



GASEOUS MERCURY IN THE MARINE BOUNDARY LAYER: MEASUREMENTS AND MODELING

PhD Thesis, 2011

Anne Lærke Sørensen



NATIONAL ENVIRONMENTAL RESEARCH INSTITUTE
AARHUS UNIVERSITY



GASEOUS MERCURY IN THE MARINE BOUNDARY LAYER: MEASUREMENTS AND MODELING

PhD Thesis

2011

Anne Lærke Sørensen



Data sheet

Title: Gaseous Mercury in the Marine Boundary Layer: Measurements and Modeling
Subtitle: PhD Thesis

Authors: Anne Laerke Soerensen
Department: Department of Atmospheric Environment & Department of Chemistry

University: The PhD was matriculated at the Department of Chemistry, Aarhus University, Aarhus Graduate School of Science (AGSoS)

Publisher: National Environmental Research Institute, Aarhus University - Denmark
URL: <http://www.neri.dk>

Year of publication: 2011

Galathea 3 contribution no: A1

Please cite as: Soerensen, A. L. 2011: Gaseous Mercury in the Marine Boundary Layer: Measurements and Modeling. PhD thesis. Department of Atmospheric Environment, NERI. National Environmental Research Institute, Aarhus University, Denmark. 176 pp.
http://www2.dmu.dk/Pub/phd_ANLS.pdf

Reproduction permitted provided the source is explicitly acknowledged

Abstract: The thesis combines analyses of observational data with biogeochemical modeling in order to explore the environmental processes that control patterns and levels of gaseous mercury concentrations in the marine boundary layer. Measurements of gaseous elemental mercury (GEM) and gaseous oxidized mercury (RGM) from the Galathea 3 circumnavigation (August 2006 to April 2007) are analyzed. A new representation of the surface ocean within the 3-D global biogeochemical model GEOS-Chem is presented. The model is used to explore mechanisms responsible for spatial and temporal trends discovered in the Galathea 3 data. The study contributes to our understanding of mercury dynamics in the marine boundary layer on diurnal, seasonal and decadal time scales. It emphasizes the importance of ocean evasion as a controlling factor for seasonal and decadal GEM variability as well as the importance of relative humidity as a controlling factor of RGM concentrations in both the polluted and pristine marine boundary layer.

Keywords: Mercury, Hg⁰, GEM, RGM, marine boundary layer, GEOS-Chem, modeling, measurements, biomass burning, anthropogenic emissions, air-sea exchange, surface ocean, Galathea 3

Supervisors: Professor Henrik Skov (National Environmental Research Institute, Aarhus University)
Associated professor Marianne Glasius (Faculty of Science, Aarhus University)
Senior scientist Jesper Christensen (National Environmental Research Institute, Aarhus Univ.)
Professor Ole John Nielsen (Faculty of Science, Copenhagen University)

Supervisor during stay at Harvard: Professor Daniel Jacob (School of Engineering and Applied Sciences, Harvard University)

Layout front page: Britta Munter

ISBN: 978-87-7073-225-3

Number of pages: 176

Internet version: The report is available in electronic format (pdf) at NERI's website
http://www2.dmu.dk/Pub/phd_ANLS.pdf

Contents

Preface 5

English resumé 7

Dansk Sammenfatning 8

1 Introduction 9

- 1.1 Problem 9
- 1.2 The aim of this work 10
 - 1.2.1 Research questions 10
 - 1.2.2 Layout of the thesis 11

2 Review of our current knowledge 13

- 2.1 Motivation for studying atmospheric and aquatic mercury 13
- 2.2 Mercury dynamics in the atmosphere 14
 - 2.2.1 Species 14
 - 2.2.2 Sources 15
 - 2.2.3 Levels 18
 - 2.2.4 Chemistry 20
 - 2.2.5 Sinks 23
- 2.3 Mercury dynamics in the surface ocean mixed layer 24
 - 2.3.1 Species 24
 - 2.3.2 Sources 24
 - 2.3.3 Levels 25
 - 2.3.4 Chemistry 26
 - 2.3.5 Sinks 27
- 2.4 Mercury dynamics in the marine boundary layer 29
 - 2.4.1 Sources 29
 - 2.4.2 Levels 30
 - 2.4.3 Chemistry 32
 - 2.4.4 Sinks 33

3 Methods 35

- 3.1 Experimental work 35
 - 3.1.1 Choice of Instruments 35
- 3.2 *Galathea 3* cruise 36
 - 3.2.1 Gaseous mercury measurements 36
 - 3.2.2 Ancillary measurements 38
 - 3.2.3 Data analysis and other data sources 38
 - 3.2.4 Hg observations that would have improved the interpretation 40
- 3.3 West Atlantic Ocean cruises 40
- 3.4 Modeling 41
 - 3.4.1 Choice of model 42
- 3.5 The GEOS-Chem model 42
 - 3.5.1 Work with the GEOS-Chem model 43
 - 3.5.2 Development of the slab-ocean model 43
 - 3.5.3 Validation of the surface ocean module 46
- 3.6 Integrating approaches 46

4	Summary and discussion of results	47
4.1	Mercury concentrations in the MBL	47
4.1.1	Spatial distribution of GEM	47
4.1.2	Spatial distribution of RGM	49
4.1.3	Diurnal variability of GEM and RGM	50
4.1.4	Seasonal variability of GEM	50
4.1.5	Do GEM MBL background concentrations exist?	54
4.2	Sources of Mercury to the MBL	56
4.2.1	Anthropogenic emissions in harbors	56
4.2.2	Anthropogenic plumes in the MBL	57
4.2.3	Influence of anthropogenic emissions on the MBL and ocean	60
4.2.4	Biomass burning emissions	61
4.2.5	Influence of biomass burning emissions	66
4.2.6	Ocean evasion of Hg ⁰	66
4.2.7	Ocean evasion of Hg ⁰ in areas with sea ice	73
4.3	Mercury Chemistry in the MBL	74
4.3.1	General Trends in RGM Dynamics in the MBL	74
4.3.2	RGM Dynamics at Antarctica	76
5	Conclusions	79
6	Outlook	82
6.1	Experimental work	82
6.2	Modeling	83
7	Glossary, Acronyms and Abbreviations	84
8	References	87
9	Appendix A List of Papers	103
9.1	Enclosed peer reviewed papers	103
9.2	Papers in preparation	103
9.3	Talks and posters (first author)	103
9.4	Popular science publications and educational material	104
10	Appendix B Enclosed Abstracts from Peer-Reviewed Papers	105
10.1	Soerensen et al. (2010a)	106
10.2	Soerensen et al. (2010b)	124
10.3	Soerensen et al. (2010c)	126
11	Appendix C Background information on the <i>Galathea 3</i> expedition	143
12	Two hour average GEM and RGM concentrations during the <i>Galathea 3</i> cruise	145
13	Appendix D Maps of input data to the GEOS-Chem slab-ocean model	146
13.1	Mixed Layer Depth	147
13.2	Chlorophyl A Concentrations	148
13.3	Net Primary Production	149
14	Appendix E Poster (Mason et al., 2009)	150

Preface

The research presented in this thesis was conducted during the period March 2008 through February 2011 with the supervisors: Prof. Henrik Skov, Associated Prof. Marianne Glasius and Senior Scientist Jesper Christensen all from Aarhus University, Prof. Ole John Nielsen from the University of Copenhagen, and Prof. Daniel Jacob from Harvard University. I carried out my research at National Environmental Research Institute (NERI), Aarhus University with Henrik Skov as the main supervisor, and spent 13 month at Harvard University under the supervision of Prof. Daniel Jacob.

My work is based on a combination of original analyses of observational data and biogeochemical modeling. I wanted to obtain a high level of experience in treatment and analyses of both observational data and model simulations. I also wanted to obtain the skills to use different programming languages and develop models. With a M.Sc. in biology, the chance to embrace the marine processes and air-sea exchange as a part of my research has been exciting. In the ocean, the biological controlled mercury processes play a more important role than they do in the atmosphere. Thus it has been possible for me to link knowledge on biological processes obtained during my M.Sc. with my PhD research in atmospheric chemistry.

My Ph.D. research has been supported by the NERI, Aarhus University. Research funding for travelling and other minor costs was funded by Andreassens & Hougaards Foundation, the Oticon Foundation, and the Hakun Lunds foundation.

There are a number of people whom I wish to acknowledge:

I would like to thank all my supervisors. I greatly appreciate the trust that you have shown me these last three years and your ability to only interfere with my research when asked to. This, and the fact that I have been able to learn from such different personalities, has made it a strength to have five supervisors.

I would like to thank Ole John Nielsen for initiating the contact to Harvard University. I also appreciate that you always have the time to listen when I struggle to understand the unwritten rules of the scientific community.

I would like to thank Elsie Sunderland for deciding I was worth mentoring. I have learned a lot and I am looking forward to our continued collaboration.

I would like to thank Daniel Jacob for making me feel part of his group at Harvard. I would also like to thank all the great people I met during my stay there. You all made me feel very welcome. And a special thanks to the people in Team-Hg.

I would like to thank my mom and dad for being who they are. I love you.

I would like to thank Maria Andersson and Robert Mason for providing the West Atlantic Cruise observations used in the thesis.

I would like to thank Ralf Ebinghaus and Hans Kock for providing the Mace Head observations used in the thesis.

Last I would like to thank Britt Tang Sørensen, Henrik Skov, Henrik Madsen, Bjarne Jensen, Christel Christoffersen, the entire crew of the *Galathea 3* as well as everybody else that helped with the collection of the mercury data during the *Galathea 3*. Without your effort this thesis could not have been written.

English resumé

The atmosphere is the primary pathway from emission to marine ecosystems around the world. When atmospheric mercury deposits to marine systems, it can be transformed to the neurotoxin methyl mercury, which biomagnifies in the food web. Mercury is therefore found in harmful concentrations in some top predators including humans. Knowledge about mercury in the marine boundary layer (MBL) is important as the MBL is the interface between the atmosphere and the marine systems.

This thesis combines analyses of observational data with biogeochemical modeling to explore the environmental processes that control patterns and levels of gaseous mercury concentrations in the MBL.

Measurements of gaseous elemental mercury (GEM) and gaseous oxidized mercury (RGM) from the *Galathea 3* circumnavigation (August 2006 to April 2007) are analyzed. GEM and RGM were measured continuously with a Tekran 2537A mercury vapor analyzer equipped with a Tekran 1130 automated denuder unit and pump module. Measurements were available for 114 days, which make the *Galathea 3* data the largest single data set on mercury in the MBL. In the 3-D global biogeochemical model GEOS-Chem the slab-ocean module is updated with a representation of the surface ocean. It includes redox processes and coupling between mercury cycling and organic carbon dynamics. After evaluation the model is used to explore spatial and temporal trends in the MBL discovered in the *Galathea 3* data.

It is found that midday peaks in RGM concentrations are common in the MBL during cruise sections with mean midday insolation $> 500 \text{ W m}^{-2}$ and mean relative humidity $< 85\%$. They indicate a photo-induced oxidation of GEM and a rapid uptake of RGM to water droplets in the air. GEM enhancements of $0.1\text{-}0.5 \text{ ng m}^{-3}$ are found in episodic plumes but RGM enhancements only in two cases. The low RGM in polluted air is suggested not to be due to a lack of RGM emissions but rather due to a rapid uptake into the water phase as a consequence of the high relative humidity in the MBL. The possible implications are that RGM emitted in coastal urban areas will deposit rapidly and be a source for the coastal ocean. The GEM variability in the MBL within each hemisphere is found to be higher than has so far been implied by relevant studies. This could be due to variable influence of continental outflow and ocean evasion but also suggest that the lifetime of GEM in the MBL might be at the low end of previous estimates. The model results suggest that 80% of mercury deposited to the ocean will re-evade. The results show that ocean evasion drives the seasonal variability of GEM in the MBL. The first estimate of seasonal variability in the MBL (Atlantic Ocean) based on cruise data is presented. Many of these cruise data have concentrations higher than at terrestrial sites. The model can explain these observations as seasonally dependent GEM evasion from the ocean driven by legacy mercury in subsurface waters. Also the Atlantic Ocean is found to currently be a net source of mercury to the atmosphere. This result combined with the result from the *Galathea 3* cruise implies that the concept of background concentrations does not apply to the MBL.

Dansk Sammenfatning

Kviksølv transporteres gennem atmosfæren, fra de kilder der udleder det, til økosystemer rundt om på jorden. Når kviksølv afsættes til marine økosystemer kan det omdannes til metylkviksølv. Methylkviksølv ophobes i fødekæden og påvirker nervesystemet i levende organismer. Det kan findes i skadelige koncentrationer i de øverste led af fødekæden, heriblandt mennesket. Det er vigtigt at forøge vores viden om kviksølv i det marine grænselag, fordi det repræsenterer overgangen fra atmosfæren til de marine økosystemer.

I denne afhandling kombineres analyser af skibsobservationer med biogeokemisk modellering for at undersøge de processer der kontrollerer koncentrationerne af gasformigt kviksølv i det marine grænselag.

Der arbejdes med målinger af gasformigt elementært kviksølv (GEM) og gasformigt oxideret kviksølv (RGM) fra *Galathea 3*'s jordomsejling (august 2006 til april 2007). GEM og RGM blev målt kontinuerligt med en Tekran 2537A udstyret med en Tekran 1130 enhed. Der var målinger fra i alt 114 dage, hvilket gør datasættet til det hidtil mest omfattende datasæt for kviksølv i det marine grænselag. I den 3-D globale biogeokemiske model GEOS-Chem opdateres havmoduliet med en ny repræsentation af kviksølvsprocesserne i havet. Efter at modellen er blevet evalueret, bruges den til at undersøge rumlige og tidsmæssige tendenser fundet under arbejdet med *Galathea 3* dataene.

Målingerne viser, at daglige variationer for RGM er almindelige i det marine grænselag. De opstår i perioder, hvor den gennemsnitlige instråling midt på dagen overstiger 500 W m^2 og den gennemsnitlige relative luftfugtighed er mindre end 85 %. Variationerne indikerer en lysinduceret oxidering af GEM og et hurtigt optag af RGM i dråber i luften. Det observeres, at GEM er $0,1-0,5 \text{ ng m}^{-3}$ højere i røgfaner fra land end i "ren" luft i det marine grænselag, men at RGM kun i to tilfælde er forhøjet. De lave RGM koncentrationer i røgfanerne skyldes højst sandsynligt, den høje relative luftfugtighed i det marine grænselag, der fører til et hurtigt RGM optag i dråber og ikke mangel på RGM emissioner fra byområder. Dette kan føre til høj våddeposition i kystområder. Variabiliteten af GEM i det marine grænselag i begge hemisfærer ser ud til at være højere end det i øjeblikket antages. Dette kan dels skyldes påvirkning fra land og hav, men kan skyldes at levetiden af GEM i det marine grænselag er i den lave ende af hidtidige antagelser. Modellen viser at 80 % af det kviksølv der afsættes til havet igen vil afgasse og at emissioner fra havet driver sæsonvariationen af GEM i det marine grænselag. Et første estimat for en sæsonvariation af GEM baseret på skibsobservationer i det marine grænselag præsenteres. Mange af disse observationer er højere end målinger på land. Modellen kan forklare dette som grundet i sæsonafhængige emissioner af GEM drevet af historisk kviksølv ophobet i havet og det vises at Atlanterhavet i øjeblikket er en kilde til kviksølv i atmosfæren. Dette resultat kombineret med resultaterne fra *Galathea 3* indikerer, at det nuværende koncept med en snæver baggrundskoncentration af GEM ikke kan bruges for det marine grænselag.

1 Introduction

1.1 Problem

Mercury is a toxic element. One third of the mercury emitted today is thought to come from direct anthropogenic emissions, and humans currently increase both the atmospheric and marine mercury pools. The mercury in the atmosphere is inorganic and not dangerous in itself. However, the atmosphere is the primary transport pathway from emission sources to terrestrial and aquatic ecosystems around the world (Figure 1). Inorganic mercury can be transformed into methyl mercury that biomagnifies in the food web, especially when mercury deposits to water bodies. Mercury can therefore be found in harmful concentrations in some top predators of aquatic animals including humans. Despite the importance of understanding the dynamics at the atmosphere-ocean interface (i.e. MBL) in order to understand the entire biogeochemical circulation of mercury, there is still a significant lack of knowledge about the processes controlling mercury in the MBL.

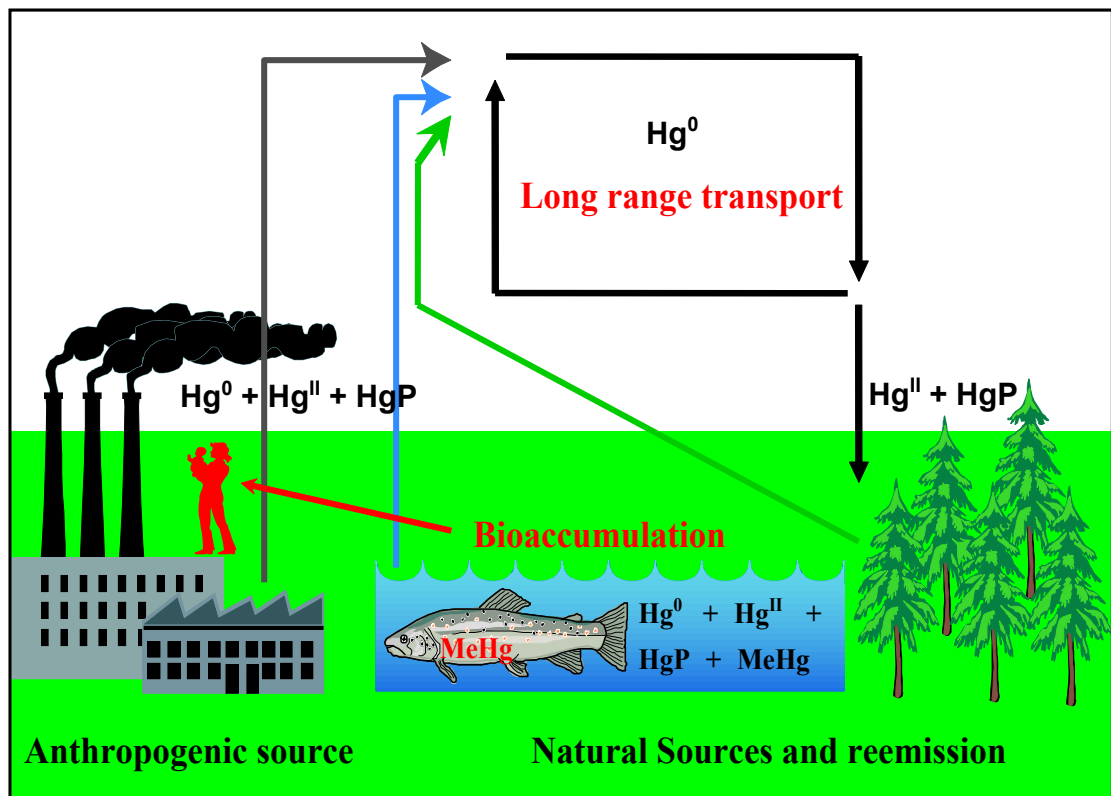


Figure 1. Overview of the biogeochemical mercury circulation. Hg^0 is gaseous elemental mercury, Hg^{II} is gaseous oxidized mercury, HgP is particular bound mercury and MeHg is methyl mercury (NERI illustration).

1.2 The aim of this work

The aim of this PhD thesis is to present my research that focuses on mercury concentrations, sources and dynamics in the marine boundary layer (MBL). I have conducted substantial research outside of this focal area. This research is included in the enclosed papers (Appendix B Enclosed Abstracts from Peer-Reviewed Papers). Thus reading the three accompanying papers in addition to the thesis provides a more complete impression of my PhD research. I have chosen the approach of presenting only parts of my research in the thesis in order to bring together my results for mercury in the MBL in a new, more coherent way than is presented in the three separate papers. Reviewing my results with the MBL as the main theme has helped me create a more complete picture of what has been accomplished during my PhD and has also allowed me to see new patterns in the data and provided insight into future research directions. The work presented here combines original analyses of observational data with biogeochemical modeling.

1.2.1 Research questions

The overarching research question for my dissertation is:

- *What environmental processes control patterns and levels of gaseous mercury concentrations in the marine boundary layer?*

To answer this question I have addressed five underlying research questions. These concentrate on factors governing the fate and dynamics of mercury in the MBL.

- 1) *Is there spatial variability of mercury in MBL? (latitudinal, longitudinal, hemispheric)*
- 2) *Is there temporal variability of mercury in MBL (diurnal, seasonal, decadal)?*
- 3) *What is the role of outflow of different continental air masses into MBL? (anthropogenic emissions, biomass burning reemissions)*
- 4) *What is the role of ocean evasion to MBL?*
- 5) *What is the role of GEM oxidation, aqueous phase RGM uptake and RGM deposition in MBL?*

I used data from the *Galathea 3* circumnavigation as the basis for investigating the five research questions given above. To help interpret the *Galathea 3* data, I applied and later enhanced the GEOS-Chem global biogeochemical mercury model. I improved the parameterization of mercury in the surface ocean including redox processes and coupling between mercury cycling and organic carbon dynamics. I used this model to further explore mechanisms responsible for spatial and temporal trends I discovered in the *Galathea 3* cruise data. My updated model has already been incorporated into the standard code of the GEOS-Chem that is presently used by 50 research groups worldwide. I am now using the model to interpret new aquatic and MBL cruise data from the Atlan-

tic Ocean (work in progress included in the section on “Ocean evasion” (4.2.6)).

The results, which are found in the enclosed papers (Appendix B) and discussed in this thesis, include:

Material from Soerensen et al., (2010a) is used in: Choice of Instruments (3.1.1), *Galathea 3* cruise (3.2), Spatial distribution of GEM (4.1.1), Spatial distribution of RGM (4.1.2), Diurnal variability of GEM and RGM (4.1.3), Seasonal variability of GEM (4.1.4), Biomass burning emissions (4.2.4), General Trends in RGM Dynamics in the MBL (4.3.1), RGM Dynamics at Antarctica (4.3.2), Ocean evasion of Hg⁰ in areas with sea ice (4.2.7).

Material from Soerensen et al., (2010b) is used in: *Galathea 3* cruise (3.2), Anthropogenic emissions in harbors (4.2.1), Anthropogenic plumes in the MBL (4.2.2).

Material from Soerensen et al., (2010c) is used in: Development of the slab-ocean model (3.5.2), Validation of the surface ocean module (3.5.3), Seasonal variability of GEM (4.1.4), Ocean evasion of Hg⁰ (4.2.6).

The results, which are found in the enclosed papers (Appendix B) but not discussed in this thesis, include:

Results on harbor concentrations, Hg/CO ratios, emission estimates and comparison to the AMAP mercury inventory for four cities and analysis of harbor concentrations for two cities are presented in Soerensen et al. (2010b).

Results on the aquatic mercury processes, concentrations and dynamics and their influence on the evasion flux from the ocean are found in Soerensen et al. (2010c).

1.2.2 Layout of the thesis

A review chapter (page 13-34) presents sections on our current knowledge regarding the general understanding of mercury in the troposphere and surface ocean (Figure 2, thin arrows) and then continues with a section focusing on the marine boundary layer and how concentrations, chemistry and dynamics of mercury and associated compound differ from what is found in the free troposphere (Figure 2, thick arrows).

A chapter on methodology (page 35-47) presents an evaluation of the choice of instrumentation and the model used as well as the methods of measurements, model development and data analysis.

A chapter on results (page 47-78) presents and discusses the main findings with a focus on results on mercury in the MBL. Most of these findings are published and can be found in “Appendix B Enclosed Abstracts from Peer-Reviewed Papers” but this chapter also presents new results that are not found in the enclosed papers. These unpublished results will be treated in depth, while published results are more briefly discussed and references of where to find in depth information on these results is given in the text. The three papers found in Appendix B will in the text be referred to Soerensen et al. (2010a, 2010b, 2010c).

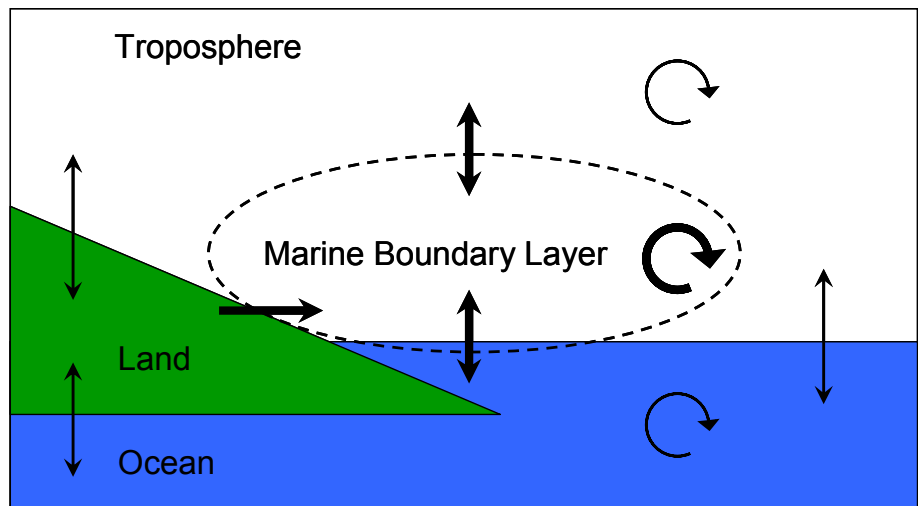


Figure 2. Schematic illustration of the levels in which fluxes and processes are treated (own illustration).

The last two chapters contain respectively the conclusions and an outlook (79-83).

2 Review of our current knowledge

2.1 Motivation for studying atmospheric and aquatic mercury

Mercury is toxic in all its forms. Compared to other heavy metals it also has unique biogeochemical cycling. Where all other heavy metals are found in the atmosphere only associated with particles, mercury is found predominantly in the gas phase. The lifetime of gaseous atmospheric mercury is thought to be around 1 year (Lamborg et al., 1999; Slemr and Langer, 1992) and thus it is globally distributed in the atmosphere (e.g. Sprovieri et al., 2010). The mercury in the atmosphere is inorganic and at current atmospheric concentrations it is not dangerous in itself. However, the atmosphere is the primary distribution pathway from emission sources to terrestrial and aquatic ecosystems around the world (Sprovieri et al., 2010). When mercury deposits to water bodies, a small portion of the inorganic mercury is transformed into highly toxic methylmercury (MeHg) (Cossa et al., 2009) by microorganisms in the water (e.g. Kerin et al., 2006). After the incorporation into the microorganisms MeHg can bioaccumulate in organisms and biomagnify through the food web. In this way it ends up in high concentrations in top predators of aquatic animals, including humans. The biomagnification process results in MeHg concentrations in predatory fish that can be elevated relative to the water by a factor of $\geq 10^6$ (Engstrom, 2007).

As one third of the current mercury emissions are thought to originate from direct anthropogenic sources, humans currently increase the globally circulated mercury pool.

Exposure to MeHg through food can result in reproductional problems, damage to the nervous system, hormonal changes and changes in behavioral patterns (Mergler et al., 2007; Scheulhammer et al., 2007). Mercury therefore has serious effects on an animal's ability to reproduce and survive. This can have severe consequences for the ecosystems in which these animals live.

The severe human health problems related to mercury exposure have for a long time not been fully recognized (Grandjean et al., 2010). Mercury was previously considered a local problem in populations with a high intake of aquatic animals but with the increasing mercury contamination, it is now being acknowledged as a global concern (Mergler et al., 2007). In a recent study in the US it was found that 5% of all women in the child bearing age had blood level concentrations of MeHg higher than $5.8 \mu\text{g L}^{-1}$ (Mahaffey et al., 2009), which is the concentration the US-EPA has used to calculate their reference level (the level below which no harm is assumed) (U.S.EPA.-IRIS, 2001). To stay below harmful concentrations as an adults EFSA (European Food Safety Authority) recommends a maximum intake of $1.6 \mu\text{g kg}^{-1}$ body weight per week and the US-National Research Council recommends a maximum intake of $0.7 \mu\text{g kg}^{-1}$ body weight per week.

One of the main concerns with mercury is that it can damage the human nervous system at the fetal stage (e.g. Mergler et al., 2007). Mercury is transferred from mother to fetus through the placenta and is found in higher concentration in the blood of the fetus than in the blood of the mother (Mergler et al., 2007). When this is considered in the study on women in the US, more than 10% of women exceeded a level, which could be of danger for the fetus (Mahaffey et al., 2009). Pregnant women therefore need to be particularly aware of how much mercury they are exposed to. Due to this concern both the EU and the US-EPA have special guidelines for pregnant women, which recommend a maximum intake of fish. The Danish Ministry of Family and Consumer Affairs is advising pregnant women to eat less than 100 gr. of large predatory fish per week (www.foedevarestyrelsen.dk [accessed January 2011]).

Avoiding mercury pollution has been shown to be far more efficient than remediating polluted sites (Hylander and Goodsite, 2006). Mercury is now listed as a priority element in a large number of international agreements and conventions aimed at protecting the environment (Ebinghaus et al., 2002). The European Union has had a strategy on mercury since 2005 (<http://ec.europa.eu/environment/chemicals/mercury> [accessed January 2011]). It contains 20 methods for reducing mercury emissions, decreasing demands in the industry and protecting citizens against exposure to MeHg in fish.

This makes it clear that mercury emitted to and transported through the atmosphere is associated with global human health problems. As the MBL is the interface between the mercury transported in the atmosphere and the mercury in the water bodies, it is important to understand what drives the processes there.

Despite the problems associated with mercury the species, sources, sinks and chemistry for atmospheric mercury are still not well understood. Here I present a review of the current knowledge.

2.2 Mercury dynamics in the atmosphere

This section will focus on the mercury cycle in the atmosphere. In Figure 3b (from Sunderland and Mason, 2007) a global budget for mercury in the atmosphere is presented including estimates on current sources and sinks.

2.2.1 Species

In the atmosphere mercury (Hg) is found as three inorganic species (GEM, RGM and TPM), which are defined from the analytic method of measurements (Steffen et al., 2008). It is believed that the three species can be converted between each other (Lindberg et al., 2007 and references therein) although the rates, with which this takes place, are very different.

TGM (total gaseous mercury) is the sum of the gaseous mercury species. TGM is split into gaseous elemental mercury (GEM/Hg⁰) and gaseous oxidized mercury (RGM/Hg^{II}).

GEM is found in the gas phase in the atmosphere and is measured in ng m^{-3} or ppq ($\sim 112 \text{ ppq} = 1 \text{ ng m}^{-3}$). GEM is not very reactive and with a vapor pressure of 0.18 Pa at 20°C (Skov et al., 2008) it is not readily taken up in the water-phase. The atmospheric lifetime in the free troposphere is around 1 year (Hedgecock and Pirrone, 2004; Lamborg et al., 1999; Slemr and Langer, 1992). GEM is the dominant mercury species in the atmosphere (Steffen et al. 2007) and it makes up > 95% of the mercury load (Fitzgerald et al., 1986; Gustin and Jaffe, 2010).

RGM is mercury in its oxidized form. It is measured in pg m^{-3} or ppq. It is believed to be constituted of compounds like HgBr_2 , HgBrO , HgO , HgClBr , Hg(OH)_2 or HgCl_2 (Ebinghaus et al., 2009; Gustin and Jaffe, 2010; Hedgecock et al., 2005; *references in* Ariya et al., 2008) although the exact composition is unknown and most likely depends on its origin. RGM is either primary emitted or created as an oxidation-product of GEM. RGM (in the form of HgCl_2) has a vapor pressure of 0.009 Pa at 20°C (Skov et al., 2008) and is more water soluble than GEM. RGM rapidly reacts with wet surfaces (Lindberg et al., 2007) and the lifetime of RGM is shorter than for GEM, in some cases only a few hours (Holmes et al., 2009). RGM is therefore only transported tens to hundreds of kilometers before it is deposited (Schroeder and Munthe, 1998). In the troposphere a presence will be maintained as an equilibrium is established between input through GEM oxidation and output through deposition. With the current measurement technique RGM taken up into water droplets is detected as TPM, but in many cases modeling papers still consider this product as RGM. It is therefore convenient to separate RGM in the water droplet and TPM. I will therefore refer to RGM that is taken up in water droplets as RGM_w .

TPM is mercury associated with particles and is measured in pg m^{-3} or ppq. Like RGM it is deposited on local to regional scales.

2.2.2 Sources

Mercury emissions have both a natural and anthropogenic component. Mercury has always been present in the environment (Figure 3a) but since industrialization the burden of anthropogenic emissions has increased the atmospheric loading (Figure 3b). Important natural sources include volcanoes, oceans and soils (Biswas et al., 2007). Important anthropogenic sources include coal burning power plants, waste incineration, and metal production (especially gold mining)(Pacyna et al., 2010; Pirrone et al., 2010).

Global emission loads

Present emission estimates attribute 25 Mmol Hg y^{-1} (1 Mmol \sim 200 Mg) to natural emissions and reemissions and 12.5 Mmol Hg y^{-1} to anthropogenic emissions (Mason and Sheu, 2002; Pirrone et al., 2010). Primary natural emissions from weathering of soil and volcanic activity are only a small part of the total emissions (0.3-2.5 Mmol Hg y^{-1}) (AMAP/UNEP., 2008 *and references therein*). Emission inventories show that most anthropogenic emissions take place in the northern hemisphere (NH) (Figure 4). There is a general lack of knowledge on emissions in especially the southern hemisphere (SH) and some newer estimates for SH countries (Dabrowski et al., 2008; Nelson, 2007) indicate that global emission inventories for 2000 (Pacyna et al., 2006b) may have overestimated anthro-

pogenic sources. This has been addressed in the 2005 inventory by Pacyna et al. (2010). There are however still many unknowns for SH emissions.

Anthropogenic emissions

There are several published global anthropogenic emission inventories, the most recent being Pacyna et al. (2010) and Pirrone et al. (2010). Anthropogenic mercury emission are generally estimated using emission estimates collected by governments, and based on emission factors and statistical data on the production of industrial goods and consumption of raw materials (Pacyna et al., 2006b). An attractive alternative is to use a GEM/CO relationship from plume measurements (Jaffe et al., 2005; Radke et al., 2007; Slemr et al., 2006; Talbot et al., 2008; Weiss-Penzias et al., 2006; Weiss-Penzias et al., 2007) since CO emissions are more accurately known than mercury emissions. The ratio between the two species can therefore be used to derive an estimate of mercury emissions for an area, based on CO inventories.

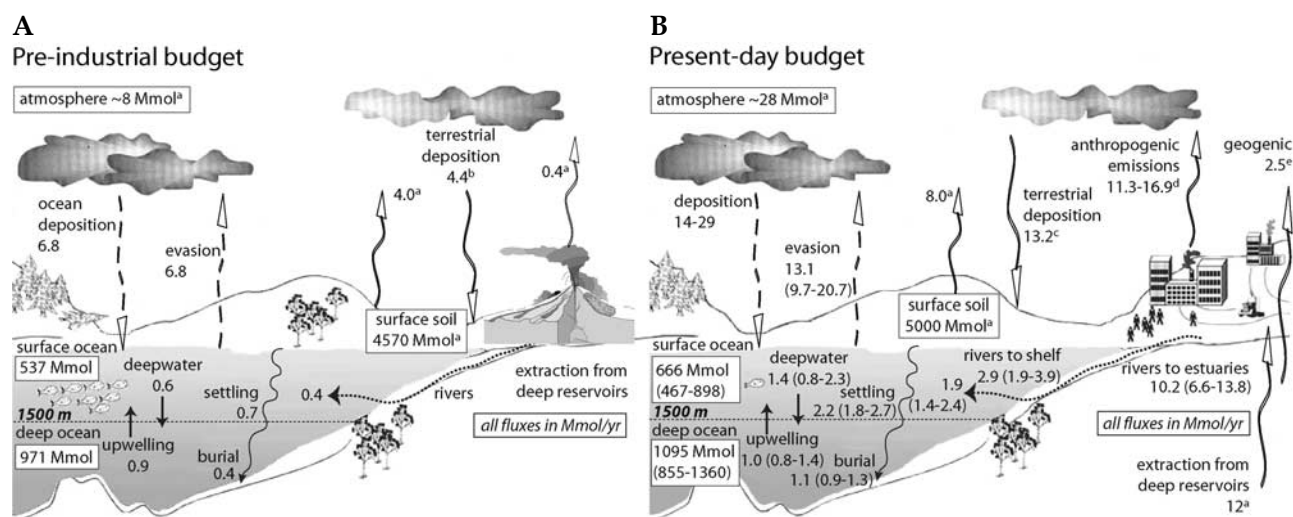


Figure 3. Global A) pre-industrial and B) present-day budgets of mercury in Mmol. The budget shows the increase in the mercury pools that have been caused by humans in the last 200 years (illustration from Sunderland & Mason, 2007).

The fraction of the different mercury species in the emissions depends on the source. Some anthropogenic emissions have a large fraction of RGM, e.g. coal combustion with 60%, while others consist of more than 80% GEM, e.g. mining and cement production (Pacyna et al., 2008). TPM is most often a smaller fraction of emissions contributing 10 % or less (Pacyna et al., 2008).

Trends in anthropogenic emissions

Until the 1990s Western Europe and North America were the largest emitters of mercury but due to legislation and changes in industrial practice emissions have now decreased in these areas (Pacyna et al., 2006a). Asia (especially China) is becoming dominant with large emission increases (Pacyna et al., 2010).

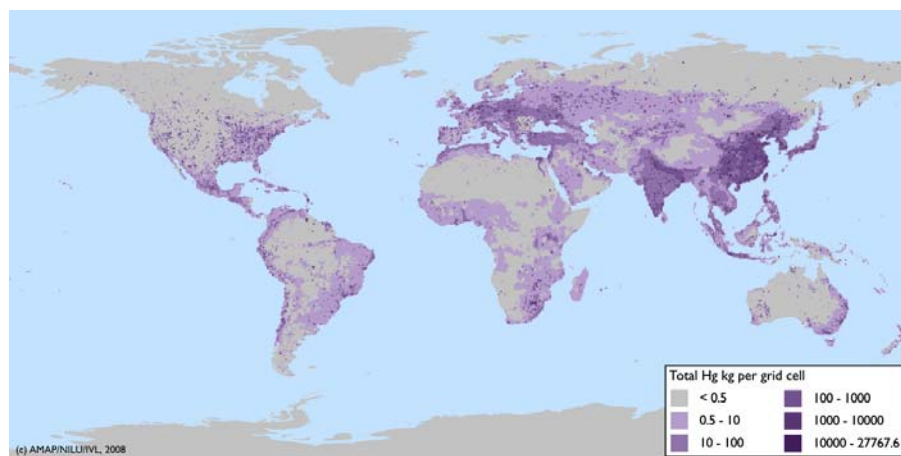


Figure 4. Map showing a 2005 estimate of the spatial distribution of anthropogenic emissions (illustration from AMAP/UNEP., 2008)

Natural emission and reemission

Most of the primary natural emissions are from volcanoes, geothermal sources and enriched top soil. Volcanoes mostly emit GEM with only 1-5% TPM (Bagnato et al., 2007; Witt et al., 2008) and a small amount (~1%) of RGM (Witt et al., 2008).

RGM will not be reemitted after deposition due to its low vapor pressure. But RGM can be reduced to form GEM, which can be reemitted due to its higher vapor pressure. Reduction of RGM takes place in water bodies and soil (e.g. Qureshi et al., 2010; Selin, 2009; Whalin et al., 2007; *references in* Smith Downey et al. 2010). GEM can also be released when organic matter is burned during fires (Friedli et al., 2009; Selin, 2009; Smith-Downey et al., 2010).

Reemissions of previously deposited mercury, which contains a component of both natural and anthropogenic mercury, are dominated by GEM. Emissions from the ocean are predominantly in the form of GEM (e.g. Schroeder et al. 1998) while biomass burning besides GEM emits a small amount of 0-15% TPM (Finley et al., 2009; Friedli et al., 2003a; Friedli et al., 2003b).

Trends in reemissions

Due to the ability of GEM to reemit from terrestrial and aquatic surfaces and during biomass burning it keeps circulating in the environment, with burial into ocean sediments as the only long term sink (Horvat, 2005). As a consequence a large part of the 25 Mmol of yearly emissions from natural sources is actually reemissions of previously deposited mercury, much of which has an anthropogenic origin. In this way anthropogenic emissions influence the amount of mercury circulating in the biogeochemical compartments and will keep doing this for a long time into the future, even if all anthropogenic emissions were stopped today. We will therefore unambiguously see the legacy of emissions today as reemissions from e.g. forest fires (*references in* Friedli et al., 2009) or evasion from the ocean (Lindberg et al., 2007; Sunderland and Mason, 2007) in centuries to come.

2.2.3 Levels

Rural areas

The current consensus is that average global background concentrations of GEM at sea level are 1.5-1.7 ng m⁻³ in the NH and 1.1-1.3 ng m⁻³ in the SH (Lindberg et al., 2007). Concentrations are higher in the NH than the SH because most anthropogenic sources are located in the NH and the mixing time between hemispheres is around 1 year. Vertical profiles up to a few kilometers indicate that GEM is well mixed within the troposphere and that GEM concentrations do not deviate much from the rural surface concentrations (Banic et al., 2003) or decrease only slightly (Holmes et al., 2010 *figure 11 and references therein*; Landis et al., 2005) with height. At the upper troposphere observations and model simulations indicate that GEM could be depleted (Dastoor and Larocque, 2004; Swartzendruber et al., 2006).

RGM concentrations measured in rural areas are low (<10 pg m⁻³) at the planetary boundary layer and highest in the upper troposphere (up to 600 pg m⁻³). The concentrations in the upper troposphere could be caused by extensive GEM oxidation (Swartzendruber et al., 2006; Swartzendruber et al., 2008), which would also cause GEM to deplete.

TPM is in the range from below detection limit (DL) to 40 pg m⁻³ at Mt. Bachelor for air in the planetary boundary layer and in the free troposphere (Swartzendruber et al., 2008).

Trends in rural areas

Most studies have shown no consistent trend in NH TGM/GEM concentrations since the 1990s based on rural sites and cruise measurements, especially in Europe and the Atlantic Ocean (e.g. Temme et al., 2007 *and references therein*; Wangberg et al., 2007). Where decreasing trends are observed this could be due to local changes in emissions as well as a global trend (Temme et al., 2007). However, a new study from Slemr et al. (2011) for the first time presents very convincing evidence for a general downward trend at the coast of the East Atlantic Ocean in both NH and SH with a rate of 1-2% decrease per year since 1996 (Figure 5). Unfortunately the cruise data used to back up this hypothesis do not agree with other recent cruise observations (Witt et al., 2010; Xia et al., 2010)(see Table 2).

As the increase in Asian emissions is most likely causing an overall global increase in GEM emissions (Streets et al., 2009) we are still waiting to see if the decrease in regional emissions in Europe and North America will lead to regional decreases in GEM levels or if the decreases in European and North American emissions are counteracted by the increasing emissions in Asia?

Seasonal variation in rural areas

NH rural monitoring sites show slight seasonal variability with highest concentrations in winter and spring (*references in* Temme et al., 2007). This is true both for inland and coastal sites. This has been attributed to the indirect influence of high anthropogenic emissions in winter and spring (Kock et al., 2005; Sprovieri et al., 2010) or seasonal changes driven by meteorological changes in circulation, boundary layer height, clouds, rain and dry deposition (Dastoor and Larocque, 2004; Kock et al., 2005).

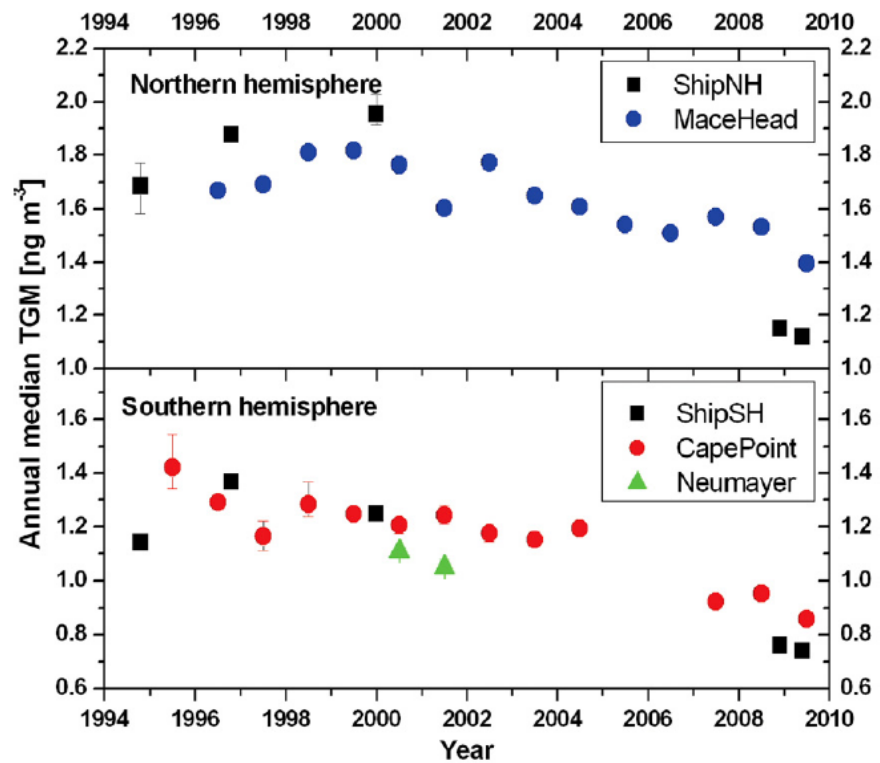


Figure 5. Trends of GEM concentrations in the NH and SH. The points and bars represent the annual medians and the 95% confidence intervals of the medians, respectively. The annual medians at Mace Head were calculated from baseline hourly mean concentrations. The median confidence intervals for the continuous measurements are smaller than the symbols (illustration from Slemr et al. (2011)).

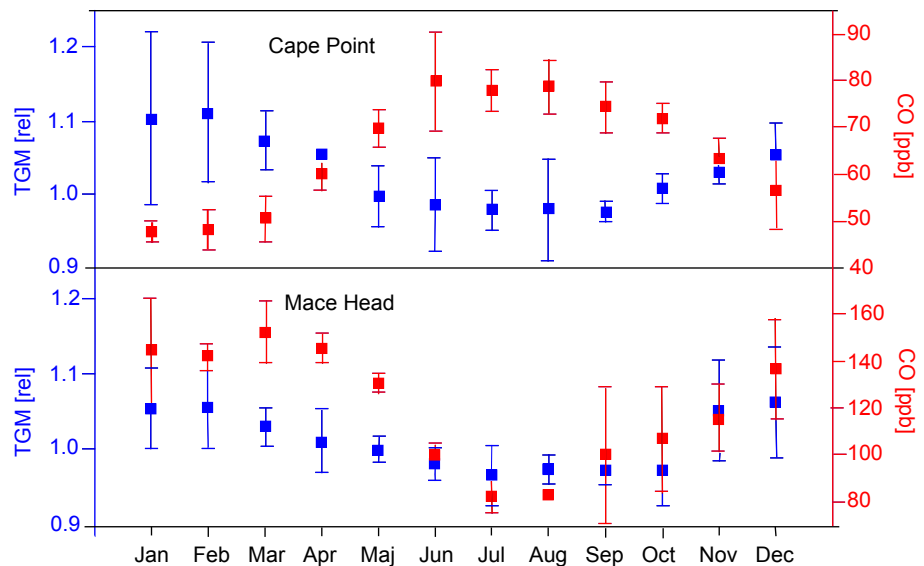


Figure 6. Seasonal variation of TGM at Cape Point and Mace Head (illustration redrawn from Slemr et al. (2006)). Shown are relative (TGM) and absolute (CO) monthly averages and their standard deviation. Only baseline data (not influenced from local sources) are considered.

Only one site in the SH has long term monitoring of mercury; Cape Point in South Africa (Brunke et al., 2010; Slemr et al., 2006). This location has a seasonal variability correlating with the one seen in the NH (Figure 6). The reason for this is not understood.

The seasonal variability of GEM has not been measured in the MBL. Rural coastal stations like Mace Head and Cape Point are used as indicators of MBL variability (Figure 6).

Urban areas

The concentration and speciation of mercury in urban areas have been investigated during campaigns in different cities around the world. The knowledge gained from combining the information from these publications is evaluated by Sprovieri et al. (2010). Most campaigns have taken place inland in North America, Europe and Asia, while there is a lack of information on urban areas in the SH. Thus the importance of anthropogenic emissions for local contamination and long range transport in the SH is not well understood (Pacyna et al., 2008).

In larger urban areas in North America, 2-10 times higher TGM (or GEM) concentrations are often observed in near-source areas compared to 40-120 km from the emission sources (*references in* Ebinghaus et al., 2009). In urban areas RGM levels are mainly above an average of 10 pg m^{-3} and often have peaks around several hundreds pg m^{-3} (Engle et al., 2010; Laurier and Mason, 2007; *references in* Ebinghaus et al., 2009), dependent on the type of industry. TPM can also reach several hundreds pg m^{-3} in peak areas (Engle et al., 2010) although the mean concentrations are much lower (*references in* Ebinghaus et al., 2009).

2.2.4 Chemistry

Halogens have long been proposed to be of importance for GEM oxidation in the MBL and atomic bromine (Br) is now emerging as the possibly most important oxidant of GEM in the troposphere (Hynes et al., 2009; Skov et al., 2008). The importance of Br was first discovered in the Arctic during analysis of atmospheric mercury depletion events (AMDEs) (Schroeder et al., 1998; Skov et al., 2004). The depletion of GEM simultaneously with dramatic increases in Br and RGM in the Arctic spring strongly emphasized the role of Br (Figure 7). The lifetime of GEM during AMDEs can be as short as hours (Goodsite et al., 2004; Skov et al., 2004).

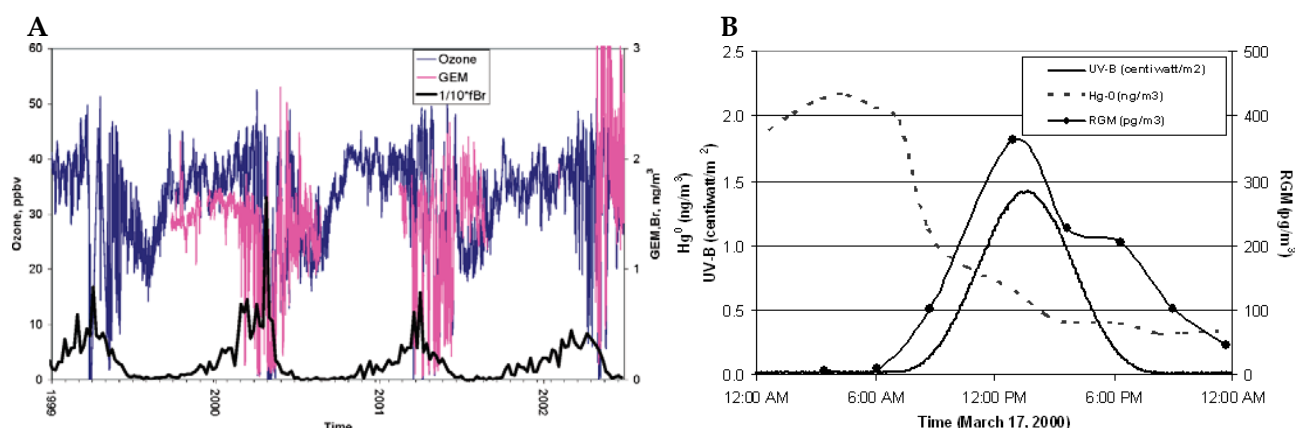


Figure 7. A) Hourly ozone mixing ratios and weekly concentration of filterable (gasphase) bromine (fBr) measured from 1999 to 2002 at Station Nord, Northeast Greenland (illustration from Skov et al., 2004). B) A 24 h time series of gaseous Hg species measured at Barrow, Alaska, during a mercury depletion event, illustrating how GEM is rapidly converted to RGM during full sunlight (Illustration from Lindberg et al., 2002).

Br is produced from naturally and anthropogenically emitted bromocarbons (Yang et al., 2005), sea salt aerosols in the MBL (Vogt et al., 1996), and by evaporation from leads during refreezing of seawater in Polar Regions (Simpson et al., 2007). Bromocarbons are emitted from anthropogenic sources, biomass burning and the ocean (Skov et al., 2008; Yang et al., 2005) but are only converted to Br-atoms during photolysis in the upper troposphere (Skov et al., 2008; Yang et al., 2005). Sea salt dominates the Br supply in the MBL (see "Chemistry" (2.4.3)). The total bromine pool in the atmosphere is made of non-radical reservoir species dominant during the night and radical species (Br and BrO) dominant during day when they are photochemically produced (Pszenny et al., 2004; von Glasow et al., 2002).

During the last ten years the role in GEM oxidation by halogens in general and Br in particular has been the focus of much research in the form of laboratory experiments and theoretical calculations (see Ariya et al. (2008) for a summary), and global scale (Dastoor et al., 2008; Holmes et al., 2010; Seigneur and Lohman, 2008) and regional/box modeling (Hedgecock et al., 2005; Hedgecock and Pirrone, 2004; Holmes et al., 2009; von Glasow, 2010).

Experiments have shown that the reaction between GEM and Br is temperature dependent (Table 1) with highest oxidation rate at cold temperatures, as is found in the polar regions (Figure 8). However Br is also an important oxidant outside the polar regions. In the MBL photo-induced oxidation is supported by cruise measurements (Hedgecock et al., 2005; Laurier and Mason, 2007; Laurier et al., 2003). Although GEM depletion is seldom seen outside the polar regions (Cape Point in South Africa being so far the only exception (Brunke et al., 2010)) diurnal variation of RGM indicates oxidation of GEM by photochemical compounds. The amplitude of the diurnal RGM variability and lack of diurnal GEM variation indicates that the strength of the oxidation is lower than in the Arctic. Models of the MBL that simulate the temporal variations of mercury species (Hedgecock et al., 2005; Hedgecock and Pirrone, 2004; Holmes et al., 2009) show that oxidation by Br can reproduce the diurnal variation of RGM better than other oxidation candidates. Br oxidation is important also in the free troposphere (Holmes et al., 2006; Lindberg et al., 2007) where the oxidation is favored by the temperature dependence of the chemical reactions (Table 1 and Figure 8). Thus the importance of Br oxidation is global.

The most important reaction pathways for the GEM oxidation are believed to be summarized by reaction 1-4 in Table 1. For a more thorough treatment of possible compounds and reactions see Ariya et al. (2008). Once GEM is oxidized to RGM, RGM can be taken up into the aqueous phase creating RGM_w. As discussed in "Species" (2.2.1) the precise composition of RGM is not known. Even if the original oxidation product is HgBr₂ or HgBrOH, it is thought that most RGM could end up as HgCl₂ in water droplets (Ebinghaus et al., 2009; Hynes et al., 2009).

Aqueous phase GEM oxidation does not seem to be as important as gaseous phase reactions most probably due to the low solubility of GEM.

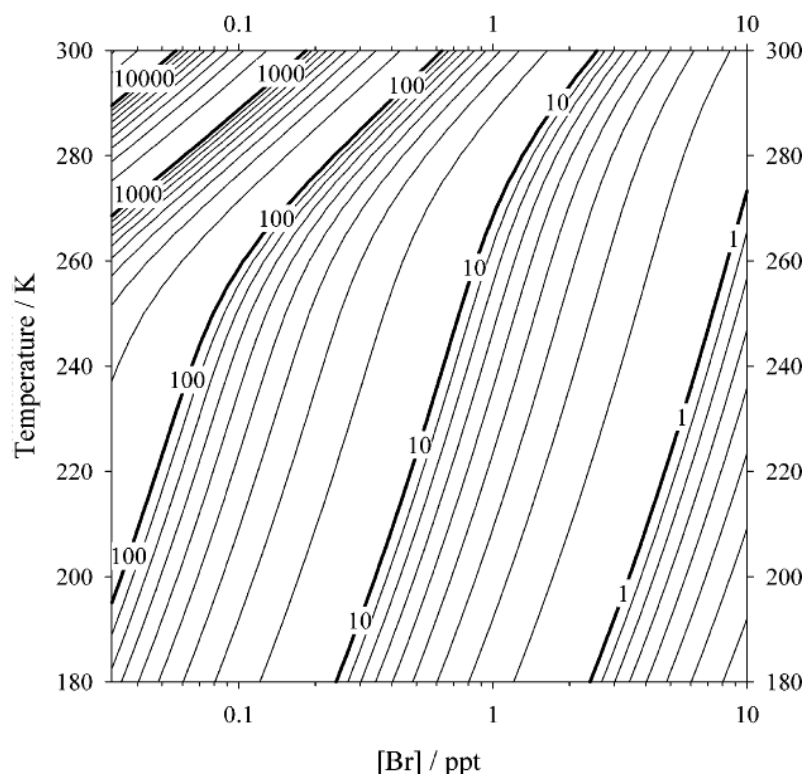


Figure 8. Contour plot of the lifetime in hours for GEM oxidation to HgBr_2 , plotted as a function of $[\text{Br}]$ in parts per trillion and temperature in Kelvin (illustration from Goodsite et al., 2004).

There is not much support for the existence of comprehensive reductive reactions of RGM in the atmosphere although it cannot be ruled out (Skov et al., 2008). One of the reactions suggested (Balabanov et al., 2005) and used in some mercury models (Holmes et al., 2009; Holmes et al., 2010) is reaction 5 in Table 1.

Table 1. Temperature dependent expressions for reactions, which include Hg and Br.

#	Reaction	Reaction rate constant at 298 K	Method	Author
1	$\text{Hg}^0 + \text{Br} + \text{M} \rightarrow \text{HgBr}$	$1.46(\pm 0.34) \times 10^{-32} \times (T/298)^{-(1.86 \pm 1.49)} \text{ cm}^6 \text{ molecules}^{-2} \text{ s}^{-1}$	Experi.	Donohoue et al. 2006
	$\text{Hg}^0 + \text{Br} \rightarrow \text{HgBr}$	$1.1 \times 10^{-12} (T/298\text{K})^{-2.37} \text{ cm}^3 \text{ molecules}^{-1} \text{ s}^{-1}$	Theoreti.	Goodsite et al. 2004
2	$\text{HgBr} \rightarrow \text{Hg}^0 + \text{Br}$	$1.2 \times 10^{10} \exp(-8357/T) \text{ s}^{-1}$	Theoreti.	Goodsite et al. 2004
3	$\text{HgBr} + \text{Br} \rightarrow \text{HgBr}_2$	$2.5 \times 10^{-10} (T/298\text{K})^{-0.57} \text{ cm}^3 \text{ molecules}^{-1} \text{ s}^{-1}$	Theoreti.	Goodsite et al. 2004
4	$\text{HgBr} + \text{OH} \rightarrow \text{HgBrOH}$	$2.5 \times 10^{-10} (T/298\text{K})^{-0.57} \text{ cm}^3 \text{ molecules}^{-1} \text{ s}^{-1}$	Theoreti.	Goodsite et al. 2004
5	$\text{HgBr} + \text{Br} \rightarrow \text{Hg}^0 + \text{Br}_2$	$3.9 \times 10^{-11} \text{ cm}^3 \text{ molecules}^{-1} \text{ s}^{-1}$	Theoreti.	Balabanov et al. 2005

Although Br is currently considered to be the globally most important oxidant there are also other possible candidates (see Ariya et al. (2008)). The two most discussed candidates are OH and O_3 , which were earlier believed to be the main GEM oxidants. Some other possible oxidants that have been tested and 1) were found to be of none or minor importance are Br_2 , BrO, and ClO, or 2) are still under consideration are I and IO. Recently Cl, Cl_2 and BrCl have been proposed to play an important part in the Arctic troposphere where chlorine concentrations are much higher than elsewhere (Holmes et al., 2010).

The reaction between OH and GEM has been found to be either too slow (Calvert and Lindberg, 2005; Goodsite et al., 2004) to play an important

role or not consistent with known thermochemistry (Hynes et al., 2009). However, some newer studies still refer to this reaction as the most likely driver in the MBL (Chand et al., 2008; Engle et al., 2010).

The direct reaction between GEM and O₃ is very unlikely to take place since the reaction is endothermic (Calvert and Lindberg, 2005). A theory that includes the creation of an intermediate (HgO₃) that will deposit on wet aerosols could however make an oxidative reaction possible (Calvert and Lindberg, 2005). The reaction between GEM and O₃ thus still needs more investigation before any conclusion can be reached about its importance (Ariya et al., 2008).

2.2.5 Sinks

Mercury is removed from the atmosphere by deposition. As the atmospheric load does not change much on yearly basis depositions must approximately equal emissions. The global deposition (wet and dry) is estimated to be around 23 to 44 Mmol y⁻¹ (Holmes et al., 2010; Sunderland and Mason, 2007). Model simulations indicate that for North America wet deposition accounts for one third of the total deposition (Miller et al., 2005; Selin and Jacob, 2008). It is plausible to assume that something similar applies for the rest of the world, although the type of deposition is highly influenced by the amount of precipitation and the roughness of the landscape (Miller et al., 2005). Model simulations with the GRAHM model indicate that dry deposition has a more local impact than wet deposition (Dastoor and Larocque, 2004).

The dominant form of mercury in wet deposition is RGM_w (Lindberg et al., 2007; Selin and Jacob, 2008). It is scavenged into droplets in the atmosphere. In this way rain events can drain at least the lower troposphere of most RGM (Laurier and Mason, 2007; Mason and Sheu, 2002). TPM in the precipitation accounts for the rest of the wet deposition (Selin and Jacob, 2008). Selin and Jacob (2008) (GEOS-Chem model) and Dastoor and Leroqueu (2004) (GRAHM model) find that half of the wet deposition and a significant portion of the wet deposition, respectively, is from scavenging above the boundary layer. Thus much of the wet deposition is not from the local pool but from the global pool of long ranged transported mercury.

Most dry depositions are in the form of GEM and RGM, while TPM is found to account for a much smaller fraction (Lindberg et al., 2007; Miller et al., 2005).

Trends

Deposition rates have increased from a preindustrial level of 5-20 nmol m⁻²y⁻¹ (1-4 µg m⁻²y⁻¹) (Givelet et al., 2003; Sunderland et al., 2008) to present day (North American) levels of 20-125 nmol m⁻²y⁻¹ (4-25 µg m⁻²y⁻¹) (Keeler et al., 2005; Miller et al., 2005; Selin et al., 2008 *and references therein*). Deposition rates in North America and Europe have declined again in recent years (Skov et al., 2008; Sunderland et al., 2008) often due to large local reduction in emissions (e.g. Givelet et al., 2003; Sunderland et al., 2008). The consequence is that the global pool now contributes with a larger fraction of the total depositions than it used to do. This trend is assumed to be consistent with the pattern in Europe, where emissions have also decreased in the past decades, but for other locations

in the world where local emissions are increasing, local depositions are likely to do the same.

2.3 Mercury dynamics in the surface ocean mixed layer

Mercury concentrations in the surface ocean mixed layer equilibrate with the atmospheric inputs on timescales of approximately one year (Strode et al., 2007; Sunderland and Mason, 2007) and the marine mercury concentrations in the surface ocean therefore rapidly react to changes in atmospheric concentrations. Intermediate and deep ocean waters respond much more slowly to changes in atmospheric inputs due to the decadal or longer timescales required for ocean circulation and vertical transport (Sunderland and Mason, 2007). Intermediate ocean waters receive mercury from the atmosphere primarily through down-welling regions and sinking of mercury bound to particulate organic material. As a consequence the ocean is not in steady state with the anthropogenically enhanced atmospheric concentrations (Sunderland and Mason, 2007) resulting in a global net flux of mercury from the atmosphere to the deep oceans (Figure 3).

2.3.1 Species

The inorganic forms of mercury in the ocean are elemental mercury (Hg^0), divalent mercury (Hg^{II}) and particulate bound mercury (HgP). It has been shown that Hg^{II} complexes with halides such as chloride in saline waters. These Hg^{II} complexes are not as available for reduction and methylation (Gardfeldt et al., 2003; Whalin et al., 2007) as the rest of the Hg^{II} pool. Here $\text{Hg}^{\text{II}}_{\text{red}}$ denotes the fraction of the Hg^{II} that is easily available for reduction. Dissolved gaseous mercury (DGM), which is a fraction often measured, is the product of both Hg^0 and Me_2Hg (Lamborg et al., 1999; Mason et al., 1995b) but Hg^0 is the dominant form in the upper ocean (Gardfeldt et al., 2003; Laurier et al., 2003).

2.3.2 Sources

Mercury is transported mainly through the atmosphere from natural and anthropogenic sources to the ocean (Sprovieri et al., 2010). Away from river mouths and continental shelves only 7-10% of the mercury input to the ocean originates from rivers (Mason and Sheu, 2002; Sunderland and Mason, 2007). In local areas, like coastal regions and the Arctic Ocean, rivers can however be the dominant source of mercury (Sunderland and Mason, 2007). Exchange with the deep ocean through ocean circulation contributes with redistribution of mercury (between the surface and sub-surface ocean) that is already in the aquatic system (Strode et al., 2007; Sunderland and Mason, 2007).

Atmospheric mercury mainly enters the surface ocean through wet deposition of RGM and TPM (Holmes et al., 2010; Sunderland and Mason, 2007) and the net flux from the atmosphere to the ocean is estimated to be $10\text{-}29 \text{ Mmol y}^{-1}$ (Strode et al., 2007 and references therein; Holmes et al., 2010; Sunderland and Mason, 2007)(Figure 3b). During specific circumstances the MBL can also be a net source of Hg^0 to the ocean (see "Sinks" (2.4.4)).

2.3.3 Levels

The number of aquatic measurements of inorganic mercury species in the open ocean regions is severely limited maybe even more so than atmospheric observations in the MBL. The observations of total inorganic mercury ($\text{Hg}^0 + \text{Hg}^{\text{II}} + \text{HgP}$) in surface waters vary substantially (0.6-3.3 pM for average concentrations during cruises) (Gill and Bruland, 1987; Gill and Fitzgerald, 1988; Kirk et al., 2008; Laurier et al., 2004; Mason et al., 1998; Mason et al., 2001; Mason and Fitzgerald, 1990; Mason and Fitzgerald, 1993; Mason and Sullivan, 1999; Sunderland et al., 2009). DGM (i.e. Hg^0) concentrations are also highly variable (0.08-0.4 pM for average concentrations during cruises) (Andersson et al., 2008c; Kim and Fitzgerald, 1988; Kim and Fitzgerald, 1986; Kirk et al., 2008; Mason et al., 2001; Mason and Fitzgerald, 1990; Mason and Fitzgerald, 1993). It is seen that these observations have been collected during several decades and more observational data is strongly needed.

Interpreting spatial and seasonal patterns in mercury concentrations in the surface ocean is challenging without additional observational data. Modeling studies allow us to use existing information on mercury speciation and dynamics in the ocean (particulate organic carbon dynamics, solar radiation, winds, and temperature) to gain further insight into temporal and spatial patterns. In one of the few global modeling studies Strode et al. (2007) found the average concentrations in the surface ocean to be 1.50 pM for total Hg ($\text{Hg}^0 + \text{Hg}^{\text{II}} + \text{HgP}$) and 0.07 pM for Hg^0 . Knowledge of aquatic mercury processes has expanded in recent years and updated model parameterizations taking new results into account are needed to understand spatial and temporal patterns.

Trends in aquatic concentrations

Using available observational data Sunderland and Mason (2007) estimated the different concentrations in the world's ocean basins and looked at what processes could drive the difference in estimated concentrations (Figure 9). The authors found that compared to the atmosphere, where concentrations have increased by 300-500% since industrialization, on a global scale concentrations in surface and intermediate ocean waters (0-1500 m) and deep waters (1500 m - bottom) have increased by 25% and 10% respectively. Much greater enrichment is observed in specific ocean basins like the Atlantic Ocean and Mediterranean Sea where anthropogenic enrichment of intermediate waters is greater than 50% (Sunderland and Mason, 2007). The physical dynamics of different oceans govern the temporal lag in response to changing atmospheric inputs. Generally intermediate waters require on the order of decades to achieve steady state with atmospheric inputs while deep ocean waters in some basins like the Pacific requires centuries (Sunderland and Mason, 2007). Another recent box model study by Strode et al. (2010) considered vertical transport processes in greater detail but did not consider differences among ocean basins. On a global scale, Strode et al. (2010) estimated that the increase in ocean mercury since industrialization is 280 Mmol (18%) and that the top 100 meters have increased by 150%.

Sunderland and Mason (2007) showed that concentrations in the Atlantic Ocean are considerably higher than in the Pacific Ocean due to higher historic anthropogenic enrichment of the Atlantic Ocean and the smaller size of the Atlantic Ocean basin. Based on observations from a 2006 cruise in the North Pacific Ocean Sunderland et al. (2009) concluded that

the concentrations in the North Pacific Ocean are currently increasing as the result of enhanced near-field deposition from Asian sources that are transported laterally in the ocean in intermediate water masses. This is the first sign that the changed distribution of anthropogenic emissions sources has an influence on the Pacific Ocean concentrations.

2.3.4 Chemistry

Conversion between the inorganic aqueous species is suggested to be a dynamical process where both reduction and oxidation takes place. A combination of biologically mediated (Mason et al., 1995b; Rolfhus and Fitzgerald, 2004; Whalin et al., 2007) and photochemical processes (Amyot et al., 1997; Mason et al., 2001) reduce $\text{Hg}^{\text{II}}_{\text{red}}$ in the water column to Hg^0 . Abiotic (dark) reduction mediated by bacteria is slower than photoreduction. Whalin et al. (2007) found that abiotic reduction was 2-20 times slower at the surface and Qureshi et al. (2009) found that abiotic reduction had no real significance. However, as abiotic reduction is not light dependent it can be found throughout the water column and can therefore be important in some scenarios (Qureshi et al., 2010). Studies suggest that aqueous Hg^0 oxidation occurs (Mason et al., 2001) through reaction with photochemically produced OH^\bullet (Gardfeldt et al., 2001; Lalonde et al., 2004; Whalin et al., 2007).

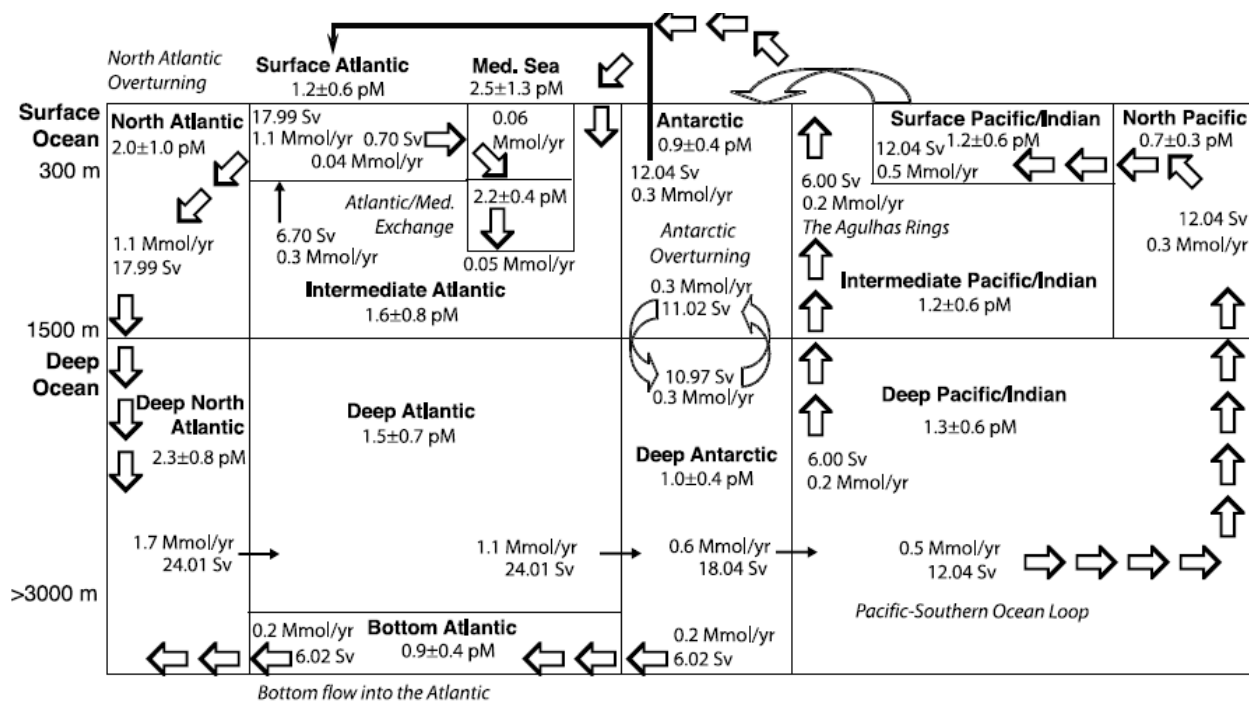


Figure 9. Overview of a 14 compartment model showing major ocean currents (block arrows) and steady state flows (smaller arrows) ($1 \text{ Sv} = 10^6 \text{ m}^3 \text{ s}^{-1}$). Also shown are average present-day mercury concentrations (mean \pm standard deviation) for each compartment and mercury fluxes from seawater flow (Mmol y^{-1}). Note that sizes of model compartments are not to scale (Illustration from Sunderland and Mason, 2007).

From experiments in saltwater Qureshi et al. (2009) recently suggested a pseudo first order rate constant for photoreduction of $\text{Hg}^{\text{II}}_{\text{red}}$ in the range of $4.0 \times 10^{-5} - 25.8 \times 10^{-5} \text{ s}^{-1}$ and a pseudo first order rate constant for photooxidation of Hg^0 in the range of $11.1 \times 10^{-5} - 52.7 \times 10^{-5} \text{ s}^{-1}$. Abiotic reduction of $\text{Hg}^{\text{II}}_{\text{red}}$ has previously been estimated to be $2.7 \times 10^{-5} - 6.7 \times 10^{-7} \text{ s}^{-1}$ (Amyot et al., 1997; Whalin et al., 2007).

Sorption of Hg^{II} to organic material, which produces Hg^{P} , is a reversible process (Guentzel et al., 1996). The partitioning has been shown to vary as a function of the particulate organic carbon content of the solids in the water (e.g. (Hammerschmidt et al., 2008; Hammerschmidt and Fitzgerald, 2006) and observed partitioning coefficients are in the range between 10^5 and 10^6 L kg^{-1} (Mason et al., 1998; Mason and Fitzgerald, 1993). Hg^{II} is released when particulate organic material is remineralized in the water column (Strode et al., 2010; Sunderland et al., 2009).

Inorganic mercury in the form of Hg^{II} is converted to organic mercury through a methylation process that is biologically mediated (e.g. Engstrom, 2007; Kerin et al., 2006). Organic mercury can subsequently demethylate to Hg^{II} in the surface ocean in the presence of sunlight (Whalin et al., 2007). However, the organic mercury processes are outside the scope of this thesis and will not be treated further.

2.3.5 Sinks

Air-sea exchange

Mercury leaves the ocean by evasion of Hg^0 when it is present at supersaturated concentration in the surface waters. As most marine surface waters are supersaturated in Hg^0 (Andersson et al., 2008c; Gardfeldt et al., 2003; Kim and Fitzgerald, 1986; Mason et al., 2001; Rolfhus and Fitzgerald, 2004; Whalin et al., 2007) this induces a global net upward flux. This is however not always the case and periodic net downward fluxes have been observed (Andersson et al., 2008c).

Mean flux rates of Hg^0 are estimated to be $2.5\text{-}400 \text{ pmol m}^{-2} \text{ h}^{-1}$ ($0.5\text{-}80 \text{ ng m}^{-2} \text{ h}^{-1}$) with a mean flux below $25 \text{ pmol m}^{-2} \text{ h}^{-1}$ ($5 \text{ ng m}^{-2} \text{ h}^{-1}$) (references in Sprovieri et al., 2010), and global yearly flux estimates based on a modeling approach suggest a net evasion from the ocean of $4\text{-}14 \text{ Mmol y}^{-1}$ (Figure 3)(Strode et al., 2007; Sunderland and Mason, 2007; Strode et al., 2007 and references therein).

Gas exchange of Hg^0 at the air-sea interface is calculated based on observations of Hg^0 in air and water as well as meteorological data. The estimated flux rates are therefore very dependent on the choice of model. For the calculation a two-layer thin film transfer model is most often used (eq. 1). This type of model suggests that the exchange is moderated by both a thin aqueous and a thin gaseous film at the air-sea interface. Based on experiments several relationships for the transfer velocity (K_w) of gasses have been suggested (e.g. Liss and Merlivat, 1986; Nightingale et al., 2000; Wanninkhof, 1992)(Figure 10). Common for all relationships is a strong dependence on wind speed. A gas transfer velocity for mercury has not been measured but Wanninkhof (1992) derived an empirical relationship relating the mass transfer coefficient of other gasses to the mass transfer of CO_2 (eq. 2). For an example for the gas transfer velocity proposed by Nightingale et al. (2000) A equal 0.25 in eq. 2. Figure 10 shows a range of proposed relationships for the gas transfer velocity and indicate how they depend on the wind speed. The parameterizations are different especially for wind speeds above 15 m s^{-1} and will therefore give highly varying predictions of the air-sea exchange.

$$Hg_{evasion}^0 = K_w \left(Hg_{aq}^0 - \frac{GEM}{H'} \right) \quad \text{Eq 1}$$

$$K_w = A \times u_{10}^2 \left(\frac{Sc_{Hg}}{Sc_{CO_2}} \right)^{-0.5} \quad \text{Eq 2}$$

H' is the dimensionless Henry's law coefficient, K_w is the gas transfer velocity, Sc_{Hg} is the Schmidt number of mercury, Sc_{CO_2} is the Schmidt number for CO_2 and u_{10} is the wind speed at 10 m height, A is a constant.

Even though a broad range of transfer velocities for poorly soluble gases are found at a given wind speed (Woolf, 2005) the solely wind dependent transfer velocity is still the most commonly used parameterization. However, a range of new parameterizations try to capture the complex structure of the transfer velocity by including the effect of breaking waves by including e.g. wave height and wave age. These parameterizations are becoming more common for other gasses (e.g. Fangohr and Woolf, 2007; Frew et al., 2007; Woolf, 2005; Zha and Xie, 2010) but have so far not been used in the calculation of air-sea exchange of mercury.

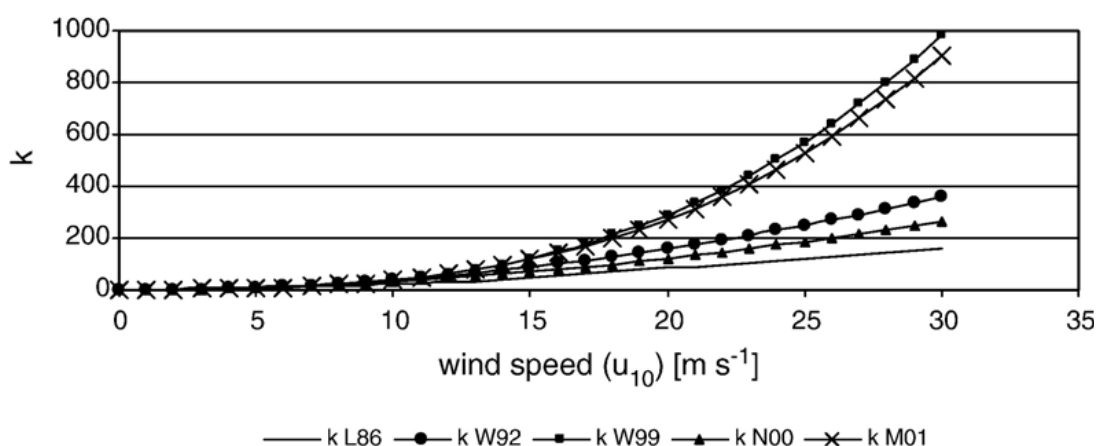


Figure 10. Comparison between different methods for calculation of the transfer velocity (k) used in flux calculations. L86 corresponds to Lis and Merlivat (1986), W92 to Wanninkhof (1992), W99 to Wanninkhof and McGillis (1999), N00 to Nightingale et al. (2000) and M01 to McGillis et al. (2001) (illustration from Andersson et al. 2007).

Sinking and sedimentation

Mercury is removed from the surface ocean by sinking adsorbed to particulate organic carbon (HgP) or by diffusion across the interface between the surface ocean mixed layer and the intermediate waters (Strode et al., 2010). HgP that has entered the subsurface ocean can be returned to the Hg^{II} pool as the organic carbon remineralizes (Sunderland et al., 2009). There is an optimum for remineralization in the subsurface ocean (500 meters depth) just below the surface ocean mixed layer (Strode et al., 2010). Some of the produced Hg^{II} can later re-enter the surface ocean through transport by ocean currents, yearly changes in the mixed layer depth and Ekman pumping. The mercury that reaches and gets buried in the sea floor of the deep ocean is thought to have entered a long term sink in the biogeochemical cycling (Horvat, 2005). The sedimentation has been estimated to be 0.9-1.3 $Mmol\ y^{-1}$ (Mason and Fitzgerald, 1996; Sunderland and Mason, 2007).

2.4 Mercury dynamics in the marine boundary layer

The MBL is the interface between the ocean and the troposphere. The sources, sinks, and chemistry of mercury in the MBL are similar to those in the rest of the troposphere. However, the relative importance of sources and sinks as well as the drivers of the chemical processes are different.

The MBL is the lowest part of the troposphere in direct contact with the ocean. The vertical mixing is strong and there are large fluctuations in temperatures, wind directions and relative humidity (RH). The height of the MBL in the mid-latitudes is typically about 300 meter but can be 50m/2000m during the right conditions in the Arctic/Tropics. Close to the coast large variations in the MBL height can be expected due to the rapid heating and cooling of the nearby land (Hedgecock et al., 2005). This leads to sea-land breeze circulation in coastal areas (Malcolm et al., 2003). The MBL differs from the terrestrial boundary layer in terms of meteorology and chemical composition of the air, e.g. wind patterns (Engle et al., 2008; Malcolm et al., 2003), RH (Sigler et al., 2009), sea salt aerosol concentration (Gustafsson and Franzen, 2000) and GEM oxidation potential (Sigler et al., 2009).

GEM oxidation by Br in the MBL indicates that the lifetime in the MBL is shorter (10-100 days) (Donohoue et al., 2006; Hedgecock et al., 2005; Hedgecock and Pirrone, 2004; Holmes et al., 2009) than the ½-1 year proposed for the general troposphere.

2.4.1 Sources

Plumes created by anthropogenic sources and biomass burning

One third of emitted mercury today is estimated to be primary anthropogenic emissions (Pirrone et al., 2010). This results in emission hotspots in urban and industrial areas many of which are located close to the coast where a large part of the world's population lives (Figure 4). Plumes from these areas as well as from biomass burning can extend into the MBL. The further inland the emission sources are located, the more RGM and TPM will have deposited before the plume reaches the MBL. However, high concentrations of RGM and TPM could be present in plumes in the MBL especially if these have an anthropogenic origin (see "Sources" (2.2.2) for the fractionation in emissions). Several cruises have recorded plumes in the MBL (e.g. Fu et al., 2010; Temme et al., 2003b; Xia et al., 2010). These show that GEM concentrations are enhanced (only in some cases significantly). Unfortunately RGM and TPM have not been measured during these episodes and there is still a limited knowledge on the influence from inland sources on the MBL.

Entrainment from the free troposphere

High concentrations of RGM and TPM have been found in the free troposphere (Fain et al., 2009; Sillman et al., 2007; Swartzendruber et al., 2006). If these air masses intrude and mix into the MBL they are a source of RGM (Holmes et al., 2009). Holmes et al. (2009) used a box model to investigate RGM in the MBL and found that 25-40% of RGM entered through entrainment from the free troposphere. As a net flux this however only accounted for about half as much, as MBL RGM is also ventilated back into the free troposphere (Holmes et al., 2009). They also pro-

posed that most of the GEM oxidized in the MBL originated in the global tropospheric mercury pool and not in ocean evasions. This is not consistent with the model results of Mason and Sheu (2002) (see below).

Ocean evasion of GEM

As described earlier the ocean is a strong source of GEM to the troposphere. Model results show that 62 % of the load deposited to the ocean surface from the entire column of the troposphere is expected to re-enter the MBL via evasion (Strode et al., 2007). The flux from the ocean to the MBL varies both spatially and temporally and the global evasion pattern does not necessarily follow the global deposition pattern (Strode et al., 2007) due to redistribution of mercury in the ocean. Eventually GEM emitted from the ocean is mixed into the tropospheric pool but it is reasonable to assume that the influence of the ocean is stronger and more immediate in the MBL especially during stable meteorological conditions. To explain high evasion rates from the ocean observed during campaigns Mason and Sheu (2002) developed a hypothesis of a fast recycling at the air-sea interface, which they tested in a box model. In order to explain the high evasion rates they suggested that more than 40% of the evaded GEM was oxidized in the MBL and redeposited to the ocean before eventually being ventilated into the free troposphere

2.4.2 Levels

Despite the many cruises that have measured GEM in the MBL (Table 2) we have an incomplete picture of temporal and spatial variability. Furthermore global models have been unable to simulate the full range of observations (Selin et al., 2007).

A gradient in GEM concentrations between NH and SH is a recurrent pattern in cruise observations (e.g. Slemr, 1996; Slemr et al., 2011). The presence of a gradient corresponds with the hemispheric gradient at sea level proposed by Lindberg et al. (2007) of a GEM concentration of 1.5-1.7 ng m⁻³ for the NH and 1.1-1.3 ng m⁻³ for the SH. It is generally agreed (Sprovieri et al. (2010), Table 2, Figure 21) that SH MBL GEM observations are fluctuating less than NH observations. Repeated observations of GEM in the NH have shown higher concentrations in the MBL than nearby rural land based observations (Table 2 show that mean cruise observations are often above 2 ng m⁻³ for the NH). Intercomparison of land based sites shows higher concentrations at Mace Head (west coast of Ireland) than at rural European sites further from the Atlantic Ocean during the period 1998 to 2004 (Kock et al., 2005; Munthe et al., 2003). Global models have not been able to account for the high MBL concentrations in the Atlantic and Pacific Ocean (Dastoor and Larocque, 2004; Holmes et al., 2010; Seigneur and Lohman, 2008; Selin et al., 2007). It has been proposed that there is a source in the MBL that is unaccounted for, and which could be the ocean (Gardfeldt et al., 2003; Kock et al., 2005; Pirrone et al., 2003).

GEM has been observed to show diurnal variation during parts of some cruise campaigns (Laurier et al., 2003; Sommar et al., 2010; Witt et al., 2010; Xia et al., 2010) but for most cruises this has not been reported. In a box model study Holmes et al. (2009) showed that the levels of RGM observed during cruises can for the most part be explained by oxidation of such a small part of the GEM pool that it would not create visible diurnal GEM variations. Another possibility is diurnal variations in ocean eva-

sion if evasion is present (Gardfeldt et al., 2001) could influence the GEM concentration on a diurnal basis.

RGM has only been measured on a couple of recent cruise campaigns in the open ocean (Aspmo et al., 2006; Laurier and Mason, 2007; Laurier et al., 2003; Temme et al., 2003a) as well as the Mediterranean Sea (Sprovieri et al., 2003). During these campaigns mean RGM concentrations were between 2.4-10 pg m⁻³. Although these limited measurements are not sufficient to establish a general consensus on worldwide MBL concentrations under changing meteorological conditions, a recurrent pattern showing diurnal variations with midday peaks and nightly minimums has been reported for most of the campaigns (Laurier and Mason, 2007; Laurier et al., 2003; Sprovieri et al., 2003).

Table 2. Cruise observations of TGM (i.e. GEM) from open oceans (not including the Mediterranean Sea).

Place	Date	TGM (ng m ⁻³)	Reference
Southern Hemisphere			
South Atlantic Ocean	Oct 77	1.19±0.25	Slemr et al. 1996
South Atlantic Ocean	Nov-Dec 78	1.35±0.21	Slemr et al. 1996
South Atlantic Ocean	Jan-Feb 79	1.26±0.22	Slemr et al. 1996
South Atlantic Ocean	Oct-Nov 80	1.45±0.16	Slemr et al. 1996
South Atlantic Ocean	Oct-Nov 90	1.50±0.30	Slemr et al. 1996
South Atlantic Ocean	Oct-Nov 94	1.18±0.17	Slemr et al. 1996
South Atlantic Ocean	Oct-Nov 96	1.39±0.13	Temme et al. 2003b
South Atlantic Ocean	Dec 99-Jan 00	1.27±0.09	Temme et al. 2003b
South Atlantic Ocean	Feb-Mar 00	1.00±0.12	Temme et al. 2003b
South Atlantic Ocean	Feb 01	1.07±0.10	Temme et al. 2003b
Antarctic – South America	Dec 01 – Feb 02	1.1±0.2	Temme et al 2003a
Indian Ocean	Nov 07	1.2 (1.05-1.51)	Witt et al. 2010
East Indian and Southern Ocean	Dec 07	1.47±0.84	Xia et al. 2010
Atlantic Ocean	2008	~0.76 ^B	Slemr et al. 2011
Atlantic Ocean	2009	~0.74 ^B	Slemr et al. 2011
Northern Hemisphere			
Eastern Atlantic Ocean	Oct 77	1.76±0.36	Slemr et al. 1996
Eastern Atlantic Ocean	Nov-Dec 78	1.85±0.31	Slemr et al. 1996
Eastern Atlantic Ocean	Jan-Feb 79	2.17±0.38	Slemr et al. 1996
Eastern Atlantic Ocean	Oct-Nov 80	2.09±0.35	Slemr et al. 1996
Eastern Atlantic Ocean	Oct-Nov 90	2.25±0.41	Slemr et al. 1996
North Atlantic Ocean	Aug 93	2.1±0.8	Mason et al. 1998
Atlantic Ocean	Oct-Nov 94	1.79±0.4	Temme et al. 2003b
Eastern Atlantic Ocean	Oct-Nov 96	2.12±1.0	Temme et al. 2003b
Western Atlantic Ocean	Sep 99	2.00±0.4	Mason et al. 2001
Eastern Atlantic Ocean	Dec 99-Jan 00	2.02±0.3	Temme et al. 2003b
Western Atlantic Ocean	Aug-Sep 03	1.63±0.08	Laurier and Mason 2007
North Atlantic Ocean	July 05	~1.7 ^A	Sommar et al. 2010
North Pacific Ocean	May 02	2.5	Laurier et al. 2003
South Chinese Sea	August 07	2.62	Fu et al. 2010
Yellow Sea and West Pacific Ocean	Nov 07	1.75±0.50	Xia et al. 2010
Atlantic Ocean	2008	~1.15 ^B	Slemr et al. 2011
Atlantic Ocean	2009	~1.12 ^B	Slemr et al. 2011

A) Arctic data not included, B) approximate concentrations taken from figure 2 in Slemr et al. (2011)

2.4.3 Chemistry

Some of the most important parameters thought to control the oxidation of GEM and the removal of RGM from the gaseous phase are described here. Many of these parameters are linked and will influence each other, which should be kept in mind when reading the section.

Wind speed

Several cruises report that the highest RGM concentrations are found at lowest wind speeds (Laurier and Mason, 2007; Laurier et al., 2003). Looking at an ensemble of RGM measurements from four different datasets (cruise and coastal data) Holmes et al. (2009) furthermore found that particular nighttime RGM observations tended to decrease as wind speed increased. They suggested that this is due to a fast deposition sink rather than chemical loss of RGM. RGM dry deposition and uptake in sea-salt aerosols has been suggested to increase with increasing wind speeds (Holmes et al., 2009; Laurier et al., 2003).

The wind speed also influences the amount of sea salt aerosols emitted from the ocean surface (Monahan et al., 1986), which could have the opposite (a positive) effect on daytime RGM concentrations (see “Br production” later).

Relative humidity

At high RH RGM is more likely to absorb into sea salt aerosols or aerosols with other origin present in the air. Mason and Sheu (2002) found that lowest nighttime RGM concentrations were associated with high RH and low daytime RGM concentrations were associated with fog. During a cruise in the Arctic, Aspino et al. (2006) observed low RGM concentrations and no recurrent diurnal variations and attributed this to high RH and fog patches as well as low insolation during the cruise.

Absorption into wet aerosols does not necessarily mean that RGM will be lost by wet deposition. Mason and Sheu (2002) found that highest RGM was observed on days with high insolation after nights with high RH. Thus volatilization of RGM_w from the water phase as RH decrease could also influence the daytime RGM concentration in the MBL.

On the other hand high, RH could also cause an increase in the release of bromine from sea salt aerosols. High RH has through calculations been shown to decrease sea salt aerosol pH (von Glasow and Sander, 2001) increasing acid catalyzed displacement of bromine. Increased release of bromine could lead to higher oxidation than at lower RH. Further it has been proposed that low RH increases aqueous uptake of RGM (in the form of HgCl₄²⁻), due to increased Cl⁻ concentration in the sea salt aerosols (Holmes et al., 2010). In this case RGM concentrations should be higher at high RH. To support this hypothesis Laurier et al. (2003) observed low RGM during low RH (66%) despite high insolation, and high RGM when RH was high (80%) and insolation was high. A clear picture of how RH influences GEM and RGM concentrations is still lacking.

Br production

In the MBL the bromine released from sea salt aerosols constitutes 70-90% of Br in the air (Yang et al., 2005). Br is found in trace amounts in sea water. Br is volatilized from the aqueous phase as Br₂ or BrCl when breaking waves create sea salt aerosols (see R1-R4). These aerosols are

suspended in the air for a period before most deposits back to the sea surface. Br⁻ deficits in sea salt aerosols compared to sea water have been observed to be large, averaging 30% to 50% on an annual basis, but with strong seasonality ranging from about 10% in some winter samples to 80% in some summer samples (Ayers et al., 1999). Acidity can enhance volatilization of halogenated compounds from sea-spray and aerosols, giving the MBL a higher reactivity (Sander et al., 2003; Vogt et al., 1996) (R1-R4). The Br⁻ deficits can be linked to acidity in the aerosol, which suggest the importance of acid catalysis to the dehalogenation process (Ayers et al., 1999).



Insolation

As described above Br₂ and BrCl are released from sea salt aerosols in the MBL. During the night when no sunlight is present these species will build up in the MBL. Sunlight will rapidly photolyse them to create atomic bromine (Hedgecock et al., 2005). A photochemically induced oxidation and a rapid deposition of RGM will result in diurnal variation of RGM. In agreement with this, maximum diurnal RGM concentrations have been found in the MBL during maximum insolation (Laurier and Mason, 2007; Laurier et al., 2003; Mason and Sheu, 2002). By inducing the creation of atomic bromine from Br₂ and BrCl, insolation controls an important part of the diurnal variability of RGM in the MBL.

Another possible influence of insolation is on the RH. The RH decreases during the day as the air is heated. This can lead to a shift in the equilibrium of RGM between air and the aqueous phase resulting in release of RGM into the gaseous phase.

Temperature

Due to the dependency of the bromine oxidation on temperature (Goodsite et al., 2004 and Figure 8), Lindberg et al. (2007) speculate that a more rapid oxidation of GEM could take place at higher (colder) latitudes in the MBL than at lower (warmer) latitudes. A trend that indicates this is a controlling factor of RGM concentrations in the MBL has as far as I know not been shown for the MBL.

2.4.4 Sinks

Wet and dry deposition

The removal rate of RGM is rapid enough that RGM concentrations decrease or even deplete during the night (Holmes et al., 2009) when RGM production does not take place. Removal takes place both by uptake of RGM into sea salt aerosols and other wet aerosols followed by wet deposition, and by dry deposition (Figure 11). Deposition of RGM_w with sea salt aerosols is through modeling estimated to be the most important sink of RGM in the MBL (Holmes et al., 2009). Mason and Sheu (2002) es-

estimated dry deposition to account for around 35% of depositions using a box model while the estimate of Holmes et al. (2009) is smaller (10-20%).

Diffusion flux across the air-sea interface

The direction of the net GEM diffusion flux across the air-sea interface is driven by the supersaturation of Hg^0 in the water and the concentration gradient between GEM in the air and Hg^0 in the water. The net flux could thus periodically be negative as found by Andersson et al. (2008). The extent of periods with a net downward flux of Hg^0 in the MBL is not well investigated.

Ventilation

Based on box-model studies Mason and Sheu (2002) suggested that 60% of the GEM flux out of the MBL would be through ventilation to the free troposphere and Holmes et al. (2009) suggested that 10-20% of the RGM flux out of the MBL would be through ventilation to the free troposphere.

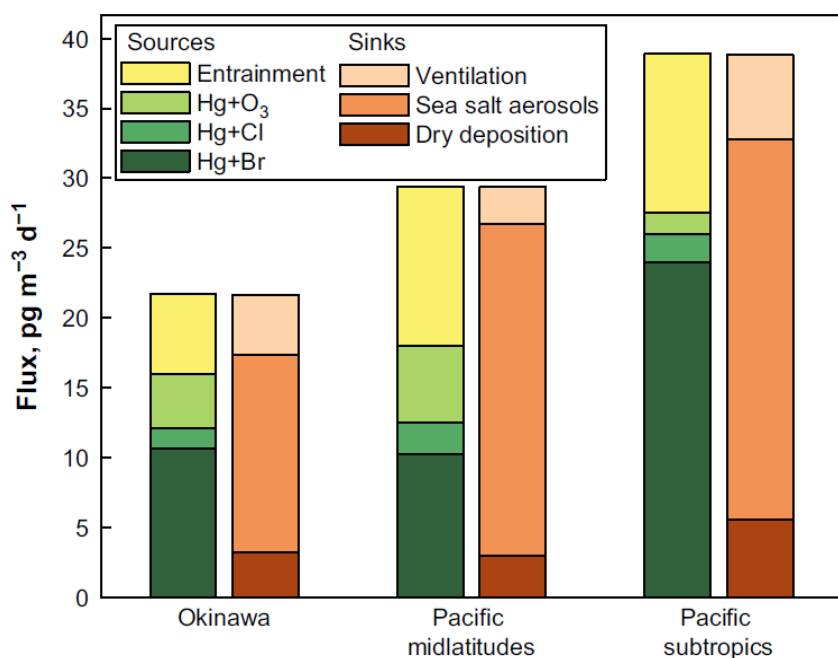


Figure 11. Model budgets of RGM sources and sinks in the marine boundary layer. Values are 24 h averages at steady state (illustration from Holmes et al., 2009).

3 Methods

3.1 Experimental work

Most mercury measurements take place at sites in the terrestrial boundary layer. These measurements sites are immobile and generate knowledge about diurnal variation, seasonal variations and long term trends in a single location. This is a relatively inexpensive type of measurements and therefore often used. But the spatial resolution is poor in a global perspective even if measurements from many sites are available.

Measurements collected on cruise and aircraft campaigns do not generate an impression of long term temporal changes but instead give insight into the spatial resolution of the measured species. These measurements mainly reveal concentrations gradients across distances for example between hemispheres or of the vertical profiles of the atmosphere.

To obtain a better understanding of the exchange of mercury between the atmosphere and the ocean, measurements in the MBL are necessary. At the moment there are no stationary sites where measurements are conducted on the ocean and coastal sites like Mace Head, Ireland (Ebinghaus et al., 2002), Cheeka Peak, Washington state, USA (Weiss-Penzias et al., 2003), and Cape Point, South Africa (Brunke et al., 2010) are therefore used to represent MBL conditions. As a supplement to these coastal sites and to generate a more detailed picture of mercury in the MBL cruise campaigns are vital. Cruise observations will be from different areas and source regions and thus giving a spatial understanding, which coastal sites cannot provide.

3.1.1 Choice of Instruments

The choice of the Tekran instruments was influenced by the type of campaign. For a cruise campaigns a manual system able to perform continuous measurements is ideal. The Tekran 2537A is one of two systems that measure GEM continuously and have a detection limit low enough ($\leq 0.1 \text{ ng m}^{-3}$) to collect measurements in the MBL (Gustin and Jaffe, 2010). The other system is the Gardis (Urba et al., 1995). The Tekran has been used widely since it came on the market more than 10 years ago and it is a common choice of instrument. An inter-comparison study including four manual and two types of automated analysis for GEM showed that automated and manual methods compared well (Ebinghaus et al., 1999) and a study including six groups that measured GEM with Tekran 2537A's showed that the precision between each group was consistently good (within 5%)(Aspmo et al., 2005). The Tekran 2537A has furthermore been used on a number of cruise campaigns (e.g. Aspmo et al., 2006; Fu et al., 2010; Laurier et al., 2003; Sommar et al., 2010; Temme et al., 2003b; Temme et al., 2003a; Xia et al., 2010) and has proven to be able to withstand the exposure to sea spray, temperature changes and movements due to waves.

RGM is a method defined parameter and thus the method has to be considered as a reference method, where the reproducibility of the method gives the best estimate of the uncertainty. Although several manual methods exist for measuring RGM only a Tekran 2537A equipped with a Tekran 1130 sampling unit allows for continuous measurements. In an inter-calibration exercise carried out at Svalbard, Norway, in 2003 (Aspmo et al., 2005) the uncertainty of RGM measurements was found to be very large. Participating laboratories used a Tekran 2537A equipped with a Tekran 1130 sampling unit; agreement was at best to within an order of magnitude. Parallel measurement of RGM were also carried out at Barrow, Alaska, where one group used a Tekran 2537A equipped with a Tekran 1130/5 sampling unit and the other only a Tekran 2537A equipped with 1130 (Henrik Skov, unpublished results). Because of the use of sampling cycles of different duration, a direct comparison of measurements was not possible but 3 day averages showed very good agreement 1.7 % (one std. dev.). In Skov et al. (2006) a Tekran 2537A equipped with a Tekran 1130 sampling unit was compared to one with manual denuders (Landis et al., 2002). Manual and automated methods were found to agree to within 25% (95% confidence interval). Due to the uncertainty of the method, which does not seem to be consistent for different comparison studies, the RGM results needs to be treated with care in the analyses.

The Tekran is the only choice for cruise campaigns if GEM and RGM are to be measured continuously.

3.2 Galathea 3 cruise

3.2.1 Gaseous mercury measurements

GEM and RGM measurements were conducted onboard the ship *Vædderen*, during the cruise campaign *Galathea 3*, from August 2006 to April 2007. The campaign was a circumnavigation resulting in mercury observations from 114 days. The route can be seen in Figure 40. A more thorough description of the *Galathea 3* expedition can be found in "Appendix C Background information on the *Galathea 3* expedition" and in the book "Galathea 3" (Joergensen, 2008)(in Danish).

GEM and RGM were measured with a Tekran 2537A mercury vapor analyzer equipped with a Tekran 1130 automated denuder unit and pump module. The Tekran was mounted on the starboard side of the ship 6 meters above sea level next to the smokestack (Figure 12). Measurements were collected by Britt Tang Sørensen, Henrik Skov, Henrik Madsen, Bjarne Jensen, and Christel Christoffersen.

On Figure 13 flow diagrams of the Tekran 2537A and the 1130 speciation subunit are shown. The Tekran 2537A monitor sucks air samples through a gold trap, which retains the mercury by forming an amalgam. Two gold traps are placed in parallel and when the first trap has completed its sampling, the second trap starts sampling, while the first trap is desorbed thermally at 500°C in a flow of argon. In this way GEM is measured continuously. The quantity of sampled mercury is detected by cold vapor atomic fluorescence spectrometry (CVAFS). The sample flow rate is controlled and adjusted by a mass flow controller. The 1130 speci-

ation module is integrated into the Tekran 2537A so that continuous measurements of both GEM and RGM are possible.



Figure 12. The location of the inlet for the Tekran (red circle) onboard the ship and the inside of the thermostated container where the instruments were located.

The Tekran system was programmed so that GEM was measured at 5 min intervals for a period of 80 min. During this period RGM was sampled on an annular quartz denuder (Figure 13 B first state). An 80 min collection time is needed since RGM is present at much lower concentrations than GEM. After the 80 min a 40 min period followed in which RGM sampled on the denuder was determined by thermal desorption and analyzed with the Tekran 2537A (Figure 13 B second state).

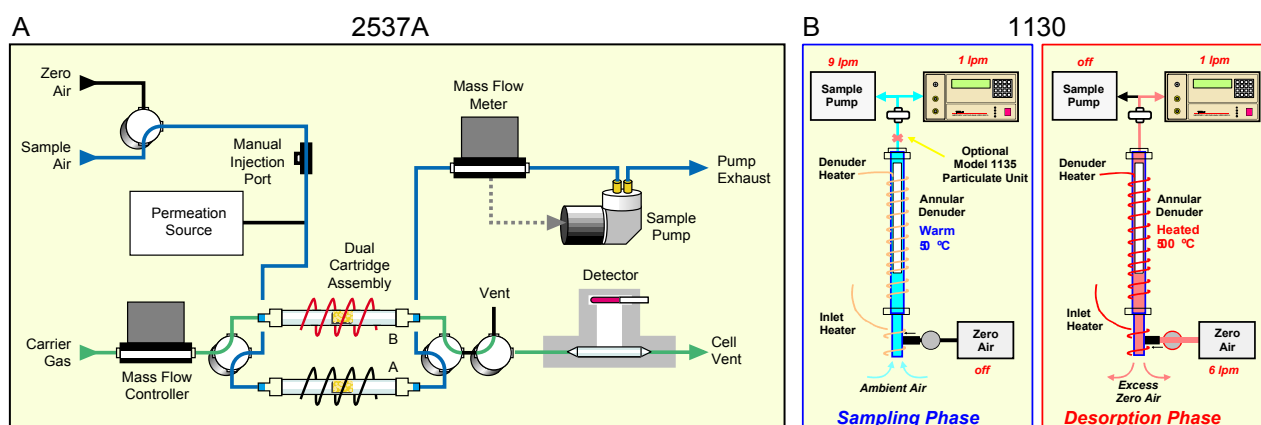


Figure 13. A setup of A) the Tekran 2537A and B) the Tekran 1130 system (illustrations taken from the Tekran homepage: www.tekran.com [accessed January 2011]).

The detection limit of GEM was 0.1 ng m^{-3} (Skov et al., 2004). The method's detection limit for RGM was calculated as $3 \times \text{std. dev.}$ on blank values obtained during the analysis of the annular quartz denuder and was better than 2 pg m^{-3} . The response of the detector was checked every 25 h by adding clean air and air with a known amount of GEM from an internally thermostatted permeation tube. The stability of the instrument was checked by parallel measurements with two Tekran 2537A instruments. Before and after the cruise the permeation rate was determined using manual injections of known quantities of mercury, and it was found to be constant within the uncertainty of the instrument. The reproducibility of GEM measurements is 20% at a 95% confidence interval above 0.5 ng m^{-3} . For RGM there is not sufficient data from the literature or from experiments at NERI (Aarhus University) to calculate the reproducibility of the measurements. Moreover the collected RGM pool

is probably made up of different gaseous Hg^{II} species in different air masses as the ship moves in time and space. Therefore 10% was added to an uncertainty to make a conservative estimate. The expanded reproducibility of RGM is thus 28%, using a factor of 2 to get a 95% confidence interval.

During the cruise, problems with the Tekran were encountered several times due to the exposure to conditions much harder than normally experienced at landbased site. One example is the extensive sea salt concentrations in the air. There are therefore periods during the cruise without measurements. Along the coast of Africa the addition from the permeation source was missing for 22 days. Fortunately the detector signal only drifted a few percent during this time and a linear interpolation spanning the period was applied. The resulting contribution to the uncertainty is therefore minimal.

3.2.2 Ancillary measurements

To help with the interpretation of the Hg data NO, NO_x, CO and O₃ were also measured during the cruise. NO_x (NO and NO₂) is a tracer for the influence of smoke from the smokestack on the ship and CO is a tracer for combustion of fossil fuels or biomass burning. Unfortunately these data were not always available, and CO and O₃ measurements were therefore not included in Soerensen et al. (2010a). For a thorough description of the methods and uncertainties used for collection of these data see Soerensen et al. (2010a; 2010b).

Black carbon (BC) was used in only one case (see Soerensen et al., 2010a) as the entire dataset has not been quality controlled. BC data for the cruise track along the African coast was made available by Matthias Ketzel (NERI, Aarhus University). A description on the collection method can be found in Soerensen et al. (2010a).

The meteorological data from the *Galathea 3* cruise is public available from <http://galathea.oersted.dtu.dk/GE.html>. The data was not quality controlled before it was made available online and quality control was made as part of this work to ensure confidence in the data.

3.2.3 Data analysis and other data sources

Data from the cruise were broken into 12 legs based on ocean basin and origin of air mass (Table 3) in order to analyze the data in smaller sections.

RGM was measured with a temporal resolution of 2 h. In order to have a uniform temporal resolution of the dataset all other parameters were averaged to 2 h. Figures and statistical tests are made with the 2 h resolution, except when GEM is treated by itself, in which case the resolution is 5 min. If the resolution deviates from 2 h this is stated explicitly.

T-tests were used to determine if concentrations during different parts of the cruise had significantly different GEM concentrations. T-tests were also used to determine if concentrations in harbor were significantly different compared to the MBL for GEM concentrations or DL and 2×DL for RGM. To investigate the presence of diurnal variations in RGM during

the 12 legs RGM was divided into daytime (6-18) and nighttime (18-6, local time) values and a t-test was used on the data. In the t-tests the null hypotheses is that the mean of the two samples are the same. Spearman's rank correlation and Pearson's rank correlation was used in different cases to determine if correlation were present in periods of the data.

GEM/CO and RGM/CO relationships were used to give an estimate of yearly GEM and RGM emissions in the areas of origin of anthropogenic pollution plumes that were intercepted at the ship. To do this a correlation between CO and the gaseous mercury species were needed. The emission estimates were computed by use of the EDGAR 2000 CO emission estimates (GEIA/ACCENT 2000 emissions, see <http://accent.aero.jussieu.fr/EDGAR32.php>, [accessed December 2010]) combined with the ratio of mercury and CO in the plumes (see Soerensen et al., 2010b). GEM/CO ratios have previously been used to estimate mercury emissions for large areas like Europe, North America and Asia (Jaffe et al., 2005;Radke et al., 2007;Slemr et al., 2006) but also for smaller areas and single cities (Talbot et al., 2008) like it is done with the *Galathea 3* data. GEM/CO ratios with values of 0.0005-0.002 ng m⁻³ ppb⁻¹ have been observed for biomass burning (*references in* Friedli et al., 2009) while the ratios for anthropogenic sources are most often higher and ratios with values of 0.0013-0.006 ng m⁻³ ppb⁻¹ have been observed (Friedli et al., 2004;Jaffe et al., 2005;Mao et al., 2008;Obrist et al., 2008;Radke et al., 2007;Slemr et al., 2006;Weiss-Penzias et al., 2006;Weiss-Penzias et al., 2007).

Table 3. Legs, latitudes and dates for the *Galathea 3* cruise.

Leg	Abbreviations used in the text	Dates	Latitudes of the given leg (°)	Origin ^A
Global		16 th Aug – 24 th Apr	-65 : 67	
NH summer		16 th Aug – 1 st Sep	58 : 67	
NH spring		30 th Mar – 24 th Apr	23 : 59	
SH		8 th Oct – 8 th Feb	-65 : -3	
North Atlantic	NA	16 th Aug – 1 st Sep	58 : 67	Ocean
Atlantic Ocean	AT	15 th Apr – 24 th Apr	43 : 59	Ocean
Sargasso Sea	SS	30 th Mar – 11 th Apr	23 : 45	Mixed
South African coast	SA	8 th Oct – 21 st Oct	-39 : -3	Mixed
Indian Ocean	IO	22 nd Oct – 29 th Oct	-39 : -33	Ocean
West Australia	WA	3 rd Nov – 6 th Nov	-22 : -17	Ocean
East Australian coast	EA	23 rd Nov – 15 th Dec	-44 : -26	Mixed
Coral Sea	CS	16 th Dec – 3 rd Jan	-27 : -7	Mixed
New Zealand	NZ	3 rd Jan – 14 th Jan	-56 : -26	Mixed
Antarctic Ocean	AO	14 th Jan – 24 th Jan	-65 : -55	Ocean
Antarctic Coast	AC	25 th Jan – 28 th Jan	-65 : -63	Mixed
Coast of Chile	CC	31 st Jan – 8 th Feb	-58 : -33	Mixed

^A Ocean = no important influence from terrestrial sources, Mixed = influence from terrestrial sources during the entire or smaller but significant portions of the leg.

For the quality control and data analysis several databases and information found on relevant web-pages as well as unpublished data were used:

- Hysplit back trajectory model (from now on referred to as HYSPLIT) (<http://ready.arl.noaa.gov/HYSPLIT.php> [accessed January 2011])
- FIRMS Web Fire Mapper (from now on referred to as FIRMS data) (<http://maps.geog.umd.edu/firms/> [accessed January 2011])

- MOPITT CO data (Emmons et al. 2009), Ice Charts (from now on referred to as NATICE) (www.natice.noaa.gov [accessed December 2009])
- Global Volcanism Program (www.volcano.si.edu/ [accessed April 2010])
- Australian Mercury Programme: NSW government, department of Environment, Climate Change and Water (www.environment.nsw.gov.au [accessed July 2010])
- AMAP Hg 2000 emission inventory (www.amap.no/Resources/HgEmissions/ [accessed 3 December 2010])
- GEIA/ACCENT 2000 CO emissions inventory (<http://accent.aero.jussieu.fr/EDGAR32.php> [accessed December 2010])
- Sciamachy satellite data, Instit. of Environmental Physics, University of Bremen (http://www.iup.uni-bremen.de/doas/scia_data_browser.htm [accessed February 2011])
- Mace Head data (Hans H. Kock, GKSS, 2010: personal communication)
- GEM data from the Nuuk research station (Henrik Skov, Aarhus University, 2010: personal communication)

3.2.4 Hg observations that would have improved the interpretation

The interpretation of the cruise data would have benefited substantially if measurements had included TPM and aqueous Hg^0 . It was planned to measure TPM with a Tekran 1135 subunit but for technical reasons this instrument was not included in the campaign. DGM (i.e. Hg^0) can be measured at high resolution by a method presented in Andersson et al. (2008a). Combining this method with GEM measurements in the air makes it possible to estimate fluxes across the air-sea interface. The system is described in “West Atlantic Ocean cruises” (3.3). Hg^0 concentrations in the ocean were not collected due to a lack of instrumentation.

3.3 West Atlantic Ocean cruises

High resolution data of DGM and TGM were measured in August 2008 on the New England shelf and in September 2008, June 2009 and September 2009 on cruises near Bermuda. The experimental work was performed by Maria Andersson, Robert P Mason, and others at the University of Connecticut. The method for collection of the data is described in Mason et al., 2009 (see “Appendix E Poster (Mason et al., 2009)”) and shortly summarized below:

TGM (treated as GEM in this data analyses) was measured using a Tekran 2537A mercury analyzer (resolution 5 min) (as described above for the *Galathea 3* measurements). The DGM (i.e. Hg^0) was determined with a purging system, where the equilibrium distribution between air and water for Hg^0 was used to calculate the Hg^0 concentration in the incoming surface waters (resolution 5 min)(Figure 14). Seawater was constantly pumped through the jacketed Plexiglas cylinder. The opposite flow principle was used in order to achieve higher contact time. The Hg^0 in the water phase achieves equilibrium with the gas phase passing through the cylinder and by calculation the DGM concentration can be deter-

mined from the gas phase concentration. Using this method the DGM concentration was measured with high resolution (5 min) using a Tekran 2537A. Another Tekran 2537A was used to quantify the atmospheric Hg^0 .

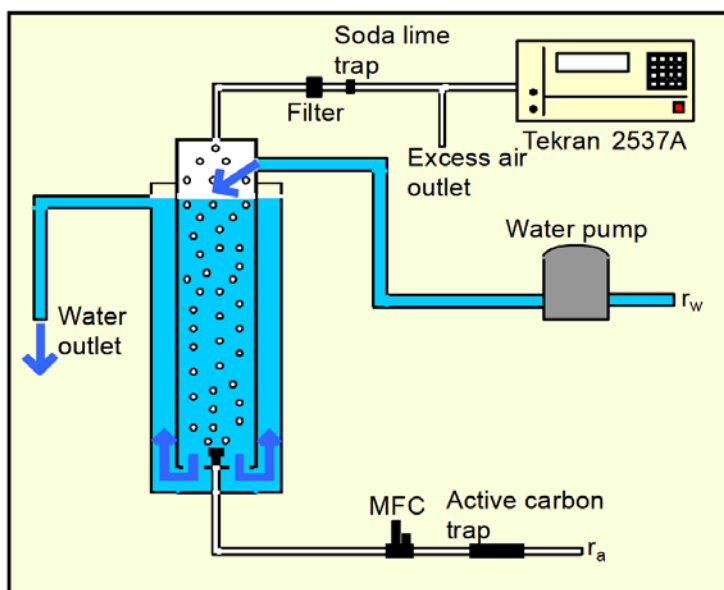


Figure 14. Purging system used in combination with a Tekran 2537A to measure DGM in the surface water (from Andersson et al., 2008a).

To calculate the mercury flux the two layer thin film model with the Nightingale et al. (2000) transfer velocity parameterization for instantaneous winds were used.

The data presented in the section on “Ocean evasion” is preliminary results from work in preparation with these data and only mean values for the West Atlantic cruises are discussed.

3.4 Modeling

The application of models is necessary to understand the dynamics of something as complex as the biogeochemical cycling of mercury. Models are mathematical realizations of the physical system under study based on current knowledge. Models employ assumptions and simplifications to fill the knowledge gaps and achieve efficiency in performing simulations.

Models serve different purposes and aim at exploring different subsets of the world. Models can reveal system properties, the weakness in our knowledge and where to focus our efforts in data collection. Models are furthermore very useful in testing scientific hypothesis. Depending on what the goal is with the model a certain complexity that can fulfill this goal has to be chosen. A complex model contains more parameters and increases the level of uncertainty because each parameter has to be estimated and thus is connected with an uncertainty (Joergensen and Bendricchio, 2001). A complex model is also more computational heavy, which is a consideration in 3-D atmospheric modeling. In the cases where our knowledge is limited or the underlying scenario does not warrant a complex model the aim should be to simplify the parameterizations in the model as much as possible.

3.4.1 Choice of model

The criterion for the initial choice of model was a global 3-D atmospheric mercury model that covered the period of the *Galathea 3* cruise. Although there were several global 3-D atmospheric mercury models to choose between (Skov et al., 2008 Appendix B), the GEOS-Chem model was the only model that included a slab-surface ocean representation of the mixed layer (Strode et al., 2007), which is essential when working with measurements in the MBL. Other models operate with the ocean surface as a boundary condition or with simple reevaporation parameterizations (Dastoor et al., 2008, Jesper H. Christensen (personal communication, NERI)). None of the possible models included a bromine scheme at the planning state of my PhD (summer 2007) although a few were about to publish bromine versions (Dastoor et al., 2008; Seigneur and Lohman, 2008). Work to include a bromine scheme in the GEOS-Chem model was under preparation (published in Holmes et al., 2010). The GEOS-Chem model also has an extensive user community and with continuous updates it is a state of the art model among the global 3-D chemical transport models. The GEOS-Chem model was chosen for the data interpretation.

3.5 The GEOS-Chem model

The GEOS-Chem 3-D global atmospheric chemistry transport model (Bey et al., 2001) uses assimilated meteorological observations from the Goddard Earth Observing System (GEOS) of the NASA Global Modeling and Data Assimilation Office (GMAO). It provides a mechanistic representation of the global biogeochemical cycling of mercury including dynamic coupling of the atmosphere to the surface reservoirs (Selin et al., 2007; Strode et al., 2007). For all the simulations in this project GEOS-5 meteorological fields were used. The model has a horizontal resolution of $4^{\circ} \times 5^{\circ}$ (45×72 grids) with the possibility to run with $2.5^{\circ} \times 2.5^{\circ}$, and 48 or 72 vertical layers. The time step is 30 or 60 minutes.

An emission inventory for anthropogenic mercury emissions based on the AMAP inventory for the year 2000 (Pacyna et al., 2006b) but adjusted for the year 2006 based on projections by Streets et al. (2009) is used (Table 4). To simulate the effect of biomass burning GFED2 CO emissions are used. They are converted to GEM emissions by the use of an Hg/CO factor of 1.05×10^{-7} molHg molCO⁻¹ (see Soerensen et al., 2010b for an explanation of the Hg/CO factor). Mean monthly emission estimates are used for biomass burning.

The model has a large atmospheric chemistry scheme, but the mercury model is run with a reduced scheme including only mercury species (GEM, RGM and TPM) (Selin et al., 2007). For a good overview of possible chemistry schemes see the GEOS-Chem wiki (<http://wiki.seas.harvard.edu/geos-chem/>). The mercury simulation has an associated slab-ocean model representing Hg⁰, Hg^{II} and HgP in the surface ocean (Strode et al., 2007) and in the new GEOS-Chem version v8-03-02 there is also a representation of terrestrial exchange with the atmosphere (Table 4). The slab-ocean model of the mixed layer was introduced by Strode et al. (2007). The slab-ocean model has the same horizontal resolution as the atmospheric model and a vertical depth that varies depending on the monthly mixed layer depth (MLD) of the ocean

(Kara et al., 2003; Montegut et al., 2004). The model recently went from using O₃ and OH as GEM oxidants (Selin et al., 2007) to using Br as the GEM oxidant (Holmes et al., 2010).

3.5.1 Work with the GEOS-Chem model

Simulations with the GEOS-Chem version v8-01-01 (Table 4) were compared to the *Galathea 3* GEM and RGM observations. This comparison led to a hypothesis about the oceanic origin of elevated GEM concentrations in the MBL and consequently to improvements to the slab-ocean model parameterization. The work with the slab-ocean model was done in close collaboration Elsie Sunderland at Harvard University.

As the GEOS-Chem model was being updated with bromine-mercury chemistry parallel with my work (Holmes et al., 2010 and Table 4) it was possible to include a version with bromine chemistry in the final version of the updated model. Different versions of the GEOS-Chem model have however been used during the PhD due to continuous update to the v8-01-01 version available at the start of my work. The different versions are presented in Table 4. The original version of the Hg model was developed by Noelle Selin (Selin et al., 2007) and included the ocean parameterization developed by Sarah Strode (Strode et al., 2007). In this thesis only results from the Soerensen version of the model are discussed (this is the version presented in Soerensen et al. 2010c). The v8-03-02 is publicly available at: <http://acmg.seas.harvard.edu/geos/index.html>.

Table 4. The different versions of the GEOS-Chem mercury model that I have worked with during the PhD. Results in the Summary and Discussion chapter are all from the Soerensen et al. (2010c) version unless otherwise stated.

Version	Atmospheric scheme	Oxidants	Ocean scheme	Inventory
v8-01-01	Selin et al., 2007	OH + O ₃	Strode et al., 2007	GEIA 2000
Holmes	Holmes et al., 2010	Br	Strode et al., 2007	GEIA 2000 scaled to Streets et al., 2009
Soerensen	Holmes et al., 2010*	Br	Soerensen et al., 2010c	GEIA 2000 scaled to Streets et al., 2009
v8-03-02	Holmes et al., 2010	Br	Soerensen et al., 2010c	GEIA 2000 scaled to Streets et al., 2009

*This version of the atmospheric mercury module differs slightly from the final version published by Holmes et al. (2010) due to overlapping development. The v8-03-02 version is the integrated publicly available version.

3.5.2 Development of the slab-ocean model

The improvements to the slab-ocean model were based on new results from the experimental and modeling community. Thus it was possible to enhance the complexity of the model parameterization compared to Strode et al. (2007).

Exchange with the atmosphere and subsurface waters

Air-sea fluxes of Hg⁰ were modeled using the parameterization of Nightingale et al. (2000), the Henry's law coefficient for Hg⁰ (Andersson et al., 2008b), a temperature-corrected Schmidt number for CO₂ (Poissant et al., 2000), and the Wilke-Chang method for estimating a temperature and salinity-corrected Hg⁰ diffusivity in different ocean regions (Wilke and Chang, 1955) (see Soerensen et al. 2010c Supporting Information (SI) Table S4). The vertical exchanges between the surface ocean and intermediate waters were retained through entrainment/detrainment of the mixed layer (Appendix D Maps of input data to the GEOS-Chem slab-ocean model: Mixed Layer Depth) and Ekman (wind-driven) pumping included in the original GEOS-Chem slab ocean model (Strode et al., 2007).

Deepening of the surface ocean mixed layer (Montegut et al., 2004) results in entrainment of Hg from intermediate waters and seasonal surface stratification resulting in detrainment. The original GEOS-Chem slab ocean model (Strode et al., 2007) assumed a globally uniform subsurface ocean Hg concentration. This was updated (Figure 15) using observations compiled by Sunderland and Mason (2007), and new data for the North Pacific Ocean (Sunderland et al., 2009) and Arctic Ocean (Kirk et al., 2008).

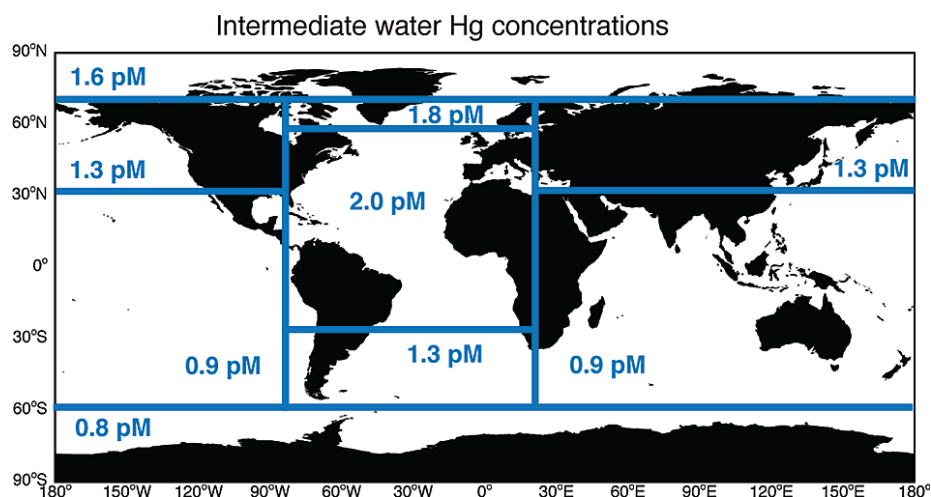


Figure 15. Subsurface ocean concentrations of inorganic total Hg based on observations compiled by Sunderland and Mason (2007), with recent measurement updates (Kirk et al., 2008; Sunderland et al., 2009).

Surface ocean redox reactions

The model incorporates separate terms for photolytic and biotic reduction, and photochemical and dark oxidation. The reducible fraction of the dissolved Hg^{II} pool was based on estimates from freshwater systems (O'Driscoll et al., 2006) and data indicating that stable chloride complexes abundant at high salinities are more resistant to reduction processes (Stumm and Morgan, 1996; Whalin et al., 2007). Reported ranges for the reducible pool ($\text{Hg}^{\text{II}}_{\text{red}}$) from the above studies vary between approximately 40% and 60% of total Hg^{II} . A value of 40% was implemented to best match the observational constraints provided by speciated surface ocean and atmospheric Hg concentrations. Re-equilibration of all reactive and nonreactive pools and Hg speciation occurs at each time step (60 min) in the model simulation. Measured biotic Hg reduction rate coefficients in dark seawater incubation experiments range from $3.5 \times 10^{-7} \text{ s}^{-1}$ (Mason et al., 1995a) to $8.3 \times 10^{-5} \text{ s}^{-1}$ (Amyot et al., 1997). These experiments assume instantaneous equilibration of any added Hg to mimic Hg speciation under natural conditions (i.e., the rate coefficients apply only to $\text{Hg}^{\text{II}}_{\text{red}}$). Many studies report relationships between biotic reduction rate coefficients in natural waters and factors such as productivity, particulate matter and bacterial activity (Mason et al., 1995a; Poulain et al., 2007; Whalin et al., 2007). A variety of rate coefficient data for $\text{Hg}^{\text{II}}_{\text{aq}}$ photoreduction are also available (Amyot et al., 2000; Lalonde et al., 2001; Lalonde et al., 2004; Qureshi et al., 2010; Rolfhus and Fitzgerald, 2004). While these data provide guidance, most cannot be implemented directly in the model because they reflect net Hg^{II} reduction rate coefficients, are for unfiltered waters (do not isolate photoreduction and biotic reduction), and/or do not report radiation intensities. Dual isotope addition data from Whalin et al. (2008), who measured simultaneous photooxidation (k_{OX1}), photoreduction (k_{RED1}), and biotic reduction (k_{RED2}) rate

coefficients (s^{-1}) in Chesapeake Bay seawater were therefore used. By least squares fit to the Whalin et al. (2008) data, linear relationships between total shortwave solar radiation (R , $W m^{-2}$), net primary productivity (NPP, $gC m^{-2} d^{-1}$) and k_{OX1} , k_{RED1} , and k_{RED2} were derived. NPP values for this derivation were for the outer and shelf region of Chesapeake Bay characteristic of the measurement period (Cerco, 2000). The rate coefficients were further adjusted within observational confidence limits to be consistent with the ratio between photo-oxidation and photoreduction measured by Qureshi et al. (2010), resulting in the following relationships being implemented in the model: $k_{OX1} = 6.6 \times 10^{-6} \times R$; $k_{RED1} = 1.7 \times 10^{-6} \times R$; $k_{RED2} = 4.5 \times 10^{-6} \times NPP$. A term for dark oxidation ($k_{OX2} = 1.0 \times 10^{-7} s^{-1}$) based on Lalonde et al. (2001) is also included. Spatial and seasonal variability in redox rates was modelled based on light attenuation in the surface mixed layer, the surface local shortwave radiation flux from GEOS-5, and global NPP distributions from MODIS satellite data (Behrenfeld and Falkowski, 1997). Light attenuation with depth is estimated from empirically determined effective light absorption coefficients for seawater, dissolved organic carbon (DOC) and pigments, and their respective concentrations (Wozniak and Dera, 2007) (Soerensen et al. 2010c SI Table S3). Pigment concentrations are derived from MODIS satellite data, while DOC is based on a global mean of $1.5 mg L^{-1}$ in the surface mixed layer, scaled by the distribution of global NPP to account for productivity related concentration differences (Chester, 2003).

Sorption of Hg^{II} to particles and export fluxes

HgP removal from the surface ocean is modelled by linking Hg^{II} sorption to particulate matter and settling to organic carbon export fluxes (the ocean's biological pump). The affinity of aqueous Hg^{II} for the solid phase is described using an empirically measured partition coefficient (K_D , $L kg^{-1}$):

$$K_D = \frac{C_S}{C_D}$$

Where C_S is the suspended particulate matter (SPM) concentration of Hg^{II} on a dry weight (mass/mass) basis ($pg kg^{-1}$) and C_D is the filtered concentration (mass/volume) of Hg^{II} in seawater ($pg L^{-1}$). The model re-equilibrates the Hg^{II} pool between the dissolved and solid phases at each time step, prior to calculating the reducible and non-reducible dissolved Hg^{II} pools.

A log K_D value based on North Pacific and North Atlantic measurements (5.5 ± 0.5) were used (Mason et al., 1998; Mason and Fitzgerald, 1993). Since no global data sets for SPM concentrations in ocean surface waters are available, integrated water column algal biomass derived from MODIS chlorophyll a data and statistical relationships from (Uitz et al., 2006) for subsurface algal productivity were used (see Soerensen et al. 2010c SI Section II). Settling fluxes of HgP are calculated using the parameterization described in Sunderland and Mason (2007) for export of particulate organic carbon with depth and HgP to carbon ($Hg:C$) ratios. Spatially and temporally variable $Hg:C$ ratios are calculated at each time step in the model (global mean of $0.16 ng Hg per mg C$) from the reservoir of HgP (derived from K_D) and the standing stock of organic carbon in the surface ocean (Soerensen et al. 2010c SI Table S2).

3.5.3 Validation of the surface ocean module

After introducing the new parameterization into the slab-ocean module the GEOS-Chem model was validated against available marine and atmospheric observations. An example of seawater Hg^0 is seen in Figure 16 and for GEM in Figure 19. Correlation between simulations and measurements of aquatic and atmospheric mercury were used to evaluate the models performance (for details see Soerensen et al., 2010c).

Although a very detailed sensitivity analysis is hard to conduct on a global model a sensitivity analysis for the most important parameters and most uncertain variables was performed (see Soerensen et al. 2010c SI Section I).

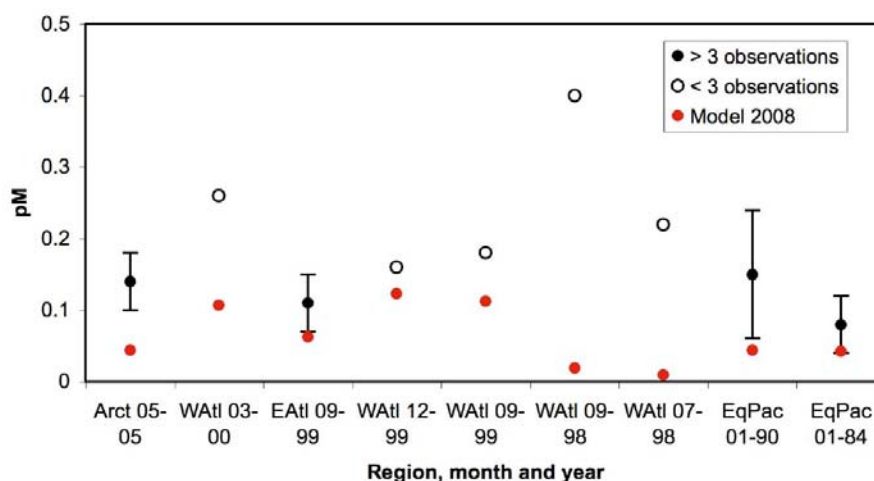


Figure 16. Comparison of monthly modeled (2008) and observed (various years) seawater Hg^0 concentrations. Pacific Ocean: (Kim and Fitzgerald, 1988; Kim and Fitzgerald, 1986; Mason and Fitzgerald, 1990; Mason and Fitzgerald, 1993); Atlantic Ocean (Gardfeldt et al., 2003; Mason et al., 2001); Arctic Ocean: (Kirk et al., 2008). (illustration from Soerensen et al., 2010c Supporting Information).

After the validation the model was used to investigate patterns of mercury levels and fluxes in the global MBL. Thus it is possible to supplement the cruise observations with model estimates of mercury concentrations improving the spatial and temporal knowledge of mercury levels in the MBL and the different source contributions. The present-day simulation was conducted for 5 years (2004-2008) to equilibrate the surface ocean and the stratosphere. Monthly output from 2008 was used for the global analyses while daily output from the exact time of the cruises in 2008 and 2009 were used in the comparison to the West Atlantic cruises.

3.6 Integrating approaches

Model development and experimental work should be planned together in an integrated monitoring approach (Hertel et al., 2009). When modelers use the experimental results for development of parameterizations and model validation, they are able to determine where the largest uncertainties lies and which new measurements are most urgent in order to improve the model parameterization and our understanding in the bigger perspective. If this information is given back to the experimentalists they will be able to better direct their campaigns at the right questions and experimentalist can thus identify new areas of research and uncertainties in models which need to be addressed.

4 Summary and discussion of results

The chapter presents results that have not previously been addressed in peer reviewed publications as well as results from the three enclosed papers (Appendix B Enclosed Abstracts from Peer-Reviewed Papers). The reader is referred to the actual papers for in depth information on some analyses and results that fall outside the main focal area discussed in this summary.

4.1 Mercury concentrations in the MBL

Due to the combination of the extensive cruise data and the GEOS-Chem model simulations, information on both the temporal and spatial resolutions of gaseous mercury concentrations have been obtained.

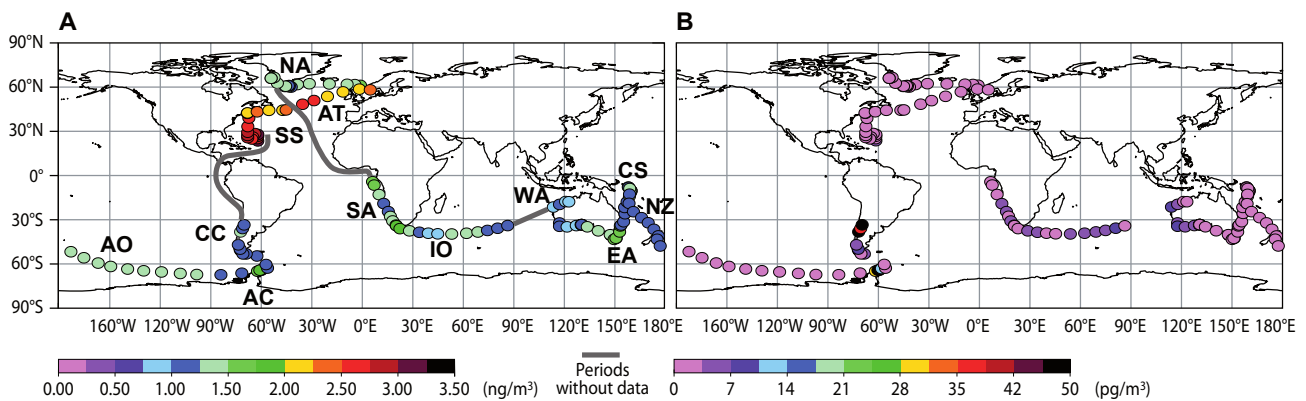


Figure 17. The navigation route of the *Galathea 3* expedition. Shown are daily mean concentrations of (A) GEM and (B) RGM. The gray line indicates the route during periods without measurements and the names are the abbreviations of the 12 cruise legs (see Table 7) (illustration from Soerensen et al., 2010a).

4.1.1 Spatial distribution of GEM

Large scale

Average NH GEM concentrations from *Galathea 3* are significantly different ($P < 0.05$) from the SH average ($1.27 \pm 0.2 \text{ ng m}^{-3}$, $n = 848$). NH spring concentrations are $2.62 \pm 0.4 \text{ ng m}^{-3}$ ($n = 241$) and late summer concentrations are $1.32 \pm 0.2 \text{ ng m}^{-3}$ ($n = 190$) (Table 7 and Figure 17). This confirms the presence of a hemispheric gradient in concentrations as observed by others (Fitzgerald et al., 1986; Lamborg et al., 1999; Slemr, 1996; Slemr et al., 2011; Temme et al., 2003a) (Figure 21). The GEM gradients between the two hemispheres in the Atlantic Ocean has ranged between 1.35-1.70 (NH/SH) the last decades (Slemr et al., 2011) (Figure 5). The data from the *Galathea 3* cruise have a gradient of 1.72 (NH median: 2.17 ng m^{-3} , SH median: 1.26 ng m^{-3}). This is in the higher end of reported gradient from the Atlantic Ocean and is the result of the high springtime GEM concentrations observed during the cruise. With the median that is observed in the SH, the NH median could potentially be as low as 1.70 ng m^{-3} and still be within the 1.35-1.70 gradient range. This suggests that there is much variability hidden in the range of NH/SH gradients reported the last decades.

The hemispheric gradient is reproduced by the GEOS-Chem model. There is a gradient in GEM concentrations around 5°N-5°S for all seasons (Figure 18). The model results indicate that the gradient is not constant throughout the year but that it will be most pronounced in spring (NH/SH=1.49) and least pronounced during summer (NH/SH=1.05). The yearly mean gradient in the model is 1.27. This seasonal variability could possibly explain why the observed gradients are also variable. The summer gradient predicted by the model is smaller compared to cruise observations in the Atlantic Ocean and this indicates that the model might be overestimating summer concentrations in the SH. At the moment there are not enough cruise observations to either confirm or reject the seasonal variability in the hemispheric gradient predicted by the model.

The *Galathea 3* cruise was broken down into 12 individual legs (Table 5). This reveals that variations in GEM concentrations are also seen within each hemisphere. For the NH large differences between spring and late summer are seen in the Atlantic Ocean. This will be discussed in “Seasonal variability of GEM” (4.1.4). For the SH differences in average concentrations are less pronounced between legs but still present. Minimum average on a leg in the SH is 1.03 ± 0.19 ng m⁻³ and maximum average is 1.55 ± 0.38 ng m⁻³. The ship covers a large spatial and temporal range during this part of the cruise as well as the source region of the air masses changes between marine and terrestrial. This makes it difficult to infer when the variability is caused by seasonal dependent changes and when it is caused by spatial dependent changes.

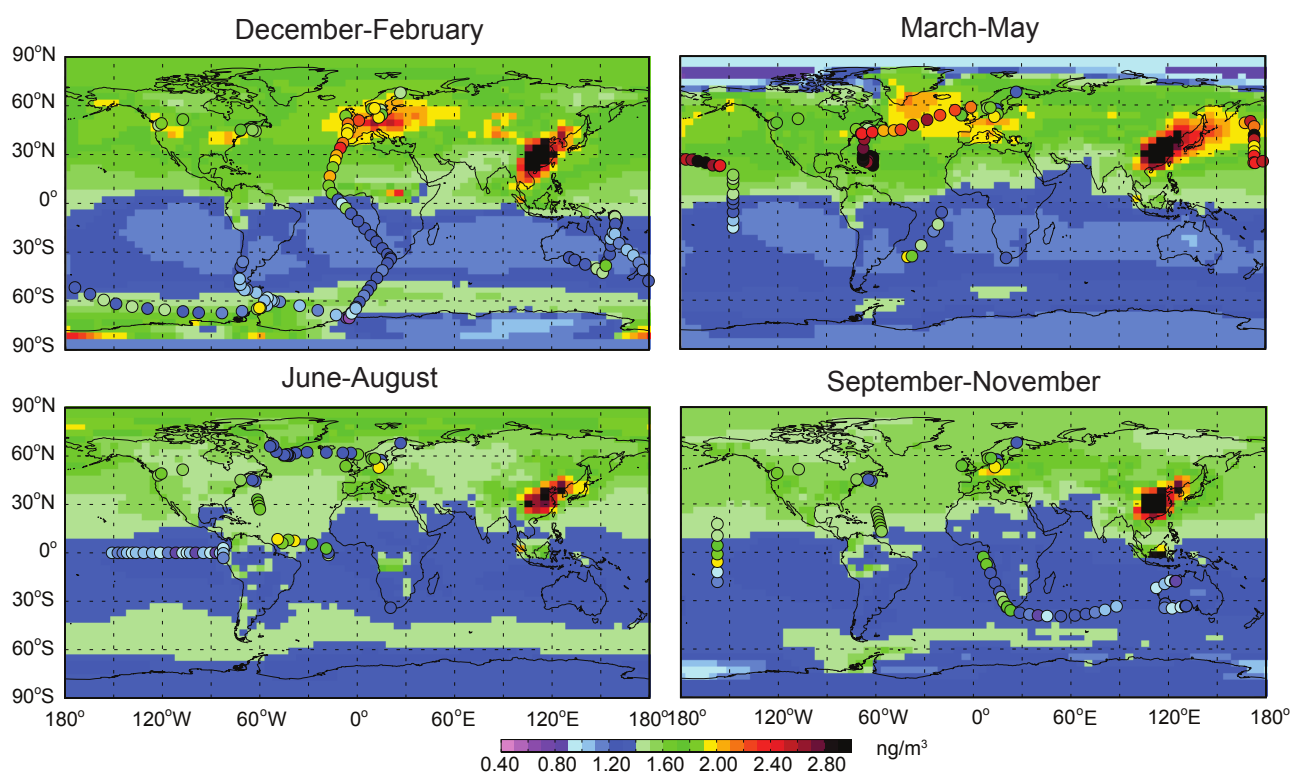


Figure 18. GEOS-Chem model output of the mean GEM concentration in the MBL for the four seasons. Overlaid are cruise and terrestrial observations from Selin et al. (2007) and Soerensen et al. (2010a) and references therein (illustration from Soerensen et al., 2010c).

Slemr et al. (2011) propose that atmospheric mercury concentrations have decreased by 20-38% since 1996 and that this has led to 2008-2009 MBL levels ~ 1.1 ng m⁻³ in the NH and ~ 0.75 ng m⁻³ in the SH. This is not

confirmed by the *Galathea 3* measurements. On the contrary, data from the *Galathea 3* (2006-2007) (Table 7) and data from the West Atlantic Ocean (2008-2009) (Table 8, see “Ocean evasion” (4.2.6)) suggest that MBL concentrations have not decreased substantially in either the NH or SH since the 90ties, where mean cruise concentrations between 1.18 ng m⁻³ and 1.50 ng m⁻³ were reported (Table 2)(Slemr, 1996;Temme et al., 2003b). This is supported by other recent SH observations from Witt et al. (2010) who finds 1.2 ng m⁻³ (range: 1.05-1.51 and no reported plume events) in the Indian Ocean in 2007 and Xia et al (2010) who finds a median of 1.28 ng m⁻³ (average was 1.47±0.84 ng m⁻³ but many episodic events were observed so the median might give a better estimate) in the East Indian and Southern Ocean in 2007 (see Table 2). The difference between the cruises presented in Slemr et al. (2011) and other cruise data suggest that there is variability in concentrations within each hemisphere that is not understood. Furthermore, a decreasing trend within the MBL is not consistent with most of the recent cruise observations despite the clear decreasing trend observed at Mace Head and Cape Point since 1996 (Figure 5). I have no suggestions as to why the data from the two cruise campaigns presented in Slemr et al. (2011) is so much lower than other MBL observations from the same period.

Local scale

During *Galathea 3*, episodic changes significantly deviated from the running mean of GEM concentrations in the SH were observed (Table 6) and GEM almost always showed enhanced concentrations in urban harbor areas. The magnitude of the enhancements in harbor areas can be seen in Figure 23 and in Soerensen et al. (2010b Table 1). These local scale events will be discussed further in “Sources of Mercury to the MBL” (4.2).

The GEOS-Chem model is not a good tool for simulating small scale episodic transport events or in harbor concentrations although it has previously been used to simulate large scale Asian transports (Strode et al., 2008). This is due to the spatial resolution of the model (4°×5°), where small point source emissions will be diluted into the grid-box and not create a point source or plume pattern. Especially in coastal areas sea-breezes and other wind patterns are not well captured with the spatial resolution of the model. Only in one case has the model been used in the understanding of a plume event with GEM enhancement (see “Biomass burning emissions” (4.2.4)).

4.1.2 Spatial distribution of RGM

During the cruise RGM concentrations were mostly < 10 pg m⁻³ and the global mean concentration was 3±11 pg m⁻³ (Figure 17).

RGM concentrations were enhanced above 10 pg m⁻³ during only two episodes lasting longer than a day. The first episode was between the 24th and 28th of January 2007 near the coast of Antarctica where mean concentrations reached 43±39 ng/m³ ($n = 47$). For a thorough discussion see “RGM Dynamics at Antarctica” (4.3.2). The second episode was during the 6th to 8th of February 2007 when the ship passed along the coast of Chile. Here the mean concentration was 43±31 pg m⁻³ ($n = 21$) (for a thorough description see “Anthropogenic plumes in the MBL” (4.2.2) and (Soerensen et al., 2010b)).

During the periods where the ship was in harbor areas RGM was almost always below $2 \times \text{DT}$ (detection limit = 2 pg m^{-3}). The exceptions were Perth, Australia ($19.9 \pm 10.3 \text{ pg m}^{-3}$, $n=11$) and Valparaíso, Chile ($69.0 \pm 64.0 \text{ pg m}^{-3}$, $n=25$) (see Soerensen et al., 2010b).

The low concentrations of RGM in harbor areas and during periods in the MBL where GEM concentrations indicate plumes from anthropogenic sources or biomass burning are unexpected. Possible reasons for these observations will be discussed in “Mercury Chemistry in the MBL” (4.3).

4.1.3 Diurnal variability of GEM and RGM

The presence of diurnal variations in GEM and RGM was investigated individually for each of the 12 cruise legs of the *Galathea 3* (see Figure 17 and Table 3). The procedure is described in Soerensen et al. (2010a).

Previous cruises have reported both an absence and a presence of diurnal GEM variations, some have even observed both within the same campaign (Laurier et al., 2003; Sommar et al., 2010; Witt et al., 2010; Xia et al., 2010). GEM variations have been proposed to be driven by ocean evasion through diurnal variations in the evasion flux. Diurnal variations in the evasion flux have been observed in coastal areas using flux chamber measurements (see for example Gardfeldt et al., 2001) although not yet in the open ocean (Andersson et al., 2007). No recurrent diurnal GEM variations were found during any of the 12 legs during the *Galathea 3* cruise. This suggests that it is not a common feature for the MBL and might rely on specific and as yet unidentified conditions.

Diurnal variations of RGM have been reported in all the limited number of cruise measurements in temperate latitudes that I am aware of (Hedgecock et al., 2003; Laurier and Mason, 2007; Laurier et al., 2003; Mason and Sheu, 2002) while observations in the Arctic report lack of diurnal variations (Aspmo et al., 2006; Sommar et al., 2010). RGM observations from *Galathea 3* revealed significant ($P < 0.1$) diurnal variation with midday peaks in 5 of the 12 legs (Table 7). This will be discussed further in “General Trends in RGM Dynamics in the MBL” (4.3.1).

4.1.4 Seasonal variability of GEM

Significantly different ($P < 0.001$) concentrations of GEM were found in the NH Atlantic Ocean MBL in late summer 2006 and spring 2007 using a t-test (Table 7 and filled triangles on Figure 19). To ensure that the observations did not have systematic errors they were validated against data from the Mace Head research station. Mace Head is located at the western tip of Ireland and receives air primarily from the Atlantic Ocean. This validation is presented in Soerensen et al. (2010a) and the results support confidence in the large differences in concentrations between spring and summer.

To confirm that the difference in concentrations in NH between August 2006 and April 2007 was part of a recurrent pattern all available information on former cruises in the NH Atlantic Ocean were collected. With the use of this ensemble of data a rough estimate of the seasonal variability of GEM in the Atlantic Ocean was made (Figure 19) (see Soerensen et al.,

2010a). A seasonal GEM variability in the Atlantic MBL was found, with minimum concentrations during summer and maximum concentrations during fall to spring (Figure 19). The seasonal variability corresponds to the one observed at Mace Head ($R^2=0.7$) (Ebinghaus et al., 2002) but its amplitude is larger.

The new version of the GEOS-Chem model is able to simulate the seasonal variation above the Atlantic Ocean (R^2 of 0.82 when comparing monthly means in the model with the observed seasonal variation in the Atlantic Ocean from cruises (Figure 19)). This is a clear improvement compared to previous versions of the model that have not been able to capture the seasonal variability of the Atlantic Ocean. For a discussion on what drives the seasonal variability of mercury in the Atlantic Ocean see “Ocean evasion” (4.2.6).

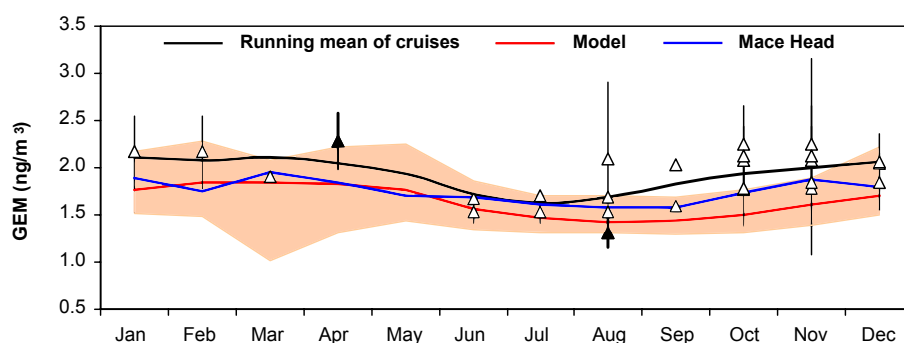


Figure 19. Season variability in GEM concentrations in the Atlantic Ocean (NH) and at coastal stations in model results and measurements. Filled triangles are *Galathea 3* cruise data, unfilled triangles are from Mason et al. 1998; 2001, Lamborg et al. 1999, Temme et al. 2003, Aspomo et al. 2006, Laurier and Mason 2007, the black line is the running mean of cruise observations (see text), the blue line is the mean concentrations at Mace Head (1995-2001)(Ebinghaus et al 2002), the red line is GEOS-Chem model data and hatched area represent highest and lowest simulated concentrations in ocean grids in the North Atlantic at the given month. Illustration modified from illustrations in Soerensen et al., 2010a and Soerensen et al., 2010c.

The model also predicts distinct seasonal variations in other ocean basins (Figure 20), which the limited number of cruise observations cannot yet confirm. The model predicts a seasonal variation in the North Pacific Ocean equal to the one in the North Atlantic Ocean ($R^2=0.96$, $n=12$) although the variation between summer and winter is less pronounced (Table 5). According to the model the South Atlantic and South Pacific Oceans have a seasonal variability anti-correlated to the one in NH ($R^2=-0.86$ between North Atlantic and South Atlantic) with peak concentrations in July to September. The mean GEM concentrations are also lower in SH and the seasonal variability less pronounced (Table 5 and Figure 20) as also suggested by measurements (Figure 21). In the Southern Ocean no distinct periods with minimum or maximum concentrations are found. Unfortunately this version of the model still has problems with the polar air-sea-ice interactions and data for the Arctic Ocean and coastal Antarctica has therefore not been derived.

The anti-correlation in the seasonal variation between the mid-latitudes of the SH and NH predicted by the model is not supported by data from the two east Atlantic coastal sites; Mace Head, Ireland in the NH and Cape Point, South Africa in the SH (Slemr et al., 2008). Measurements suggest that the two sites have similar seasonal variability (Figure 6) and

the authors propose that the seasonal variation at Cape Point is driven by emission sources (ocean evasion, biomass burning, anthropogenic emissions and inflow from the NH). It could be that the influence from one of these emission sources is misrepresented in the model. Another possibility is that the seasonal variation at Cape Point is not representing conditions throughout the hemisphere. Although Slemr et al. (2009) suggests that the seasonal variation at Cape Point is source driven new information (Brunke et al., 2010) also indicate that rapid removal of gaseous mercury take place at Cape Point in some cases. More long term monitoring of mercury at coastal sites and on cruises in the SH is clearly needed to clarify if the seasonal variation seen at Cape Point is the general hemispheric pattern for the MBL, if the model is misrepresenting the seasonal variability or if seasonal variations are different at different places in the SH.

Table 5. Output from the GEOS-Chem for the five ocean basins shown in Figure 20.

Ocean basin	Yearly mean \pm stdv. ^A ng m ⁻³
North Atlantic Ocean	1.71 \pm 0.19
North Pacific Ocean	1.64 \pm 0.13
South Atlantic Ocean	1.24 \pm 0.08
South Pacific Ocean	1.26 \pm 0.06
Southern Ocean	1.35 \pm 0.06

^A The output is in monthly means, which have been used to derive the stdv.

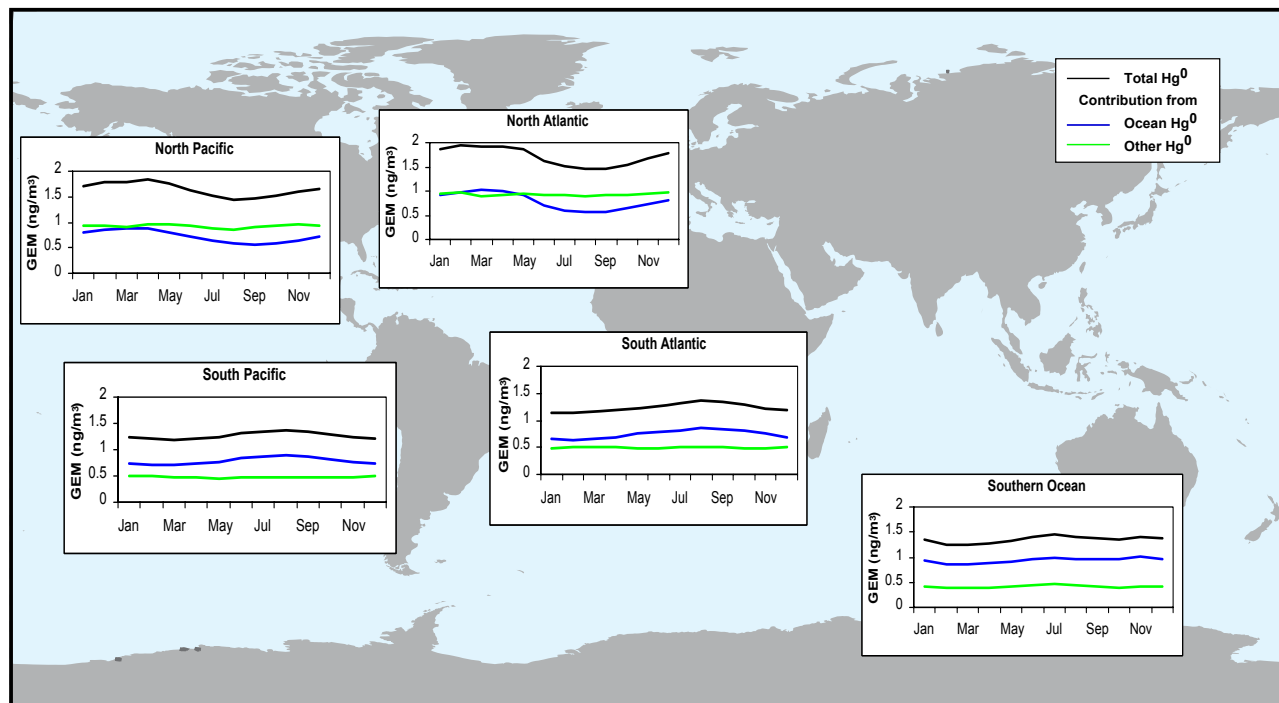


Figure 20. GEM monthly variation from the GEOS-Chem model for North Atlantic Ocean (-35:0°N, 30:66°S), North Pacific Ocean [150:-140 °N, 18-62°S], South Atlantic Ocean (-30:10°N, -30:-2°S), South Pacific Ocean (160:-90°N, -38:-10°S) and the Southern Ocean (-58:-42°S).

Table 6. Information on observed plume events during the cruise (see Table 7 for mean concentrations during each leg).

Location	Leg	Period	GEM	GEM prior/after event	GEM t-test ^A p	RGM	GEM,RGM no. obs	CO	NOx	O3	GEM/CO ^C (R ²) ^p
W. coast of Africa	SA	8 th -9 th Oct 06	1.70±0.06	1.25±0.14	0.001	2±3	13, 11	NA	NA	35.6±2.8	NA
S. coast of Africa	SA-IO	18 th -19 th Oct 06	1.73±0.15	NA	NA	3±3	19	70.6±20.0	NA	30.9±3.8	not sign
S. coast of Australia 1 st	EA	5 th - 5 th Dec 06	1.70±0.14 ^B	~1.4	NA	0.5	25 ^B , 2	71	4	22	NA
S. coast of Australia 2 nd A	EA	5 th -6 th Dec 06	1.50±0.06	1.23±0.16	0.001	0	17	65.7	53±128	18.7±6.8	not sign
S. coast of Australia 2 nd B		8 th -9 th Dec 06	1.63±0.06	1.23±0.16	0.001	0	21	68.0	9±20	15.8±2.4	not sign
Coast of Antarctica	AC1	25 th -27 th Jan 07	1.80±0.26	1.30±0.16	0.001	56±39	29,29	71.5±56.3	3.5±6.4	10.0±2.2	-0.74 ^{0.001}
Coast of Chile	CC	6 th -7 th Feb 07	1.17±0.17	1.07±0.07	0.01	43±31	21,21	150±36	81±180	3.9±8.5	0.18 ^{0.07}

^A GEM is tested to see if it is significantly enhanced compared to measurement just prior and/or after the episodic event. ^B 5 min values used. ^C Spearman's rank correlation used.

Table 7. Global, Hemispheric and Sectional Data from the *Galathea 3* cruise (table from Soerensen et al., 2010a).

leg	Ab ^a	dates	lat ^b (deg)	origin ^c	GEM (ng/m ³) mean(±std)	RGM (pg/m ³) mean(±std)	no obs GEM/RGM	RGM t test day vs night	RGM-Rad ^d PCC	RGM-RH ^d PCC
Global		16th August to 24th April	-65: 67		1.53(±0.58)	3.1(±11)	1279/1174			
NH summer		16th August to 1st September	58: 67		1.32(±0.16)	0.4(±3)	190/172			
NH spring		30th March to 24th April	23: 59		2.61(±0.36)	0.8(±2)	241/218			
SH		8th October to 8th February	-65: -3		1.27(±0.25)	4.3(±14)	848/784			
North Atlantic	NA	16th August to 1st September	58: 67	ocean	1.32(±0.16)	0.4(±3)	190/172			0.31
Atlantic O.	AT	15th April to 24th April	43: 59	ocean	2.26(±0.26)	0.1(±1)	100/92		0.89 ^f	-0.83 ^f
Sargasso Sea	SS	30th March to 11th April	23: 45	mixed	2.86(±0.17)	1.2(±2)	141/126		-0.49	0.31
South Africa	SA	8th October to 21st October	-39: -3	mixed	1.36(±0.24)	3.4(±4)	113/101		-0.60	0.43
Indian Ocean	IO	22nd October to 29th October	-39: -33	ocean	1.11(±0.19)	4.6(±5)	88/79	e	0.83 ^f	-0.66 ^{0.16}
West Australia	WA	3rd November to 6th November	-22: -17	ocean	1.03(±0.16)	5.0(±6)	32/26	g	0.77 ^e	-0.94 ^g
East Australia	EA	23rd November to 15th December	-44: -26	mixed	1.33(±0.24)	1.9(±3)	185/175	e	0.94 ^g	-0.77 ^e
Coral Sea	CS	16th December to 3rd January	-27: -7	mixed	1.21(±0.18)	0.3(±1)	130/124	g	0.71 ^{0.11}	-0.89 ^f
New Zealand	NZ	3rd January to 14th January	-56: -26	mixed	1.19(±0.17)	0.1(±0)	108/104	g	0.89 ^f	-0.83 ^f
Antarctic O.	AO	14th January to 24th January	-65: -55	ocean	1.30(±0.16)	0.0(±0)	105/92		0.09	-0.09
Antarctic Coast	AC	25th January to 28th January	-65: -63	mixed	1.55(±0.38)	43.0(±39)	49/47		-0.2	-0.03
Coast of Chile	CC	31st January to 8th February	-58: -33	mixed	1.11(±0.11)	28.6(±30)	37/36		-0.49	0.54

^a Abbreviations used in the text. ^b The latitude that the given leg includes. ^c Ocean = no influence from terrestrial sources, Mixed = influence from terrestrial sources during the entire or smaller but significant portions of the leg. ^d PCC (*r*) = Pearson's correlation coefficient (with significance level given in footnotes e-h. ^e *P* < 0.1. ^f *P* < 0.05. ^g *P* < 0.01.) between mean diurnal RGM and radiation and relative humidity during the given leg.

4.1.5 Do GEM MBL background concentrations exist?

In the last decade there has been a consensus that a so called “background concentration” for the NH and SH exist in the MBL and at rural terrestrial sites due to the long atmospheric lifetime of mercury. This has most clearly been expressed in Lindberg et al. (2007). This is a paper synthesizing knowledge from the Panel on Source Attribution of Atmospheric Mercury, which was convened during the 8th International Conference on Mercury as a Global Pollutant. In Lindberg et al. (2007) it is stated that the term “Global background concentration refers to the average sea-level atmospheric concentration of Hg^0 at remote sites and is currently taken as $1.5\text{--}1.7\text{ ng m}^{-3}$ in the Northern Hemisphere, $1.1\text{--}1.3\text{ ng m}^{-3}$ in the Southern Hemisphere”. That this is still considered to be valid is seen by the reference to this statement in a newly published review by Sprovieri et al. (2010). They state “Based on the existing data, there is a scientific consensus about the current global background concentration of airborne Hg which is considered to be in the range of 1.5 to 1.7 ng m^{-3} in the Northern Hemisphere and 1.1 to 1.3 ng m^{-3} in the Southern Hemisphere (Lindberg et al., 2007)”.

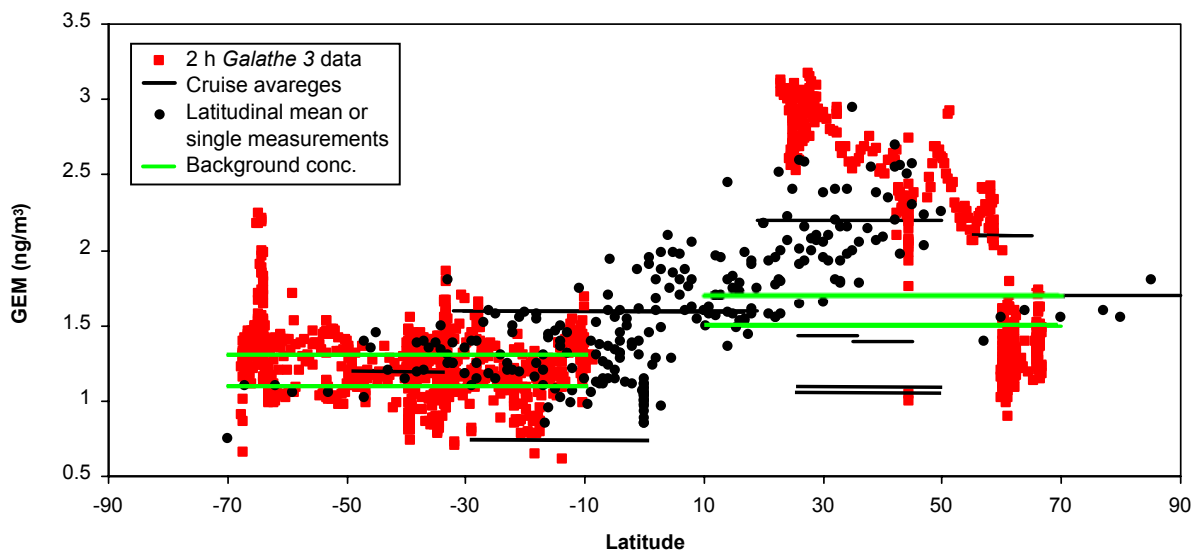


Figure 21. Compilation of cruise measurements from 1977 and until today. Black dots and lines show data from previous cruises (Andersson et al., 2008c; Aspino et al., 2006; Fitzgerald et al., 1984; Fitzgerald et al., 1986; Kim and Fitzgerald, 1986; Lamborg et al., 1999; Laurier and Mason, 2007; Laurier et al., 2003; Mason et al., 1998; Mason et al., 2009; Slemr, 1996; Slemr et al., 2011; Slemr and Langer, 1992; Temme et al., 2003b). The black lines indicate mean concentrations given for a certain range of latitudes; black dots indicate individual measurements or a mean of measurements at the given latitudes depending on the form of the data available. Red dots indicate 2 h mean concentrations during the *Galathea 3* cruise, with all data where influence from anthropogenic sources or biomass burning is suspected has been removed. Green lines indicate the upper and lower limits of the background concentrations in the two hemispheres as suggested by Lindberg et al. (2007).

In the NH (North America and Europe) average mercury concentrations at rural terrestrial sites are mostly within the limit of the background concentrations given by Lindberg et al. (2007) and, although present the amplitude of the seasonal variation is small (Sprovieri et al. 2010 and references therein). However, the NH MBL GEM concentrations measured during *Galathea 3* supports measurements from previous cruise campaigns: reported mercury concentrations are inconsistent with the suggested average background concentrations (Figure 21). Furthermore it has already been shown that the seasonal variability in the NH MBL is considerable. The lower end of average cruise concentrations have sev-

eral times been observed to be well below 1.5 ng m^{-3} (Slemr et al., 2011; the *Galathea 3* data and data from West Atlantic Ocean (see Table 8)) but it is the tendency for MBL observations to be above 1.7 ng m^{-3} that is most striking. Observations are often $> 2 \text{ ng m}^{-3}$ (Table 2) and have been observed to be more than twice as high as the proposed background level. It is also seen that NH cruise data have a bell shape across latitudes. Highest concentrations as well as the largest variability in the concentrations are seen around $20\text{-}50^\circ\text{N}$ (Figure 21). It is not possible to calculate an accurate yearly mean for the NH MBL but using the running mean from the ensemble of Atlantic cruise data described in “Seasonal variability of GEM” (4.1.4) a yearly average concentration of $1.93 \pm 0.17 \text{ ng m}^{-3}$ can be approximated. This is well above the “background concentration”.

Previous cruise campaigns in the SH Atlantic (Lamborg et al., 1999; Slemr, 1996; Temme et al., 2003b; Temme et al., 2003a; Witt et al., 2010) have measured more uniform concentrations across all latitudes than in the NH MBL (Figure 21)(Slemr et al. 2011). Average cruise concentrations mostly fall within the range of $1.1\text{-}1.5 \text{ ng m}^{-3}$ (Table 2), the new cruise data from Slemr et al. (2011) being the exception. The average concentration of GEM in the SH during *Galathea 3* was $1.27 \pm 0.25 \text{ ng m}^{-3}$ ($n = 848$ five min obs). At first sight this supports the proposed average background concentrations, however if the average leg concentrations or the 2 h average concentrations are considered it is seen that this average is masking a large variability in the data with periods well below and above the “background concentration”. This implies that so far there is not enough information to disregard that some locations in the SH pristine MBL could have yearly averages either well above or below the suggested background concentrations. The enhancements above 1.3 ng m^{-3} could for older publications be due to episodic plumes from biomass burning or anthropogenic sources but the known episodes have been removed from the 2 h average *Galathea 3* data presented in Figure 21. The variability in the 2 h average data could indicate that the lifetime of GEM in the MBL is too short to create a uniform hemispheric average. At the only long term monitoring site in the SH (Cape Point, South Africa) an average yearly concentration below 1 ng m^{-3} has been observed the last couple of years (Slemr et al., 2011). At this site frequent GEM depletion events are also reported (Brunke et al., 2010) indicating that a fast removal of mercury is occurring at least at some locations in the SH. What drives this variability at Cape Point and to a lesser extent in the MBL during the *Galathea 3* cruise is still not understood.

It seems that the concentrations in the MBL are much more variable than the defined “background concentrations” for remote sites suggest as well as the yearly average most likely is much higher in the NH MBL than it should be by the definition. The high variability suggests a lifetime of mercury in the MBL much shorter than one year as also suggested by others (Donohoue et al., 2006; Hedgecock et al., 2005; Hedgecock and Pirrone, 2004; Holmes et al., 2009). The bell shape of GEM observations present across the latitudes in the NH but not in the SH could be caused by a higher anthropogenic influence on the MBL in the $20\text{-}50^\circ\text{N}$ region. This could either be through directly emitted mercury transported out above the ocean or through re-evasions from the ocean (see “Ocean evasion” (4.2.6) for a description of the influence ocean evasion can have on MBL concentrations). The variability and the levels of GEM in the MBL

leads to the questions of whether the MBL can be considered a “remote” site with “background concentrations”? I therefore propose that the term “background concentrations” as defined by Lindberg et al. (2007) should not be used for the MBL.

4.2 Sources of Mercury to the MBL

Figure 22 shows the locations where episodic plume events were recorded as well as the harbor areas where GEM and RGM were measured.

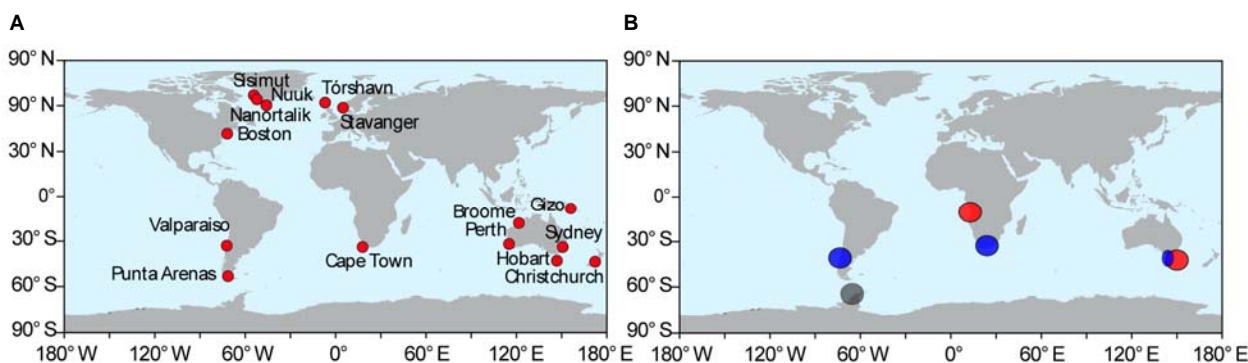


Figure 22. The figure shows A) the towns where measurements were taken and B) the areas where it is believed that plumes from biomass burning (red circles), anthropogenic plumes (blue circle) and unidentified sources (grey circle) were encountered. The ocean surface is furthermore an emission source. Illustration modified from Soerensen et al. (2010b).

4.2.1 Anthropogenic emissions in harbors

During the *Galathea 3* cruise anthropogenic influences were encountered many times. The most pronounced impact on concentrations was encountered close to urban areas (see Soerensen et al., 2010b for a thorough discussion on the harbor observations). In the 15 harbors where GEM was measured the concentrations were significantly elevated ($P < 0.001$) in all but three harbors where no statistically significant enhancement was found (Figure 23, harbors marked with * and Table 1 in Soerensen et al., 2010b). The average harbor concentrations of GEM ranged from 0.05 ng m⁻³ below to 1.18 ng m⁻³ above the concentrations in the MBL in the vicinity of the harbors. The three cities where no enhancements were found all had less than 30,000 inhabitants, while the range of inhabitants in all cities recorded was between 2,000 and 4.5 million (Figure 23).

Interestingly, there were only two harbor areas with significantly increased RGM concentrations (compared to 2×detection limit); Perth, Australia and Valparaíso, Chile. This is not consistent with inland observations of urban areas where RGM is mostly found above 10 pg m⁻³ (Sprovieri et al., 2010 and references therein). The lack of elevated RGM concentrations could be caused by low primary emissions of RGM or a rapid removal of the emitted RGM from the gaseous phase converting it to RGM_w. Based on inland observations it seems unlikely that RGM is not emitted in the urban areas where enhancements in GEM indicate that GEM is emitted. Unfortunately TPM was not measured. TPM could have helped create a more nuanced picture of the possible near coast enhancements of RGM_w (which is detected as TPM with the Tekran instrument).

See Soerensen et al., 2010b for a thorough discussion on harbor observations.

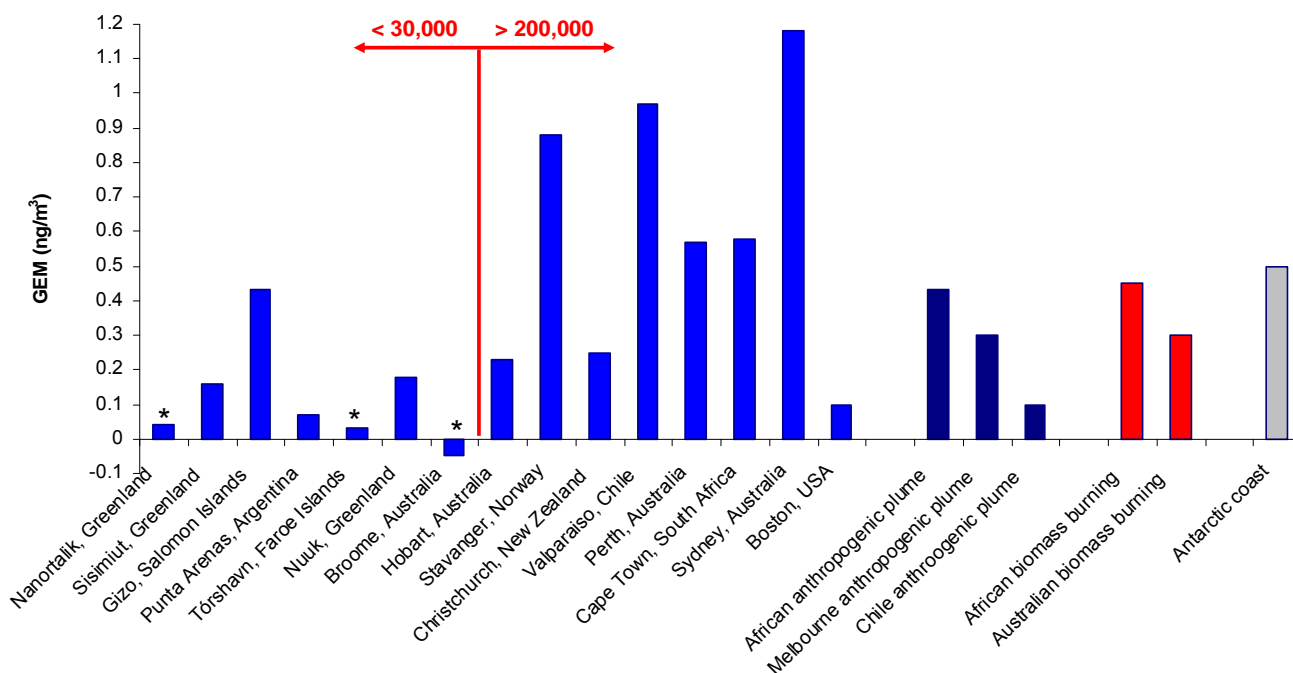


Figure 23. GEM enhancements (ng m^{-3}) in harbor areas (blue bars), during interception of anthropogenic plume events (dark blue bars), during interception of biomass burning events (red bars) and during possible evasion from breaking sea-ice (gray bar). Enhancements are calculated based on comparison to MBL concentrations in the vicinity of harbor areas or before/after the enhancement episodes. Measurements in harbor areas are shown with increasing number of inhabitants. The red line indicate the change from smaller cities (<30.000 inhabitants) to larger cities (> 200.000 inhabitants). A * indicates the only three harbor areas where no statistically significant ($P < 0.05$) enhancements were found using a t-test on measurements from the harbor and the nearby MBL (own illustration).

4.2.2 Anthropogenic plumes in the MBL

A few times air masses with an anthropogenic origin were intercepted at the ship in the MBL. This happened in South-Southwest of South Africa, in the waters between the Australian mainland and Tasmania and as the ship passed along the coast of Chile. Enhancements include episodes where one gaseous mercury species was enhanced while the other was not. When sources or source regions are explored in connection with enhancements in mercury concentrations intercepted at the ship, it is imperative to take into account the chemistry and dilution that take place between the source and the place of interception.

African anthropogenic plume

On October 18th 2007 at 21:00 *Vædderen* left Cape Town. During the next 36 hours (until 21st 9:00) GEM slowly decreased from 1.9 ng m^{-3} to 1.3 ng m^{-3} (2 h means). The average concentration was $1.73 \pm 0.15 \text{ ng m}^{-3}$ ($n=19$). Thereafter GEM continued to decrease until it reached 0.8 ng m^{-3} on the 22nd. RGM was not increased above average MBL concentrations and the average concentration was $2.84 \pm 2.84 \text{ pg m}^{-3}$ during the first 36 hours. CO decreased rapidly from 150 ppb to below 100 ppb within the first 6 hours after the ship left Cape Town and then more slowly continued to decrease until it reached 50 ppb on the 22nd. O_3 increased from a concentration of 15 ppb when the ship left Cape Town to a maximum of 35 ppb on the 21st, which was then followed by a slow decrease. The behavior of GEM, CO and O_3 suggest that the ship moved in a plume at least the first 36 hours after the departure from Cape Town. The most likely origin of

the plume is the South African mainland. For the first 12 hours wind direction observed at the ship agrees with back trajectories from HYSPLIT (Draxler and Rolph, 2003). They show that the air masses arrive from land. This most probably implies that the source is anthropogenic as no extensive fires were found with FIRMS fire mapping system (FIRMS data). However, during the next 24 hours when the ship sailed east towards the Indian Ocean the back trajectories and the wind direction observed at the ship were not consistent. The observations on the ship indicate that air masses arrive from north-northwest (Figure 25 case 4) consistent with continued influence from the continent. Back trajectories (Figure 24 A-C) show an origin of the air masses from northeast suggesting that the influence from the continent should slowly decrease and no longer be present on the 19th at 19:00. At this time GEM was still enhanced above 1.5 ng m^{-3} .

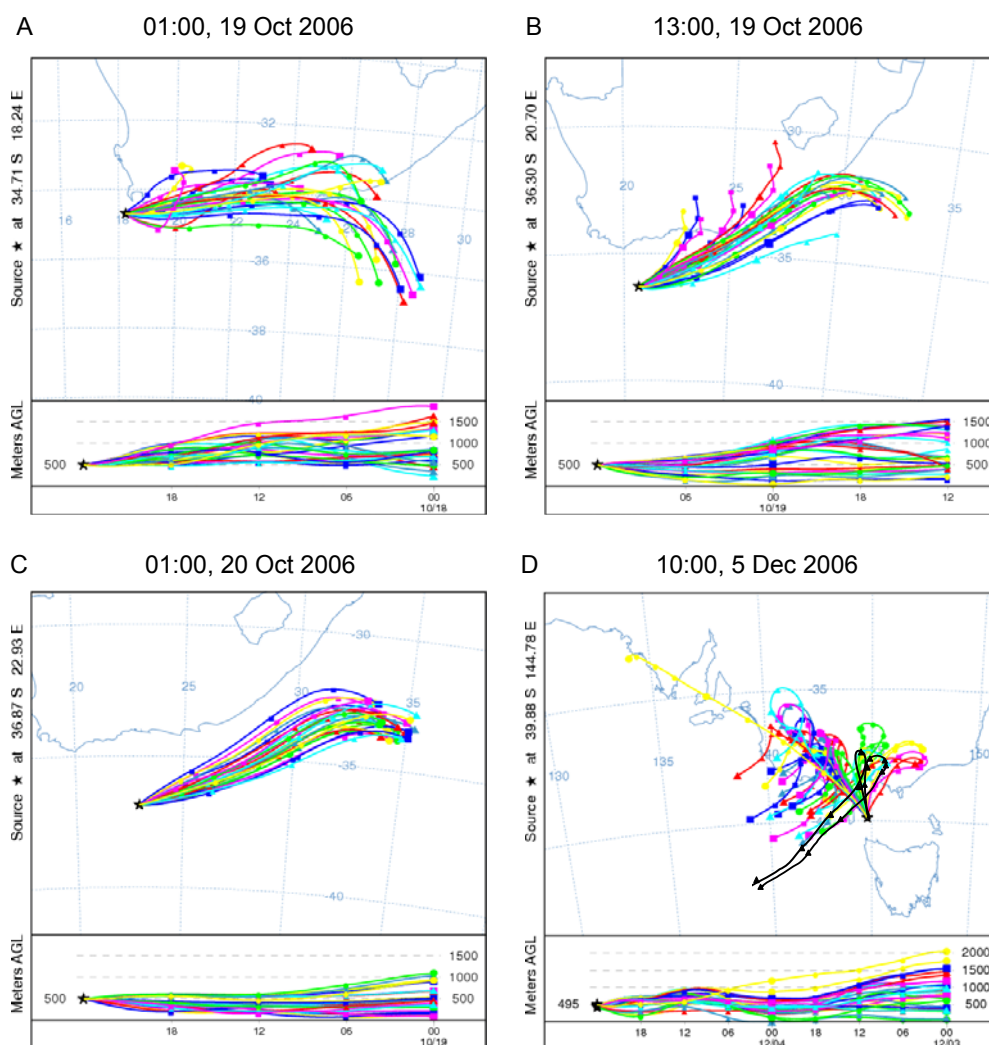


Figure 24. A-C) Waters south of Africa. HYSPLIT ensemble back trajectories from the ship at 500 m, which show the most likely wind directions (Draxler and Rolph, 2003) for the local times 19th October at A) 01:00 and B) 13:00 and C) 20th October 01:00. D) Waters southeast of Australia. HYSPLIT ensemble back trajectories at 500 m showing the origin of the air mass arriving at the ship on the 5th of December 10:00 (local time) within the 5 hour GEM peak. The black lines are single back trajectories at 100 m and 150 m and indicate the most likely trajectory close to the surface indicating Melbourne as a possible source. The location of Melbourne can be found on Figure 27. All times are local times.

Despite the discrepancies in the determination of the source area based on origin of air masses the observations of GEM, CO and O₃ concentrations all indicate that the plume intercepted at the ship was polluted. As the enhanced GEM levels were observed while the ship crossed a distance of 500 km, the outflow was not coming from a specific city but from a larger catchment area in the southern South Africa. This is not an area with large coal fired power plants. These are located further North in South Africa (Dabrowski et al., 2008). But other industries and domestic cooking at open fires as well as small scale gold mining could lead to high mercury emissions.

Melbourne anthropogenic plume

On December 5th 2006 between 6:30 and 11:30 in the waters linking the Australian mainland with Tasmania (EA leg) a five hour enhancement of GEM concentrations were recorded (1.70 ± 0.14 ng m⁻³, $n=25$, 5 min values) with peaks above 1.9 ng m⁻³ (Figure 26). Although not all species were enhanced during the entire period half hour measurements showed CO up to 100 ppb, O₃ above 25 ppb and NO₂ above 2.3 ppt as well as NO₂ contributed 80% to the total NO_x. RGM was not enhanced compared to the general level in the MBL during the cruise. Back trajectories point to an origin of the air mass in the southeastern Australian mainland (Figure 24D). A large forest fire was burning east of Melbourne on the 5th (see “Biomass burning emissions” (4.2.4)) but it seems unlikely (although not impossible) that the GEM concentrations in the plume were higher at this point than seen later. Also the ancillary data point to two different air masses signatures during this event and the one described in “Biomass burning emissions” (4.2.4). More likely the intercepted plume was from the largest city in the area with 4 million inhabitants, the city of Melbourne on the Australian mainland 180-240 km away (for the location of Melbourne see Figure 27).

Chile Anthropogenic Plume

During a 700 km voyage south of Valparaíso (CC leg) at a distance of 5-50 km from the coast of Chile (6th - 7th of February) RGM was observed at a mean concentration of $43(\pm 31)$ pg m⁻³ ($n=21$). During this period RGM did not show diurnal variations. The mean GEM concentration was $1.17(\pm 0.17)$ ng m⁻³ ($n=21$). This is significantly higher ($P = 0.01$) than a mean GEM concentration of $1.07(\pm 0.07)$ ng m⁻³ ($n=25$) measured at more southerly locations along the Chilean coast (2nd - 4th of February). During this segment CO increased relative to background (~50 ppb) to a mean concentration of $150(\pm 36)$ ppb ($n=21$). Back trajectories and the wind directions observed at the ship did not indicate an explicit area of origin for the polluted air, other than from the south along the coastline. Maximum incoming insolation reached 1000 W m⁻² and RH was on average 65% (37-85%). The RH was very low compared to the cruise's mean concentration of $79(\pm 13\%)$. Highest RHs were observed just before the ship reached Valparaíso. During these two days there was a correlation between GEM and CO ($R^2=0.18$, $P=0.07$, $n=18$); and the slope of the linear regression was 0.0018 ng m⁻³ ppb⁻¹. RGM and CO were correlated ($R^2=0.16$, $P=0.11$, $n=18$) with a linear regression slope of 0.00036 ng m⁻³ ppb⁻¹. Although the low GEM/CO ratio could indicate plumes from forest fires (Friedli et al., 2009), no extensive fires were observed along the coastline during this period (Davies et al., 2009; FIRMS data), although domestic use of wood cannot be ruled out as a source. The GEM enhancement compared to concentrations on the 2nd-4th combined with the

high RGM concentrations points to an influence from primary sources. The high RGM levels could be caused by a high fraction of RGM in the emissions as in e.g. power plant emissions from plants without purification systems (Pacyna et al., 2008). In addition the low RH may have slowed down the removal of RGM from the gas phase. Several larger cities are located in the area south of the ship (e.g. Puerto Montt, Osorno, Temuco and Concepcion) as well as smaller coastal towns. Based on the correlation of both gaseous mercury species with CO it seem reasonable to assume that GEM and RGM enhancements results from direct anthropogenic emission.

By use of the GEM/CO ratio a GEM emission of 0.05 Mmol y^{-1} was estimated to be emitted from the southern Chilean coastal area. This emission estimate represents only 25% of the AMAP 2000 estimate (Pacyna et al., 2005). By use of the RGM/CO ratio a RGM emission of $0.001 \text{ Mmol y}^{-1}$ was also estimated for the area. The AMAP 2000 estimate for RGM emissions is $0.005 \text{ Mmol y}^{-1}$ for the same area. Due to the rapid conversion of RGM to RGM_w and loss due to dry deposition combined with the distance from emission sources to the ship, a large part of the RGM emitted should be expected to be lost from the air mass before it is intercepted at the ship. The AMAP 2000 emission estimate is therefore not unreasonable for RGM, although GEM is lower than expected from the results in the AMAP inventory.

The high RGM concentrations in the air masses intercepted at the ship as well as the possible loss of around $0.004 \text{ Mmol y}^{-1}$, primarily to the coastal areas (land and MBL), indicate that both soil and aquatic systems are exposed to enhanced mercury deposition at the Chilean coast.

4.2.3 Influence of anthropogenic emissions on the MBL and ocean

Only a couple of clear anthropogenic pollution plumes extending into the MBL were encountered during the *Galathea 3* cruise. Some pollution plumes might however not have been identified due to inconsistent data. High GEM concentrations in the Sargasso Sea are an example where the information is insufficient to conclude anything (see Soerensen et al. 2010a). In other cases the signal from pollution plumes are diluted to an extent where it is hard to determine if they should be categorized as part of the global mixed pool or independent plumes.

In most cases urban point source enhancements of GEM (and in rare cases RGM) seem to dilute rapidly in the atmosphere once they are emitted (as e.g. experienced in observations when the ship entered or left harbor areas). Plumes could therefore be of greater concern as sources to the global atmospheric mercury pool than as sources to the nearby MBL. However, the low concentrations of RGM observed during most interceptions of anthropogenically polluted air masses are disturbing especially in the harbor measurements. These observations could imply that special conditions are present in the MBL (like high RH), which could influence the speed with which RGM is removed from the air. If this is the case it is not possible to determine the importance of RGM emissions and the following deposition in coastal areas without simultaneous TPM measurements. The RGM dynamics will be discussed further in "Mercury Chemistry in the MBL" (4.3).

4.2.4 Biomass burning emissions

Elevated GEM west of Angolan Coast, Africa

One incident that with great certainty could be attributed to biomass burning from African forest fires was encountered during the first part of the South African leg (SA leg Figure 17, Figure 25 case 1) north of 8°S (see Soerensen et al., 2010a). During the episode GEM concentrations were elevated with a mean of $1.70 \pm 0.06 \text{ ng m}^{-3}$ ($n=13$) and the wind direction was from the southeast (Figure 25 and Table 6). Black carbon data from the ship show elevated spectral absorption (median absorption coefficient: $1.6(\pm 1.0) \times 10^{-6} \text{ m}^{-1}$, $n=13$) compared to remote ocean sites ($0.1 \times 10^{-6} - 0.5 \times 10^{-6} \text{ m}^{-1}$). An origin of enhancements of black carbon and GEM from biomass burning is supported by observations off extensive fires at the Angolan coast (Davies et al. 2009), and by MOPITT (V3) CO satellite data (Emmons et al., 2009). MOPITT data show high CO column concentrations off the coast in the cruise track between 5°S and 13°S (See Soerensen et al., 2010a SI S6). Unfortunately CO measurements from the *Galathea 3* cruise are not available during this period. Biomass burning is likely to be the most important source of mercury to the atmosphere from Africa (Streets et al., 2009) and previous measurements during African biomass burning episodes have shown a GEM enhancement of 45% close to the source (Brunke et al., 2001). This is in good agreement with the 35% increase observed at *Vædderen* 1000 km from the source in Angola. GEM decreased as the wind direction changed to a southerly direction. Between 13°S and 27°S when the ship was no longer intercepting air from the continent GEM had decreased to $1.25 \pm 0.14 \text{ ng m}^{-3}$ ($n=37$) which is within the expected level for pristine air in the SH (Figure 25 case 2).

RGM levels were not increased relative to the rest of the cruise but did not show distinct diurnal variability either. From previous studies it is known that forest fires primarily emit GEM and TPM (Finley et al., 2009; Friedli et al., 2003a; Friedli et al., 2003b), so high levels of RGM are not expected. On the other hand neither maximum insolation (884 W m^{-2}) nor RH (74%, $n = 12$) should be at levels that would interrupt the expected diurnal variations (see "General Trends in RGM Dynamics in the MBL" (4.3.1)). But as is the case with the rest of the dataset, diurnal variations are not present during all days, even in the cases where the leg as a mean had diurnal variation.

Elevated GEM southeast of Australia

During the last part of the trip from Perth to Hobart (5th-6th December 2006) and the trip from Hobart to Sydney (8th-9th December 2006) (both EA leg) average GEM concentrations were $1.50 \pm 0.06 \text{ ng m}^{-3}$ ($n=17$) and $1.63 \pm 0.06 \text{ ng m}^{-3}$ ($n=21$), respectively (Figure 27). These periods were significantly enhanced ($p < 0.001$) compared to the period before (1-4 Dec) and after (15-17 Dec) ($1.23 \pm 0.16 \text{ ng m}^{-3}$, $n=87$). The enhancements did not coincide with enhancements of CO, which was 65.7 ppb and 68.0 ppb, respectively during the periods. No significant correlation between GEM and CO was found and CO observations were very variable (in the range of 0-116 ppb). RGM was not elevated compared to other places in the MBL (Figure 26). RGM enhancements would however not be expected if the source of the plume was biomass burning (Finley et al., 2009; Friedli et al., 2003a; Friedli et al., 2003b). Neither O₃ nor NO_x were enhanced.

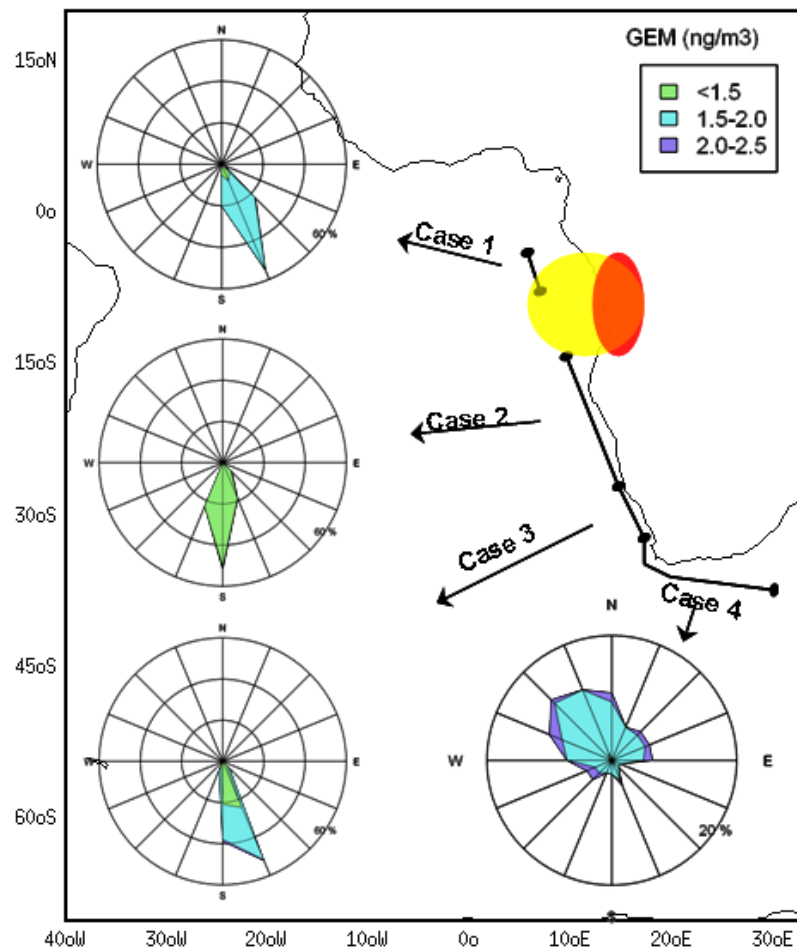


Figure 25. Four cases during the cruise close to the African continent showing GEM concentrations and wind directions during biomass burning (Case 1), free MBL (case 2) and possible anthropogenic influence (case 3 and 4).

From fire count data for December (FIRMS data) and a 2006 mercury emission inventory from Australia (Cope et al., 2009) it is known that there was a biomass burning hot spot east of Melbourne in 2006. This is not a yearly recurrent phenomenon (FIRMS data) but an exceptional large biomass burning event in 2006 (Cope et al., 2009). From fire counts and satellite photos it was found that the biomass burning coincided with the period that GEM was enhanced (Figure 27). Active fires initiate on the 2nd and have increased in strength on the 5th when the ship entered the range of the plume (based on satellite photos) and the first enhancements were observed. The fires continued until after the ship left the area of influence and reached the Sydney harbor. During this period there were also small fires close to Hobart (Tasmania) that could influence the air masses when the ship was close to Hobart on the 6th (Figure 27).

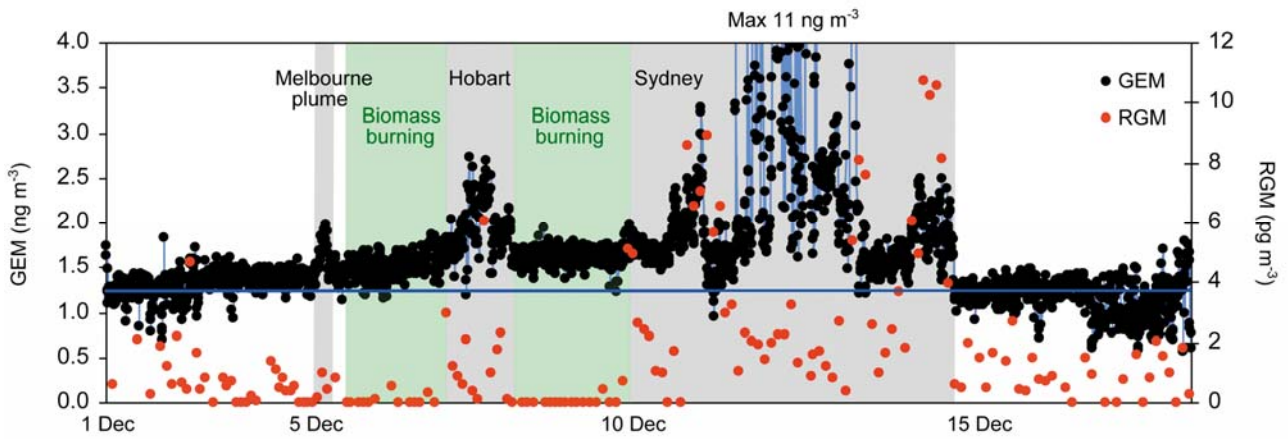


Figure 26. GEM 5 min measurements and RGM 2 h measurements from the 1st to 17th December 2006 (local time). Blue line shows baseline measurements during the period (1-4 and 15-17 December), hatched grey areas indicate influence from different anthropogenic sources and hatched green areas indicate periods of possible influence from biomass burning plumes.

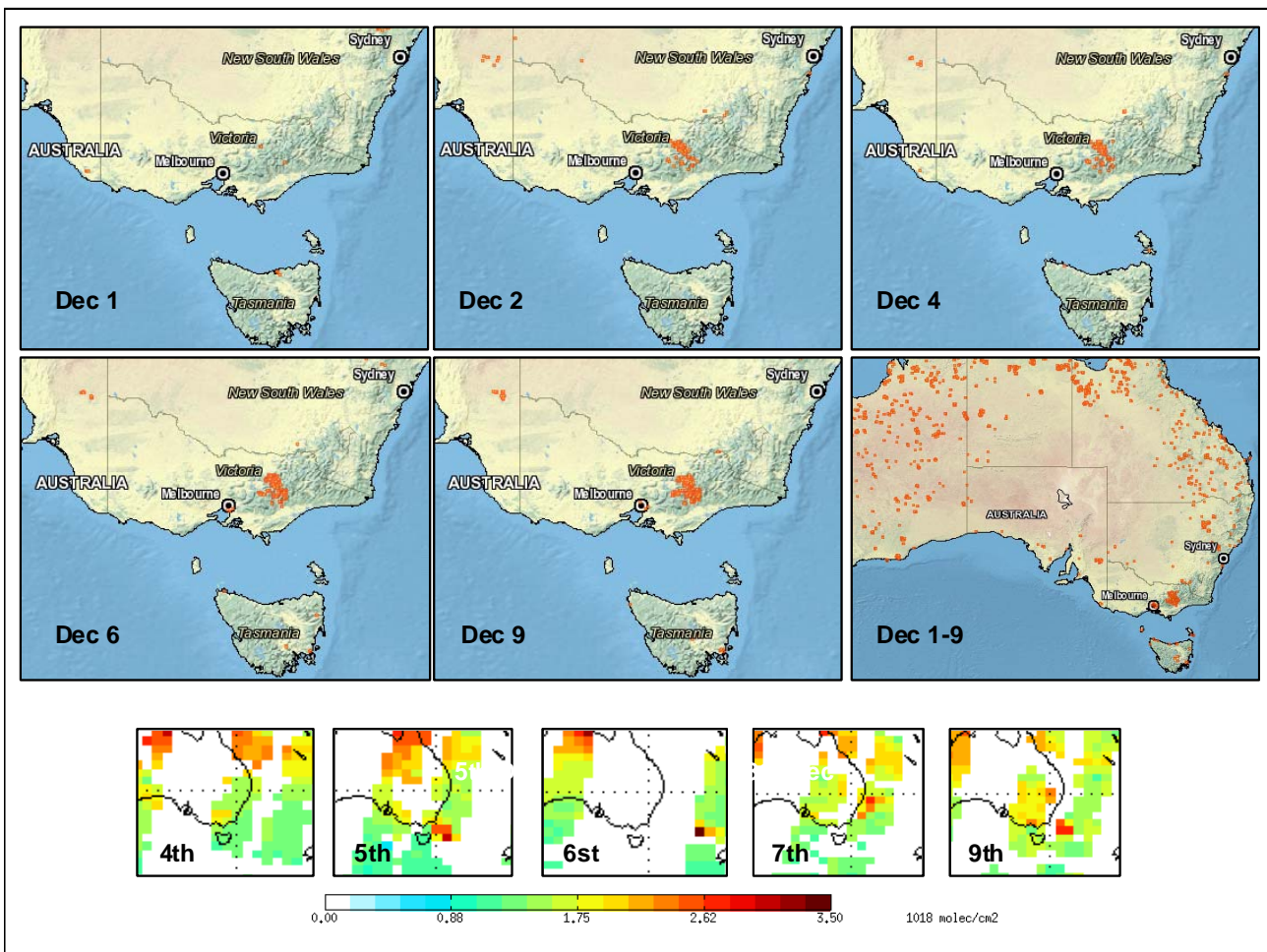


Figure 27. Fire counts and CO column data from MOPITT from the southeast of Australia. The “Web Fire mapper” fire counts indicate a large source of biomass burning east of Melbourne in southern Australia. CO column data from the MOPITT satellite indicates high CO southeast of Australia during the time the ship is in these waters (unfortunately there is no useable satellite data for all days e.g. not the 8th).

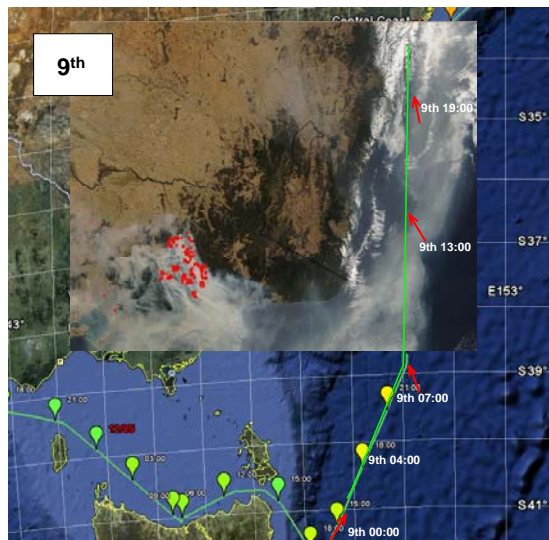
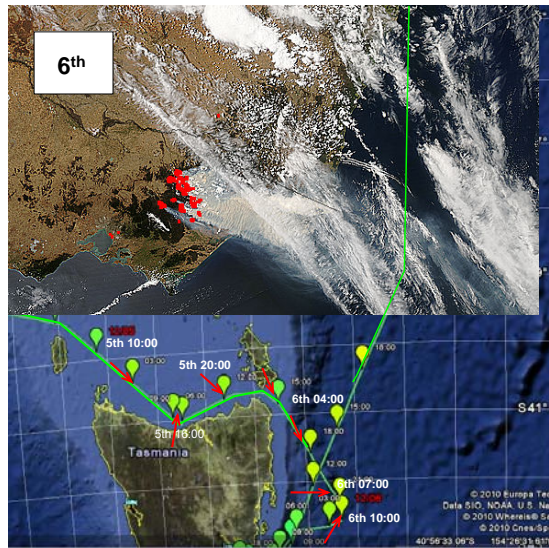


Figure 28. MODIS satellite images (FIRMS data) of the south eastern part of Australia from the 5th, 6th and 9th of December overlaid with the ship route as well as the local times and wind directions measured onboard the ship. MODIS satellite images are snapshots of the plume but can be used to get a general idea of the prevailing wind systems.

Due to the mountain range that runs along the southeastern coast of Australia and which makes forward trajectories from the biomass burning area unreliable, HYSPLIT cannot be used convincingly in this case. Instead satellite pictures are used to identify the spatial coverage of the plume. This is combined with measurements of wind directions at the ship (Figure 28). The satellite pictures show a large plume that crosses the ship's path on both the 5th and the 9th, while the overlap is less clear on the 6th.

In spite of the lack of elevated CO concentrations in ship measurements, the CO columns show elevated concentrations in the ship's path on the 5th and the 9th of December (no data is available for the 6th). This does not mean that concentrations are high in the MBL but only that enhancements are present somewhere in the atmospheric column. It is also seen that the enhancements are not as pronounced as for the CO column observed west of the Angolan coast during the interception of a biomass plume (see Soerensen et al., 2010a SI S6). A plume that extends out above the ocean could do so at an altitude that would not allow for mixing with the MBL. This would explain the high CO column data despite the lack of enhancement in the CO concentrations measured at the ship. If this scenario is true for the biomass burning plume the plume is not intercepted at the ship, and the reason for the GEM enhancements should be found elsewhere. One possibility could be that what was observed between the 1st and 17th December 2006 was air masses from different regions, e.g. terrestrial and marine, resulting in periods with measurements of different GEM levels at the ship.

Results from GEOS-Chem model simulation showing GEM in the MBL in December 2006 are presented in Figure 29. The emission hotspot due to the biomass burning is clearly seen. The model result indicates that the intensive biomass burning has the possibility to influence a very large area of southern Australia and the MBL southeast of Australia. Unfortunately the model resolution ($4^{\circ} \times 5^{\circ}$) and the proximity of the ship to the emission source does not allow for a closer comparison of model simulation to cruise observations.

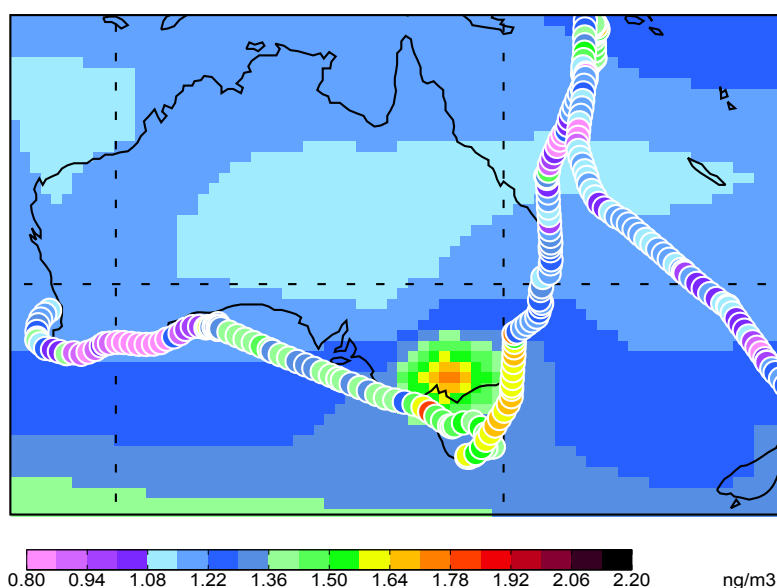


Figure 29. GEOS-Chem results for December 2006 in the MBL southeast of Australia, 2-h mean GEM concentrations from the *Galathea 3* cruise are overlaid on the map (own illustration).

Although the *Galathea 3* data is not unambiguously pointing in one direction I speculate that the enhancement of GEM in the MBL southeast of the Australian continent during December 2006 could be caused by biomass burning. If this is true, biomass burning enhances the GEM concentrations 450-550 km from the source area by 30% compared to measurements along the coast further north.

4.2.5 Influence of biomass burning emissions

Measurements from the African and Australian coast support the conclusion by others that biomass burning is an emission source of GEM (Finley et al., 2009; Friedli et al., 2009) and it is found that fires can lead to enhanced GEM concentrations in the MBL. As expected in biomass burning elevated RGM is not found.

4.2.6 Ocean evasion of Hg^0

Large Scale Evasion

The ocean is a strong source of mercury to the atmosphere. With the improved version of the GEOS-Chem model I find that the net GEM evasion flux from the ocean to the MBL is 14.7 Mmol y^{-1} (Figure 30). The estimate falls within 90% confidence limits of previous estimates that ranged between 9.7 and 20.7 Mmol y^{-1} (Sunderland and Mason, 2007) and is in the same range as the estimate found with the previous ocean module in GEOS-Chem (14.1 Mmol y^{-1}). Ocean evasion is thus approximately equal to estimated anthropogenic emissions (Mason and Sheu, 2002; Pirrone and Mason, 2009).

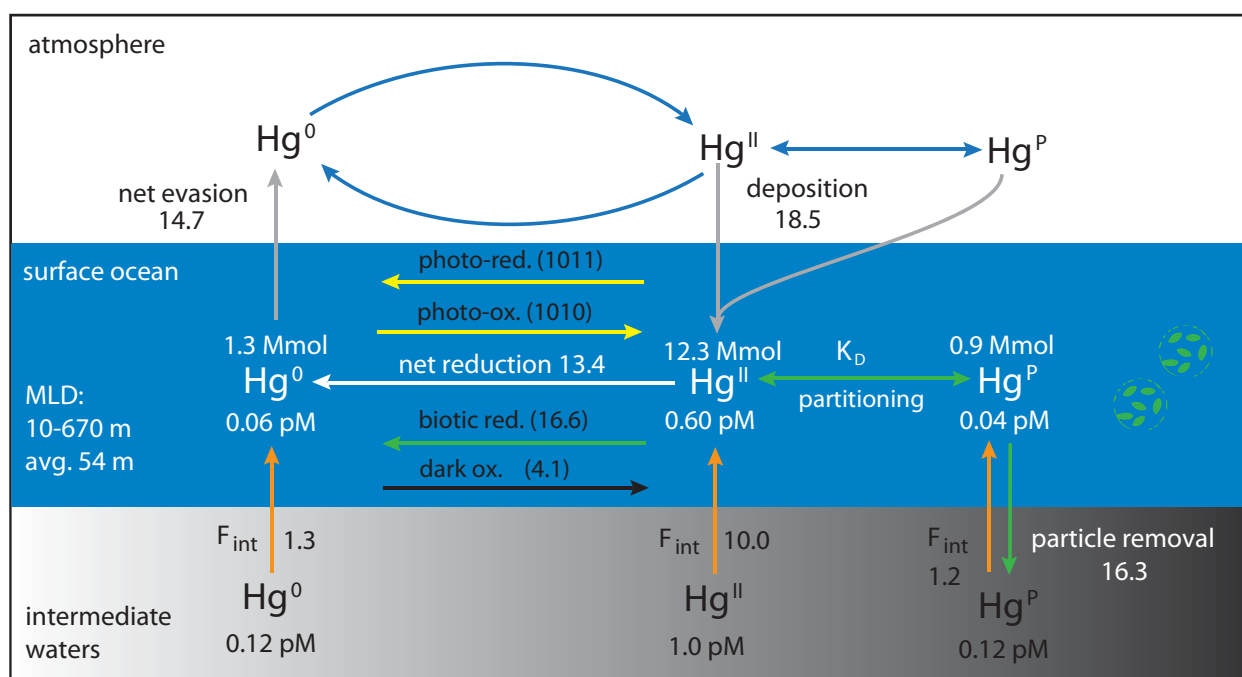


Figure 30. GEOS-Chem global budget of Hg in the surface ocean. Units are Mmol y^{-1} unless noted. F_{int} denotes net fluxes from intermediate waters through entrainment/detrainment of the mixed layer and Ekman pumping. MLD denotes mixing layer depth (illustration from Soerensen et al., 2010c).

The surface ocean is a temporary reservoir on shorter timescales. The lifetime of mercury in the surface ocean is according to the model half a year. About half of the exchange is with the atmosphere and the other half with the intermediate waters. This implies a fast response to deposi-

tions. 20% (3.8Mmol y^{-1}) of the Hg deposited to the surface ocean on a global scale will enrich the subsurface waters mainly through particle-associated scavenging of HgP from the surface ocean. Thus in a global perspective subsurface Hg concentrations are increasing.

The ocean evasion is not uniformly distributed but varies both spatially and temporally (Figure 31). Figure 20 divides the atmospheric GEM concentrations for five ocean basins in the MBL into emission contributions from the ocean and from other sources. It is seen that the ocean evasion controls the seasonal variability in the MBL. This is due to a complex set of interactions. The Atlantic Ocean (NH) is treated as a case here but for a more general discussion of drivers see Soerensen et al. (2010c). Previous efforts to model Hg air-sea exchange (Strode et al., 2007) and atmospheric transport (Dastoor and Larocque, 2004; Seigneur et al., 2004; Seigneur and Lohman, 2008; Selin et al., 2007) have been unable to reproduce high atmospheric concentrations observed in the NH MBL during previous ocean cruises (Laurier et al., 2003; Slemr et al., 2003; Temme et al., 2003b) as well as during the *Galathea 3*. Furthermore as far as I know no previous models have been validating against cruise measurements distributed into month of measurement. With the new version of the model both these trends have been reproduced for the first time (Figure 18 and Figure 19). The winter and spring peak in the North Atlantic Ocean is caused by a combination of elevated entrainment of aqueous Hg^{II} into the surface mixed layer, enhanced Ekman pumping, and high winds increasing air-sea exchange rates and subsurface Hg entrainment compared to other regions. In the Atlantic Ocean the wind driven winter mixing increases the mixed layer depth from $<50\text{m}$ the summer to more than 600m , which create high entrainment. Furthermore intermediate waters are relatively enriched in Hg compared to other oceans due to legacy Hg. Conversely, in the summer and early fall mixed layer depth decreases (detrainment) and the reservoirs of Hg^0 and reducible Hg^{II} are more limited, lowering seawater Hg^0 saturation values relative to the atmosphere. In addition, enhanced productivity in the ocean during summer months increases scavenging of HgP and can lower evasion by depleting the reducible Hg^{II} pool. I hypothesize that the observations of high concentrations in the MBL in certain months is a result of the influence from subsurface seawater Hg enrichment, reflecting the legacy of past anthropogenic inputs and that the ocean evasion controls MBL GEM concentrations through seasonally dependent evasion. The consequence of the subsurface enrichment in the Atlantic Ocean is that although globally the ocean is a net Hg sink (the ocean is enriched with 3.8Mmol y^{-1}), much of the Atlantic Ocean is a net source to the atmosphere (see Figure 19 and Soerensen et al, 2010c Figure 3F).

The same factors that control the Atlantic Ocean air-sea exchange also control the North Pacific air-sea exchange. However, the annual variability of the MLD is less pronounced in the North Pacific Ocean (Appendix D Maps of input data to the GEOS-Chem slab-ocean model), and the subsurface concentrations are less influenced by legacy anthropogenic depositions (Figure 15). This results in a less pronounced influence from ocean evasion in winter and a lower total contribution from ocean evasion to MBL GEM.

My results do not agree with Slemr et al. (2011) who propose that the main factor controlling the trend of decreasing atmospheric Hg at coastal

sites and in the MBL is changes in the long term soil reservoir, while they reject the ocean as a long term reservoir with any influence on the atmosphere Hg concentrations. They base this argument on results from surface ocean modeling that show a short lifetime of Hg in the surface ocean. My findings indicate that despite the short lifetime of mercury in the surface ocean historic enhancements of subsurface waters are very likely to influence concentrations in the atmosphere today and in the future.

The ocean is contributing around one third of the yearly emissions to the atmosphere. The fluctuating strength of the evasion controls much of the seasonal variability in the MBL in most ocean basins (Figure 20 and Figure 31). It is therefore not possible to consider the MBL as a remote location far from potential sources and the term “background concentrations” as defined by Lindberg et al. (2007) does not apply to the MBL.

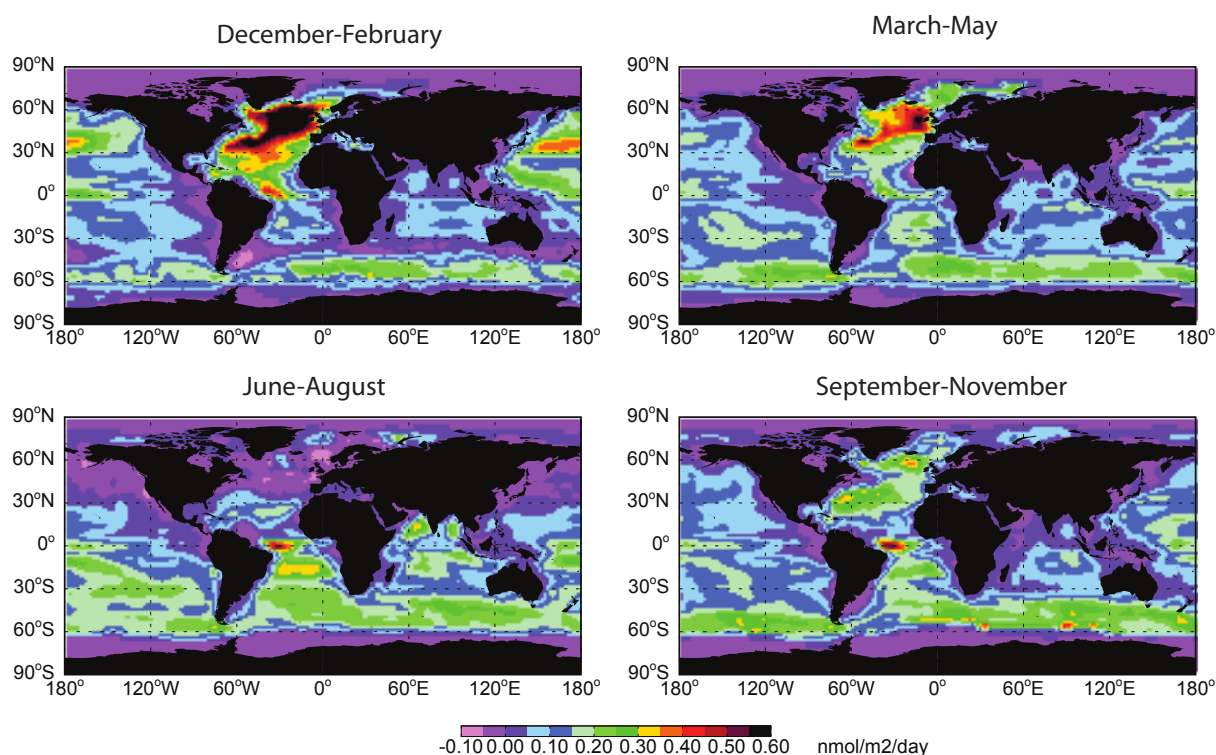


Figure 31. Seasonal variability in modeled oceanic Hg⁰ evasion for 2008 (illustration from Soerensen et al., 2010c Supporting Information).

Local Scale Evasion - Box Model Approximation

It is possible to consider a gridbox from the surface ocean and a gridbox from the lowest level in the atmosphere as a semi-closed system. By neglecting the influence of transport this two-cell system can be seen as an approximation of a box model. This exercise is done in order to investigate the drivers of the air-sea exchange of Hg⁰ on shorter timescales. For the surface ocean this is a fair approximation due to the lack of vertical flows. For the lowest atmospheric gridbox I assume that the large grid size and the uniform concentrations in the MBL on short timescales will justify this assumption.

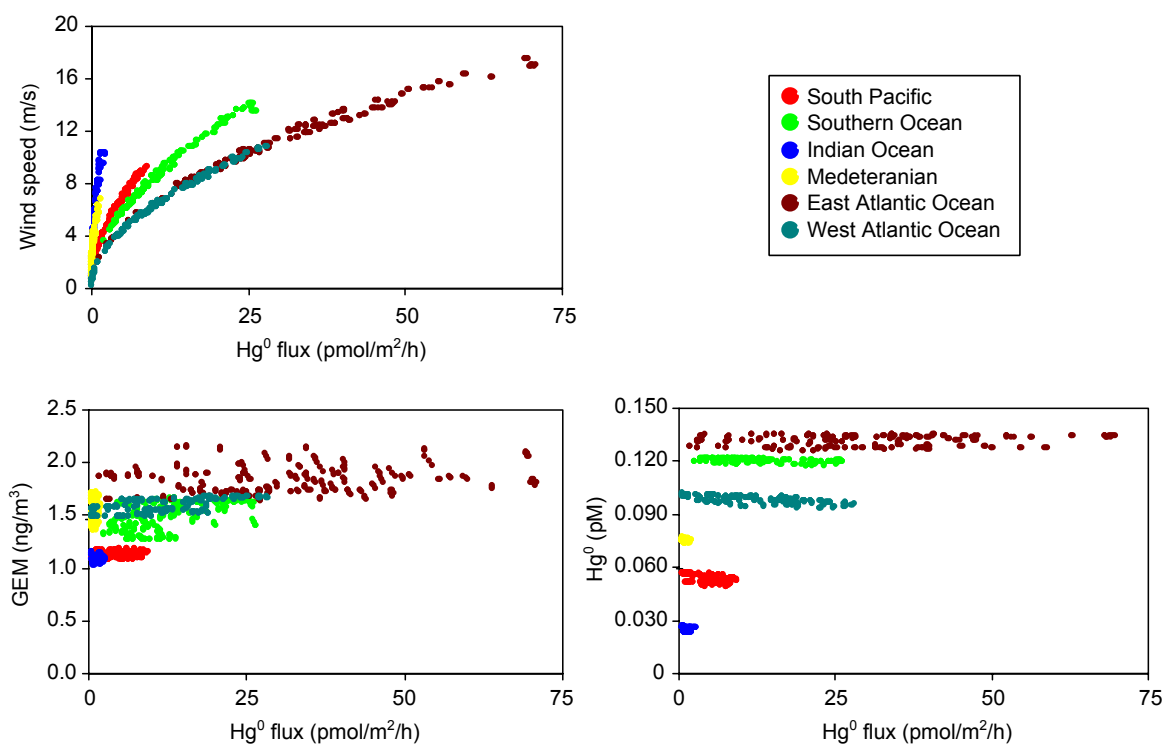


Figure 32. Example of the relationship between the ocean evasion flux and A) wind speed, B) GEM and C) aqueous Hg^0 taken from a GEOS-Chem simulation. Simulation outputs are from 6 ocean basin 14 days in January 2006. The temporal resolution is one hour. Data on temperature and insolation are not shown (own illustration).

14 days of data with 1 h resolution from 6 locations in different ocean basins and during 4 seasons (Jan, Apr, Jul, Oct) were extracted from the model (Figure 32, only January shown and Figure 33). The extracted variables were Hg^0 flux, wind speed, GEM, seawater Hg^0 , temperature and insolation. The Hg^0 flux was correlated with the other variables within sites and seasons in order to determine which variables that control the flux. The correlation within sites showed that the Hg^0 flux and the wind speed always had an $R^2 > 0.85$ while the correlation with the other variables always had an $R^2 < 0.52$. On the short timescale the evasion flux in the model is thus primarily controlled by the wind speed (as a proxy for turbulence at the air-sea interface). This implies that in the model the seawater Hg^0 is quickly replenished in the surface ocean and that a constant loss of GEM in the MBL keeps the GEM variability at a minimum despite fluctuating evasion fluxes. Although the wind speed is driving evasion on the short timescales in the model different parameters controls the flux on larger spatial scales (Figure 32) and longer timescale of months (Figure 33) for instance as the equilibrium relationship between GEM and seawater Hg^0 changes. To explore the various factors driving the evasion flux at the air-sea interface in the model, additional model parameters like subsurface inflow and reduction and oxidation flows need to be extracted and included in the analysis. This will be explored in a future study.

Local Scale Evasion – West Atlantic Ocean

Results from the four cruises in the West Atlantic Ocean carried out by Maria Andersson, Rob Mason and others at University of Connecticut (see “Appendix E Poster (Mason et al., 2009)”) show average Hg^0 fluxes in the range of 10-24 $\text{pmol m}^{-2} \text{h}^{-1}$. In Table 8 both cruise averages and GEOS-Chem model output are listed. When extracting data from the model the location and the exact cruise period were considered. Extracting the specific periods is important since the flux relies on meteorologi-

cal variables that differ on short timescale as well as annually. In the comparison it is however important to remember that observations are snapshots of the concentrations in a very limited region, while the domain of each grid represents a much larger area.

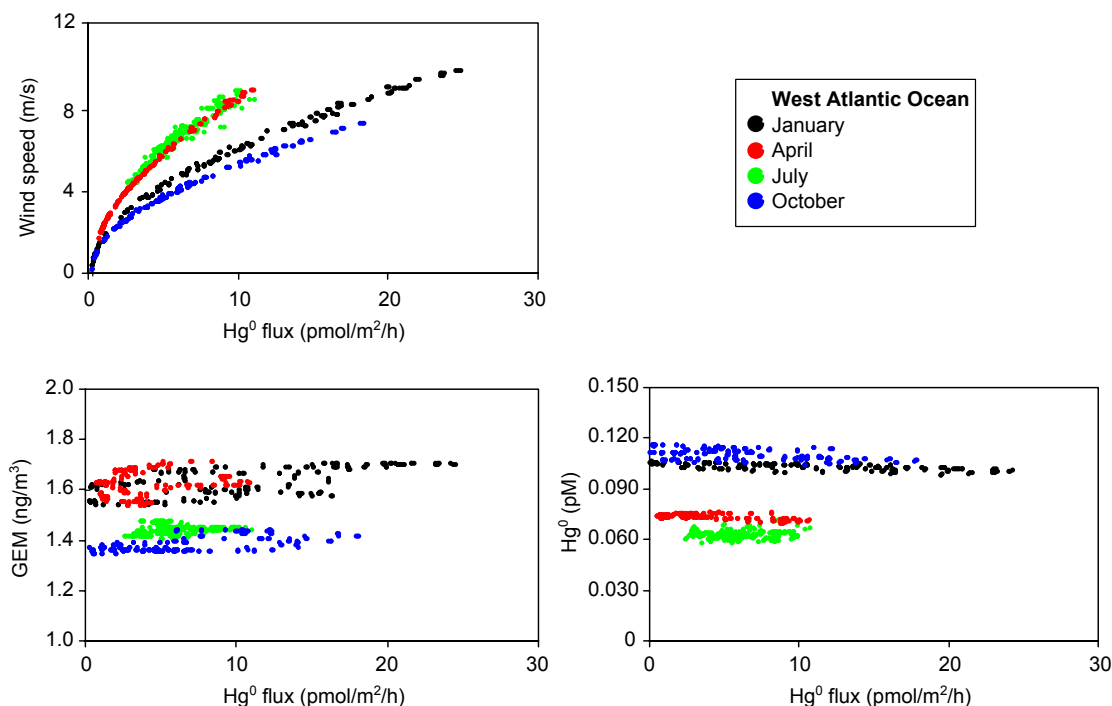


Figure 33. Example of the relationship between the Hg⁰ evasion flux and A) wind speed, B) GEM and C) seawater Hg⁰ taken from a GEOS-Chem simulation. Data is from 14 days in January, April, July and October in the West Atlantic Ocean. Model output has a temporal resolution of one hour (own illustration).

In Table 8 it is seen that the model fluxes are all lower than observations but still within 35% difference for the September 2008 (BERsep08) and September 2009 (BERsep09) cruises. To understand what drives the flux difference between observations and model the other variables given in Table 8 are examined. Average wind speeds and temperatures are comparable ($\pm 25\%$) for observations and model, except for the August 2008 (NEau08) cruise (41%). The NEau08 cruise took place close to the coast where the variability of the wind can be hard to describe with the $4^\circ \times 5^\circ$ grid size resolution of the model. Modelled estimates of the atmospheric GEM concentrations are within $\pm 5\%$ of cruise observations while seawater Hg⁰ always is underestimated by at least 20% and up to 98%. Considering the variables given in Table 8 it is reasonable to conclude that the deviations between calculated and modelled fluxes should be explained by the difference in seawater Hg⁰. For the BERsep08 and BERsep09 the underestimation of seawater Hg⁰ is around 20% and thus within a level of uncertainty that can be expected for a comparison of point specific measurements to $4^\circ \times 5^\circ$ grid sizes model simulations. For these two cruises the model does a good job reproducing observations. For the BERjun09 cruise the difference is 63% and for the NEaug08 the model predicts net deposition of Hg⁰ and not net evasion as seen in observations. By exploring the model parameterization and how it relates to specific circumstances during the cruises the drivers of the discrepancies can be found.

Table 8. Average values for four cruises in the West Atlantic Ocean.

	GEM (ng/m ³)	Hg⁰_{aq} (pM)	Flux (pmol/m ² /h)	Wind speed (m/s)	Saturation (%)	MLD (m)	Temperature (°C)
New England Aug 2008	1.4±0.2	0.140±0.060	15±20	6.4	NA	NA	NA
GEOS-Chem	1.47	0.003	-1.1	3.8	12	9.5 (E)	19.7
% difference	-5 %	98 %	NA	41 %			
Bermuda Sep 2008 (primo)	1.46	0.123	16	5.1	610	NA	27.4±1.4
GEOS-Chem	1.43	0.098	14.1	6.3	516	43.5 (E)	26.9
% difference	2 %	20 %	12 %	-24 %	15 %		2 %
Bermuda June 2009	1.43	0.120	24	7.4	530	NA	24.4±0.6
GEOS-Chem	1.41	0.044	6.8	8.3	235	15.4 (D)	26.2
% difference	1 %	63 %	72 %	-12 %	56 %		-7 %
Bermuda Sep 2009 (ultimo)		0.111	10	5.2	470	NA	28.7±0.7
GEOS-Chem	1.41	0.088	6.7	5	473	27.1 (E)	27.5
% difference		21 %	33 %	4 %	-1 %		4 %

NA = data is not available, E = entrainment is taking place during the period due to changes in the MLD, D = detrainment is taken place during the period due to changes in the MLD.

As stated above the difference in the fluxes between cruise observations and model is found in the concentrations of seawater Hg⁰ and thus in the supply of Hg to the aqueous Hg⁰ pool. During the BERjun09 cruise in June 2009 the MLD should be at a minimum at the West Atlantic Ocean (Appendix D Maps of input data to the GEOS-Chem slab-ocean model: Mixed Layer Depth). The Hg supply to the Hg⁰ pool in the surface waters therefore primarily relies on Hg entering the ocean through RGM and TPM depositions. However, just prior to the BERjun09 cruise a storm passed the area around Bermuda (Appendix E Poster (Mason et al., 2009)). The effects of this are expressed in a mean wind speed of 7.5 m s⁻¹ during the cruise, which is the highest of the four cruises. According to the climatologic monthly mean MLD used in the model (Montegut et al., 2004) the depth should be around 15 m during the cruise (see Strode et al. (2007) for an explanation of the parameterization of changes of MLD in the model). A strong storm might create enough turbulence in the water to account for the high concentrations observed during the cruise through mixing of the depleted surface water (as is observed in the model simulation) with intermediate waters of higher total Hg concentrations. Although the model use meteorological wind speeds these do not influence the climatologic MLD used and a storm will therefore not induce a change in the entrainment of Hg from the intermediate waters in the model. A passing summer storm could therefore explain the high evasion rates during the period of the cruise and why the enhanced evasion was not simulated by the model.

The 98% difference between seawater Hg⁰ concentrations during the NEau08 cruise and in the corresponding model simulation is an example that exposes a general problem with the current version of the model. It underestimates Hg⁰ in coastal areas. A reason for this is that the main Hg source to coastal and shelf regions is fluvial inputs, which are presently not included in the model but is expected to be included in the next version. My result emphasise the importance of river outputs as a source to the oceans as proposed for example by Sunderland and Mason (2007).

The model is able to present a spatial pattern that is not obtained through observations. As the ship during the cruise campaigns moves between grid boxes it is important for the understanding of average values to understand the spatial distribution predicted by the model. Figure

34 shows GEM and seawater Hg^0 concentrations as well as the Hg^0 flux. From right to left the figure represents a timeline with a seasonal dependent order from June to September. Here a seasonal recurrent pattern for the Hg^0 flux is seen as well as its dependency on the aqueous Hg^0 concentration on this monthly timescale. For an impression on how the flux will change during the four different seasons in the West Atlantic Ocean see Figure 33. On Figure 34 is also seen that where the atmospheric GEM concentrations are quite constant the seawater Hg^0 concentrations vary considerably both temporally as well as spatially. Due to the large spatial changes in the modelled concentrations, concentrations can be very abrupt between adjacent grid boxes. These steep spatial differences in the model simulation imply that a high uncertainty on the flux estimate should be expected.

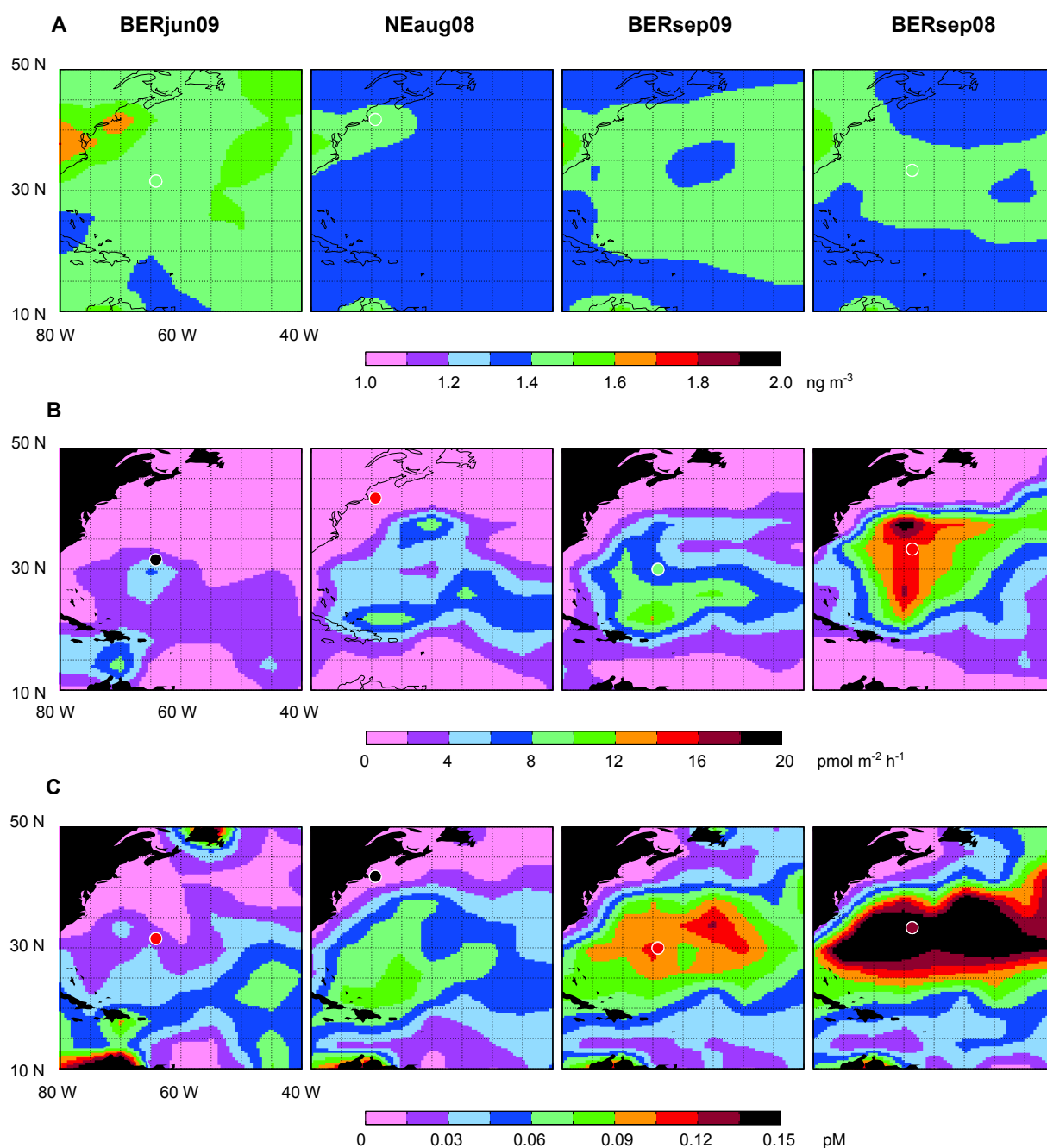


Figure 34. Model output for A) GEM, B) Hg^0 flux and C) seawater Hg^0 during the four cruise periods. Overlaid is a circle representing the mean observed concentration in the area of sampling (but not covering the entire sampling area). The maps represent the spatial and temporal changes in the model from June, August, primo September and ultimo September.

Even though the model captures the BERsep08 and BERsep09 fluxes better than the NEau08 and BERjun09 fluxes, the model has a lower Hg^0 flux than observations for all four cruises due to lower seawater Hg^0 concentrations. This supports findings during the model validation (See Sorensen et al., 2010c, Supporting Information section 1). Modeling the Hg^0 concentrations in the surface waters so they match observations leads to a global flux estimate much higher than previously suggested estimates. Furthermore, such a high flux is not supported by model simulations when considering the consequences this would have on the global deposition. This suggests that parameterization currently used to calculate the air-sea exchange from observations (see “Sinks” (2.3.5)) overestimate the flux.

The comparison between cruise observations and the GEOS-Chem model thus indicates that more studies need to be carried out on alternative parameterizations of the air-sea exchange, and that the validity of the variables included in the current parameterizations needs to be strengthened.

4.2.7 Ocean evasion of Hg^0 in areas with sea ice

An episodic transport event between the 25th and 27th of January 2007 rapidly increased GEM concentrations from 1.3 ng m⁻³ to 2.2 ng m⁻³ and RGM concentrations from below detection limit to >100 pg m⁻³ (Table 6). This event was encountered close to the coast of Antarctica in a non ice covered area (Figure 38, AC1 leg). For a thorough description of the behavior of the gaseous mercury species and the ancillary data see Sorensen et al. (2010a). RGM dynamics will be described in “Mercury Chemistry in the MBL” (4.3).

The wind direction measured at the ship as well as results from back trajectories indicate that the air mass was arriving from along the coastline and inland when GEM enhancements were highest (Figure 35). Periodically enhanced GEM concentrations have previously been observed in the Arctic summer at terrestrial sites and in the MBL (Aspmo et al., 2006; Lindberg et al., 2002; Sommar et al., 2010) and at Antarctica at terrestrial sites (Sprovieri et al., 2002; Temme et al., 2003a). These observations have been attributed to re-emissions from snow covered areas (Lindberg et al., 2002) or ocean evasion from beneath breaking sea-ice (Andersson et al., 2008a; Aspmo et al., 2006; Kirk et al., 2006). Lindberg et al. (2002) found that after the end of AMDEs in the Arctic GEM peaked in the air above the snow and remained elevated for several weeks, while snow mercury decreased by 92%. Concentrations above the snow exceeded 3 ng m⁻³. Kirk et al. (2006) on the other hand observed that reemissions were occurring continuously after each AMDE during spring. They thought it more likely that the observed elevated terrestrial concentrations after the end of the AMDE season observed by Lindberg et al. (2002) was an effect of breaking sea-ice and not snow re-emissions. They supported this with observations of enhanced sea water GEM concentrations beneath the sea ice in the Hudson Bay area during the post AMDE period. In the case of Antarctica, Temme et al. (2003a) dismissed that enhanced GEM concentrations measured at Neumayer could be attributed to reemissions from snow or ocean surfaces. They based this interpretation on the fact that they found no correlation with UV-radiation and temperature to the “infrequent and short lived” enhancement episodes

they observed. Although the enhancement episodes found by Temme et al. (2003a) does not seem to correspond well with slow continuous release from snow or water surfaces, it is seen in Figure 6 from Temme et al. (2003a) that each enhancement episode (with GEM levels up to 2 ng m^{-3}) lasts at least 24 hours. Thus observations from Temme et al. (2003a) could support the theory of a Hg^0 buildup beneath sea-ice that is released in smaller or larger event when the sea-ice breaks (Andersson et al., 2008c; Kirk et al., 2006).

The back trajectories and the wind-roses based on the wind direction measured onboard *Vædderen* during the interception of the plume with enhanced GEM concentrations indicate that the primary wind trajectory is from along the coastline passing partly ice-covered surfaces (Figure 35). This is supported by the change air mass from warmer air of marine origin (not enriched in GEM) to colder air coming from the ice and snow covered areas (enriched in GEM) (Figure 38). Thus it seems likely that the enhancement observed was from GEM recently released through volatilization from the ocean surface as sea-ice broke up.

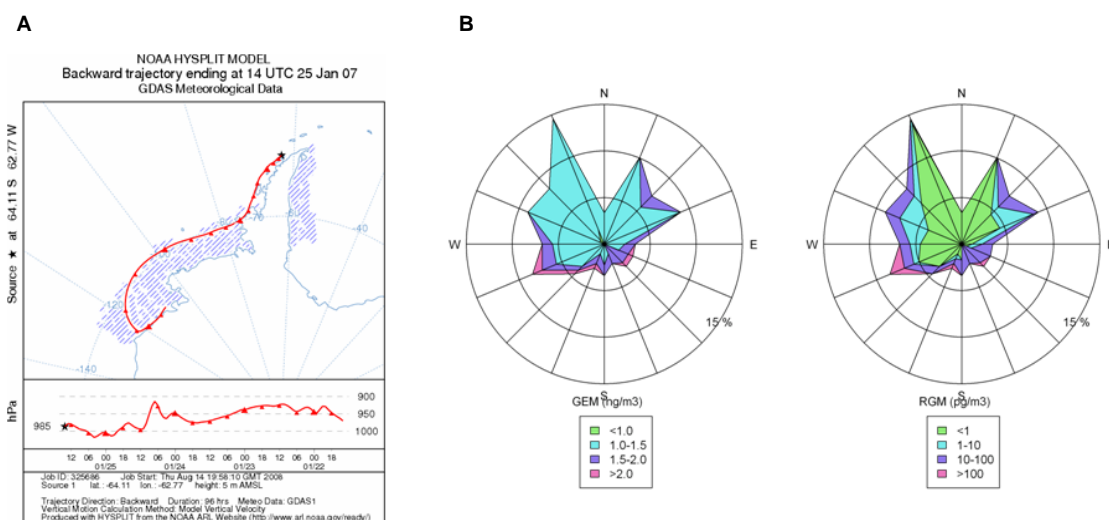


Figure 35. A) Back trajectory for the period of elevated GEM and RGM at the Antarctic coast (Draxler and Rolph, 2003). The wind direction along the back trajectory was consistent for the period with elevated GEM. Hatched areas indicate partly ice-covered sea (NATICE). B) Wind-roses show the origin of GEM and RGM during the campaign south of 60° .

4.3 Mercury Chemistry in the MBL

4.3.1 General Trends in RGM Dynamics in the MBL

During the *Galathea 3* cruise five legs (IO, WA, EA, CS, NZ) showed a statistically significant diurnal variation of RGM ($P = 0.1$) (Table 7 and Figure 36). These legs as well as the Atlantic Ocean leg also showed a positive correlation ($P = 0.1$) with radiation and negative correlation with RH (Table 7).

The 5 legs that showed statistically significant diurnal variation had a minimum mean midday peak in insolation of around 500 W m^{-2} and a mean maximum RH of around 80% (Table 9). The North Atlantic, Antarctic Ocean and Atlantic Ocean legs all lacked diurnal variations. They all have mean RH above 90% and low insolation (Table 9). Mean incoming insolation at midday (11-13, local time) during the AO leg was low

with 235 W m^{-2} (there is no observations of radiation from the North Atlantic leg). The Atlantic Ocean leg did not show a significant difference between RGM concentrations during daytime and nighttime but did show significant correlation with radiation and anticorrelation with RH ($P > 0.01$). A closer look at the data for the AO leg (Figure 37) showed that RGM variations were present when midday insolation was $>500 \text{ W m}^{-2}$ and midday RH $\leq 85\%$ but not when average midday insolation of 350 W m^{-2} and average RH below 92%. One instance with a small RGM midday peak was present at insolation of 200 W m^{-2} and RH of 91% and one instance without RGM peak when midday insolation of 500 W m^{-2} and RH just $< 90\%$ were found. This implies that the insolation and RH levels are not representing an exact rule but general tendencies. The lowest mean midday insolation for a leg with a diurnal RGM variations occurred on the New Zealand leg with mean incoming solar radiation of 493 W m^{-2} .

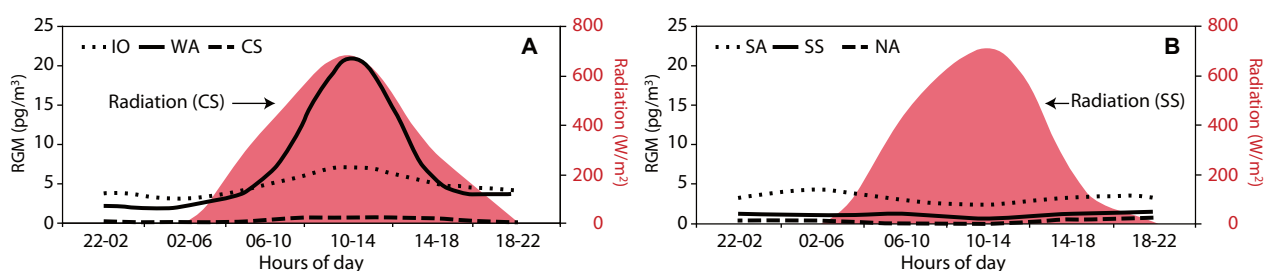


Figure 36. Examples of diurnal cycles of RGM and radiation during (A) selected legs that show diurnal variation and, (B) selected legs that do not show diurnal variation due to low radiation and RH $> 90\%$, or anthropogenic/biomass burning influence. A list of abbreviations is found in Table 7.

A lack of diurnal variation has previously been observed in the Arctic (Aspmo et al., 2006; Sommar et al., 2010) and was suggested to be a consequence of high RH, fog, and insolation below 200 W m^{-2} (Aspmo et al., 2006). The *Galathea 3* data indicate that lack of diurnal variation is not a specific Arctic occurrence but is controlled by meteorological parameters like insolation and RH. Periods without diurnal RGM variability can thus be expected at all latitudes in the MBL during specific meteorological circumstances. The *Galathea 3* data thus support the theory that photoinduced oxidation controls the production of RGM in the MBL but also emphasize the importance of RH in controlling the removal of RGM by uptake the aqueous phase at a rate that in some cases are equal to or faster than production.

Table 9. Variables that could control the diurnal variability of RGM in the MBL

Diurnal variations	Legs	Mean RH (%)	Mean midday insolation (W m^{-2})
Present	IO, WA, EA, CS, NZ	71-83	493-907
Absent	NA, AT, AO	90-93	235-339
Not considered due to uncertainty about anthropogenic influences	SS, SA, CC, (AC)		

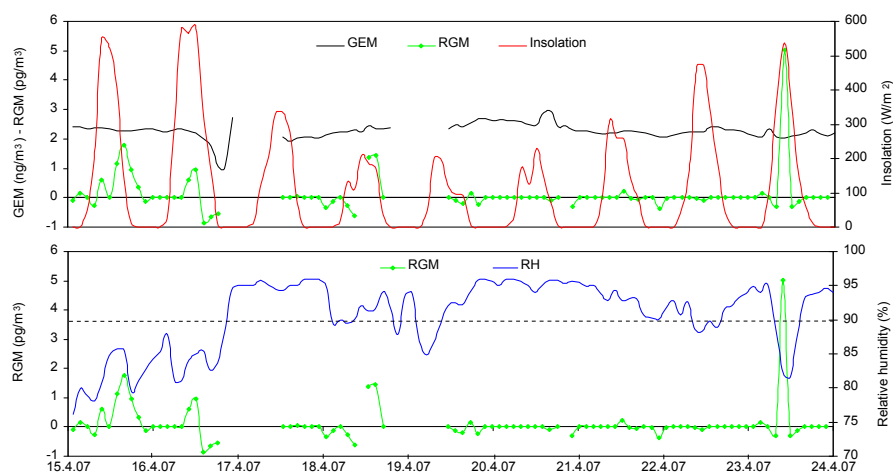


Figure 37. Atlantic Ocean leg showing the importance of insolation and relative humidity for observed diurnal RGM variations. RH of 90% is shown by the punctuated line.

4.3.2 RGM Dynamics at Antarctica

Eight RGM peaks (30-140 pg m^{-3}) were observed during the AC leg (Figure 38, punctuated lines). Six of these took place during cold conditions between the 24th and 27th (AC1), and two after (AC2). While no single common factor correlates with all of the general changes seen in the meteorology, a pattern can still be discerned. In the AC leg RGM concentrations always had a midday peak indicating the importance of insolation induced oxidation, but during AC1 4 nighttime peaks were also observed. During AC2 GEM had decreased to background concentrations and the temperature was 2-6 °C. However the oxidation potential still seemed to be large (and wind speed low), giving midday RGM peaks above 30 pg m^{-3} . This is high relative to typical MBL concentrations, $3 \pm 11 \text{ pg m}^{-3}$. During AC1 each RGM peak is seen to correlate with a small GEM peak (0.2-0.4 ng m^{-3} above baseline for the period) and a temperature between 1.4 and 2 °C, which represent an increase relative to an AC1 mean temperature of 0.9 °C. The wind speed decreased to below 3.0 m s^{-1} during all RGM peaks, and wind speed and RGM are anti-correlated ($R^2 = -0.3$, $n = 29$). This could be explained by a higher aerodynamic resistance at low wind speeds.

High concentrations of RGM have been observed in the Antarctic austral summer at Neumayer (Temme et al., 2003a) and Terra Nova Bay (Sproveri et al., 2002). At Neumayer GEM and RGM are anti-correlated (Temme et al., 2003a). I know of no previous observations of simultaneous peaks of GEM and RGM during a period where GEM in general is enhanced. The large fluctuations in RGM concentrations indicate that specific circumstances are needed for high concentrations of RGM to build up. One possibility is that RGM originates from oxidation of GEM during transport above sea ice (Temme et al., 2003a) or snow. However the four RGM peaks, correlated with maximum radiation, indicate that in these cases oxidation takes place close to the ship, where no sea ice is found (National Ice Center, www.natice.noaa.gov/ [accessed December 2009]). Relatively large diurnal variability in RGM is also seen after GEM returns to its background level and the wind no longer arrives from along the coast (AC2 in Figure 38). This indicates that the factors controlling RGM are independent of the GEM source.

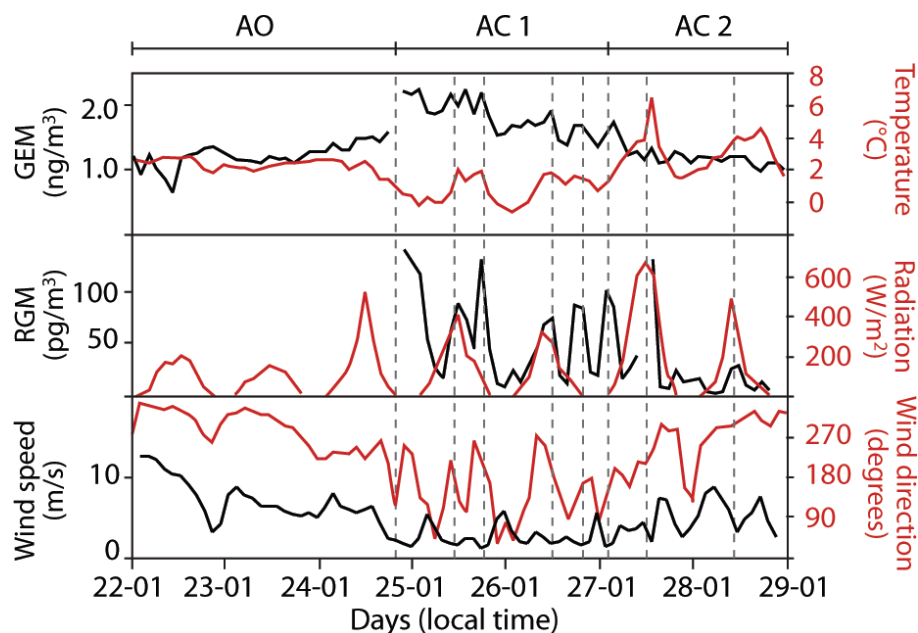


Figure 38. Concentrations of GEM, RGM, temperature, radiation, wind speed and wind direction close to the Antarctic continent. Punctuated lines indicate a recurrent pattern of peaks in RGM and GEM observed when wind speed is low; wind direction is from 130-250° and temperature shows small maxima around 2 °C.

Satellite observations do not indicate any extensive occurrence of BrO as is seen in the polar spring during AMDEs (see Figure 39). Small scale enhancement in bromine concentrations would most likely not be visible on the resolution of satellite images and one possibility could be local bromine sources. Volcanic plumes are enriched in bromine (von Glasow et al., 2009) and fumaroles are located 200 km northeast of the ship at Deception Island (Global Volcanism Program: www.volcano.si.edu/ [accessed April 2010]). However the dominant wind direction from southeast and the low wind speed during RGM events makes a scenario with enhanced bromine concentrations from volcanic emissions unlikely.

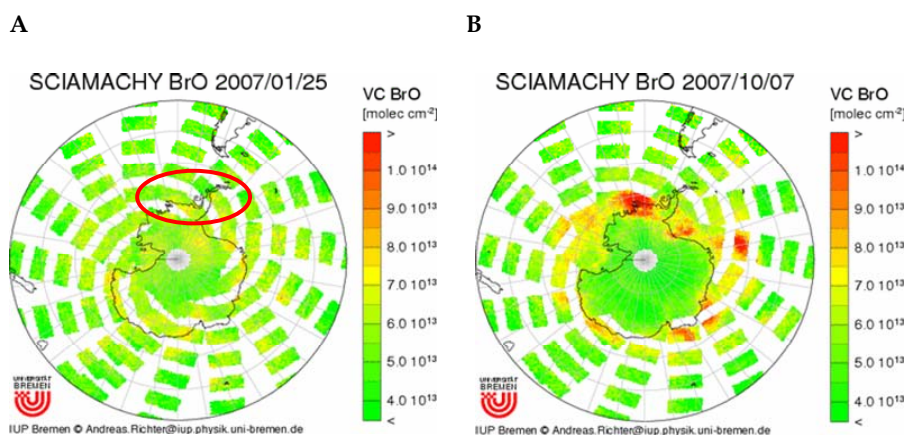


Figure 39. BrO satellite data during A) the enhanced RGM observations and B) an example of spring time concentrations in the area (data from Institute of Environmental Physics, University of Bremen: http://www.iup.uni-bremen.de/doas/scia_data_browser.htm [accessed February 2011]).

A last possibility is that normal rate of formation of RGM in the MBL in combination with very low deposition velocity at low wind speed is enough to explain the RGM build up despite a RH of $92.5 \pm 4.0\%$, ($n=49$). The insolation is quite high during the AC leg ($451 \pm 176 \text{ W m}^{-2}$, $n=5$) and

a normal rate of RGM formation would not affect GEM concentrations (Holmes et al., 2009), while a low boundary layer height might even slightly enhance concentrations. If this is true high RGM should also be observed in stagnant air arriving at the ship at night (as is the case), as the deposition would be at a minimum. A final explanation of the observed RGM concentrations close to the Antarctic coast cannot be given at this point.

5 Conclusions

In this thesis the results from the *Galathea 3* mercury data are presented together with results from my updated version of the GEOS-Chem mercury model.

The *Galathea 3* data is the largest single data set on GEM and RGM in the MBL and it is an essential collection on gaseous mercury. In addition to the results gained from the *Galathea 3* data during my work the data is an important contribution to future data ensembles and model simulations when spatial and temporal trends are to be investigated.

My update to the slab ocean module in GEOS-Chem is a unique representation of the processes in the surface ocean and it has already been incorporated into the standard code of the GEOS-Chem model. The update has helped answer long standing questions on the drivers behind mercury observations in the MBL and the new version of GEOS-Chem will be used in future biogeochemical studies on mercury dynamics.

Five underlying research questions were addressed in the thesis.

1. *Is there spatial variability of mercury in MBL?*

I found a gradient between the NH and the SH of 1.72 in the *Galathea 3* GEM concentrations, supporting previous findings of different hemispheric GEM levels. I also found that the GEM variability in the MBL within each hemisphere is higher than most published studies imply. This could be due to varying influence from continental outflow and ocean evasion (see research question 3 and 4). But periods with concentrations well below the suggested mean concentrations also imply that the lifetime of GEM in the MBL might be in the low end of previous estimates. The stable GEM concentrations within periods of days could be maintained through fast re-cycling of deposited mercury at the air-sea interface. My results imply that the term “background concentrations” in its current form cannot be used for the MBL (see research question 4).

I found that RGM concentrations do not vary a lot in the MBL and are mostly below 10 pg m⁻³. As few measurements of RGM in the MBL are available at this time this is an important result. I am for the first time able to establish that there is little variability in RGM concentrations when no outside sources influence the MBL. My results suggest that the polar areas might be an exception to this rule, in agreement with previous observations.

2. *Is there temporal variability of mercury in MBL?*

In contrast to recent suggestions I found no strong evidence for a downward trend in MBL GEM concentrations in the *Galathea 3* and West Atlantic Cruise data when compared to observations during the last decades.

Combining *Galathea 3* data on GEM concentrations from the NH Atlantic Ocean with previous cruise observations I have been able to present the first estimate for a seasonal variation of GEM in the MBL. The discovery of the strong seasonal variability has helped with the interpretation of the large variation in measured concentrations during previous cruises (see research question 4). With my new version of the GEOS-Chem model I am also able to simulate the seasonal variability in the Atlantic Ocean. This is the first time that a model is validated not only against seasonal data at terrestrial sites but also seasonal data in the MBL. I have found that the amplitude of the temporal variability in the Atlantic MBL is higher than at rural terrestrial sites and that the variability is driven by different processes in the ocean. That seasonal variability for the Atlantic Ocean is now assessable is an important contribution to future validations of global atmospheric models.

I found that diurnal variations of RGM are common in the MBL but that their presence is very dependent on meteorological variables like insolation strength and RH (see research question 5).

3. *What is the role of outflow of different continental air masses into MBL?*

I found that GEM is significantly enhanced in almost all coastal urban areas although GEM in most cases seems to rapidly dilute and mix into the global atmospheric mercury pool. In a few instances plumes from anthropogenic sources or biomass burning were encountered and I found GEM enhancements of 10-40% ($0.1-0.5 \text{ ng m}^{-3}$) but only in one case RGM enhancements. In inland urban areas $\text{RGM} > 10 \text{ pg m}^{-3}$ is commonly observed. Based on the unexpected distribution of gaseous mercury species measured in coastal urban areas I suggest that low RGM in air enriched with anthropogenically emitted GEM is not due to a lack of RGM emissions. Rather high RH at the coast causes rapid uptake of RGM into water droplets and it will therefore not be detected in measurements. Thus based on measurements it could look like plumes in the MBL contribute mostly to the global GEM pool however measurements of TPM (RGM_w) are needed before it is possible to conclude anything on the importance of RGM emissions.

4. *What is the role of ocean evasion?*

My results show that the surface ocean is very dynamic. I found that 80% of mercury deposited to the ocean will re-evade and the lifetime of Hg^0 in the surface ocean is only half a year. Ocean evasion therefore is an important source of Hg^0 to the MBL and my results show that evasion drives the seasonal variability of GEM in the MBL.

In the North Atlantic Ocean cruise observations have shown that GEM concentrations in the MBL are often higher than at rural sites at the same latitude and my results from an ensemble of cruise data have revealed that there is a seasonal dependency on GEM in the MBL. I have with the model for the first time been able to explain these observations as a cause of seasonally dependent Hg^0 evasion from the ocean driven by historic enrichment of subsurface waters. I have found that the Atlantic Ocean currently is a net source of mercury to the atmosphere. This is an important result as it implies that despite the fast equilibrium between the sur-

face ocean and the atmosphere the subsurface ocean can also influence the atmospheric concentrations. This influence could be the reason why I found no decreasing trend in MBL GEM during the *Galathea 3* cruise.

From my model simulations I have found a strong influence of ocean evasion on the MBL GEM concentrations in most ocean basins. I have found that the ocean accounts for one third of current emissions to the atmosphere but that evasions are very spatially and temporally variable. I therefore suggest that no place in the MBL can be considered a location remote from sources, even if the source is not a primary anthropogenic one. This result combined with the result from the *Galathea 3* cruise on the variability of GEM concentrations in the MBL implies that the concept of “background concentrations” does not apply to the MBL.

I compared the model to cruise observations in the West Atlantic Ocean and found that current flux parameterizations might overestimate the flux across the air-sea interface. This is an important result since it is currently not possible to measure the flux across the air-sea interface and both experimentalists and modelers rely on parameterizations to calculate flux estimates. The result emphasizes the need for a reevaluation of current used flux parameterizations.

5. *What is the role of GEM oxidation, aqueous phase RGM uptake and RGM deposition in MBL?*

My results suggest that the MBL in both hemispheres is more spatially and temporally dynamic than is currently suggested. Results with the model show that this variability is partly controlled by emission to the MBL. However measurements also indicate that rapid removal of mercury from the MBL could influence the concentrations considerably. The diurnal variations of RGM, which I found in the MBL during high insolation and average RH below 85%, indicate a photo-induced oxidation of GEM and a rapid uptake of RGM to water droplets in the air. Low RGM concentrations were observed in the harbor areas during the *Galathea 3* cruise. These observations do not agree with inland urban observations of RGM concentrations. High RH in the MBL could in most cases induce a fast uptake of RGM to droplets. From this, it follows that although low concentrations of RGM were found during the *Galathea 3* cruise these observations could mask an actual higher production of RGM than currently believed. The *Galathea 3* data is the first dataset presented on GEM and RGM from a broad range of coastal urban areas and it is imperative to follow up on these results. The possible implications are that RGM emitted in coastal urban areas will deposit rapidly and therefore be a mercury source to the coastal MBL. Furthermore GEM oxidation in the MBL might be faster than currently inferred from observations of RGM concentrations. Additional investigations into the role of RGM uptake in the water phase during high RH regimes (through Tekran TPM measurements) in both anthropogenic plumes and in the pristine MBL are needed to answer these questions.

6 Outlook

6.1 Experimental work

More laboratory experiments and analytic calculations on GEM oxidation are necessary in order to understand which species that drive the oxidation of GEM in the MBL as well as elsewhere.

One of the most important challenges in the understanding of the mercury chemistry and dynamics in the atmosphere is to discover which species constitute the “RGM” pool? What is measured with the Tekran and how do fractions of the different RGM forms vary at different locations in the atmosphere? Knowing the specific chemical forms of RGM will be one of the most important improvements to our understanding of the atmospheric processes. It will also result in important improvements to current mercury models, which at the moment attempt to simulate an Hg^{II} compound, for which the chemical form is unknown.

In recent years there have been a number of papers published with GEM data from cruise campaigns. However a much better spatial coverage of the ocean basins is needed. Recent cruise campaigns all take place in June to September while there were a few cruises in October to February in the 90ties. Very few other cruises than the *Galathea 3* have measured mercury in the MBL in March to May. To understand the seasonal variations in the MBL in both hemispheres cruise campaigns need to be distributed across the seasons.

My findings suggest that RGM could be taken up rapidly in the aqueous phase in the MBL. To understand the mercury dynamic and deposition to the MBL it is imperative to get a better understanding of the role of TPM and RGM_w in the MBL. Cruises that measure GEM, RGM and TPM during conditions similar to the ones observed during the *Galathea 3* will reveal how large the mercury burden really is in plumes and during pristine condition in the MBL. Many cruises still only measure GEM, and TPM and RGM should be prioritized on upcoming cruises.

My findings indicate that evasion from the ocean is an important source of mercury to the MBL and that 80% of mercury depositing to the ocean will leave it again through evasion. This hypothesis needs to be confirmed through simultaneous measurements of GEM (in the MBL) and Hg^0 (in the ocean) at different locations and times of year. With these observations it will be possible to determine spatial and temporal changes in the net evasion flux. Especially in the North Atlantic Ocean this could reveal how important evasion is for explaining the high GEM concentrations observed in winter and spring. To explore this, improved parameterizations of the air-sea flux are also necessary as the current parameterizations might underestimate the complexity in the exchange processes. It is furthermore very important to get more accurate information on the internal processes in the ocean.

6.2 Modeling

In order to provide guidance for policy makers to design effective regulations aimed at abating mercury contamination at global and national levels, and thereby reducing health impacts we need to take atmospheric modeling a step further and develop them into fully integrated earth system models. These should simulate mercury from emissions to its effect on consumers. To create such models the experimental work described above is essential as a good understanding of species and processes are needed to make a realistic attempt at simulating the entire system.

Several improvements to the existing version of the GEOS-Chem model will be able to provide new understanding about mercury processes as well as move the model towards a full biogeochemical model. Lateral flow of the water masses in the surface ocean will be an important improvement and will allow for fluvial inputs to the ocean from rivers to be included in the model as well. The air-sea exchange parameterization needs to be re-evaluated and a parameterization including build-up of Hg^0 beneath ice covered areas as well as release when the ice is breaking should be included. Methylmercury and dimethylmercury should also be included as species in the model as a first step of linking deposition inputs to uptake in the food web. A coupling between the current version of the GEOS-Chem model with a 3-D ocean model will allow for simulations of the long term build up of legacy mercury in the biogeochemical pool and help understand the role of the subsurface ocean as a reservoir for mercury.

7 Glossary, Acronyms and Abbreviations

The terms, acronyms and abbreviations below appear in this thesis.

AMAP - The Arctic Monitoring and Assessment Programme. One of the five Working Groups of the Arctic Council. The primary function of AMAP is to advise the governments of the eight Arctic countries (Canada, Denmark/Greenland, Finland, Iceland, Norway, Russia, Sweden and the United States) on matters relating to threats to the Arctic region from pollution, and associated issues.

AMAP 2000 Hg dataset - Global dataset of anthropogenic Hg emissions for the year 2000 with a $1^{\circ} \times 1^{\circ}$ grid resolution made available through cooperation between the Norwegian Institute for Air Research (NILU), the Arctic Monitoring and Assessment Programme (AMAP), and the Arctic Centre, University of Groningen (RuG). (Pacyna et al., 2005).

AMDE - Atmospheric Mercury Depletion Episode, name for mercury depletion episodes first observed in the Arctic in 1995.

Atlantic Ocean - referring to the Atlantic the following terminology will be used: 70-60°N is North Atlantic, 20-60°N is Atlantic and 20°N - 60°S is South Atlantic.

Background concentrations - as described by Lindberg et al. (2007) "*Global background concentration refers to the average sea-level atmospheric concentration of Hg⁰ at remote sites and is currently taken as 1.5-1.7 ng m⁻³ in the Northern Hemisphere, 1.1-1.3 ng m⁻³ in the Southern Hemisphere*"

DGM - Dissolved Gaseous Mercury. A product of Hg⁰ and Me₂Hg in water. Hg⁰ is the dominant form in the upper ocean.

DEHM - Danish Eulerian Hemispheric Model (hemispheric 3-D mercury model developed at NERI by Jesper Christensen).

DT = Detection limit - With the Tekran instrument during *Galathea 3*: RGM = 2 pg m⁻³ and GEM = 0.1 ng m⁻³

Dry deposition - process of species transport from the atmosphere to the underlying surface at their direct (without precipitation) physical-chemical interaction with elements of the underlying surface; dry deposition is of a continuous character independent of the occurrence or absence of atmospheric precipitation.

EDGAR - Emissions Database for Atmospheric Research (<http://edgar.jrc.ec.europa.eu/index.php>)

Edgar 2000 CO data - CO anthropogenic emissions estimate for the year 2000 made by EDGAR and available at the ACCENT/GEIA data portal (http://accent.aero.jussieu.fr/database_table_inventories.php).

EFSA - European Food Safety Authority

FIRMS - Fire Information for Resource Management System (<http://maps.geog.umd.edu/firms/>). FIRMS have a web fire mapping service and MODIS subset satellite photos available.

Flux - amount of mercury deposited over a defined area per a defined time interval

GEM - gaseous elemental mercury in the atmosphere. A common term for Hg⁰ in the atmosphere.

GEOS - Goddard Earth Observing System (GEOS) of the NASA Global Modeling and Assimilation Office (GMAO) (<http://gmao.gsfc.nasa.gov/systems/geos5/>).

GEOS-Chem - Global 3D atmospheric chemistry model developed by Bey et al. (2001).

Hg - mercury.

Hg⁰ - gaseous elemental mercury

Hg^{II} - divalent oxidized mercury in atmosphere or ocean

HgP - particulate bound mercury. HgP can be found both in the atmosphere and the ocean.

HYSPLIT - Hybrid Single Particle Lagrangian Integrated Trajectory Model made available by the National Oceanic and Atmospheric Administration (NOAA), United States Department of Commerce. The Hysplit model is used to make backward and forward trajectories.

MBL - marine boundary layer; the air right over the ocean surface, where exchange of mercury between the two compartments takes place;

MeHg and **Me₂Hg** - methylmercury; CH₃Hg⁺, (CH₃)₂Hg

M - metric ton - 1000 kg;

MBL - Marine Boundary Layer. It is the lowest part of the troposphere in direct contact with the ocean. The vertical mixing is strong and there are large fluctuations in temperatures, wind directions and RH. The height at typical mid-latitudes has a thickness of 300 meter but can be 50m/2000m during the right conditions in the Arctic/Tropics.

Mg - mega gram - 1000 kg

MLD - Mixed layer dept. The depth of the well mixed upper part of the ocean in which active turbulence has homogenized the water masses. The turbulence is generated by winds, cooling, or processes such as evaporation or sea ice formation, which result in an increase in salinity. Due to the changes in turbulence the MLD has seasonal variations.

Mmol - mega mol -1000 mol or 200.59 Mg

NA - not available

Natural emission - mercury input to the atmosphere, which is not connected with current or previous human activity;

NERI - National Environmental Research Institute (Aarhus University)

ng - nanogram (10⁻⁹ gram).

NH - Northern Hemisphere.

NPP - Net primary production is the part of the gross (total) primary production of organic compounds from atmospheric or aqueous carbon dioxide that is not used by the organisms for respiration production

pg - picogram (10⁻¹² gram).

ppb - parts per billion.

ppm - parts per million.

ppq - parts per quadrillion.

ppt - part per trillion.

Pre-industrial state - a conventional term implying the state of the natural mercury cycle before the beginning of human industrial activity; in Europe the beginning of a noticeable production and consumption of mercury is related to medieval centuries;

Re-emission - secondary input of mercury to the atmosphere from geochemical reservoirs (soil, sea water, fresh water bodies) where mercury has been accumulating as a result of previous and current human activity;

RGM - Reactive Gaseous Mercury or Gaseous oxidized mercury; an operationally defined term for gaseous divalent mercury compounds of the type HgXY (e.g. HgCl₂ or HgBr₂). RGM is in newer publications called GOM or Hg^{II}.

RGM_w - RGM that is taken up in water droplets as RGM_w. With the current methods of measurements RGM taken up into water droplets will be detected as TPM, but in many cases modeling papers still refer to RGM in water droplets as RGM. It is therefore convenient to have separate terms for RGM in water droplets and TPM.

RH - Relative Humidity (measured in %)

SH - Southern Hemisphere

TGM - Total Gaseous Mercury. The sum of GEM and RGM species.

TPM - Total Particulate Mercury. Mercury bound to or absorbed into particles in the atmosphere.

Wet deposition - flux of substance from the atmosphere onto the underlying surface with atmospheric precipitation

8 References

- AMAP/UNEP, Technical Background Report to the Global Atmospheric Mercury Assessment. Arctic Monitoring and Assessment Programme / UNEP Chemicals Branch. 159 pp., 2008.
- Amyot, M., G. A. Gill and F. M. M. Morel, Production and loss of dissolved gaseous mercury in coastal seawater, *Environmental Science & Technology*, 31(12), 3606-3611, 1997.
- Amyot, M., D. R. S. Lean, L. Poissant and M. R. Doyon, Distribution and transformation of elemental mercury in the St. Lawrence River and Lake Ontario, *Canadian Journal of Fisheries and Aquatic Sciences*, 57, 155-163, 2000.
- Andersson, M. E., K. Gardfeldt, I. Wangberg, F. Sprovieri, N. Pirrone and O. Lindqvist, Seasonal and daily variation of mercury evasion at coastal and off shore sites from the Mediterranean Sea, *Marine Chemistry*, 104(3-4), 214-226, 2007.
- Andersson, M. E., K. Gardfeldt and I. Wangberg, A description of an automatic continuous equilibrium system for the measurement of dissolved gaseous mercury, *Analytical and Bioanalytical Chemistry*, 391(6), 2277-2282, 2008a.
- Andersson, M. E., K. Gardfeldt, I. Wangberg and D. Stromberg, Determination of Henry's law constant for elemental mercury, *Chemosphere*, 73(4), 587-592, 2008b.
- Andersson, M. E., J. Sommar, K. Gardfeldt and O. Lindqvist, Enhanced concentrations of dissolved gaseous mercury in the surface waters of the Arctic Ocean, *Marine Chemistry*, 110(3-4), 190-194, 2008c.
- Ariya, P. A., H. Skov, M. M. L. Grage and M. E. Goodsite, Gaseous elemental mercury in the ambient atmosphere: Review of the application of theoretical calculations and experimental studies for determination of reaction coefficients and mechanisms with halogens and other reactants, *Advances in Quantum Chemistry: Applications of Theoretical Methods to Atmospheric Science*, 55, 43-55, 2008.
- Aspmo, K., P. A. Gauchard, A. Steffen, C. Temme, T. Berg, E. Bahlmann, C. Banic, A. Dommergue, R. Ebinghaus, C. Ferrari, N. Pirrone, F. Sprovieri and G. Wibetoe, Measurements of atmospheric mercury species during an international study of mercury depletion events at Ny-Alesund, Svalbard, spring 2003. How reproducible are our present methods?, *Atmospheric Environment*, 39(39), 7607-7619, 2005.
- Aspmo, K., C. Temme, T. Berg, C. Ferrari, P. A. Gauchard, X. Fain and G. Wibetoe, Mercury in the atmosphere, snow and melt water ponds in the North Atlantic Ocean during Arctic summer, *Environmental Science & Technology*, 40(13), 4083-4089, 2006.
- Ayers, G. P., R. W. Gillett, J. M. Cainey and A. L. Dick, Chloride and bromide loss from sea-salt particles in southern ocean air, *Journal of Atmospheric Chemistry*, 33(3), 299-319, 1999.

- Bagnato, E., A. Aiuppa, F. Parello, S. Calabrese, W. D'Alessandro, T. A. Mather, A. J. S. McGonigle, D. M. Pyle and I. Wangberg, Degassing of gaseous (elemental and reactive) and particulate mercury from Mount Etna volcano (Southern Italy), *Atmospheric Environment*, 41(35), 7377-7388, 2007.
- Balabanov, N. B., B. C. Shepler and K. A. Peterson, Accurate global potential energy surface and reaction dynamics for the ground state of HgBr₂, *Journal of Physical Chemistry A*, 109(39), 8765-8773, 2005.
- Banic, C. M., S. T. Beauchamp, R. J. Tordon, W. H. Schroeder, A. Steffen, K. A. Anlauf and H. K. T. Wong, Vertical distribution of gaseous elemental mercury in Canada, *Journal of Geophysical Research-Atmospheres*, 108(D9), 2003.
- Behrenfeld, M. J. and P. G. Falkowski, Photosynthetic rates derived from satellite-based chlorophyll concentration, *Limnology and Oceanography*, 42(1), 1-20, 1997.
- Bey, I., D. J. Jacob, R. M. Yantosca, J. A. Logan, B. D. Field, A. M. Fiore, Q. B. Li, H. G. Y. Liu, L. J. Mickley and M. G. Schultz, Global modeling of tropospheric chemistry with assimilated meteorology: Model description and evaluation, *Journal of Geophysical Research-Atmospheres*, 106(D19), 23073-23095, 2001.
- Biswas, A., J. D. Blum, B. Klaue and G. J. Keeler, Release of mercury from Rocky Mountain forest fires, *Global Biogeochemical Cycles*, 21(1), 2007.
- Brunke, E. G., C. Labuschagne, R. Ebinghaus, H. H. Kock and F. Slemr, Gaseous elemental mercury depletion events observed at Cape Point during 2007-2008, *Atmospheric Chemistry and Physics*, 10(3), 1121-1131, 2010.
- Brunke, E. G., C. Labuschagne and F. Slemr, Gaseous mercury emissions from a fire in the Cape Peninsula, South Africa, during January 2000, *Geophysical Research Letters*, 28(8), 1483-1486, 2001.
- Calvert, J. G. and S. E. Lindberg, Mechanisms of mercury removal by O₃ and OH in the atmosphere, *Atmospheric Environment*, 39(18), 3355-3367, 2005.
- Cerco, C. F., Phytoplankton Kinetics in the Chesapeake Bay Eutrophication Model, *Water Quality and Ecosystem Modeling*, 1, 5-49, 2000.
- Chand, D., D. Jaffe, E. Prestbo, P. C. Swartzendruber, W. Hafner, P. Weiss-Penzias, S. Kato, A. Takami, S. Hatakeyama and Y. Z. Kajii, Reactive and particulate mercury in the Asian marine boundary layer, *Atmospheric Environment*, 42(34), 7988-7996, 2008.
- Chester, R., *Marine Geochemistry*, 2nd Ed., Blackwell Science Ltd., Berlin, Germany, 506 pp., 2003.
- Cope, M. E., M. F. Hibberd, S. Lee, H. R. Malfroy, J. R. McGregor, C. P. Meyer, A. L. Morrison and P. F. Nelson, *The Transportation and Fate of Mercury in Australia: Atmospheric Transport Modelling and Dispersion*. Appendix 1 to Report RFT 100/0607 to Department of Environment, Water, Heritage & the Art, The Centre for Australian Weather and Climate Research, 60 pp., 2009.

- Cossa, D., B. Averty and N. Pirrone, The origin of methylmercury in open Mediterranean waters, *Limnology and Oceanography*, 54(3), 837-844, 2009.
- Dabrowski, J. M., P. J. Ashton, K. Murray, J. J. Leaner and R. P. Mason, Anthropogenic mercury emissions in South Africa: Coal combustion in power plants, *Atmospheric Environment*, 42(27), 6620-6626, 2008.
- Dastoor, A. P., D. Davignon, N. Theys, M. Van Roozendael, A. Steffen and P. A. Ariya, Modeling dynamic exchange of gaseous elemental mercury at polar sunrise, *Environmental Science & Technology*, 42(14), 5183-5188, 2008.
- Dastoor, A. P. and Y. Larocque, Global circulation of atmospheric mercury: a modelling study, *Atmospheric Environment*, 38(1), 147-161, 2004.
- Davies, D. K., S. Ilavajhala, M. M. Wong and C. O. Justice, Fire Information for Resource Management System: Archiving and Distributing MODIS Active Fire Data, *Ieee Transactions on Geoscience and Remote Sensing*, 47(9), 3298, 2009.
- Donohoue, D. L., D. Bauer, B. Cossairt and A. J. Hynes, Temperature and pressure dependent rate coefficients for the reaction of Hg with Br and the reaction of Br with Br: A pulsed laser photolysis-pulsed laser induced fluorescence study, *Journal of Physical Chemistry A*, 110(21), 6623-6632, 2006.
- Draxler, R. P. and G. D. Rolph, HYSPLIT (HYbrid Single-Particle Lagrangian Integrated Trajectory) Model access via NOAA ARL READY Website (<http://www.arl.noaa.gov/ready/hysplit4.html>). NOAA Air Resources Laboratory, Silver Spring, MD., 2003.
- Ebinghaus, R., C. Banic, S. Beauchamp, D. Jaffe, H. H. Kock, N. Pirrone, L. Poissant, F. Sprovieri and P. Weiss-Penzias, *Spatial Coverage and Temporal Trends of Land-Based Atmospheric Mercury Measurements in the Northern and Southern Hemispheres* in: Mercury Fate and Transport in the Global Atmosphere: Measurements, Models and Policy Implications, edited by N. Pirrone and R.P. Mason, pp. 145-167, 2009.
- Ebinghaus, R., H. H. Kock, A. M. Coggins, T. G. Spain, S. G. Jennings and C. Temme, Long-term measurements of atmospheric mercury at Mace Head, Irish west coast, between 1995 and 2001, *Atmospheric Environment*, 36(34), 5267-5276, 2002.
- Ebinghaus, R., S. G. Jennings, W. H. Schroeder, T. Berg, T. Donaghy, J. Guentzel, C. Kenny, H. H. Kock, K. Kvietkus, W. Landing, T. Muhleck, J. Munthe, E. M. Prestbo, D. Schneeberger, F. Slemr, J. Sommar, A. Urba, D. Wallschlager and Z. Xiao, International field intercomparison measurements of atmospheric mercury species at Mace Head, Ireland, *Atmospheric Environment*, 33(18), 3063-3073, 1999.
- Emmons, L. K., D. P. Edwards, M. N. Deeter, J. C. Gille, T. Campos, P. Nedelec, P. Novelli and G. Sachse, Measurements of Pollution In The Troposphere (MOPITT) validation through 2006, *Atmospheric Chemistry and Physics*, 9(5), 1795-1803, 2009.
- Engle, M. A., M. T. Tate, D. P. Krabbenhoft, J. J. Schauer, A. Kolker, J. B. Shanley and M. H. Bothner, Comparison of atmospheric mercury

- speciation and deposition at nine sites across central and eastern North America, *Journal of Geophysical Research-Atmospheres*, 115, 2010.
- Engle, M., M. Tate, D. Krabbenhoft, A. Kolker, M. Olson, E. Edgerton, J. DeWild and A. McPherson, Characterization and cycling of atmospheric mercury along the central US Gulf Coast, *Applied Geochemistry*, 23(3), 419-437, 2008.
- Engstrom, D. R., Fish respond when the mercury rises, *Proceedings of the National Academy of Sciences of the United States of America*, 104(42), 16394-16395, 2007.
- Fain, X., D. Obrist, A. G. Hallar, I. Mccubbin and T. Rahn, High levels of reactive gaseous mercury observed at a high elevation research laboratory in the Rocky Mountains, *Atmospheric Chemistry and Physics*, 9(20), 8049-8060, 2009.
- Fangohr, S. and D. K. Woolf, Application of new parameterizations of gas transfer velocity and their impact on regional and global marine CO₂ budgets, *Journal of Marine Systems*, 66(1-4), 195-203, 2007.
- Finley, B. D., P. C. Swartzendruber and D. A. Jaffe, Particulate mercury emissions in regional wildfire plumes observed at the Mount Bachelor Observatory, *Atmospheric Environment*, 43(38), 6074-6083, 2009.
- FIRMS data (Fire Information for Resource Management System); <http://maps.geog.umd.edu/firms/> (accessed September 2010).
- Fitzgerald, W. F., J. P. Kim, G. A. Gill and A. D. Hewitt, Atmospheric Cycling of Mercury Over the Pacific-Ocean, *Atmospheric Environment*, 20(10), 2075-2076, 1986.
- Fitzgerald, W. F., G. A. Gill and J. P. Kim, An Equatorial Pacific-Ocean Source of Atmospheric Mercury, *Science*, 224(4649), 597-599, 1984.
- Frew, N. M., D. M. Glover, E. J. Bock and S. J. Mccue, A new approach to estimation of global air-sea gas transfer velocity fields using dual-frequency altimeter backscatter, *Journal of Geophysical Research-Oceans*, 112(C11), 2007.
- Friedli, H. R., A. F. Arellano, S. Cinnirella and N. Pirrone, Initial Estimates of Mercury Emissions to the Atmosphere from Global Biomass Burning, *Environmental Science & Technology*, 43(10), 3507-3513, 2009.
- Friedli, H. R., L. F. Radke, R. Prescott, P. Li, J. H. Woo and G. R. Carmichael, Mercury in the atmosphere around Japan, Korea, and China as observed during the 2001 ACE-Asia field campaign: Measurements, distributions, sources, and implications, *Journal of Geophysical Research-Atmospheres*, 109(D19), 2004.
- Friedli, H. R., L. F. Radke, J. Y. Lu, C. M. Banic, W. R. Leaitch and J. I. MacPherson, Mercury emissions from burning of biomass from temperate North American forests: laboratory and airborne measurements, *Atmospheric Environment*, 37(2), 253-267, 2003a.
- Friedli, H. R., L. F. Radke, R. Prescott, P. V. Hobbs and P. Sinha, Mercury emissions from the August 2001 wildfires in Washington State and an agricultural waste fire in Oregon and atmospheric mercury budget estimates, *Global Biogeochemical Cycles*, 17(2), 2003b.

- Fu, X. W., X. B. Feng, G. Zhang, W. H. Xu, X. D. Li, H. Yao, P. Liang, J. Li, J. Sommar, R. S. Yin and N. Liu, Mercury in the marine boundary layer and seawater of the South China Sea: Concentrations, sea/air flux, and implication for land outflow, *Journal of Geophysical Research-Atmospheres*, 115, 2010.
- Gardfeldt, K., J. Sommar, R. Ferrara, C. Ceccarini, E. Lanzillotta, J. Munthe, I. Wangberg, O. Lindqvist, N. Pirrone, F. Sprovieri, E. Pesenti and D. Stromberg, Evasion of mercury from coastal and open waters of the Atlantic Ocean and the Mediterranean Sea, *Atmospheric Environment*, 37, S73-S84, 2003.
- Gardfeldt, K., X. B. Feng, J. Sommar and O. Lindqvist, Total gaseous mercury exchange between air and water at river and sea surfaces in Swedish coastal regions, *Atmospheric Environment*, 35(17), 3027-3038, 2001.
- Gill, G. A. and W. F. Fitzgerald, Vertical Mercury Distributions in the Oceans, *Geochimica et Cosmochimica Acta*, 52(6), 1719-1728, 1988.
- Gill, G. A. and K. Bruland, Mercury in the northeast Pacific Ocean (abstract), *EOS Transaction, American Geophysical Union*, 68, 1763, 1987.
- Givelet, N., F. Roos-Barraclough and W. Shotyk, Predominant anthropogenic sources and rates of atmospheric mercury accumulation in southern Ontario recorded by peat cores from three bogs: comparison with natural "background" values (past 8000 years), *Journal of Environmental Monitoring*, 5(6), 935-949, 2003.
- Goodsite, M. E., J. M. C. Plane and H. Skov, A theoretical study of the oxidation of Hg^0 to $HgBr_2$ in the troposphere, *Environmental Science & Technology*, 38(6), 1772-1776, 2004.
- Grandjean, P., H. Satoh, K. Murata and K. Eto, Adverse Effects of Methylmercury: Environmental Health Research Implications, *Environmental Health Perspectives*, 118(8), 1137-1145, 2010.
- Guentzel, J. L., R. T. Powell, W. M. Landing and R. P. Mason, Mercury associated with colloidal material in an estuarine and an open-ocean environment, *Marine Chemistry*, 55(1-2), 177-188, 1996.
- Gustafsson, M. E. R. and L. G. Franzen, Inland transport of marine aerosols in southern Sweden, *Atmospheric Environment*, 34(2), 313-325, 2000.
- Gustin, M. and D. Jaffe, Reducing the Uncertainty in Measurement and Understanding of Mercury in the Atmosphere, *Environmental Science & Technology*, 44(7), 2222-2227, 2010.
- Hammerschmidt, C. R. and W. F. Fitzgerald, Methylmercury cycling in sediments on the continental shelf of southern New England, *Geochimica et Cosmochimica Acta*, 70(4), 918-930, 2006.
- Hammerschmidt, C. R., W. F. Fitzgerald, P. H. Balcom and P. T. Visscher, Organic matter and sulfide inhibit methylmercury production in sediments of New York/New Jersey Harbor, *Marine Chemistry*, 109(1-2), 165-182, 2008.
- Hedgecock, I. M., G. A. Trunfio, N. Pirrone and F. Sprovieri, Mercury chemistry in the MBL: Mediterranean case and sensitivity studies using the

- AMCOTS (Atmospheric Mercury Chemistry over the Sea) model, *Atmospheric Environment*, 39(38), 7217-7230, 2005.
- Hedgecock, I. M. and N. Pirrone, Chasing quicksilver: Modeling the atmospheric lifetime of $\text{Hg}^0_{(g)}$ in the marine boundary layer at various latitudes, *Environmental Science & Technology*, 38(1), 69-76, 2004.
- Hedgecock, I. M., N. Pirrone, F. Sprovieri and E. Pesenti, Reactive gaseous mercury in the marine boundary layer: modelling and experimental evidence of its formation in the Mediterranean region, *Atmospheric Environment*, 37, S41-S49, 2003.
- Hertel, O. *Integrated monitoring and assessment of air pollution – Doctor's dissertation (DSc)*, National Environmental Research Institute, Aarhus University, Denmark, pp. 80, 2009.
- Holmes, C. D., D. J. Jacob, E. S. Corbitt, J. Mao, X. Yang, R. Talbot and F. Slemr, Global atmospheric model for mercury including oxidation by bromine atoms, *Atmospheric Chemistry and Physics*, 10(24), 12037-12057, 2010.
- Holmes, C. D., D. J. Jacob, R. P. Mason and D. A. Jaffe, Sources and deposition of reactive gaseous mercury in the marine atmosphere, *Atmospheric Environment*, 43(14), 2278-2285, 2009.
- Holmes, C. D., D. J. Jacob and X. Yang, Global lifetime of elemental mercury against oxidation by atomic bromine in the free troposphere, *Geophysical Research Letters*, 33(20), 2006.
- Horvat, M., *Determination of mercury and its compounds in water, sediment, soil and biological samples in: Dynamics of mercury pollution on regional and global scale*, edited by N. Pirrone and K. R. Mahaffey, pp. 153-192, Springer, New York, 2005.
- Hylander, L. D. and M. E. Goodsite, Environmental costs of mercury pollution, *Science of the Total Environment*, 368(1), 352-370, 2006.
- Hynes, A. J., D. L. Donohue, M. Goodsite and I. M. Hedgecock, *Our current understanding of major chemical and physical processes affecting mercury dynamics in the atmosphere and at the air-water/terrestrial interfaces in: Mercury Fate and Transport in the Global Atmosphere: Measurements, Models and Policy Implications*, edited by N. Pirrone and R.P. Mason, pp. 378-388, 2009.
- Jaffe, D., E. Prestbo, P. Swartzendruber, P. Weiss-Penzias, S. Kato, A. Takami, S. Hatakeyama and Y. Kajii, Export of atmospheric mercury from Asia, *Atmospheric Environment*, 39(17), 3029-3038, 2005.
- Joergensen, L. N. (eds.), *Galathea 3*, Thanning & Appel, 2008.
- Joergensen, S. E. and G. Bendoricchio, *Fundamentals of ecological modelling*, Elsevier, Oxford, 2001.
- Kara, A. B., P. A. Rochford and H. E. Hurlburt, Mixed layer depth variability over the global ocean, *Journal of Geophysical Research-Oceans*, 108(C3), 2003.
- Keeler, G. J., L. E. Gratz and K. Al-Wali, Long-term atmospheric mercury wet deposition at Underhill, Vermont, *Ecotoxicology*, 14(1-2), 71-83, 2005.

- Kerin, E. J., C. C. Gilmour, E. Roden, M. T. Suzuki, J. D. Coates and R. P. Mason, Mercury methylation by dissimilatory iron-reducing bacteria, *Applied and Environmental Microbiology*, 72(12), 7919-7921, 2006.
- Kim, J. and W. Fitzgerald, Gaseous Mercury Profiles in the Tropical Pacific-Ocean, *Geophysical Research Letters*, 15(1), 40-43, 1988.
- Kim, J. P. and W. F. Fitzgerald, Sea-Air Partitioning of Mercury in the Equatorial Pacific-Ocean, *Science*, 231(4742), 1131-1133, 1986.
- Kirk, J. L., V. L. S. Louis, H. Hintelmann, I. Lehnerr, B. Else and L. Poissant, Methylated Mercury Species in Marine Waters of the Canadian High and Sub Arctic, *Environmental Science & Technology*, 42(22), 8367-8373, 2008.
- Kirk, J. L., V. L. S. Louis and M. J. Sharp, Rapid reduction and reemission of mercury deposited into snowpacks during atmospheric mercury depletion events at Churchill, Manitoba, Canada, *Environmental Science & Technology*, 40(24), 7590-7596, 2006.
- Kock, H. H., E. Bieber, R. Ebinghaus, T. G. Spain and B. Thees, Comparison of long-term trends and seasonal variations of atmospheric mercury concentrations at the two European coastal monitoring stations Mace Head, Ireland, and Zingst, Germany, *Atmospheric Environment*, 39(39), 7549-7556, 2005.
- Lalonde, J. D., M. Amyot, J. Orvoine, F. M. M. Morel, J. C. Auclair and P. A. Ariya, Photoinduced oxidation of $Hg^{0(aq)}$ in the waters from the St. Lawrence estuary, *Environmental Science & Technology*, 38(2), 508-514, 2004.
- Lalonde, J. D., M. Amyot, A. M. L. Kraepiel and F. M. M. Morel, Photooxidation of $Hg(0)$ in artificial and natural waters, *Environmental Science & Technology*, 35(7), 1367-1372, 2001.
- Lamborg, C. H., K. R. Rolfhus, W. F. Fitzgerald and G. Kim, The atmospheric cycling and air-sea exchange of mercury species in the South and equatorial Atlantic Ocean, *Deep-Sea Research*, 46(5), 957-977, 1999.
- Landis, M. S., M. M. Lynam and R. K. Stevens, *The monitoring and modelling of Hg species in support of local, regional and global modeling*: in Dynamics of mercury pollution on regional and global scale, edited by N. Pirrone and K. R. Mahaffey, pp. 123-152, Springer, New York, 2005.
- Landis, M. S., R. K. Stevens, F. Schaedlich and E. M. Prestbo, Development and characterization of an annular denuder methodology for the measurement of divalent inorganic reactive gaseous mercury in ambient air, *Environmental Science & Technology*, 36(13), 3000-3009, 2002.
- Laurier, F. and R. Mason, Mercury concentration and speciation in the coastal and open ocean boundary layer, *Journal of Geophysical Research-Atmospheres*, 112(D6), 2007.
- Laurier, F. J. G., R. P. Mason, G. A. Gill and L. Whalin, Mercury distributions in the North Pacific Ocean - 20 years of observations, *Marine Chemistry*, 90(1-4), 3-19, 2004.
- Laurier, F. J. G., R. P. Mason, L. Whalin and S. Kato, Reactive gaseous mercury formation in the North Pacific Ocean's marine boundary layer:

A potential role of halogen chemistry, *Journal of Geophysical Research-Atmospheres*, 108(D17), 2003.

Lindberg, S., R. Bullock, R. Ebinghaus, D. Engstrom, X. B. Feng, W. Fitzgerald, N. Pirrone, E. Prestbo and C. Seigneur, A synthesis of progress and uncertainties in attributing the sources of mercury in deposition, *Ambio*, 36(1), 19-32, 2007.

Lindberg, S. E., S. Brooks, C. J. Lin, K. J. Scott, M. S. Landis, R. K. Stevens, M. Goodsite and A. Richter, Dynamic oxidation of gaseous mercury in the Arctic troposphere at polar sunrise, *Environmental Science & Technology*, 36(6), 1245-1256, 2002.

Liss, P. S. and L. Merlivat, *Air-sea exchange rates: Introduction and synthesis in: The role of Air-Sea Exchange in Geochemical Cycling*, edited by P. Buat-Menard, pp. 113-127, Reidel Publishing Company, Dordrecht, 1986.

Mahaffey, K. R., R. P. Clickner and R. A. Jeffries, Adult Women's Blood Mercury Concentrations Vary Regionally in the United States: Association with Patterns of Fish Consumption (NHANES 1999-2004), *Environmental Health Perspectives*, 117(1), 47-53, 2009.

Malcolm, E. G., G. J. Keeler and M. S. Landis, The effects of the coastal environment on the atmospheric mercury cycle, *Journal of Geophysical Research-Atmospheres*, 108(D12), 2003.

Mao, H., R. W. Talbot, J. M. Sigler, B. C. Sive and J. D. Hegarty, Seasonal and diurnal variations of Hg degrees over New England, *Atmospheric Chemistry and Physics*, 8(5), 1403-1421, 2008.

Mason, R. P., M. E. Andersson, A. L. Soerensen and E. M. Sunderland, Measurements and Modelling of the Air-Sea Exchange of Mercury (poster A51G-0197 AGU, San Francisco, USA), *AGU abstract 2009*.

Mason, R. P. and G. R. Sheu, Role of the ocean in the global mercury cycle, *Global Biogeochemical Cycles*, 16(4), 2002.

Mason, R. P., N. M. Lawson and G. R. Sheu, Mercury in the Atlantic Ocean: factors controlling air-sea exchange of mercury and its distribution in the upper waters, *Deep-Sea Research Part II-Topical Studies in Oceanography*, 48(13), 2829-2853, 2001.

Mason, R. P. and K. A. Sullivan, The distribution and speciation of mercury in the South and equatorial Atlantic, *Deep-Sea Research Part II-Topical Studies in Oceanography*, 46(5), 937-956, 1999.

Mason, R. P., K. R. Rolfhus and W. F. Fitzgerald, Mercury in the North Atlantic, *Marine Chemistry*, 61(1-2), 37-53, 1998.

Mason, R. P. and W. F. Fitzgerald, Sources, sinks and biogeochemical cycling of mercury in the ocean, *Global and Regional Mercury Cycles: Sources, Fluxes and Mass Balances*, 21, 249-272, 1996.

Mason, R. P., F. M. M. Morel and H. F. Hemond, The Role of Microorganisms in Elemental Mercury Formation in Natural-Waters, *Water Air and Soil Pollution*, 80(1-4), 775-787, 1995a.

- Mason, R. P., K. R. Rolffhus and W. F. Fitzgerald, Methylated and Elemental Mercury Cycling in Surface and Deep-Ocean Waters of the North-Atlantic, *Water Air and Soil Pollution*, 80(1-4), 665-677, 1995b.
- Mason, R. P. and W. F. Fitzgerald, The Distribution and Biogeochemical Cycling of Mercury in the Equatorial Pacific-Ocean, *Deep-Sea Research Part I-Oceanographic Research Papers*, 40(9), 1897-1924, 1993.
- Mason, R. P. and W. F. Fitzgerald, Alkylmercury Species in the Equatorial Pacific, *Nature*, 347(6292), 457-459, 1990.
- McGillis, W. R., J. B. Edson, J. E. Hare and C. W. Fairall, Direct covariance air-sea CO₂ fluxes, *Journal of Geophysical Research-Oceans*, 106(C8), 16729-16745, 2001.
- Mergler, D., H. A. Anderson, L. H. M. Chan, K. R. Mahaffey, M. Murray, M. Sakamoto and A. H. Stern, Methylmercury exposure and health effects in humans: A worldwide concern, *Ambio*, 36(1), 3-11, 2007.
- Miller, E. K., A. Vanarsdale, G. J. Keeler, A. Chalmers, L. Poissant, N. C. Kamman and R. Brulotte, Estimation and mapping of wet and dry mercury deposition across northeastern North America, *Ecotoxicology*, 14(1-2), 53-70, 2005.
- Monahan, E. C., D. E. Spiel and K. L. Davidson, *A model of marine aerosol generation via whitecaps and wave disruption in oceanic whitecaps* in: Oceanic whitecaps and their role in air-sea exchange processes, edited by E. C. Monahan and G. M. Niocaill, pp. 167-174, Reidel Publishing, Dordrecht, Holland, 1986.
- Montegut, C. D., G. Madec, A. S. Fischer, A. Lazar and D. Iudicone, Mixed layer depth over the global ocean: An examination of profile data and a profile-based climatology, *Journal of Geophysical Research-Oceans*, 109(C12), 2004.
- Munthe, J., I. Wangberg, A. Iverfeldt, O. Lindqvist, D. Stromberg, J. Sommar, K. Gardfeldt, G. Petersen, R. Ebinghaus, E. Prestbo, K. Larjava and V. Siemens, Distribution of atmospheric mercury species in Northern Europe: final results from the MOE project, *Atmospheric Environment*, 37, S9-S20, 2003.
- NATICE, National Ice Center Website; <http://www.natice.noaa.gov/> [accessed December 2009].
- Nelson, P. F., Atmospheric emissions of mercury from Australian point sources, *Atmospheric Environment*, 41(8), 1717-1724, 2007.
- Nightingale, P. D., G. Malin, C. S. Law, A. J. Watson, P. S. Liss, M. I. Liddicoat, J. Boutin and R. C. Upstill-Goddard, In situ evaluation of air-sea gas exchange parameterizations using novel conservative and volatile tracers, *Global Biogeochemical Cycles*, 14(1), 373-387, 2000.
- O'Driscoll, N. J., S. D. Siciliano, D. R. S. Lean and M. Amyot, Gross photoreduction kinetics of mercury in temperate freshwater lakes and rivers: Application to a general model of DGM dynamics, *Environmental Science & Technology*, 40(3), 837-843, 2006.
- Obrist, D., A. G. Hallar, I. Mccubbin, B. B. Stephens and T. Rahn, Atmospheric mercury concentrations at Storm Peak Laboratory in the

- Rocky Mountains: Evidence for long-range transport from Asia, boundary layer contributions, and plant mercury uptake, *Atmospheric Environment*, 42(33), 7579-7589, 2008.
- Pacyna, E. G., J. M. Pacyna, K. Sundseth, J. Munthe, K. Kindbom, S. Wilson, F. Steenhuisen and P. Maxson, Global emission of mercury to the atmosphere from anthropogenic sources in 2005 and projections to 2020, *Atmospheric Environment*, 44(20), 2487-2499, 2010.
- Pacyna, J. M., J. Munthe and S. Wilson, *Part A. Global Emissions of Mercury to the Atmosphere in: AMAP/UNEP, 2008 Technical background report to the Global Atmospheric Assessment. Arctic Monitoring and Assessment Programme / UNEP Chemicals Branch*, pp. 3-63, 2008.
- Pacyna, E. G., J. M. Pacyna, J. Fudala, E. Strzelecka-Jastrzab, S. Hlawiczka and D. Panasiuk, Mercury emissions to the atmosphere from anthropogenic sources in Europe in 2000 and their scenarios until 2020, *Science of the Total Environment*, 370(1), 147-156, 2006a.
- Pacyna, E. G., J. M. Pacyna, F. Steenhuisen and S. Wilson, Global anthropogenic mercury emission inventory for 2000, *Atmospheric Environment*, 40(22), 4048-4063, 2006b.
- Pacyna, J. M., S. Wilson and F. Steenhuisen, Spatially Distributed Inventories of Global Anthropogenic Emissions of Mercury to the Atmosphere (www.amap.no/Resources/HgEmissions/), 2005.
- Pirrone, N., S. Cinnirella, X. Feng, R. B. Finkelman, H. R. Friedli, J. Leaner, R. Mason, A. B. Mukherjee, G. B. Stracher, D. G. Streets and K. Telmer, Global mercury emissions to the atmosphere from anthropogenic and natural sources, *Atmospheric Chemistry and Physics*, 10(13), 5951-5964, 2010.
- Pirrone, N. and R. Mason (eds.), *Mercury Fate and Transport in the Global Atmosphere: Measurements, Models and Policy Implications*, pp. 182, 2009.
- Pirrone, N., R. Ferrara, I. M. Hedgecock, G. Kallos, Y. Mamane, J. Munthe, J. M. Pacyna, I. Pytharoulis, F. Sprovieri, A. Voudouri and I. Wangberg, Dynamic processes of mercury over the Mediterranean region: results from the Mediterranean Atmospheric Mercury Cycle System (MAMCS) project, *Atmospheric Environment*, 37, S21-S39, 2003.
- Poissant, L., M. Amyot, M. Pilote and D. Lean, Mercury water-air exchange over the Upper St. Lawrence River and Lake Ontario, *Environmental Science & Technology*, 34(15), 3069-3078, 2000.
- Poulain, A. J., S. M. Ni Chadhain, P. A. Ariya, M. Amyot, E. Garcia, P. G. C. Campbell, G. J. Zylstra and T. Barkay, Potential for mercury reduction by microbes in the high arctic, *Applied and Environmental Microbiology*, 73(7), 2230-2238, 2007.
- Pszenny, A. A. P., J. Moldanov, W. C. Keene, R. Sander, J. R. Maben, M. Martinez, P. J. Crutzen, D. Perner and R. G. Prinn, Halogen cycling and aerosol pH in the Hawaiian marine boundary layer, *Atmospheric Chemistry and Physics*, 4, 147-168, 2004.
- Qureshi, A., N. J. O'Driscoll, M. MacLeod, Y. M. Neuhold and K. Hungerbuhler, Photoreactions of Mercury in Surface Ocean Water: Gross Re-

action Kinetics and Possible Pathways, *Environmental Science & Technology*, 44(2), 644-649, 2010.

Radke, L. F., H. R. Friedli and B. G. Heikes, Atmospheric mercury over the NE Pacific during spring 2002: Gradients, residence time, upper troposphere lower stratosphere loss, and long-range transport, *Journal of Geophysical Research-Atmospheres*, 112(D19), 2007.

Rolfhus, K. R. and W. F. Fitzgerald, Mechanisms and temporal variability of dissolved gaseous mercury production in coastal seawater, *Marine Chemistry*, 90(1-4), 125-136, 2004.

Sander, R., W. C. Keene, A. A. P. Pszenny, R. Arimoto, G. P. Ayers, E. Baboukas, J. M. Cainey, P. J. Crutzen, R. A. Duce, G. Honninger, B. J. Huebert, W. Maenhaut, N. Mihalopoulos, V. C. Turekian and R. Van Dingenen, Inorganic bromine in the marine boundary layer: a critical review, *Atmospheric Chemistry and Physics*, 3, 1301-1336, 2003.

Scheulhammer, A. M., M. W. Meyer, M. B. Sandheinrich and M. W. Murray, Effects of environmental methylmercury on the health of wild birds, mammals, and fish, *Ambio*, 36(1), 12-18, 2007.

Schroeder, W. H., K. G. Anlauf, L. A. Barrie, J. Y. Lu, A. Steffen, D. R. Schneberger and T. Berg, Arctic springtime depletion of mercury, *Nature*, 394(6691), 331-332, 1998.

Schroeder, W. H. and J. Munthe, Atmospheric mercury - An overview, *Atmospheric Environment*, 32(5), 809-822, 1998.

Seigneur, C. and K. Lohman, Effect of bromine chemistry on the atmospheric mercury cycle, *Journal of Geophysical Research-Atmospheres*, 113(D23), 2008.

Seigneur, C., K. Vijayaraghavan, K. Lohman, P. Karamchandani and C. Scott, Global source attribution for mercury deposition in the United States, *Environmental Science & Technology*, 38(2), 555-569, 2004.

Selin, N. E., Global Biogeochemical Cycling of Mercury: A Review, *Annual Review of Environment and Resources*, 34, 43-63, 2009.

Selin, N. E. and D. J. Jacob, Seasonal and spatial patterns of mercury wet deposition in the United States: Constraints on the contribution from North American anthropogenic sources, *Atmospheric Environment*, 42(21), 5193-5204, 2008.

Selin, N. E., D. J. Jacob, R. J. Park, R. M. Yantosca, S. Strode, L. Jaegle and D. Jaffe, Chemical cycling and deposition of atmospheric mercury: Global constraints from observations, *Journal of Geophysical Research-Atmospheres*, 112(D2), 2007.

Sigler, J. M., H. Mao and R. Talbot, Gaseous elemental and reactive mercury in Southern New Hampshire, *Atmospheric Chemistry and Physics*, 9(6), 1929-1942, 2009.

Sillman, S., F. J. Marsik, K. I. Al-Wali, G. J. Keeler and M. S. Landis, Reactive mercury in the troposphere: Model formation and results for Florida, the northeastern United States, and the Atlantic Ocean, *Journal of Geophysical Research-Atmospheres*, 112(D23), 2007.

- Simpson, W. R., R. von Glasow, K. Riedel, P. Anderson, P. Ariya, J. Bottenheim, J. Burrows, L. J. Carpenter, U. Friess, M. E. Goodsite, D. Heard, M. Hutterli, H. W. Jacobi, L. Kaleschke, B. Neff, J. Plane, U. Platt, A. Richter, H. Roscoe, R. Sander, P. Shepson, J. Sodeau, A. Steffen, T. Wagner and E. Wolff, Halogens and their role in polar boundary-layer ozone depletion, *Atmospheric Chemistry and Physics*, 7(16), 4375-4418, 2007.
- Skov, H., J. H. Christensen, M. E. Goodsite, N. Z. Heidam, B. Jensen, P. Wahlin and G. Geernaert, Fate of elemental mercury in the arctic during atmospheric mercury depletion episodes and the load of atmospheric mercury to the arctic, *Environmental Science & Technology*, 38(8), 2373-2382, 2004.
- Skov, H., O. Travnikov, A. Dastoor, R. Bullock, J. H. Christensen and L. L. Soerensen, Part B. *Atmospheric Pathways, transport and fate in: AMAP/UNEP, 2008 Technical background report to the Global Atmospheric Assessment. Arctic Monitoring and Assessment Programme / UNEP Chemicals Branch*, 64-110, 2008.
- Slemr, F., E. G. Brunke, R. Ebinghaus and J. Kuss, Worldwide trend of atmospheric mercury since 1995, *Atmospheric Chemistry and Physics Discussions*, 11, 2355-2375, 2011.
- Slemr, F., E. G. Brunke, C. Labuschagne and R. Ebinghaus, Total gaseous mercury concentrations at the Cape Point GAW station and their seasonality, *Geophysical Research Letters*, 35(11), 2008.
- Slemr, F., R. Ebinghaus, P. G. Simmonds and S. G. Jennings, European emissions of mercury derived from long-term observations at Mace Head, on the western Irish coast, *Atmospheric Environment*, 40(36), 6966-6974, 2006.
- Slemr, F., E. G. Brunke, R. Ebinghaus, C. Temme, J. Munthe, I. Wangberg, W. Schroeder, A. Steffen and T. Berg, Worldwide trend of atmospheric mercury since 1977, *Geophysical Research Letters*, 30(10), 2003.
- Slemr, F., Trends in atmospheric mercury concentrations over the Atlantic Ocean and at the Wank summit, and the resulting constraints on the budget of atmospheric mercury, *Global and Regional Mercury Cycles: Sources, Fluxes and Mass Balances, Nato advanced science Institutes series, ser 2*, 21, 33-84, 1996.
- Slemr, F. and E. Langer, Increase in Global Atmospheric Concentrations of Mercury Inferred from Measurements Over the Atlantic-Ocean, *Nature*, 355(6359), 434-437, 1992.
- Smith-Downey, N. V., E. M. Sunderland and D. J. Jacob, Anthropogenic impacts on global storage and emissions of mercury from terrestrial soils: Insights from a new global model, *Journal of Geophysical Research-Biogeosciences*, 115, 2010.
- Soerensen, A. L., H. Skov, D. J. Jacob, B. T. Soerensen and M. S. Johnson, Global Concentrations of Gaseous Elemental Mercury and Reactive Gaseous Mercury in the Marine Boundary Layer, *Environmental Science & Technology*, 44(19), 7425-7430, 2010a.
- Soerensen, A. L., H. Skov, M. S. Johnson and M. Glasius, Gaseous mercury in coastal urban areas, *Environmental Chemistry*, 7(6), 537-547, 2010b.

- Soerensen, A. L., E. M. Sunderland, C. D. Holmes, D. J. Jacob, R. M. Yantosca, H. Skov, J. H. Christensen, S. A. Strode and R. P. Mason, An Improved Global Model for Air-Sea Exchange of Mercury: High Concentrations over the North Atlantic, *Environmental Science & Technology*, 44(22), 8574-8580, 2010c.
- Sommar, J., M. E. Andersson and H. W. Jacobi, Circumpolar measurements of speciated mercury, ozone and carbon monoxide in the boundary layer of the Arctic Ocean, *Atmospheric Chemistry and Physics*, 10(11), 5031-5045, 2010.
- Sprovieri, F., N. Pirrone, R. Ebinghaus, H. Kock and A. Dommergue, A review of worldwide atmospheric mercury measurements, *Atmospheric Chemistry and Physics*, 10(17), 8245-8265, 2010.
- Sprovieri, F., N. Pirrone, K. Gardfeldt and J. Sommar, Mercury speciation in the marine boundary layer along a 6000 km cruise path around the Mediterranean Sea, *Atmospheric Environment*, 37, S63-S71, 2003.
- Sprovieri, F., N. Pirrone, I. M. Hedgecock, M. S. Landis and R. K. Stevens, Intensive atmospheric mercury measurements at Terra Nova Bay in Antarctica during November and December 2000, *Journal of Geophysical Research-Atmospheres*, 107(D23), 2002.
- Steffen, A., T. Douglas, M. Amyot, P. Ariya, K. Aspmo, T. Berg, J. Bottenheim, S. Brooks, F. Cobbett, A. Dastoor, A. Dommergue, R. Ebinghaus, C. Ferrari, K. Gardfeldt, M. E. Goodsite, D. Lean, A. J. Poulain, C. Scherz, H. Skov, J. Sommar and C. Temme, A synthesis of atmospheric mercury depletion event chemistry in the atmosphere and snow, *Atmospheric Chemistry and Physics*, 8(6), 1445-1482, 2008.
- Streets, D. G., Q. Zhang and Y. Wu, Projections of Global Mercury Emissions in 2050, *Environmental Science & Technology*, 43(8), 2983-2988, 2009.
- Strode, S., L. Jaegle and S. Emerson, Vertical transport of anthropogenic mercury in the ocean, *Global Biogeochemical Cycles*, 24, 2010.
- Strode, S. A., L. Jaegle, D. A. Jaffe, P. C. Swartzendruber, N. E. Selin, C. Holmes and R. M. Yantosca, Trans-Pacific transport of mercury, *Journal of Geophysical Research-Atmospheres*, 113(D15), 2008.
- Strode, S. A., L. Jaegle, N. E. Selin, D. J. Jacob, R. J. Park, R. M. Yantosca, R. P. Mason and F. Slemr, Air-sea exchange in the global mercury cycle, *Global Biogeochemical Cycles*, 21(1), 2007.
- Stumm, W. and J. J. Morgan (eds.), *Aquatic Chemistry: Chemical Equilibria and Rates in Natural Waters*, 3rd ed., John Wiley & Sons, Inc., New York, 1996.
- Sunderland, E. M., D. P. Krabbenhoft, J. W. Moreau, S. A. Strode and W. M. Landing, Mercury sources, distribution, and bioavailability in the North Pacific Ocean: Insights from data and models, *Global Biogeochemical Cycles*, 23, 2009.
- Sunderland, E. M., M. D. Cohen, N. E. Selin and G. L. Chmura, Reconciling models and measurements to assess trends in atmospheric mercury deposition, *Environmental Pollution*, 156(2), 526-535, 2008.

- Sunderland, E. M. and R. P. Mason, Human impacts on open ocean mercury concentrations, *Global Biogeochemical Cycles*, 21(4), 2007.
- Swartzendruber, P. C., D. Chand, D. A. Jaffe, J. Smith, D. Reidmiller, L. Gratz, J. Keeler, S. Strode, L. Jaegle and R. Talbot, Vertical distribution of mercury, CO, ozone, and aerosol scattering coefficient in the Pacific Northwest during the spring 2006 INTEX-B campaign, *Journal of Geophysical Research-Atmospheres*, 113(D10), 2008.
- Swartzendruber, P. C., D. A. Jaffe, E. M. Prestbo, P. Weiss-Penzias, N. E. Selin, R. Park, D. J. Jacob, S. Strode and L. Jaegle, Observations of reactive gaseous mercury in the free troposphere at the Mount Bachelor Observatory, *Journal of Geophysical Research-Atmospheres*, 111(D24), 2006.
- Talbot, R., H. Mao, E. Scheuer, J. Dibb, M. Avery, E. Browell, G. Sachse, S. Vay, D. Blake, G. Huey and H. Fuelberg, Factors influencing the large-scale distribution of Hg degrees in the Mexico City area and over the North Pacific, *Atmospheric Chemistry and Physics*, 8(7), 2103-2114, 2008.
- Temme, C., P. Blanchard, A. Steffen, C. Banic, S. Beauchamp, L. Poissant, R. Tordon and B. Wiens, Trend, seasonal and multivariate analysis study of total gaseous mercury data from the Canadian atmospheric mercury measurement network (CAMNet), *Atmospheric Environment*, 41(26), 5423-5441, 2007.
- Temme, C., J. W. Einax, R. Ebinghaus and W. H. Schroeder, Measurements of atmospheric mercury species at a coastal site in the Antarctic and over the south Atlantic Ocean during polar summer, *Environmental Science & Technology*, 37(1), 22-31, 2003a.
- Temme, C., F. Slemr, R. Ebinghaus and J. W. Einax, Distribution of mercury over the Atlantic Ocean in 1996 and 1999-2001, *Atmospheric Environment*, 37(14), 1889-1897, 2003b.
- U.S.EPA.-IRIS, Methylmercury (MeHg); CASRN 22967-92-6 Integrated Risk Information System (US EPA), last updated 2001, 2001, Available at: <http://www.epa.gov/iris/subst/0073.htm> [accessed January 2011].
- Uitz, J., H. Claustre, A. Morel and S. B. Hooker, Vertical distribution of phytoplankton communities in open ocean: An assessment based on surface chlorophyll, *Journal of Geophysical Research-Oceans*, 111(C8), 2006.
- Urba, A., K. Kvietkus, J. Sakalys, Z. Xiao and O. Lindqvist, A New Sensitive and Portable Mercury-Vapor Analyzer Gardis-1A, *Water Air and Soil Pollution*, 80(1-4), 1305-1309, 1995.
- Vogt, R., P. J. Crutzen and R. Sander, A mechanism for halogen release from sea-salt aerosol in the remote marine boundary layer, *Nature*, 383(6598), 327-330, 1996.
- von Glasow, R., Atmospheric chemistry in volcanic plumes, *Proceedings of the National Academy of Sciences of the United States of America*, 107(15), 6594-6599, 2010.
- von Glasow, R., N. Bobrowski and C. Kern, The effects of volcanic eruptions on atmospheric chemistry, *Chemical Geology*, 263(1-4), 131-142, 2009.

- von Glasow, R., R. Sander, A. Bott and P. J. Crutzen, Modeling halogen chemistry in the marine boundary layer - 1. Cloud-free MBL, *Journal of Geophysical Research-Atmospheres*, 107(D17), 2002.
- von Glasow, R. and R. Sander, Variation of sea salt aerosol pH with relative humidity, *Geophysical Research Letters*, 28(2), 247-250, 2001.
- Wangberg, I., J. Munthe, T. Berg, R. Ebinghaus, H. H. Kock, C. Temme, E. Bieber, T. G. Spain and A. Stolk, Trends in air concentration and deposition of mercury in the coastal environment of the North Sea Area, *Atmospheric Environment*, 41(12), 2612-2619, 2007.
- Wanninkhof, R., Relationship Between Wind-Speed and Gas-Exchange Over the Ocean, *Journal of Geophysical Research-Oceans*, 97(C5), 7373-7382, 1992.
- Wanninkhof, R. and W. R. McGillis, A cubic relationship between air-sea CO₂ exchange and wind speed, *Geophysical Research Letters*, 26(13), 1889-1892, 1999.
- Weiss-Penzias, P., D. Jaffe, P. Swartzendruber, W. Hafner, D. Chand and E. Prestbo, Quantifying Asian and biomass burning sources of mercury using the Hg/CO ratio in pollution plumes observed at the Mount Bachelor Observatory, *Atmospheric Environment*, 41(21), 4366-4379, 2007.
- Weiss-Penzias, P., D. A. Jaffe, A. McClintick, E. M. Prestbo and M. S. Landis, Gaseous elemental mercury in the marine boundary layer: Evidence for rapid removal in anthropogenic pollution, *Environmental Science & Technology*, 37(17), 3755-3763, 2003.
- Weiss-Penzias, P., D. A. Jaffe, P. Swartzendruber, J. B. Dennison, D. Chand, W. Hafner and E. Prestbo, Observations of Asian air pollution in the free troposphere at Mount Bachelor Observatory during the spring of 2004, *Journal of Geophysical Research-Atmospheres*, 111(D10), 2006.
- Whalin, L., E. H. Kim and R. Mason, Factors influencing the oxidation, reduction, methylation and demethylation of mercury species in coastal waters, *Marine Chemistry*, 107(3), 278-294, 2007.
- Wilke, C. R. and P. Chang, Correlation of Diffusion Coefficients in Dilute Solutions, *Aiche Journal*, 1(2), 264-270, 1955.
- Witt, M. L. I., T. A. Mather, A. R. Baker, C. J. de Hoog and D. M. Pyle, Atmospheric trace metals over the south-west Indian Ocean: Total gaseous mercury, aerosol trace metal concentrations and lead isotope ratios., *Marine Chemistry*, 2010.
- Witt, M. L. I., T. A. Mather, D. M. Pyle, A. Aiuppa, E. Bagnato and V. I. Tsanev, Mercury and halogen emissions from Masaya and Telica volcanoes, Nicaragua, *Journal of Geophysical Research-Solid Earth*, 113(B6), 2008.
- Woolf, D. K., Parametrization of gas transfer velocities and sea-state-dependent wave breaking, *Tellus Series B-Chemical and Physical Meteorology*, 57(2), 87-94, 2005.
- Wozniak, B. and J. Dera (eds.), *Light Absorption in Sea Water*, Springer, New York, 2007.

- Xia, C. H., Z. Q. Xie and L. G. Sun, Atmospheric mercury in the marine boundary layer along a cruise path from Shanghai, China to Prydz Bay, Antarctica, *Atmospheric Environment*, 44(14), 1815-1821, 2010.
- Yang, X., R. A. Cox, N. J. Warwick, J. A. Pyle, G. D. Carver, F. M. O'Connor and N. H. Savage, Tropospheric bromine chemistry and its impacts on ozone: A model study, *Journal of Geophysical Research-Atmospheres*, 110(D23), 2005.
- Zha, D. L. and L. A. Xie, A Practical Bi-parameter Formula of Gas Transfer Velocity Depending on Wave States, *Journal of Oceanography*, 66(5), 663-671, 2010.

9 Appendix A List of Papers

9.1 Enclosed peer reviewed papers

Soerensen, A. L., H. Skov, D. J. Jacob, B. T. Soerensen and M. S. Johnson, Global Concentrations of Gaseous Elemental Mercury and Reactive Gaseous Mercury in the Marine Boundary Layer, *Environmental Science & Technology*, 44(19), 7425-7430, 2010a.

Soerensen, A. L., H. Skov, M. S. Johnson and M. Glasius, Gaseous mercury in coastal urban areas, *Environmental Chemistry*, 7(6), 537-547, 2010b.

Soerensen, A. L., E. M. Sunderland, C. D. Holmes, D. J. Jacob, R. M. Yantosca, H. Skov, J. H. Christensen, S. A. Strode and R. P. Mason, An Improved Global Model for Air-Sea Exchange of Mercury: High Concentrations over the North Atlantic, *Environmental Science & Technology*, 44(22), 8574-8580, 2010c.

9.2 Papers in preparation

Soerensen, A.L., Andersson, M., Mason, R.M., Sunderland, E.M. (in prep), Measurement and modeling of the air-sea exchange of mercury species in the vicinity of Bermuda, (2011).

9.3 Talks and posters (first author)

Soerensen, A.L., E.M. Sunderland, H. Skov, J.H. Christensen, C.D. Holmes, D.J. Jacob, *Including exchange with the ocean in a global atmospheric mercury model*, GLOREAM-Eurosap 2011 workshop, Copenhagen, Denmark, 26.01.2011-28.01.2011. Talk

Soerensen, A.L., H. Skov, M. Glasius, J.H. Christensen, E.M. Sunderland, D.J. Jacob, C.D. Holmes, B.S. Corbitt, M.S. Johnson, *Mercury in the Marine Boundary Layer: Measurements and Modeling*, University of Washington, Seattle, USA, 25.10.2010. Talk

Soerensen, A.L., H. Skov, M.S. Johnson, *The effect of anthropogenic pollution on the fractionation of gaseous mercury in coastal urban areas: Modeling observations*, iCACGP-IGAC, Halifax, Canada, 16.7.2010 - 20.7.2010. Poster

Soerensen, A.L., *Mercury dynamics in atmosphere and ocean*, Annual meeting of the Danish Chemical Society, Odense, Denmark, 4.6.2010. Invited talk

Soerensen, A.L., H. Skov, M.S. Johnson, *Summer peaks of GEM and RGM at the Antarctic coast*, IPY-2010, Oslo, Norway, 8.6.2010 - 12.6.2010. Poster

Soerensen, A.L., E.M. Sunderland, H. Skov, C.D. Holmes, D.J. Jacob, *Seasonality of mercury in the Atlantic marine boundary layer*, EGU-2010, Vienna, Austria 2.5.2010-8.5.2010. Talk

Soerensen, A.L., H. Skov, M.S. Johnsson, *Gaseous elemental mercury and reactive gaseous mercury in coastal urban areas*, EGU-2010, Vienna, Austria, 2.5.2010 – 8.5.2010. Poster

Soerensen, A.L., E.M. Sunderland, H. Skov, C.D. Holmes, D.J. Jacob, *Modeling mercury in the Ocean and it's effect on the Marine boundary layer*, ICMPG-09, Guiyang, China 7.6.2009-12.6.2009. Talk

Soerensen, A.L., H. Skov, J.H. Christensen, C.D. Holmes, D.J. Jacob, A. Steffen, M.S. Johnson, B.T. Soerensen, *The global Distribution of GEM and RGM Concentrations in the marine Boundary Layer*, INTROP (Tropospheric Chemistry conference), Portoroz, Slovenia 14.4.2009-17.4.2009. Poster

Soerensen, A.L., *Mercury in the Marine Boundary Layer*, Group Meeting presentation, Harvard University, Cambridge, March 2009. Talk

Soerensen, A.L., H. Skov, A. Steffen, M.S. Johnson B. Jensen, C. Christoffersen, H. Madsen, B.T. Soerensen, *Background concentrations of gaseous mercury measured in the marine boundary layer*, European Research Course on Atmospheres, Grenoble, France, 12.01.2009 – 13.02.2009. Talk and poster

Soerensen, A.L., H. Skov, M. Glasius, M.S. Johnson, J.H. Christensen, B. Jensen, C. Christoffersen, H.W. Madsen, A. Steffen, B.T. Sørensen, O.J. Nielsen, *Shipborne measurements of Mercury in the Marine Boundary Layer*, AGU Fall Meeting 2008, San Francisco 15.12.2008 – 19.12.2008. Poster

Soerensen, A.L., H. Skov., M. Glasius, M.S. Johnson, J.H. Christensen, O.J. Nielsen, A. Steffen, B.T. Sørensen, D.J. Jacob, *Distribution of Mercury in the Marine Troposphere*, (in Danish), Galathea-3 seminar. Hosted by the Ministry of Science Technology and Innovation, Copenhagen, 24.10.2008. Talk

Soerensen, A.L., H. Skov, J.H. Christensen, M. Glasius, *The dynamic of Mercury in the troposphere*, 9 udg., Helsingør, 6.6.2008 - 8.6.2008. Talk

9.4 Popular science publications and educational material

Soerensen, A.L., H. Skov, J.H. Christensen, S. Høgslund, M. Badger, *Kviksølv i luften*, 2009, Educational material to the website VirtuelGalathea (<http://virtuelgalathea3.dk/node/945>)

Soerensen, A.L., *A world of possibilities – Possibilities in the world, 2nd letter from Harvard* (in Danish). Article for Dansk Kemi, May 2009

Soerensen, A.L., H. Skov, M. Glasius, M.S. Johnson, J.H. Christensen, B. Jensen, C. Christoffersen, H.W. Madsen, A. Steffen, B.T. Sørensen, O.J. Nielsen, *Modeling of mercury's global distribution, 1st letter from Harvard* (in Danish), Article for Dansk Kemi, November 2008

10 Appendix B Enclosed Abstracts from Peer-Reviewed Papers

10.1 Soerensen et al. (2010a)

Global concentrations of gaseous elemental mercury and reactive gaseous mercury in the marine boundary layer

Anne L. Soerensen^{†*}, Henrik Skov[†], Daniel J. Jacob[‡], Britt T. Soerensen, and Matthew S. Johnson[§]

†National Environmental Research Institute, University of Aarhus, Frederiksborgvej 399, DK-4000 Roskilde, Denmark

‡Harvard University, School of Engineering and Applied Sciences and Department of Earth and Planetary Sciences, Cambridge MA, 02138 USA

§Copenhagen Center for Atmospheric Research, Department of Chemistry, University of Copenhagen, Universitetsparken 5, DK-2100 Copenhagen, Denmark

Environmental Science and Technology (2010a) **44**, 7425-7430

doi: 10.1021/es903839n

Supporting Information is included

Global Concentrations of Gaseous Elemental Mercury and Reactive Gaseous Mercury in the Marine Boundary Layer

ANNE L. SOERENSEN,^{*,†} HENRIK SKOV,[†]
DANIEL J. JACOB,[‡]
BRITT T. SOERENSEN,^{†,§} AND
MATTHEW S. JOHNSON[§]

National Environmental Research Institute, Aarhus University, Frederiksborgvej 399, DK-4000 Roskilde, Denmark, School of Engineering and Applied Sciences and Department of Earth and Planetary Sciences, Harvard University, Cambridge Massachusetts 02138, and Copenhagen Center for Atmospheric Research, Department of Chemistry, University of Copenhagen, Universitetsparken 5, DK-2100 Copenhagen, Denmark

Received December 18, 2009. Revised manuscript received August 20, 2010. Accepted August 24, 2010.

Gaseous elemental mercury (GEM) and reactive gaseous mercury (RGM) were measured during an eight month circumnavigation to obtain knowledge of their worldwide distributions in the marine boundary layer (MBL). Background GEM concentrations were found to be $1.32 \pm 0.2 \text{ ng/m}^3$ (summer) and $2.62 \pm 0.4 \text{ ng/m}^3$ (spring) in the northern hemisphere and $1.27 \pm 0.2 \text{ ng/m}^3$ (spring and summer) in the southern hemisphere. Radiation and relative humidity are shown to control diurnal cycles of RGM. During the cruise the ship passed areas of clean MBL air, air influenced by biomass burning (South Atlantic) and air with high concentrations of GEM and RGM of unknown origin (Antarctic). High GEM concentrations above the Atlantic indicate that emission from the ocean can be an important GEM source. Our data combined with data from earlier cruises provides adequate information to establish a seasonal cycle for the Atlantic. Results show a cycle similar to that found at Mace Head, Ireland but with larger amplitude. We have improved the basic knowledge of mean GEM and RGM concentrations in the MBL worldwide and shown how natural sources and reemissions can affect GEM concentrations in the MBL.

* Corresponding author phone: +45 4630 1154; e-mail: anl@dmu.dk.

[†] Aarhus University.

[‡] Harvard University.

[§] University of Copenhagen.

SUPPORTING INFORMATION

Global concentrations of gaseous elemental mercury and reactive gaseous mercury in the marine boundary layer

Anne L. Soerensen^{†*}, Henrik Skov[†], Daniel J. Jacob[‡], Britt T. Soerensen^{†§}, and Matthew S. Johnson[§]

[†]*National Environmental Research Institute, Aarhus University, Frederiksborgvej 399, DK-4000 Roskilde, Denmark*

[‡]*Harvard University, School of Engineering and Applied Sciences and Department of Earth and Planetary Sciences, Cambridge MA, 02138 USA*

[§]*Copenhagen Center for Atmospheric Research, Department of Chemistry, University of Copenhagen, Universitetsparken 5, DK-2100 Copenhagen, Denmark*

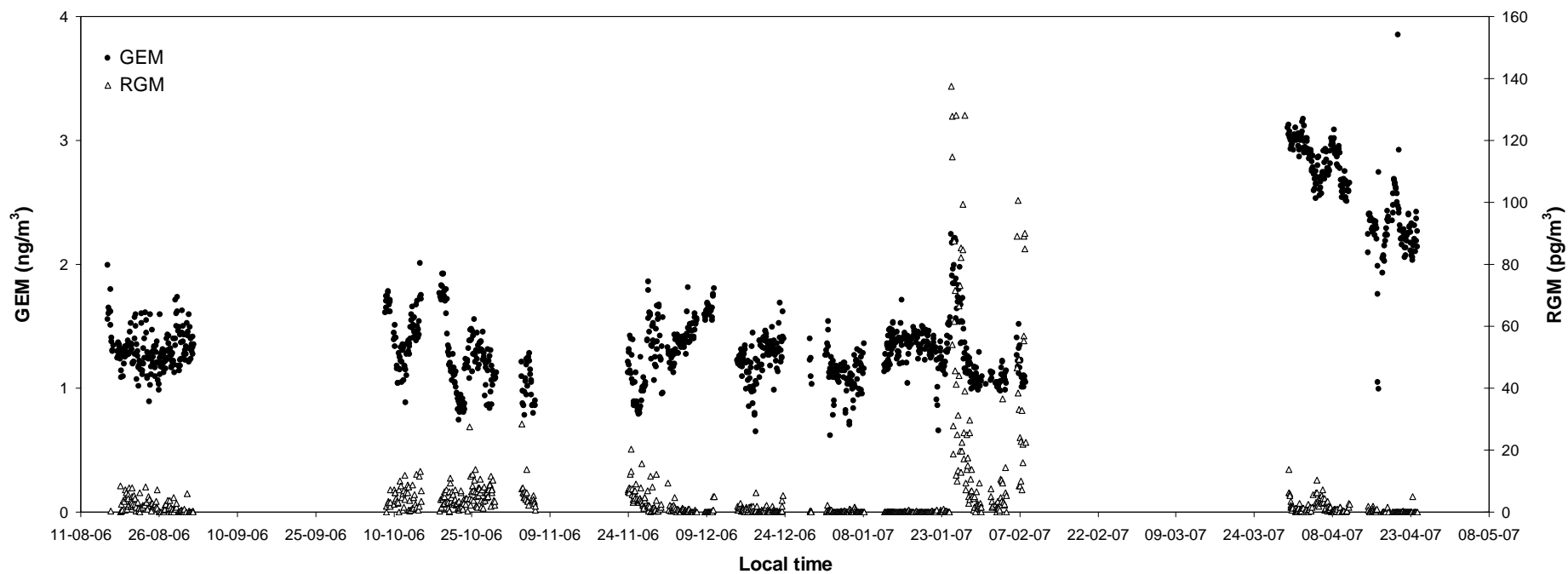
*Corresponding author, anls@dmu.dk; +45 4630 1154

Table of contents

Figure S1	2 hour average GEM and RGM concentrations during the cruise
Text T1	Placement of instruments
Text T2	Measurements of RGM
Text T3	Measurements of NO_x and soot
Table Ta1	Availability of supplementary measurements
Table Ta2	Previous measurements in the MBL
Text T4	Seasonal cycle in the Atlantic Ocean
Figure S2	Back trajectories in the Atlantic
Figure S3	Back trajectories at Mace Head during August 2006 and April
Figure S4	South Atlantic wind directions
Figure S5	CO MOPIT data
Figure S6	Fire counts in Africa during October 5th to 12th (2006)
Figure S7	Back trajectories in the Antarctic
Figure S8	Sea Ice Charts for Antarctic

Figure S1. 2 hour average GEM and RGM concentrations during the cruise

Two hour mean values for GEM and RGM during the cruise. Only measurements in the MBL are presented, while measurements from harbor areas are excluded and will be presented in another paper that is currently in review.



Text T1. Placement of instruments

All measurements were carried out from a 10' shipping container located on the port side of the ship next to the chimney and behind the bridge. The inlet was 8 meters above sea-level. The place was chosen to minimize the effect of ship emissions and Sea Spray.



Picture showing the location of the inlet for the Tekran (red circle) used and showing the inside of the thermostated container where the instruments were located.

Text T2. Measurement of RGM

RGM is a method defined parameter and thus the method has to be considered as a reference method, where the reproducibility of the method gives the best estimate of the uncertainty. In an inter-calibration exercise carried out at Svalbard in 2003 (1) the uncertainty of RGM measurements was found to be very large; agreement was at best to within an order of magnitude. Participating laboratories used a Tekran 2537A equipped with a Tekran 1130/5 sampling unit.

We carried out parallel measurement of RGM at Barrow, Alaska, where one group used a Tekran 2537A equipped with a Tekran 1130/5 sampling unit and the other only a Tekran 2537A equipped with 1130 (unpublished results). Because of the use of different sampling cycles of different duration, a direct comparison of measurements was not possible but 3 day averages showed very good agreement 1.7 % (one std. dev.). In Skov et al. (2) we compared a Tekran 2537A equipped with the Tekran 1130 automated system with manual denuders (3). Manual and automated methods were found to agree to within 25% (95% confidence interval). However we do not have sufficient data from the literature or from our own experiments to calculate the

reproducibility for RGM measurements on the Galathea 3 cruise. Moreover RGM is probably not made of the same gaseous Hg^{II} species but may differ in time and space. Therefore we added 10% to the uncertainty to make a conservative estimate. The expanded reproducibility of RGM is thus 28 %, using a factor of 2 to get a 95% confidence interval.

Text T3. Measurements of NOx and soot

NOx ($\text{NO} + \text{NO}_2$) was measured with an API Teledyne NOx analyzer Model 200 A. To ensure the quality of the NOx data zero-air was added frequently ($n=124$) and samples ($n = 10$) from a pressurized flask with a known, certified NO concentration were added every four weeks. NOx (NO and NO_2) is used as a tracer for contamination from the ship's exhaust. The uncertainty of the method is 4% for NO and 10 % for NO_2 (based on uncertainty budgets and using an expanding factor 2 following the guidelines in CEN EN 14211) for values above 1 ppbv. The detection limits are 200 and 300 pptv for NO and NO_2 respectively for the experimental setup applied. This relative high detection limit for the method is caused mainly by the quality of zero air and not by the capability of the instrument.

Soot data were only used for the (SA) leg during the passage along the Africa coast. Soot for this part of the cruise was made available by Matthias Ketzler (NERI, Aarhus University). The measurements were performed using a **P**article **S**oot **A**bsorption **P**hotometer (PSAP). A description of the instrument can be found in Krecl et al. (4). We used a median of 2 hour mean soot data ($n=13$) to be consistent with other data in the paper. Quality control checks were made on the 5-minute-interval measurements. The ship was moving against the wind for all the measurements along the African coast and we did not see indications of contamination from the ship.

Table Ta1. Availability of supplementary measurements of NO_x, soot and meteorological data

Leg	Ab ^a	Dates	Lat ^b	Origin ^c	NO Mean (ppb)	NO Median (ppb)	NO ₂ Mean (ppb)	NO ₂ Median (ppb)	Soot ^e Mean (m ⁻¹)	RH Mean (%) (no. obs) ^d	Radaition Mean midday (11-13, local time) (W/m ²) (no. obs) ^d
North Atlantic	NA	16 th Aug – 1 st Sep	58 : 67	Ocean	/	/	/	/	/	92.5±6.1 (185)	/
Atlantic O.	AT	15 th Apr – 24 th Apr	43 : 59	Ocean	13.9±34.8	0.2	1.8±3.6	0.2	/	90.4±5.6 (113)	339±160 (9)
Sargasso Sea	SS	30 th Mar – 11 th Apr	23 : 45	Mixed	11.8±24.8	3.0	4.2±3.7	3.5	/	62.6±7.1 (142)	813±150 (12)
South Africa	SA	8 th Oct – 21 st Oct	-39 : -3	Mixed	/	/	/	/	1.5*10 ⁻⁶	86.3±6.7 (120)	498±198 (10)
Indian Ocean	IO	22 nd Oct – 29 th Oct	-39 : -33	Ocean	/	/	/	/	/	80.8±12.3 (91)	617±217 (8)
West Australia	WA	3 rd Nov – 6 th Nov	-22 : -17	Ocean	/	/	/	/	/	72.1±6.2 (32)	907 (2)
East Australia	EA	23 rd Nov – 15 th Dec	-44 : -26	Mixed	32.7±76.3	1.8	2.1±8.5	0.0	/	71.6±10.2 (186)	782±205 (15)
Coral Sea	CS	16 th Dec – 3 rd Jan	-27 : -7	Mixed	77.1±131.4	10.1	5.5±8.2	1.1	/	76.1±5.8 (129)	603±287 (11)
New Zealand	NZ	3 rd Jan – 14 th Jan	-56 : -26	Mixed	18.3±49.9	1.1	0.7±4.4	0.0	/	83.0±13.0 (109)	493±258 (9)
Antarctic O.	AO	14 th Jan – 24 th Jan	-65 : -55	Ocean	27.4±76.5	0.6	0.64±4.1	0.0	/	93.1±3.7 (106)	235±133 (9)
Antarctic Coast	AC	25 th Jan – 28 th Jan	-65 : -63	Ocean	7.0±15.9	1.5	0±2.0	0.0	/	92.5±4.0 (49)	415±176 (4)
Coast of Chile	CC	31 st Jan – 8 th Feb	-58 : -33	Mixed	90.2±157.2	15.13	3.15±10.2	0.1	/	63.8±11.2 (37)	638±407 (4)

a) Abbreviations used in the text.

b) The latitude that the given leg includes.

c) Ocean = no influence from terrestrial sources, Mixed = influence from terrestrial sources during the entire or smaller but significant portions of the leg.

d) The two hour means are used to indicate the number of observations of each species or parameters.

e) Soot measurements were performed by an independent group and we therefore only have limited access to results.

Table Ta2. Previous measurements in the MBL that overlap spatially with measurements during the cruise presented in the paper

Place	Date	TGM ng/m ³	Reference
Southern Hemisphere			
South Atlantic Ocean	Oct 77	1.19±0.25	Slemr et al. 1996
South Atlantic Ocean	Nov-Dec 78	1.35±0.21	Slemr et al. 1996
South Atlantic Ocean	Jan-Feb 79	1.26±0.22	Slemr et al. 1996
South Atlantic Ocean	Oct-Nov 80	1.45±0.16	Slemr et al. 1996
South Atlantic Ocean	Oct-Nov 90	1.50±0.30	Slemr et al. 1996
South Atlantic Ocean	Oct-Nov 94	1.18±0.17	Slemr et al. 1996
South Atlantic Ocean	Dec 99-Jan 00	1.27±0.09	Temme et al. 2003b
South Atlantic Ocean	Feb-Mar 00	1.00±0.12	Temme et al. 2003b
South Atlantic Ocean	Feb 01	1.07±0.10	Temme et al. 2003b
Antarctic – South America	Dec 01 – Feb 02	1.1±0.2	Temme et al 2003a
Indian Ocean	Nov 07	1.2 (1.05-1.51)	Witt et al. 2010
Northern Hemisphere			
Eastern Atlantic Ocean	Oct 77	1.76±0.36	Slemr et al. 1996
Eastern Atlantic Ocean	Nov-Dec 78	1.85±0.31	Slemr et al. 1996
Eastern Atlantic Ocean	Jan-Feb 79	2.17±0.38	Slemr et al. 1996
Eastern Atlantic Ocean	Oct-Nov 80	2.09±0.35	Slemr et al. 1996
Eastern Atlantic Ocean	Oct-Nov 90	2.25±0.41	Slemr et al. 1996
North Atlantic Ocean	Aug 93	2.1±0.8	Mason et al. 1998
Atlantic Ocean	Oct-Nov 94	1.79±0.4	Temme et al. 2003b
Eastern Atlantic Ocean	Oct-Nov 96	2.12±1.0	Temme et al. 2003b
Western Atlantic Ocean	Sep 99	2.00±0.4	Mason et al. 2001
Eastern Atlantic Ocean	Dec 99-Jan 00	2.02±0.3	Temme et al. 2003b
Western Atlantic Ocean	Aug-Sep 03	1.63±0.08	Laurier and Mason 2007
North Atlantic Ocean	July 05	~1.7 ^A	Sommar et al. 2009

A. Arctic data not including

B. Slemr et al. 1996 (5), Mason et al. 1998 (6), Mason et al. 2001 (7), Temme et al. 2003a (8), Temme et al. 2003b (9), Laurier and Mason 2007 (10), Sommar et al. 2009 (11), Witt et al. 2010 (12)

Text T4. Seasonal cycle in the Atlantic Ocean

The seasonal cycle in the Northern Hemisphere Atlantic Ocean is found by converting the available cruise data from the Northern Hemisphere Atlantic Ocean into monthly mean values.

Mean values and standard deviations have been taken from earlier publications (6,7,9-11,13,14). When cruises had a duration of more than one month the same mean value was used to represent all months of the cruise except in the cases where information was sufficient to calculate means for the different months. This approach causes all cruises to have the same weight in the calculations despite their differences in duration and spatial coverage. This is a rough approximation but necessary at this point due to the sparse observations.

To create a smoothed line for the seasonal cycle the mean of the previous and following month were used to make a central moving average. No observations are available in May in the Atlantic Ocean and a value is estimated from the mean concentration in April and June.

Figures S3. Back trajectories at Mace Head during August 2006 and April 2007
HYSPLIT back trajectories were used from <http://ready.arl.noaa.gov/HYSPLIT.php> (15).

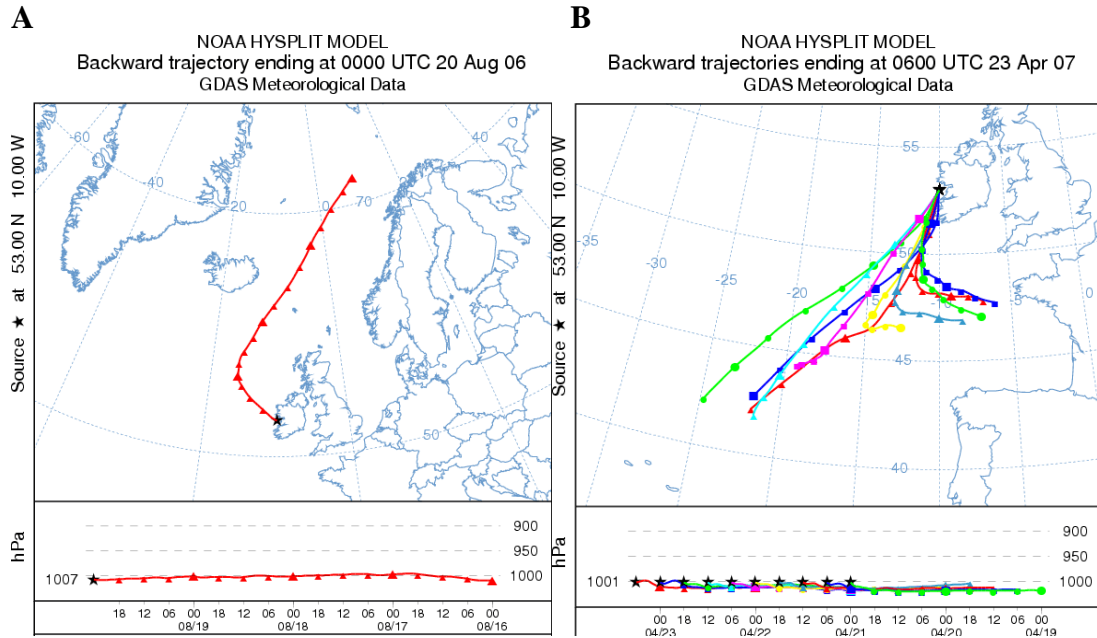


Figure S4. South Atlantic wind directions

While back trajectories for Africa are less clear, the wind direction measured at the ship, together with soot data, satellite CO data and fire counts, gave a good indication of potential mercury sources on the west coast of Africa. We think that this discrepancy between back trajectories and other data might be due to a strong sea-land breeze close to the African coast that is not caught by the HYSPLIT model.

The figure shows wind direction and GEM concentrations encountered along the coast of Africa. Case A: biomass burning, Case B: free MBL air. The red area was influenced by biomass burning (16) (see Figure S6) and the yellow area was influenced by the plume from biomass burning identified by an elevated CO column concentration on October 12th, 2006 (17) (see Figure S5).

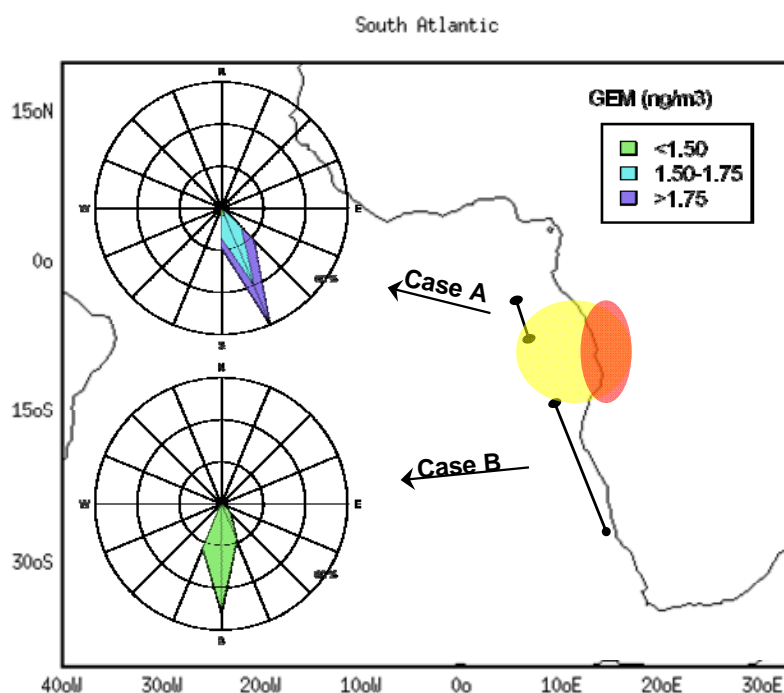


Figure S5. CO MOPIT data

Mean atmospheric CO columns (October 12th, 2006). MOPITT (V3) satellite observations obtained by the MOPIT Satellite (17).

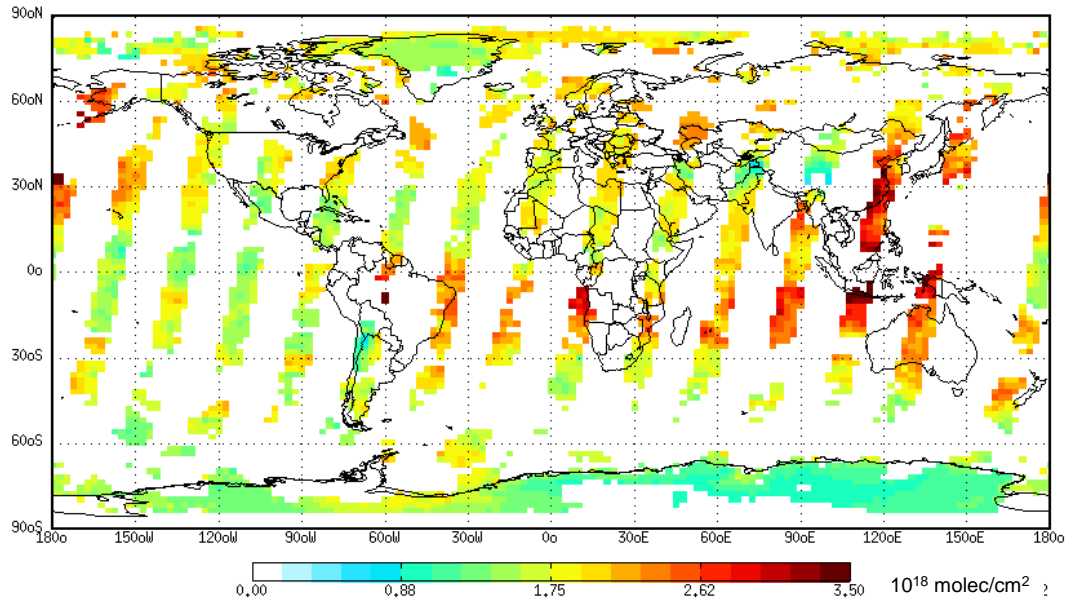


Figure S6. Fire counts in Africa during October 5th to 12th (2006).

Screen print from <http://firefly.geog.umd.edu/firemap/> (web fire mapper, accessed November 2009) (16).

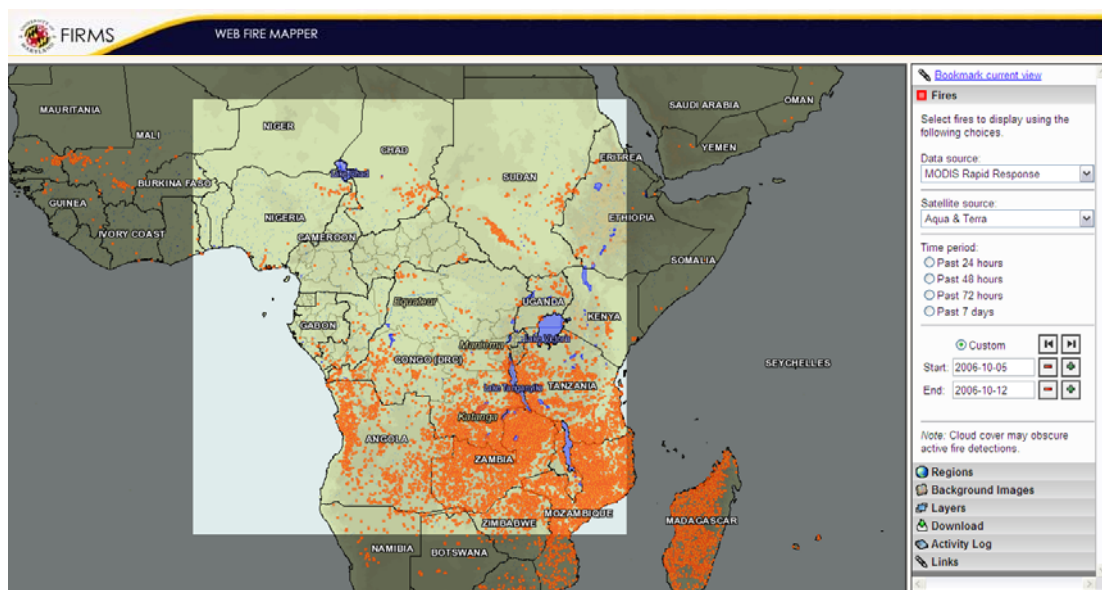


Figure S7. Back trajectories in the Antarctic

Back trajectories are from <http://ready.arl.noaa.gov/HYSPLIT.php> (15).

The heights of the trajectories are 6 meters above sea level, the duration is 96 hours.

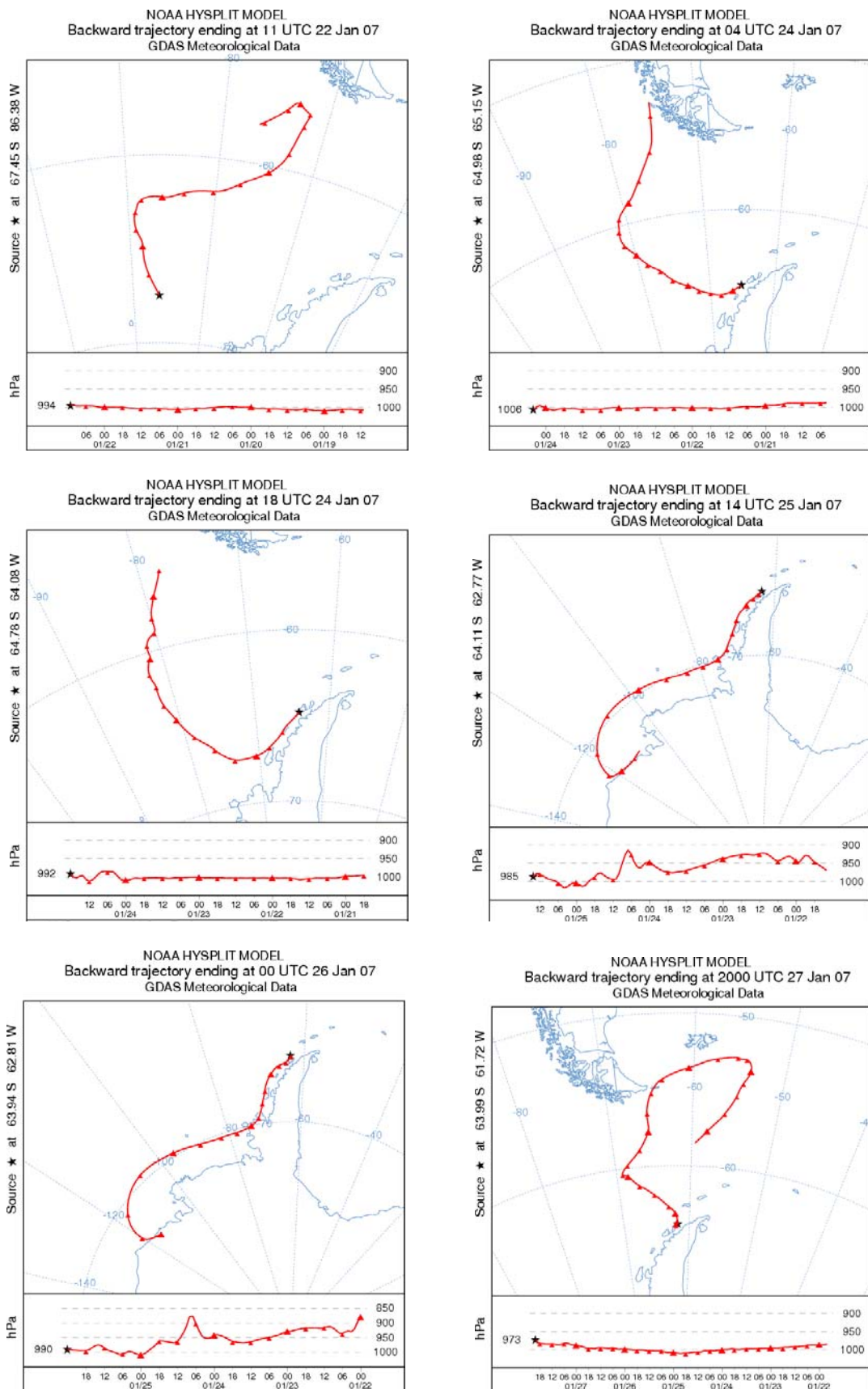
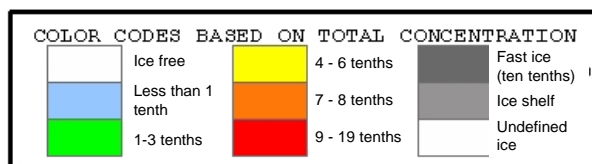
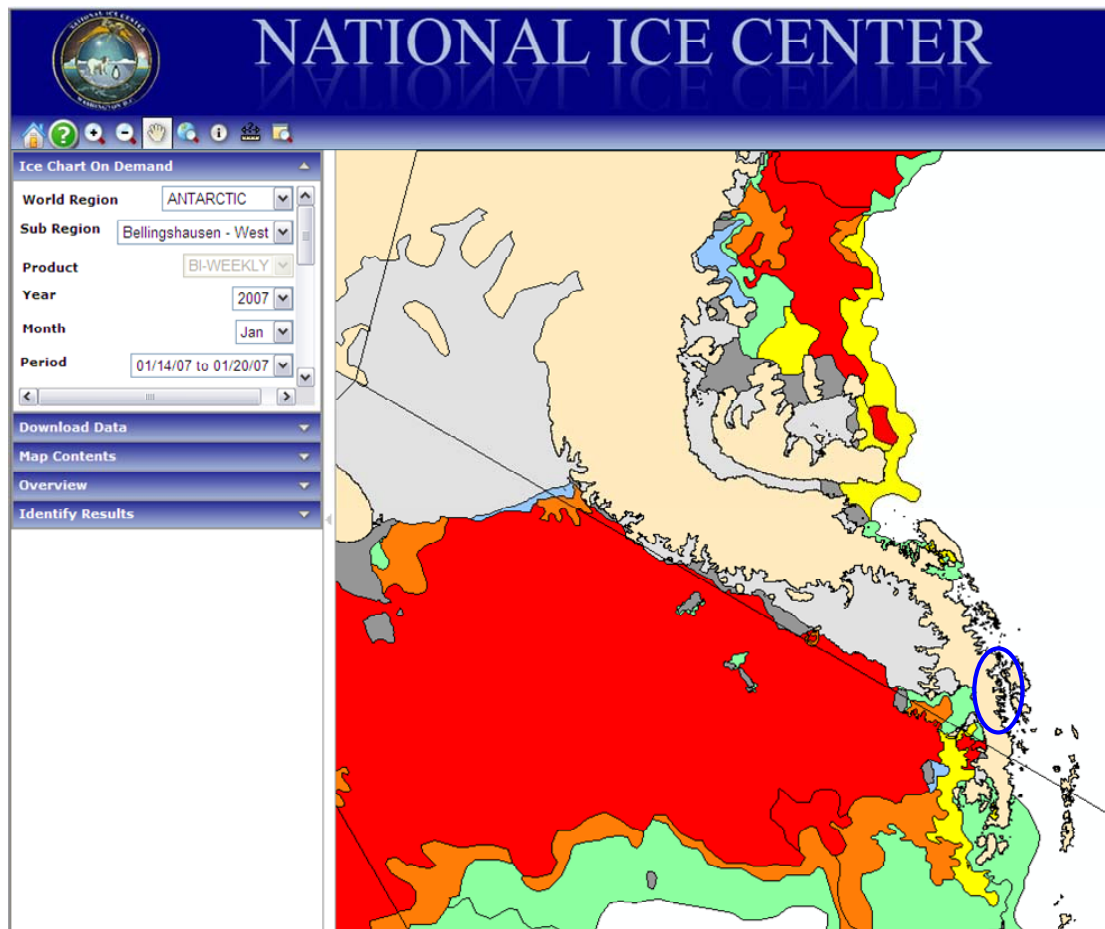


Figure S8. Ice extend (source: www.natice.noaa.gov, accessed December 2009)

Sea ice extend determined for the 14-20 January 2007.

Screen print of the ice extent at Bellingshausen West (included is a color scale that indicates the fraction of sea covered with ice). The blue circle indicates the location of the ship during the observations with high GEM and RGM concentrations.



Literature Cited

1. Aspö, K.; Gauchard, P. A.; Steffen, A.; Temme, C.; Berg, T.; Bahlmann, E.; Banic, C.; Dommergue, A.; Ebinghaus, R.; Ferrari, C.; Pirrone, N.; Sprovieri, F.; Wibetoe, G. Measurements of atmospheric mercury species during an international study of mercury depletion events at Ny-Alesund, Svalbard, spring 2003. How reproducible are our present methods? *Atmos. Environ.* **2005**, *39* (39), 7607-7619.
2. Skov, H.; Brooks, S. B.; Goodsite, M. E.; Lindberg, S. E.; Meyers, T. P.; Landis, M. S.; Larsen, M. R. B.; Jensen, B.; McConville, G.; Christensen, J. Fluxes of reactive gaseous mercury measured with a newly developed method using relaxed eddy accumulation. *Atmos. Environ.* **2006**, *40* (28), 5452-5463.
3. Landis, M. S.; Stevens, R. K.; Schaedlich, F.; Prestbo, E. M. Development and characterization of an annular denuder methodology for the measurement of divalent inorganic reactive gaseous mercury in ambient air. *Environ. Sci. Technol.* **2002**, *36* (13), 3000-3009.
4. Krecl, P.; Strøm, J.; Johansson, C. Carbon content of atmospheric aerosols in a residential area during the wood combustion season in Sweden. *Atmos. Environ.* **2007**, *41* (33), 6974-6985.
5. Slemr, F. Trends in atmospheric mercury concentrations over the Atlantic Ocean and at the Wank summit, and the resulting constraints on the budget of atmospheric mercury. In *Global and Regional Mercury Cycles: Sources, Fluxes and Mass Balances*; Baeyens, W., Ebinghaus, R., Vasiliev, O., Eds.; Kluwer Academic Publishers: Netherlands, 1996.
6. Mason, R. P.; Rolffhus, K. R.; Fitzgerald, W. F. Mercury in the North Atlantic. *Mar. Chem.* **1998**, *61* (1-2), 37-53.
7. Mason, R. P.; Lawson, N. M.; Sheu, G. R. Mercury in the Atlantic Ocean: factors controlling air-sea exchange of mercury and its distribution in the upper waters. *Deep-Sea Res. II.* **2001**, *48* (13), 2829-2853.
8. Temme, C.; Einax, J. W.; Ebinghaus, R.; Schroeder, W. H. Measurements of atmospheric mercury species at a coastal site in the Antarctic and over the south Atlantic Ocean during polar summer. *Environ. Sci. Technol.* **2003**, *37* (1), 22-31.

9. Temme, C.; Slemr, F.; Ebinghaus, R.; Einax, J. W. Distribution of mercury over the Atlantic Ocean in 1996 and 1999-2001. *Atmos. Environ.* **2003**, *37* (14), 1889-1897.
10. Laurier, F.; Mason, R. Mercury concentration and speciation in the coastal and open ocean boundary layer. *J. Geophys. Res. A.* **2007**, *112* (D6), D06302.
11. Sommar, J.; Andersson, M. E.; Jacobi, H.-W. Circumpolar measurements of speciated mercury, ozone and carbon monoxide in the boundary layer of the Arctic Ocean. *Atmos. Chem. Phys. Disc.* **2009**, *9* 20913-20948.
12. Witt, M. L. I.; Mather, T. A.; Baker, A. R.; de Hoog, C. J.; Pyle, D. M. Atmospheric trace metals over the south-west Indian Ocean: Total gaseous mercury, aerosol trace metal concentrations and lead isotope ratios. *Mar. Chem.* **2010**, *121* (1-4), 2-16.
13. Lamborg, C. H.; Rolffhus, K. R.; Fitzgerald, W. F.; Kim, G. The atmospheric cycling and air-sea exchange of mercury species in the South and equatorial Atlantic Ocean. *Deep-Sea Res. II.* **1999**, *46* (5), 957-977.
14. Aspö, K.; Temme, C.; Berg, T.; Ferrari, C.; Gauchard, P. A.; Fain, X.; Wibetoe, G. Mercury in the atmosphere, snow and melt water ponds in the North Atlantic Ocean during Arctic summer. *Environ. Sci. Technol.* **2006**, *40* (13), 4083-4089.
15. Draxler, R. P.; Rolph, G. D. *HYSPLIT (HYbrid Single-Particle Lagrangian Integrated Trajectory)*. NOAA Air Resources Laboratory: Silver Spring, MD., 2003. Website; www.arl.noaa.gov/ready/hysplit4.html.
16. Davies, D. K.; Ilavajhala, S.; Wong, M. M.; Justice, C. O. Fire Information for Resource Management System: Archiving and Distributing MODIS Active Fire Data. *Ieee Trans. Geosci. Remote Sens.* **2009**, *47* (9), 3298.
17. Emmons, L. K.; Edwards, D. P.; Deeter, M. N.; Gille, J. C.; Campos, T.; Nedelec, P.; Novelli, P.; Sachse, G. Measurements of Pollution In The Troposphere (MOPITT) validation through 2006. *Atmos. Chem. Phys.* **2009**, *9* (5), 1795-1803.

10.2 Soerensen et al. (2010b)

Gaseous Mercury in Coastal Urban Areas

Anne L. Soerensen^{†*}, Henrik Skov[†], Matthew S. Johnson[‡], Marianne Glasius[§]

†National Environmental Research Institute, Aarhus University, Frederiksborgvej 399, DK-4000 Roskilde, Denmark

†National Environmental Research Institute, Aarhus University, Frederiksborgvej 399, DK-4000 Roskilde, Denmark

‡Copenhagen Center for Atmospheric Research, Department of Chemistry, University of Copenhagen, Universitetsparken 5, DK-2100 Copenhagen, Denmark

§Department of Chemistry, Aarhus University, Langelandsgade 140, DK-8000 Århus C, Denmark

Environmental Chemistry (2010b) 7, 537-547

doi: 10.1071/EN10088

Gaseous mercury in coastal urban areas

Anne L. Soerensen,^{A,D} Henrik Skov,^A Matthew S. Johnson^B
and Marianne Glasius^C

^ANational Environmental Research Institute, Aarhus University, Frederiksborgvej 399, DK-4000 Roskilde, Denmark.

^BCopenhagen Center for Atmospheric Research, Department of Chemistry, University of Copenhagen, Universitetsparken 5, DK-2100 Copenhagen, Denmark.

^CDepartment of Chemistry, Aarhus University, Langelandsgade 140, DK-8000 Århus C, Denmark.

^DCorresponding author. Email: anl@dmu.dk

Environmental context. Mercury is a neurotoxin that bioaccumulates in the aquatic food web. Atmospheric emissions from urban areas close to the coast could cause increased local mercury deposition to the ocean. Our study adds important new data to the current limited knowledge on atmospheric mercury emissions and dynamics in coastal urban areas.

Abstract. Approximately 50% of primary atmospheric mercury emissions are anthropogenic, resulting from e.g. emission hotspots in urban areas. Emissions from urban areas close to the coast are of interest because they could increase deposition loads to nearby coastal waters as well as contribute to long range transport of mercury. We present results from measurements of gaseous elemental mercury (GEM) and reactive gaseous mercury (RGM) in 15 coastal cities and their surrounding marine boundary layer (MBL). An increase of 15–90% in GEM concentration in coastal urban areas was observed compared with the remote MBL. Strong RGM enhancements were only found in two cities. In urban areas with statistically significant GEM/CO enhancement ratios, slopes between 0.0020 and 0.0087 ng m⁻³ ppb⁻¹ were observed, which is consistent with other observations of anthropogenic enhancement. The emission ratios were used to estimate GEM emissions from the areas. A closer examination of data from Sydney (Australia), the coast of Chile, and Valparaiso region (Chile) in the southern hemisphere, is presented.

Additional keywords: emissions, gaseous elemental mercury, GEM/CO ratios, reactive gaseous mercury.

10.3 Soerensen et al. (2010c)

An Improved Global Model for Air-Sea Exchange of Mercury: High Concentrations over the North Atlantic

Anne L. Soerensen^{†‡*}, Elsie M. Sunderland^{‡§}, Christopher D. Holmes[‡], Daniel J. Jacob[‡], Robert M. Yantosca[‡], Henrik Skov[†], Jesper H. Christensen[†], Sarah A. Strode^{||}, and Robert P. Mason[⊥]

†National Environmental Research Institute, Aarhus University, Frederiksborgvej 399, DK-4000 Roskilde, Denmark

‡School of Engineering and Applied Sciences and Department of Earth and Planetary Sciences, Harvard University, Cambridge MA, 02138, USA

§Department of Environmental Health, Harvard University School of Public Health, Boston MA, 02115, USA

||Department of Atmospheric Sciences, University of Washington, Seattle, WA, 98195 USA

⊥Department of Marine Sciences, University of Connecticut, 1080 Shennecossett Road, Groton, CT, 0634, USA

Environmental Science and Technology (2010c) **44**, 8574-8580

doi: 10.1021/es102032g

Supporting Information is included

An Improved Global Model for Air-Sea Exchange of Mercury: High Concentrations over the North Atlantic

ANNE L. SOERENSEN,^{†,‡}
ELSIE M. SUNDERLAND,^{*,†,§}
CHRISTOPHER D. HOLMES,[‡]
DANIEL J. JACOB,[‡]
ROBERT M. YANTOSCA,[‡] HENRIK SKOV,[†]
JESPER H. CHRISTENSEN,[†]
SARAH A. STRODE,^{||} AND
ROBERT P. MASON[⊥]

National Environmental Research Institute, Aarhus University, Frederiksborgvej 399, DK-4000 Roskilde, Denmark, School of Engineering and Applied Sciences and Department of Earth and Planetary Sciences, Harvard University, Cambridge Massachusetts 02138, United States, Department of Environmental Health, Harvard University School of Public Health, Boston Massachusetts 02115, United States, Department of Atmospheric Sciences, University of Washington, Seattle, Washington 98195, United States, and Department of Marine Sciences, University of Connecticut, 1080 Shennecossett Road, Groton, Connecticut, 0634, United States

Received June 15, 2010. Revised manuscript received October 1, 2010. Accepted October 7, 2010.

We develop an improved treatment of the surface ocean in the GEOS-Chem global 3-D biogeochemical model for mercury (Hg). We replace the globally uniform subsurface ocean Hg concentrations used in the original model with basin-specific values based on measurements. Updated chemical mechanisms for Hg⁰/Hg^{II} redox reactions in the surface ocean include both photochemical and biological processes, and we improved the parametrization of particle-associated Hg scavenging. Modeled aqueous Hg concentrations are consistent with limited surface water observations. Results more accurately reproduce high-observed MBL concentrations over the North Atlantic (NA) and the associated seasonal trends. High seasonal evasion in the NA is driven by inputs from Hg enriched subsurface waters through entrainment and Ekman pumping. Globally, subsurface waters account for 40% of Hg inputs to the ocean mixed layer, and 60% is from atmospheric deposition. Although globally the ocean is a net sink for 3.8 Mmol Hg y⁻¹, the NA is a net source to the atmosphere, potentially due to enrichment of subsurface waters with legacy Hg from historical anthropogenic sources.

* Corresponding author phone: +1-617-384-8832; e-mail: esunder@hsph.harvard.edu.

[†] Aarhus University.

[‡] Harvard University.

[§] Harvard University School of Public Health.

^{||} University of Washington.

[⊥] University of Connecticut.

SUPPORTING INFORMATION

An Improved Global Model for Air-Sea Exchange of Mercury: High Concentrations Over the North Atlantic

Anne L. Soerensen^{†‡}, Elsie M. Sunderland[‡], Christopher D. Holmes[‡], Daniel J. Jacob[‡], Robert Yantosca[‡], Henrik Skov[†], Jesper H. Christensen[†], Sarah A. Strode[§], and Robert P. Mason^{||}*

[†]National Environmental Research Institute, Aarhus University, Frederiksborgvej 399, DK-4000 Roskilde, Denmark

[‡]Harvard University, School of Engineering and Applied Sciences and Department of Earth and Planetary Sciences, Cambridge MA, 02138, USA

[§]Department of Atmospheric Sciences, University of Washington, Seattle, WA, 98195 USA

^{||}University of Connecticut, Department of Marine Sciences, 1080 Shennecossett Road, Groton, CT, 0634, USA

Contents		Page(s)
Section I	Model Sensitivity Analyses	2
Section II	Supplemental Results	3-6
Section III	Model Updates and Formulation	6-11
Section IV	References Cited	12-14
Figure S1	Comparison of monthly modeled and observed seawater total inorganic Hg	3
Figure S2	Comparison of modeled and observed seawater Hg ⁰	3
Figure S3	Modeled seasonal surface water Hg ⁰ saturation values for 2008	4
Figure S4	Seasonal variability in modeled oceanic evasion for 2008	5
Figure S5	Modeled contribution of oceanic Hg ⁰ emissions to marine boundary Hg ⁰ concentrations	6
Table S1	Model differential equations	7
Table S2	Particle associated mercury reservoirs and fluxes	7
Table S3	Redox reactions	10
Table S4	Gas-exchange parameterization	11

Section I: Model Sensitivity Analyses

We performed a variety of sensitivity analysis to help prioritize future experimental data needs. The reducible Hg^{II} pool is rarely measured in studies collecting data on gross reaction kinetics (1) and should be a priority for future research because Hg^0 evasion increases/decreases proportionally to this pool in our simulation. Other studies have suggested that the diffusivity of Hg^0 in seawater (2) is overestimated by standard calculation methods like Wilke-Chang (3), which could lead to low retention of Hg^0 in the surface waters. However, implementing the experimentally based diffusivity term for Hg^0 proposed by Kuss et al. (4) in our model simulation only increases aqueous Hg^0 concentrations by 5% and results in a decrease in global net evasion of 14%.

We analyzed the sensitivity of modeling results to several gas transfer models. Using the gas transfer scheme developed by Liss and Merlivat (5), generally accepted as a low-end estimate, results in a 30% reduction in modeled global evasion compared to our standard simulation based on Nightingale et al. (6) but does not substantially change aqueous Hg^0 concentrations. Several ecosystem-scale studies have shown Hg^0 evasion flux estimates typically also vary by approximately 30%, depending on the choice of gas transfer model (7-9). Our results suggest that the Nightingale parameterization (6) that uses a quadratic relationship between evasion and wind speed is most appropriate because the linear dependence of evasion on wind speed in the Liss and Merlivat model (5) diminishes the modeled seasonal cycle of MBL Hg concentrations that is observed in the Northern Hemisphere (10).

Section II: Supplemental Results

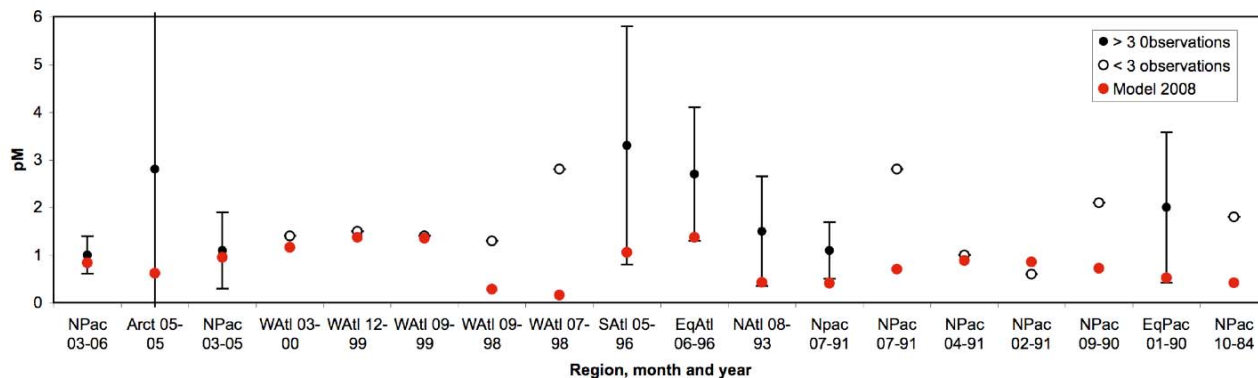


Figure S1. Comparison of monthly modeled (2008) and observed (various years) total inorganic Hg concentrations. Data sources are as follows: Pacific (11-16); Atlantic Ocean (16-19); Arctic Ocean (20).

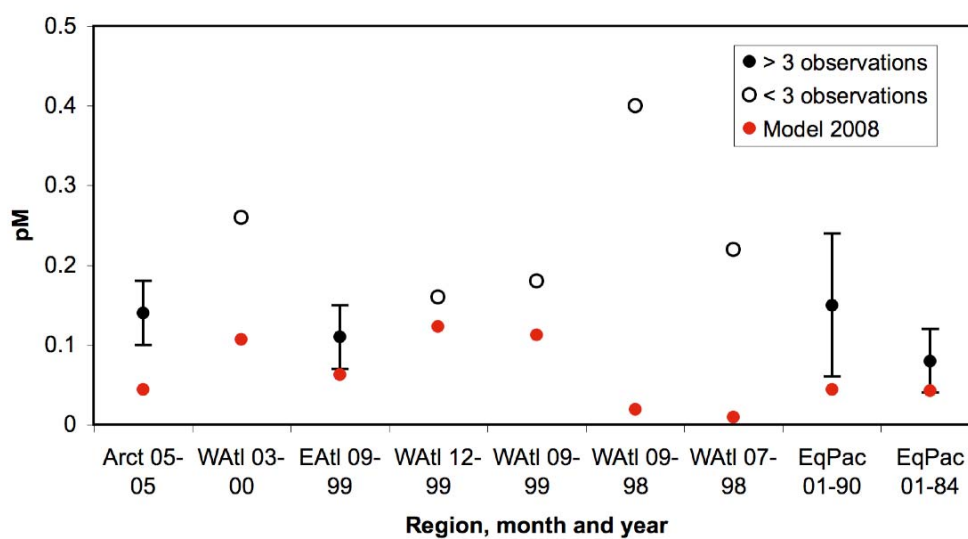


Figure S2. Comparison of monthly modeled (2008) and observed (various years) seawater Hg^0 concentrations. Pacific Ocean: (13, 14, 21, 22); Atlantic Ocean (17, 23); Arctic Ocean: (20).

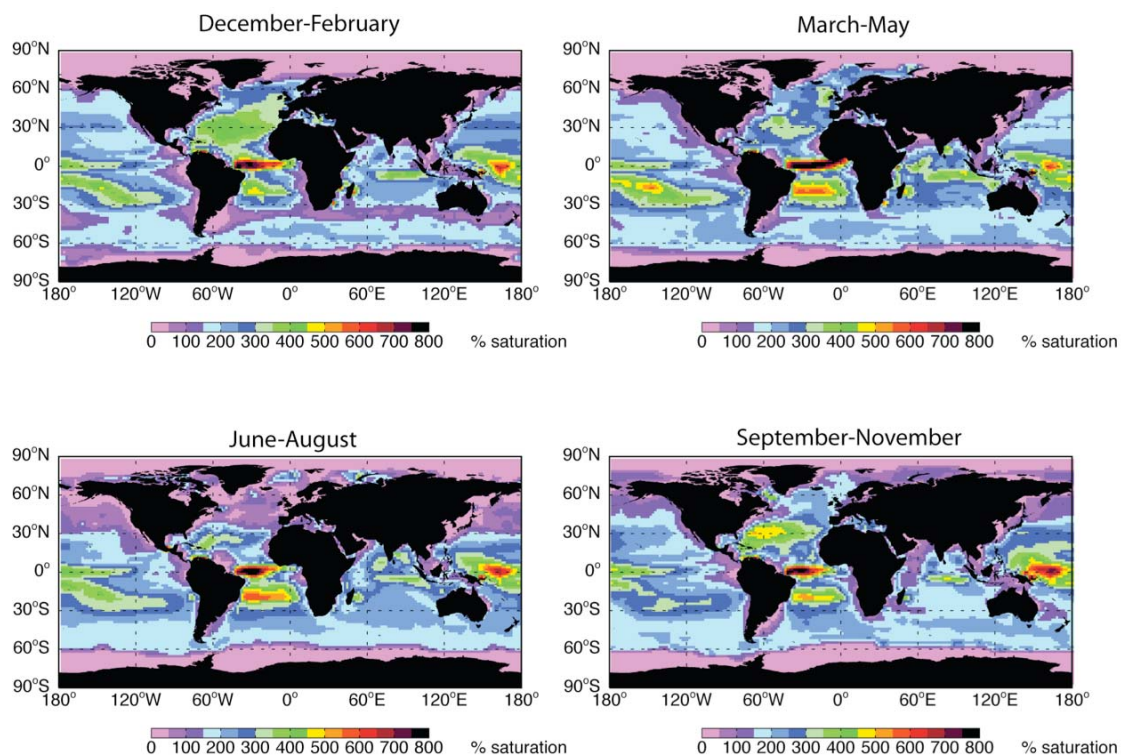


Figure S3. Modeled seasonal surface water Hg^0 saturation values for 2008. The degree of saturation indicates the direction of the flux across the air-sea interface. Less than 100% indicates net deposition and greater than 100% indicates net evasion of Hg^0 .

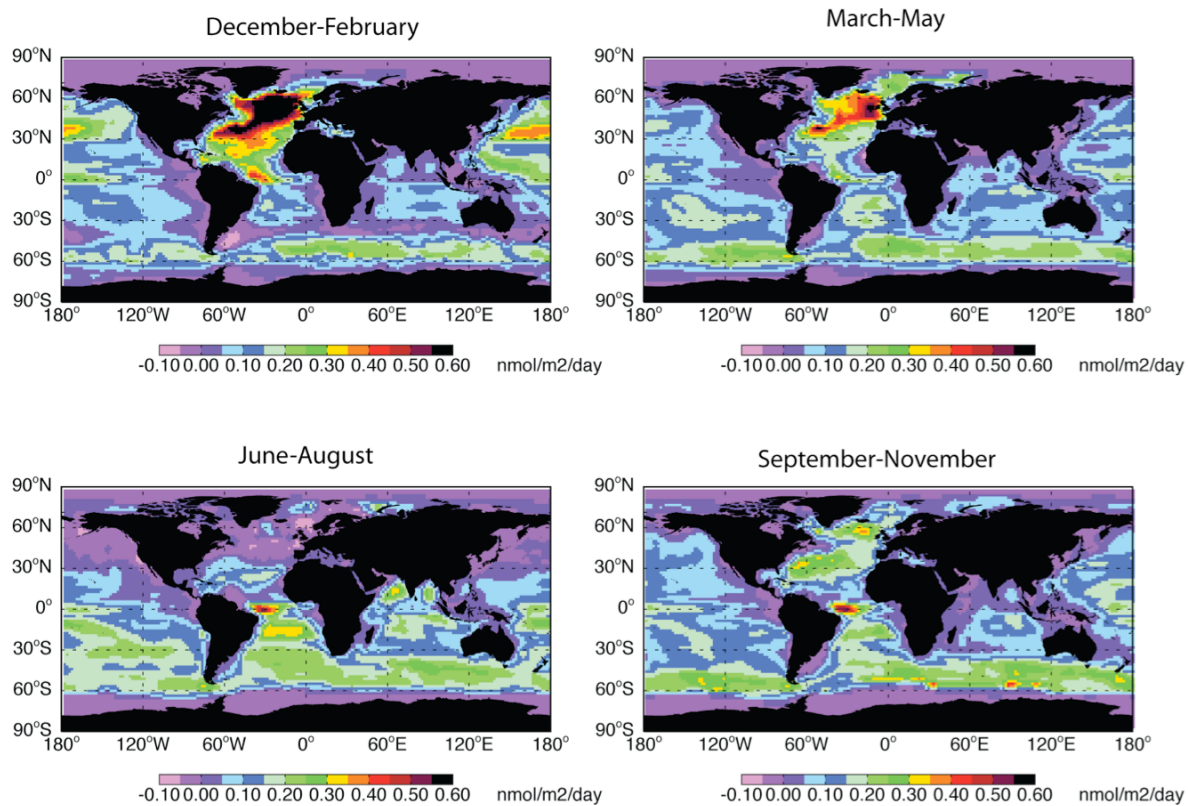


Figure S4. Seasonal variability in modeled oceanic Hg^0 evasion for 2008.

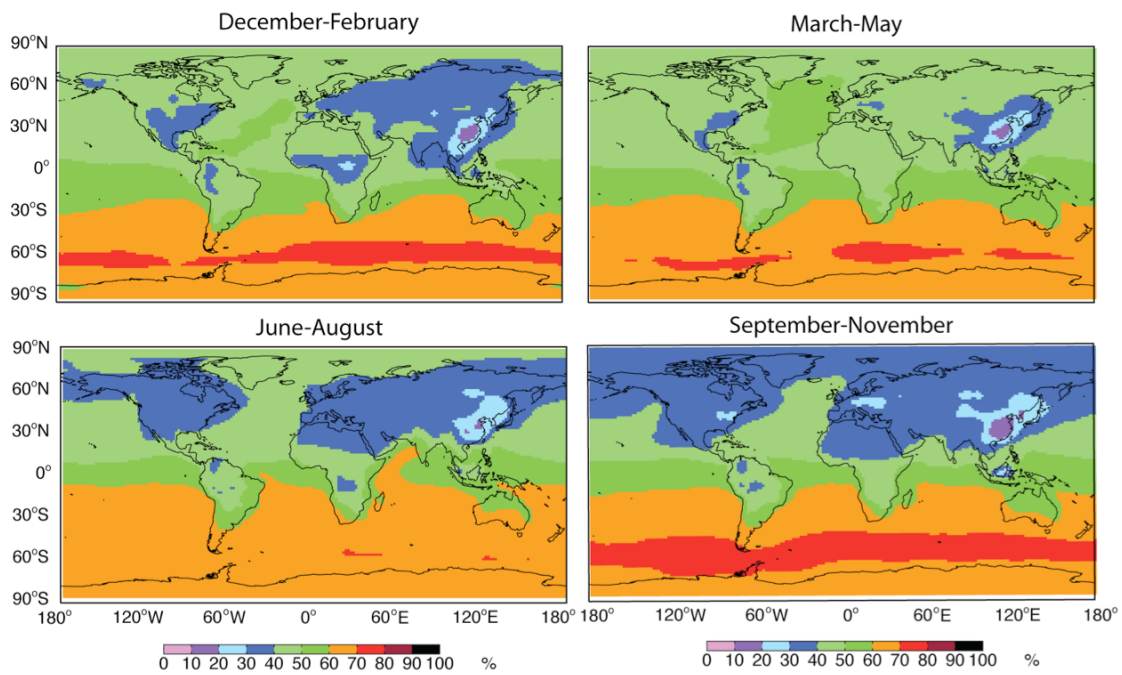


Figure S5. Modeled contribution of oceanic Hg^0 evasion to marine boundary Hg^0 concentrations.

Section III: Model Updates and Formulation

Table S1. Model differential equations

Change in Hg ⁰ mass over time (<i>dt</i>)	$\frac{dM_{Hg^0}}{dt} = M_{Ek}^{Hg^0} \pm M_{ent}^{Hg^0} \pm M_{ev} - k_{ox}M_{Hg^0} + k_r\phi_F\alpha_rM_{Hg^{II}}$	
Change in Hg ^{II} mass over time (<i>dt</i>)	$\frac{dM_{Hg^{II}}}{dt} = M_a + M_{up}^{Hg^{II}} \pm M_{ent}^{Hg^{II}} - M_p + k_{ox}M_{Hg^0} - k_r\phi_F\alpha_rM_{Hg^{II}}$	
M_a (kg)	Deposition of Hg to the ocean surface	
M_{ent} (kg)	Mass of mercury species introduced or removed due to deep convection or shoaling of the mixed-layer	
M_{Ek} (kg)	Wind-driven mass transfer of mercury species due to Ekman pumping	
M_{ev} (kg)	Mass of Hg ⁰ evaded from the ocean to the atmosphere	
M_p (kg)	Flux of Hg ^{II} lost from mixed layer with sinking particles	
$M_{Hg(0)}$ (kg)	Reservoir of Hg ⁰ in the surface mixed layer	
$M_{Hg(II)}$ (kg)	Reservoir of Hg ^{II} in the surface mixed layer	
k_{ox} (s ⁻¹)	Hg ⁰ oxidation rate	$k_{ox1} + k_{ox2}$
k_r (s ⁻¹)	Reduction rate of reducible pool of Hg ^{II}	$k_{red1} + k_{red2}$
ϕ_F (unitless)	Hg ^{II} fraction in the dissolved phase	$1/(1 + K_D SPM)$
α_r (unitless)	Reducible fraction of the filtered Hg ^{II} pool	0.40 (19, 24, 25)

Table S2. Particle associated mercury reservoirs and fluxes.

M_{Hg^p} (kg)	Hg ^{II} mass in the particulate phase	$(1 - \phi_F)M_{Hg^{II}}$
K_D (L kg ⁻¹)	Seawater partition coefficient for Hg ^{II}	3.16×10^5 (14, 19)
C_{SPM} (kg L ⁻¹)	Concentration of suspended particles	$10^3(C_{OC} \cdot M_{wet} \cdot A_w)/z_{MLD}$
z_{MLD} (m)	Mixed layer depth	WOCE data assimilation (26)
A_w (m ²)	Water surface area	
C_{OC} (mg m ⁻²)	Standing stock of organic carbon in mixed layer	$C_{T-Chl} \cdot C_C : C_{Chl_a}$
C_{T-Chl} (mg m ⁻²)	Integrated water column pigment content	See text for derivation
$r_{C:Chla}$ (unitless)	Carbon to chlorophyll a ratio	80:1 (27)
M_{wet} (unitless)	Conversion for wet weights of planktonic biomass	10 mg wet weight: mg carbon
J_{orgC} (mg C m ⁻² d ⁻¹)	Organic carbon flux out of the mixed layer	$0.1NPP^{1.77}z_{MLD}^n$
NPP (mg C m ⁻² d ⁻¹)	Net primary productivity	2003 MODIS satellite data (28)
n (unitless)	Exponent describing relationship between declines in organic carbon flux due to mineralization in the water column with depth	-0.74 (29)
$r_{Hg:C}$ (unitless)	Hg ^P to organic carbon ratio in the mixed layer	$M_{Hg(P)}/(10^6 C_{OC} \cdot A_w)$
M_p (kg)	Mass of Hg ^P lost from the mixed layer due to particle sinking	$J_{orgC} \cdot r_{Hg:C} \cdot A_w(dt)$

Method used for estimating suspended particulate matter concentrations

No global data sets on SPM concentrations in the ocean mixed layer are available. We therefore estimate SPM concentrations in the surface mixed layer based on the standing biomass in the water column derived from MODIS satellite chlorophyll a (C_{Chla} , mg m^{-3}) concentrations (<http://oceancolor.gsfc.nasa.gov/ftp.html>) for the year 2003. We calculate the water column integrated pigment content within the euphotic layer (C_{T-Chl} , mg m^{-2}) based on the statistical fits for subsurface algal productivity in the ocean developed by Morel and Berthon (30) and updated by Uitz et al. (31).

These equations are as follows:

1. STRATIFIED WATERS

For stratified waters in low and mid latitude stations, where $C_{Chla} \leq 1.0 \text{ mg m}^{-3}$

$$(1) \quad C_{T-Chl} = 36.1 C_{Chla}^{0.357}$$

For stratified waters in low and mid latitude stations, where $C_{Chla} \geq 1.0 \text{ mg m}^{-3}$

$$(2) \quad C_{T-Chl} = 37.7 C_{Chla}^{0.615}$$

2. WELL-MIXED WATERS

For well-mixed waters at high latitudes:

$$(3) \quad C_{T-Chl} = 42.1 C_{Chla}^{0.538}$$

Waters are defined as well-mixed if $z_{eu}/z_{MLD} < 1$
Conversely, if $z_{eu}/z_{MLD} > 1$ then the waters are considered stratified.

Where,

z_{eu} is the euphotic depth and is defined as the depth where the PAR irradiance is 1% of its value at the surface.

z_{MLD} (m) is the mixed layer depth derived from de Boyer Montegut et al. (26) from the National Oceanographic Data Center (NODE), World Ocean Circulation Experiment (WOCE) database, and the ARGO program (available: <http://www.locean-ipsl.upmc.fr/~cdblod/mlld.html>)

C_{T-Chl} and z_{eu} are calculated iteratively in the model to determine whether waters are stratified or well mixed and the appropriate equations for C_{T-Chl} .

z_{eu} is derived as a function of C_{T-Chl} by Morel and Maritorea (32):

$$(4) \quad z_{eu} = 912 C_{T-Chl}^{-0.839} \text{ when } 10 \text{ m} < z_{eu} < 102 \text{ m and } C_{T-Chl} > 13.65 \text{ mg m}^{-2}$$

$$(5) \quad z_{eu} = 426.3 C_{T-Chl}^{-0.547} \text{ when } 102 \text{ m} < z_{eu} < 180 \text{ m and } C_{T-Chl} < 13.65 \text{ mg m}^{-2}$$

We calculate the standing stock of organic carbon (C_{OC} , mg m^{-2}) from the integrated water column pigment content (C_{T-Chl} , mg m^{-2}) by assuming a constant C:Chl a ratio ($r_{C:Chla}$) of 80:1 based on Wetzel et al. (27). This is a simplification of real biological processes in the ocean where $r_{C:Chla}$ is known to vary as a function of light limitation, depth, and phytoplankton growth rates among other factors (33).

$$(6) \quad C_{OC} = C_{T-Chl} \cdot r_{C:Chla}$$

We approximate the concentration of suspended particles in each model grid cell from wet weights of planktonic biomass that are derived by assuming that organic carbon is 50% of the dry weight and the dry weight is 20% of the weight for phytoplankton, resulting in an overall conversion factor of 10 mg wet weight: mg carbon (34). This results in an overall conversion factor of 10 mg wet weight: mg carbon.

$$(7) \quad C_{SPM} = 10^3 (C_{OC} \cdot M_{wet} \cdot A_w) / z_{MLD}$$

Although the majority of particles in open ocean environments are living and dead planktonic biomass, we allow for up to an additional 10% increase in SPM to account for allochthonous abiotic particles such as mineral dust (35).

Table S3. Model representation of redox reactions.

k_{ox1} (s^{-1})	Photo-oxidation rate constant	$6.6 \times 10^{-6} \cdot R$ (25) When $R > 0$ <i>min</i> : $5.6 \times 10^{-6} s^{-1}$ (36) <i>max</i> : $9.7 \times 10^{-4} s^{-1}$ (25)
k_{ox2} (s^{-1})	Dark oxidation rate constant	1.0×10^{-7} (36, 37)
k_{red1} (s^{-1})	Photolytic reduction rate constant	$1.7 \times 10^{-6} \cdot R$ (25) When $R > 0$ <i>min</i> : $< 1.0 \times 10^{-7} s^{-1}$ (25, 36) <i>max</i> : $8.7 \times 10^{-4} s^{-1}$ (25)
k_{red2} (s^{-1})	Biotic reduction rate constant	$4.5 \times 10^{-6} \cdot NPP$ (25) <i>min</i> : $3.5 \times 10^{-7} s^{-1}$ <i>max</i> : $8.3 \times 10^{-5} s^{-1}$ (38)
R ($W m^{-2}$)	Average shortwave radiation intensity in the mixed layer	$\int_0^{MLD} R_i$
$\int_0^{MLD} R_i$ ($W m^{-2}$)	Total local shortwave radiation penetration in the mixed layer	$\frac{1}{x_2 - x_1} \cdot \frac{R_i}{\eta} [e^{\eta x_1} - e^{-\eta x_2}]$
R_i ($W m^{-2}$)	Total shortwave radiation intensity	GEOS-5 meteorology
x_1 (m)	Surface depth	0 m
x_2 (m)	Bottom depth	z_{MLD}
η (m^{-1})	Extinction coefficient for radiation	$\eta_w + \eta_{chl} C_{chl} + \eta_{DOC} C_{DOC}$
η_w (m^{-1})	Extinction coefficient for water	450 nm (vis) = 0.0145
η_{Chla} (m^{-1})	Extinction coefficient for pigments	450 nm (vis) = 31
C_{Chla} ($mg L^{-1}$)	Average concentration of Chl a in mixed layer	$(C_{T-Chl} \cdot A_w) / z_{MLD}$
η_{DOC} ($mg L^{-1}$)	Extinction coefficient for dissolved organic carbon (DOC)	450 nm (vis) = 0.654
C_{DOC} ($mg L^{-1}$)	Concentration of DOC in water column	$1.5 \cdot (NPP / NPP_x)$ (39)
NPP ($gC m^{-2} d^{-1}$)	NPP in model grid cell	2003 MODIS satellite data (28)
NPP_x	Global average NPP	global NPP/ocean surface area

Table S4. Gas exchange parameterization.

M_{ev} (kg s ⁻¹)	Air-sea exchange of Hg ⁰ for each model time step (dt)	$(10^{-12} F_v \cdot A_w) dt / 3600$
F_v (ng m ⁻² h ⁻¹)	Hg ⁰ air-sea exchange flux	$F_v = K_w (C_w - C_a / H'(T))$
C_{wHg^0} (ng m ⁻³)	Concentration of Hg ⁰ in seawater	See differential equations
C_{aHg^0} (ng m ⁻³)	Concentration of Hg ⁰ in air	GEOS-Chem atmospheric simulation
$H'(T)$	Temperature dependent dimensionless Henry's law constant	$\ln H' = \left(\frac{-2403.3}{T} + 6.92 \right) (40)$
K_w (m hr ⁻¹)	Water-side mass transfer coefficient for steady winds	$A \times u_{10}^2 (Sc / Sc_{CO_2})^{-0.5} (41)$
A (unitless)	Constant based on the Weibull distribution of wind speeds over oceans	0.25 (6)
u_{10} (m s ⁻¹)	Wind speed normalized to 10 m above sea surface	GEOS-5 data
Sc_{CO_2}	Schmidt number for CO ₂	$0.11T'^2 - 6.16T' + 644.7 (42)$
T' (°C)	Water temperature	GEOS-5
$Sc_{Hg(0)}$	Schmidt number for Hg(0)	ν / D
ν (cm ² s ⁻¹)	Kinematic viscosity	$N/\rho = 0.017e^{(-0.025T')} (42)$
N (cP)	Viscosity of water	See text
ρ (mg cm ⁻³)	Seawater density	
D (cm ² s ⁻¹)	Diffusivity (Wilke-Chang (3) method)	$\frac{7.4 \times 10^{-8} (\phi_w M_w)^{1/2} T}{NV_B^{0.6}}$
M_w (g mol ⁻¹)	Molecular weight of water	18.0
T (K)	Water temperature in Kelvin	GEOS-5 data
V_B (cm ³ mol ⁻¹)	Molal volume of mercury at its normal boiling temperature	12.74
ϕ_w	Solvent association factor introduced to define the effective molecular weight of the solvent with respect to the diffusion process	2.26 (43)

Aqueous Viscosity

Loux (44) provides the following relationship for estimating aqueous viscosity as a function of aqueous temperature between 0-20°C:

$$(8) \log(N) = \frac{1301}{(998.333 + 8.1855(T' - 20) + 0.00585(T' - 20)^2)} - 3.30233$$

For water temperatures 20-100°C:

$$(9) \log(N_T / N_{20}) = \frac{1.3272(20 - T') - 0.001053(T' - 20)^2}{T' + 105}$$

Where N_{20} = aqueous viscosity at 20°C.

Section IV: References Cited

- (1) Qureshi, A.; O'Driscoll, N. J.; MacLeod, M.; Neuhold, Y. M.; Hungerbuhler, K., Photoreactions of Mercury in Surface Ocean Water: Gross Reaction Kinetics and Possible Pathways. *Environmental Science & Technology* **2010**, *44*, (2), 644-649.
- (2) Loux, N. T., A critical assessment of elemental mercury air/water exchange parameters. *Chemical Speciation and Bioavailability* **2004**, *16*, (4), 127-138.
- (3) Wilke, C. R.; Chang, P., Correlation of diffusion coefficients in dilute solutions. *Aiche Journal* **1955**, *1*, (2), 264-270.
- (4) Kuss, J.; Holzmann, J.; Ludwig, R., An Elemental Mercury Diffusion Coefficient for Natural Waters Determined by Molecular Dynamics Simulation. *Environmental Science & Technology* **2009**, *43*, (9), 3183-3186.
- (5) Liss, P. S.; Merlivat, L., Air-sea exchange rates: Introduction and synthesis. In *The role of Air-Sea Exchange in Geochemical Cycling*, Buat-Menard, P., Ed. D Reidel Publishing Compant: Dordrecht, 1986; pp 113-127.
- (6) Nightingale, P.; Malin, G.; Law, C.; AJ, W.; Liss, P.; Liddicoat, M.; Boutin, J.; Upstill-Goddard, R., In situ evaluation of air-sea gas exchange parameterizations using novel conservative and volatile tracers. *Global Biogeochemical Cycles* **2000**, *14*, (1), 373-387.
- (7) Rolffhus, K.; Fitzgerald, W. F., The evasion and spatial/temporal distribution of mercury species in Long Island Sound, CT-NY. *Geochimica et Cosmochimica Acta* **2001**, *65*, (3), 407-418.
- (8) Sunderland, E. M.; Dalziel, J.; Heyes, A.; Branfireun, B. A.; Krabbenhoft, D. P.; Gobas, F., Response of a Macrotidal Estuary to Changes in Anthropogenic Mercury Loading between 1850 and 2000. *Environmental Science & Technology* **2010**, *44*, (5), 1698-1704.
- (9) Andersson, M. E.; Gardfeldt, K.; Wangberg, I.; Sprovieri, F.; Pirrone, N.; Lindqvist, O., Seasonal and daily variation of mercury evasion at coastal and off shore sites from the Mediterranean Sea. *Marine Chemistry* **2007**, *104*, (3-4), 214-226.
- (10) Soerensen, A.; Sunderland, E.; Holmes, C.; Jacob, D. J.; Yantosca, R.; Strode, S.; Skov, H.; Christensen, J.; Mason, R. P., A new global simulation of mercury air-sea exchange for evaluating impacts on marine boundary layer concentrations. *Environmental Science & Technology* **2010**, *submitted*.
- (11) Sunderland, E. M.; Krabbenhoft, D. P.; Moreau, J. W.; Strode, S. A.; Landing, W. M., Mercury sources, distribution, and bioavailability in the North Pacific Ocean: Insights from data and models. *Global Biogeochemical Cycles* **2009**, *23*, 14.
- (12) Laurier, F.; Mason, R.; Gill, G.; Whalin, L., Mercury distribution in the North Pacific Ocean - 20 years of observations. *Marine Chemistry* **2004**, *90*, (1-4), 3-19.
- (13) Mason, R. P.; Fitzgerald, W., Alkylmercury species in the equatorial Pacific. *Nature* **1990**, *347*, 457-459.
- (14) Mason, R. P.; Fitzgerald, W., The distribution and cycling of mercury in the equatorial Pacific Ocean. *Deep-Sea Research Part I: Oceanographic Research Papers* **1993**, *40*, (9), 1897-1924.
- (15) Gill, G.; Bruland, K., Mercury in the northeast Pacific Ocean. *EOS Trans. Amer. Geophys. Union* **1987**, *68*, 1763.
- (16) Gill, G.; Fitzgerald, W. F., Vertical mercury distributions in the oceans. *Geochimica Cosmochimica Acta* **1988**, *52*, 1719-1728.
- (17) Mason, R.; Lawson, N.; Sheu, G.-R., Mercury in the Atlantic Ocean: factors controlling air-sea exchange of mercury and its distribution in upper waters. *Deep-Sea Research II* **2001**, *48*, 2829-2853.

- (18) Mason, R.; Sullivan, K. A., The distribution and speciaiton of mercury in the South and equatorial Atlantic. *Deep-Sea Research II* **1999**, *46*, 937-956.
- (19) Mason, R.; Rolffhus, K.; Fitzgerald, W., Mercury in the North Atlantic. *Marine Chemistry* **1998**, *61*, 37-53.
- (20) Kirk, J. L.; St. Louis, V.; Hintelmann, H.; Lehnherr, I.; Else, B.; Poissant, L., Methylated mercury species in marine waters of the Canadian High and Sub Arctic. *Environmental Science and Technology* **2008**, *42*, (22), 8367-8373.
- (21) Kim, J.; Fitzgerald, W., Sea-Air partitioning of mercury in the equatorial Pacific Ocean. *Science* **1986**, *231*, (4742), 1131-1133.
- (22) Kim, J.; Fitzgerald, W., Gaseous mercury profiles in the tropical Pacific Ocean. *Geophysical Research Letters* **1988**, *15*, 40-43.
- (23) Gardfeldt, K.; Sommar, J.; Ferrara, R.; Ceccarini, C.; Lanzillotta, E.; Munthe, J.; Wangberg, I.; Lindqvist, O.; Pirrone, N.; Sprovieri, F.; Pesenti, E.; Stromberg, D., Evasion of mercury from coastal and open waters of the Atlantic Ocean and the Mediterranean Sea. *Atmospheric Environment* **2003**, *Supplement No. 1*, S73-S84.
- (24) Guentzel, J. L.; Powell, R. T.; Landing, W. M.; Mason, R. P., Mercury associated with colloidal material in an estuarine and open-ocean environment. *Marine Chemistry* **1996**, *55*, 177-188.
- (25) Whalin, L.; Kim, E.; Mason, R., Factors influencing the oxidation, reduction, methylation and demethylation of mercury species in coastal waters. *Marine Chemistry* **2007**, *107*, 278-294.
- (26) Montegut, C. D.; Madec, G.; Fischer, A. S.; Lazar, A.; Iudicone, D., Mixed layer depth over the global ocean: An examination of profile data and a profile-based climatology. *Journal of Geophysical Research-Oceans* **2004**, *109*, (C12), 20.
- (27) Wetzel, P.; Maier-Reimer, E.; Botzet, M.; Jungclaus, J.; Keenlyside, N.; Latif, M., Effects of ocean biology on the penetrative radiation in a coupled climate model. *Journal of Climate* **2006**, *19*, (16), 3973-3987.
- (28) Behrenfeld, M. J.; Falkowski, P. G., Photosynthetic rates derived from satellite-based chlorophyll concentration. *Limnology and Oceanography* **1997**, *42*, (1), 1-20.
- (29) Antia, A.; Koeve, W.; Fischer, G.; Blanz, T.; Schulz-Bull, D.; Scholten, J.; Neuer, S.; Kremling, K.; Kuss, J.; Peinert, R.; Hebbeln, D.; Bathmann, U.; Conte, M.; Fehner, U.; Zeitzschel, B., Basin-wide particulate organic carbon flux in the Atlantic Ocean: Regional export patterns and potential for CO₂ sequestration. *Global Biogeochemical Cycles* **2001**, *15*, (4), 845-862.
- (30) Morel, A.; Berthon, J. F., Surface pigments, algal biomass profiles, and potential production of the euphotic layer - relationships reinvestigated in view of remote-sensing applications. *Limnology and Oceanography* **1989**, *34*, (8), 1545-1562.
- (31) Uitz, J.; Claustre, H.; Morel, A.; Hooker, S. B., Vertical distribution of phytoplankton communities in open ocean: An assessment based on surface chlorophyll. *Journal of Geophysical Research-Oceans* **2006**, *111*, (C8), 23.
- (32) Morel, A.; Maritorena, S., Bio-optical properties of oceanic waters: A reappraisal. *Journal of Geophysical Research-Oceans* **2001**, *106*, (C4), 7163-7180.
- (33) Westberry, T.; Behrenfeld, M.; Siegel, D.; Boss, E., Carbon-based primary productivity modeling with vertically resolved photoacclimation. *Global Biogeochemical Cycles* **2008**, *22*, GB2024.
- (34) O'Reilly, J.; Evans-Zetlin, C.; Busch, D., Primary Production. In *Georges Bank*, Backus, R. H.; Bourne, D. W., Eds. MIT Press: Cambridge, MA, 1987; pp 220-233.
- (35) Millero, F. J., *Chemical Oceanography*, 3rd ed. CRC Press: Boca Raton, FL USA, 2006; p 496.

- (36) Lalonde, J. D.; Amyot, M.; Orvoine, J.; Morel, F. M. M.; Auclair, J. C.; Ariya, P. A., Photoinduced oxidation of Hg-0 (aq) in the waters from the St. Lawrence estuary. *Environmental Science & Technology* **2004**, *38*, (2), 508-514.
- (37) Lalonde, J.; Amyot, M.; Kraepiel, A.; Morel, F., Photooxidation of Hg(0) in artificial and natural waters. *Environmental Science and Technology* **2001**, *35*, 1367-1372.
- (38) Amyot, M.; Gill, G. A.; Morel, F. M. M., Production and loss of dissolved gaseous mercury in coastal seawater. *Environmental Science & Technology* **1997**, *31*, (12), 3606-3611.
- (39) Chester, R., *Marine Geochemistry, 2nd Ed.* Blackwell Science Ltd.: Berlin, Germany, 2003; p 506.
- (40) Andersson, M. E.; Gardfeldt, K.; Wangberg, I.; Stromberg, D., Determination of Henry's law constant for elemental mercury. *Chemosphere* **2008**, *73*, (4), 587-592.
- (41) Wanninkhof, R., Relationship between wind-speed and gas-exchange over the ocean. *Journal of Geophysical Research-Oceans* **1992**, *97*, (C5), 7373-7382.
- (42) Poissant, L.; Amyot, M.; Pilote, M.; Lean, D., Mercury water-air exchange over the upper St. Lawrence River and Lake Ontario. *Environmental Science and Technology* **2000**, *2000*, (34), 3069-3078.
- (43) Hayduk, W.; Laudie, H., Prediction of diffusion-coefficients for nonelectrolytes in dilute aqueous solutions. *Aiche Journal* **1974**, *20*, (3), 611-615.
- (44) Loux, N. T. In *Monitoring cyclical air/water elemental mercury exchange*, 2001; Royal Soc Chemistry: 2001; pp 43-48.

11 Appendix C Background information on the *Galathea 3* expedition

The *Galathea 3* expedition was a 9 month long cruise campaign with the vessel *Vædderen* starting in Copenhagen August 14th 2006 and ending the same place April 25th 2007. During the cruise more than 39.000 nautical miles were crossed (Figure 40). Onboard the ship or linked to the destinations of it, 48 research projects took place. A more thorough description of the *Galathea 3* expedition can be found in the book “*Galathea 3*” edited by Lisbeth Nannested Jørgensen (in Danish) (available at: <http://130.226.56.246/dk/Menu/Ekspeditionen+2006-2007/Publikationer/Galathea+3+2006-2007> [accessed Jan 2011]) and at the internet portals from Virtuel Galathea (<http://virtuelgalathea3.dk/> [accessed Jan 2011]) the news paper Jyllands Posten (<http://viden.jp.dk/galathea/ekspeditionen/> [accessed Jan 2011]).

One of the projects was “Kviksølv i Troposfæren” (Mercury in the Troposphere). This project was one of the few that were onboard during the entire duration of the cruise. The aim was to give a global insight into mercury in the marine boundary layer. Measurements were carried out by PhD student Britt Tang Sørensen and her supervisor Henrik Skov as well as technicians Bjarne Jensen, Henrik W.Madsen and Christel Christoffersen. Britt decided not to continue her PhD after the cruise. This left the data unexplored for almost a year until the opportunity to incorporate them into my PhD project arose.



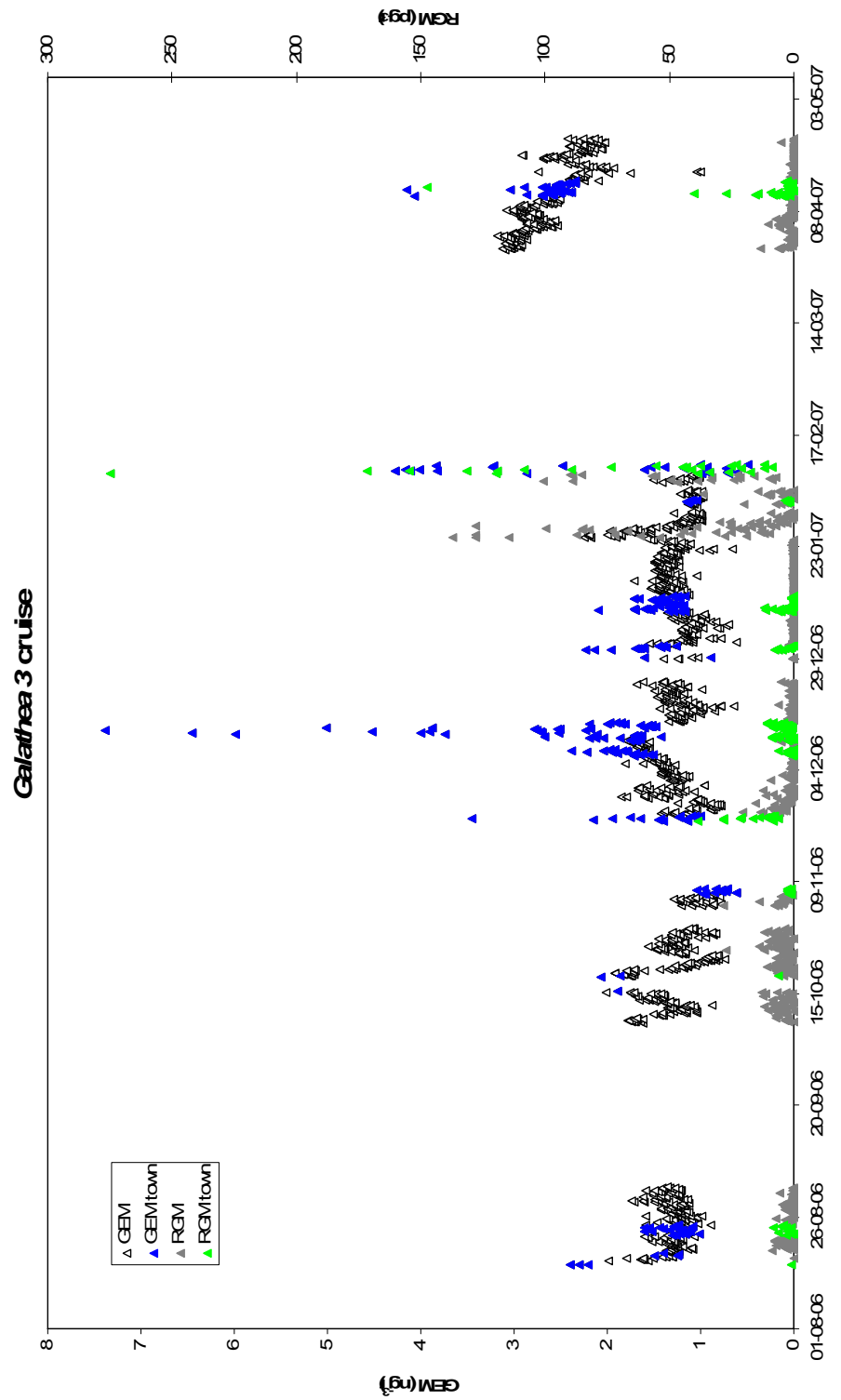
Figure 40. The track of the *Galathea 3* expedition.

The *galathea 3* expedition is following in the footsteps of earlier Danish global circum navigations carried out in the name of science. The first *Galathea* expedition took place in 1845-1847. The second *Galathea* expedition took place in 1950-1952. In addition to the scientific purpose an aim of the second expedition was to deliver information to the Danish public about the progress and findings of the expedition.

Information about science to the public has also been one of the main aims of the *Galathea 3* expedition. Focus was from the start not only on the 48 scientific projects but also on an attempt to create public interest for science. To create publicity during the cruise, journalists were invited onboard the ship, but the aim of making science public continued to be

followed after the cruise. Through educational material composed on the basis of the findings during the cruise students can be exposed to science from the cruise that they can relate to. The internet portal "Virtuel Galathea" (<http://virtuelgalathea3.dk/>) has a collection of educational material for elemental and high school students, which also including material and assignments on mercury in the project "Kviksølv i luften" (Mercury in the air) written by A.L. Soerensen, H. Skov, J. Christensen, S. Høgslund and M. Badger (2009).

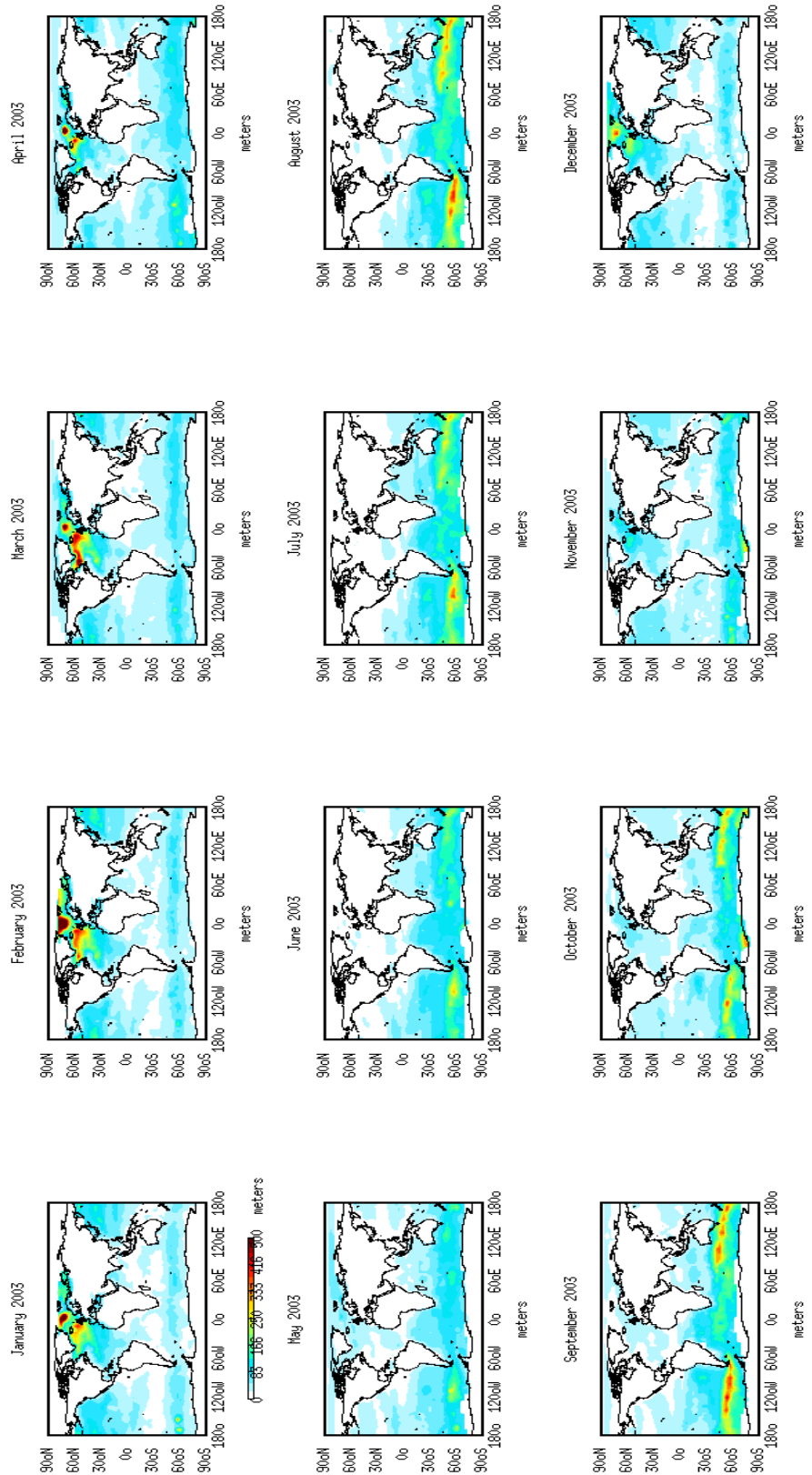
12 Two hour average GEM and RGM concentrations during the *Galathea 3* cruise



13 Appendix D Maps of input data to the GEOS-Chem slab-ocean model

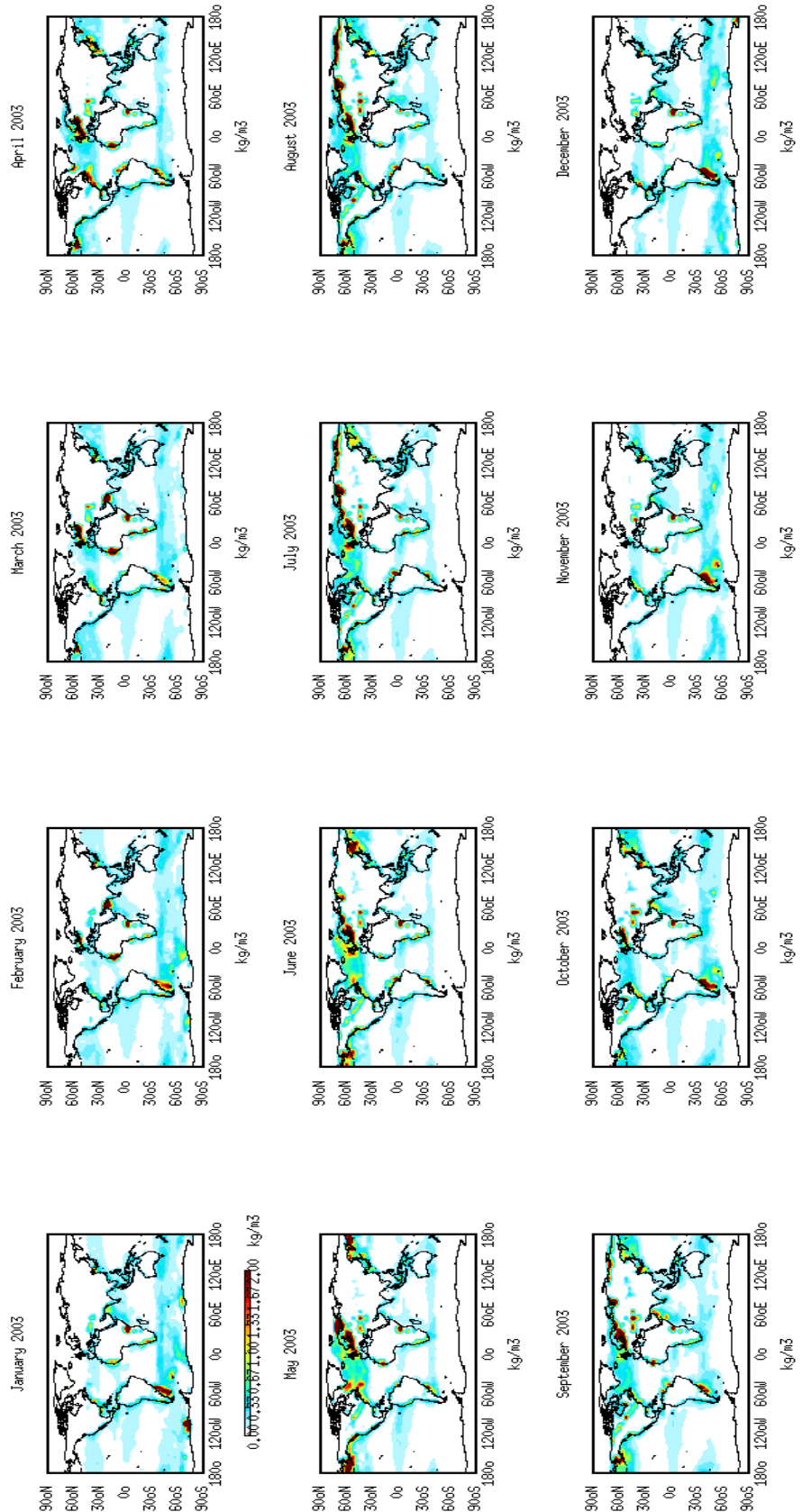
13.1 Mixed Layer Depth

From the National Oceanographic Data Center (NODE), World Ocean Circulation Experiment (WOCE) database, and the ARGO program (<http://www.loceanipsl.upmc.fr/~cdblod/mld.html>) (Montegut et al., 2004)



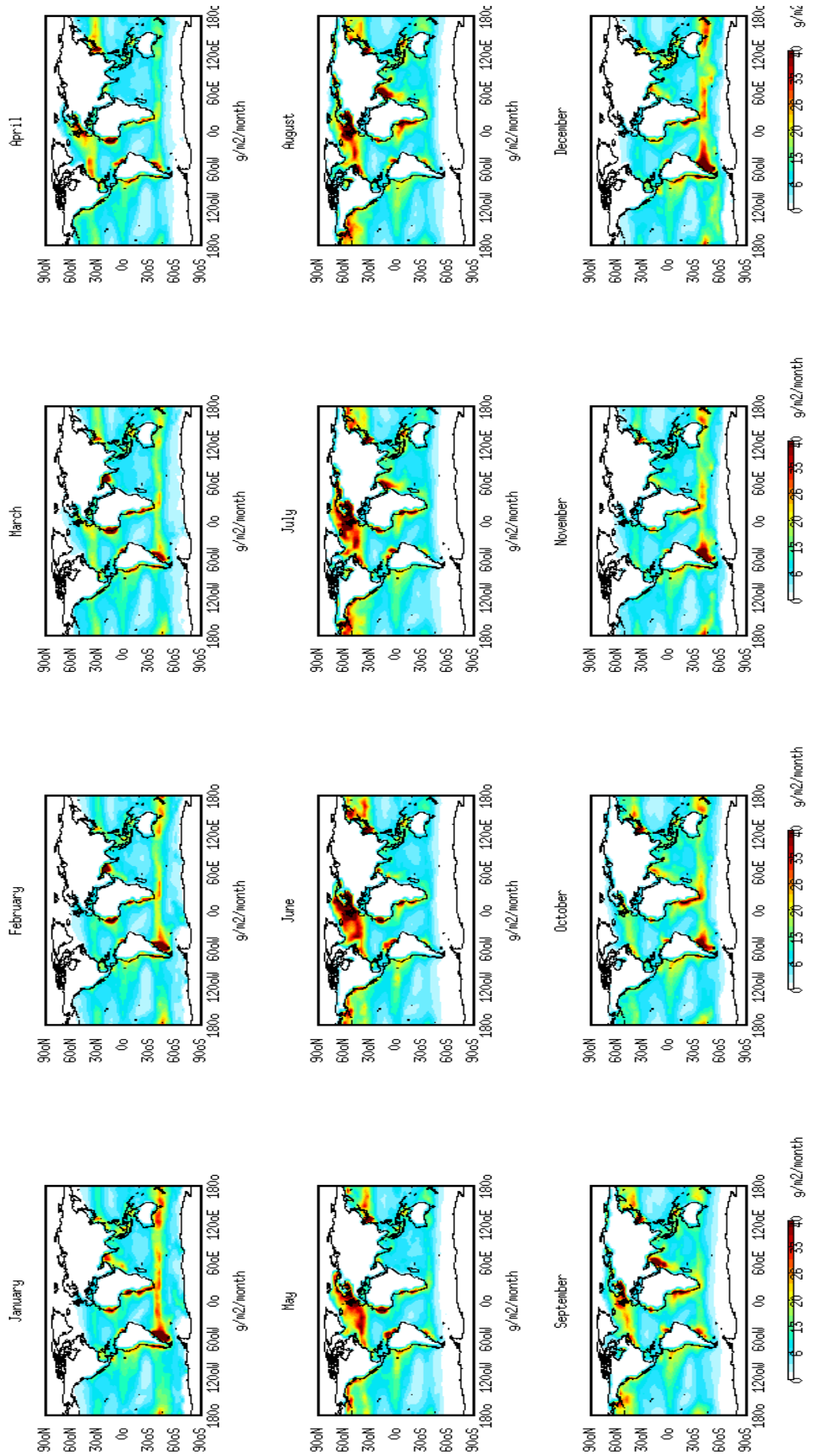
13.2 Chlorophyll A Concentrations

MODIS satellite chlorophyll a (C_{Chla} , mg m^{-3}) concentrations for the year 2003 (<http://oceancolor.gsfc.nasa.gov/ftp.html>).



13.3 Net Primary Production

Global NPP distributions from MODIS satellite data (Behrenfeld and Falkowski, 1997).



A51G-0197

Measurements and Modelling of the Air-Sea Exchange of Mercury

Robert P. Mason¹, Maria E. Andersson², Anne Sorensen³ and Elsie M. Sunderland⁴

1. Dept. Marine Sciences, Univ. of Connecticut, Groton, CT, USA; 2:Dept. Chemistry, Univ. of Goteborg, Sweden; 3: Dept. Atmospheric Environment, NERI, Univ. of Aarhus, Roskilde, Denmark; 4: School of Eng. & Appl. Sci., Harvard Univ., Cambridge, MA, USA

Introduction

Mercury (Hg) is released to the environment both via natural and anthropogenic sources, with ocean Hg⁰ emission being a major global flux (Sunderland and Mason, 2007). In the atmosphere, Hg exists as gaseous elemental mercury (Hg⁰), gaseous ionic mercury and mercury attached to particles. Once deposited to the ocean, mostly as ionic Hg, it can be transformed into methyl mercury, and into Hg²⁺ (measured as dissolved gaseous Hg (DGHg)), taken up into particles and removed by settling, and mixed to depth. The formation and evasion of Hg⁰ is the result of the net transformation, through biotic and photochemical redox processes. This is illustrated in Figure 1, which shows the current parameterization of these processes in the Geos-Chem Model (Soerensen et al., in prep), which is an update on Strode et al. (2007). Most ocean surface waters are supersaturated with Hg⁰, resulting in net evasion to the atmosphere globally, although model simulations suggest that not all waters are supersaturated and deposition of Hg⁰ may occur (e.g. Strode et al., 2007). Measurements have been historically sparse but new techniques (Andersson et al., 2008a; 2008b) are improving the overall database. Such data are discussed here and contrasted with the results of the current version of the Geos-Chem model.

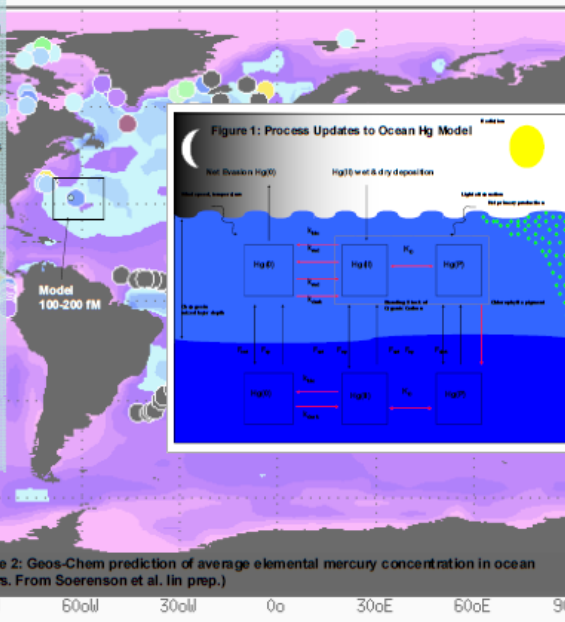


Figure 3: Measured elemental mercury during cruises in 9/08, 6/09 & 9/09

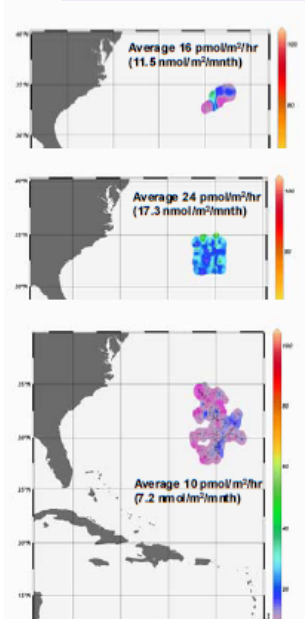
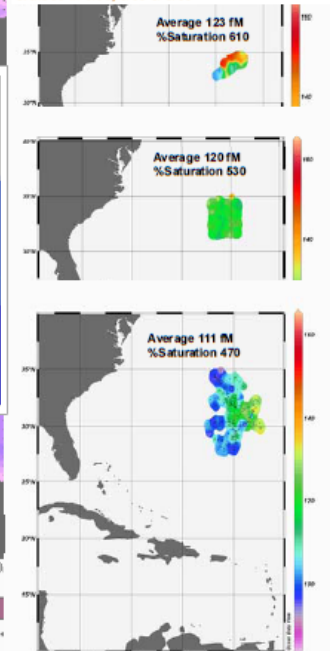
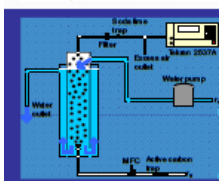
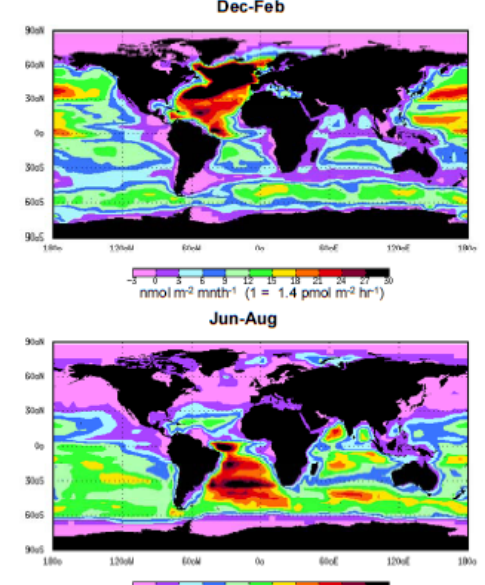


Figure 2: Geos-Chem prediction of average elemental mercury concentration in ocean waters. From Soerensen et al. in prep.)

Results and Discussion

DGHg (Hg²⁺) was measured during three cruises off Bermuda (Fig. 3). The observed DGHg concentrations and range were similar for all cruises. There was no strong indication of a diurnal variation and flux differences are mostly driven by differences in wind speed during the cruises (Fig. 4). Fluxes were estimated from measured parameters (wind speed, temp, air and water Hg⁰ concentrations). For example, winds were higher during the June 09 cruise due to a strong storm prior to the cruise, resulting in higher fluxes. The model output is shown in Fig. 2 for Hg⁰ and Fig. 5 for flux. Comparison of the measurements and model show that Hg⁰ values are similar for the observation region (box region in Fig. 2), while the flux estimates from the model are slightly lower than those estimated from measurements. This may reflect differences in the wind fields used in the model compared to during the cruises. However, it does appear that the model is providing a reasonable simulation of the concentration, changes with time and the overall flux. The model suggests a strong inter-annual variation but the data is limited to the spring-summer period and therefore can't be used to test this model result.

Figure 5: Model estimated fluxes of elemental mercury for two seasons. From Soerensen et al. (in prep.)



Method: Continuous measurements of DGHg (Hg²⁺) were made using the continuous sparging set-up in Fig. 6 (Andersson et al., 2008a). Seawater flow was 10-16 L/min and Hg-air flow 1.5 L/min; i.e. a high water/air flow ratio that ensured air equilibration with the water. The air Hg⁰ was then quantified at high resolution (5 min) using a Tekran 2537A, and the water Hg²⁺ concentration (Fig. 3) determined using Henry's Law (Andersson et al., 2008b). The flux (Fig. 4) was estimated using measured temperatures and wind speed (u) and the model of Nightingale et al. (2000), which relies on the Schmidt number (Sc_{DGHg}): $k = 0.333u + 0.22u^2 (Sc_{DGHg}/660)^{-0.5}$. As shown in Fig. 1, the model includes biotic processes that are linked to the extent of primary production, and photochemical processes that are related to light intensity and depth. The model output of Hg⁰ is shown in Figure 2, which is presented in the background, with other literature data superimposed as circles (Soerensen et al., in prep).

Acknowledgement
The Captain/crew of the RV Atlantic Explorer are acknowledged for all their help during the cruises. Mason's research funded by NSF Chemical Oceanography

References
1. Andersson et al. 2008a, Anal. Bioanal. Chem. 391: 2277
2. Andersson et al. 2008b, Chemosphere 73: 957
3. Nightingale et al. 2000, Global Biogeochem Cycles 14: 373
4. Strode et al. (2007) Global Biogeochem Cycles 21: Art #GB1017
5. Soerensen et al., in preparation
6. Sunderland and Mason (2007) Global Biogeochem Cycles 21: Art# GB4032

GASEOUS MERCURY IN THE MARINE BOUNDARY LAYER: MEASUREMENTS AND MODELING

The thesis combines analyses of observational data with biogeochemical modeling in order to explore the environmental processes that control patterns and levels of gaseous mercury concentrations in the marine boundary layer. Measurements of gaseous elemental mercury (GEM) and gaseous oxidized mercury (RGM) from the Galathea 3 circumnavigation (August 2006 to April 2007) are analyzed. A new representation of the surface ocean within the 3-D global biogeochemical model GEOS-Chem is presented. The model is used to explore mechanisms responsible for spatial and temporal trends discovered in the Galathea 3 data. The study contributes to our understanding of mercury dynamics in the marine boundary layer on diurnal, seasonal and decadal time scales. It emphasizes the importance of ocean evasion as a controlling factor for seasonal and decadal GEM variability as well as the importance of relative humidity as a controlling factor of RGM concentrations in both the polluted and pristine marine boundary layer.